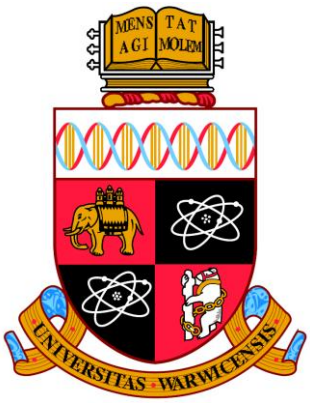

Modelling endocrine regulation of glycaemic control in animal models of diabetes

by

Edmund Michael Watson

MEng (Hons)

for

Doctor of Philosophy in Engineering

at

School of Engineering

University of Warwick

and

Cardiovascular & Gastrointestinal Research Area

AstraZeneca

Submitted: December 2014

My piece of resistance.

Table of Contents

Table of figures

Table of tables

Acknowledgments

Thank you to all my supervisors for all their patience and understanding over the years:

- Dr. Michael Chappell (University of Warwick)
- Dr. Simon Poucher (AstraZeneca then private consultancy)
- Frederic Ducrozet (AstraZeneca, October 2006-March 2008)
- Dr. Gary Wilkinson (AstraZeneca, from March 2008)
- Dr. James Yates (AstraZeneca, from March 2008)

In particular, thank you for helping out even when you weren't obligated to. I would also like to thank Dr. Phil Arundel (formerly AstraZeneca and Visiting Professor at Warwick) and Chris Allott (formerly AstraZeneca).

Also I would like to briefly thank people that have helped me with my modelling work at conferences, especially Dr. Andrea De Gaetano (BioMathMed, Warwick Summer School), Dr. Jerry Batzel (BioMathMed, Warwick Summer School) and Dr. Susanne Ditlevsen (BioMathMed).

I would like to thank all the people at AstraZeneca who helped collect data for me and allowed me to observe experiments to gain a better understanding of what was going on: Alice Yu, Dr. Amie Gyte, Ruth MacDonald (nee Potter), Dr. Georgia Frangioudakis, Sue Loxham and Dr. Steve Wang.

I would like to thank AstraZeneca for funding my PhD.

Lastly, I would like to thank my now-wife, Jenn, for all her patience and understanding, Kate Houston for interpreting my random presses of keys on a keyboard and Amy Cheung and James Chapman for their friendship whilst doing this PhD.

Declaration

This thesis is the original work of the author, with the following publications describing parts of the work:

Papers

E. Watson, S. Poucher, M. J. Chappell, and J. Teague, "Short term and long term disease mathematical modelling of diabetes in Zucker and ZDF rats," *Diabetologia*, vol. 52, pp. S240, 2009.

E. Watson, M. Chappell, F. Ducrozet, S. M. Poucher, and J. Yates, "A new general glucose homeostatic model using a proportional-integral-derivative controller," *Modelling and Control in Biomedical Systems*, 2009, pp. 79-84.

P. Arundel, C. Allott, and E. Watson. (2010, Double-pole in closed-loop minimal model of insulin kinetics. *IET Conference Proceedings,* 85-90. Available: http://digital-library.theiet.org/content/conferences/10.1049/ic.2010.0261

J. W. Yates and E. M. Watson, "Estimating Insulin Sensitivity From Glucose Levels Only: Use of a non-linear mixed effects approach and Bayesian estimation," *Proceedings of UKACC International Conference on Control,* 2010, pp. 1-5.

E. M. Watson, M. J. Chappell, F. Ducrozet, S. Poucher, and J. W. Yates, "A new general glucose homeostatic model using a proportional-integral-derivative controller," *Computer methods and programs in biomedicine*, vol. 102, pp. 119-129, 2011.

J. W. Yates and E. M. Watson, "Estimating insulin sensitivity from glucose levels only: Use of a non-linear mixed effects approach and maximum a posteriori (MAP) estimation," *Computer methods and programs in biomedicine*, vol. 109, pp. 134-143, 2013.

Conferences

Paper and poster presentation: "A New General Glucose Homeostatic Model using a Proportional-Integral-Derivative Controller"; published in *Computer Methods*, August 2009: IFAC; Aalborg, Denmark

Poster presentation: "Modelling of Blood Glucose Dynamics: New Approaches to a Growing Problem". March 2009: SET for Britain; London, UK

Oral presentation: "Hepatic blood flow variations affect insulin 1st pass absorption and clearance rates". November 2008: PKUK; Stansted, UK

Oral presentation: "Deconvolution of C-peptide to estimate insulin secretion and clearance in Han Wistar rats". August 2008: BioMedMath Event 2; Middelfart, Denmark

Oral presentation: "Structural identifiability of the Minimal Model with insulin and glucose regulation in rat animal models". November 2007: PKUK; Edinburgh, UK

Other declarations

The implementation of the Maximum Entropy deconvolution technique used in Chapter 7 C-peptide was a collaborative work by the author and Dr. John Hattersley. The application to the C-peptide data was solely the work of the author.

The data from the animal models was collected at AstraZeneca, Alderley Park, Cheshire, UK, and is described in Chapter 4.

Summary

This thesis is concerned with mathematical modelling of the glucose-insulin homeostatic system, with the specific aim of mathematically modelling diabetes and diabetes-like conditions in animals. Existing models were examined and critiqued in this thesis. Additionally, structural identifiability analysis of the most widely-used model in the field, the Minimal Model, was performed using Taylor series and similarity transformation approaches. It was shown under certain assumptions that it was theoretically possible to obtain a unique set of parameters for the model from only measuring glucose.

C-peptide deconvolution was performed using the WinNonLin algorithm and Maximum Entropy technique implemented in MATLAB. This was used to calculate insulin secretion, the percentage of insulin appearing in the periphery and insulin clearance rate. This was then further developed to model insulin appearance and clearance based on hepatic blood flow changes.

A short-term model of the glucose-insulin and C-peptide system was initially formulated using a PID controller concept and later refined to reduce the number of model parameters. Structural identifiability analysis was performed using the Lie symmetries approach, followed by parameter estimation on rat and mice data from IVGTTs, OGTTs and hyperglycaemic clamps and sensitivity analysis. This short-term model was integrated into a long-term model to analyse Zucker and ZDF rat data to create a single model to cater for both short- and long-term dynamics. Finally, a software tool was developed to allow non-mathematical scientists to use and access the benefits of the model.

Glossary and abbreviations

Accuchek®	Roche's glucose monitoring device
Adipose tissue	Collection of cells which store fat
ADP	Adenosine diphosphate
AIDA model	Automated insulin dosage advisor model, see section 5.4
AIR	Acute insulin response
Animal model	Model where an animal (in this case often a rat) is used to represent a human
ATP	Adenosine triphosphate
AUC	Area under curve
β-cell	Cell in the pancreas which secretes insulin
Basal level	Level a concentration returns to naturally (steady state)
Berkeley-Madonna	Mathematical modelling software [1]
BFGS algorithm	Broyden-Fletcher-Goldfarb-Shanno algorithm; used to solve ordinary differential equations
Bioavailability	Amount of drug or substance entering systemic circulation
Biomarker	Indicator of a biological state

C57BL/6J mice	Standard mouse used in scientific research, see section 4.3.4
CAC	Citric acid cycle (also known as Krebs cycle or tricarboxylic acid cycle)
CGM	Continuous glucose monitoring
Clearance	Rate at which a substance is removed
Cleaving	Process by which C-peptide is removed from proinsulin, causing insulin to be released
CNS	Central nervous system
Compartmental model	Mathematical model which uses compartments to represent aspects of the system
Control system state space form	Standard form for mathematical model equations given in section 2.3.2
C-peptide	By-product of insulin secretion
Critically damped (system)	System which returns to its steady state as quickly as possible
CVGI	Cardiovascular gastro-intestinal (department at AstraZeneca)
Deconvolution	Process whereby system input is determined from its output and knowledge of the system
Deterministic	System whose response is uniquely determined by the input and parameters, with no random component

ELISA assay	Enzyme-linked immunosorbent assay; biological test used to measure insulin and C-peptide levels
Enzyme	Biological catalyst
Euglycaemic-hyperinsulinaemic clamp	An experiment where glucose is maintained at a normal concentration and insulin is maintained at a high concentration for a period of time
First order ODE	Ordinary differential equation containing only first derivative terms
First pass effect	Amount of drug or substance removed before being measured
First phase response	Initial reaction of a system to an impulse
Gear's stiff algorithm	Algorithm for solving ordinary differential equations, see section 2.5
GIM	Glucose insulin model; software tool developed from the Cobelli model, see section 5.7
GLS	Generalised least squares
Globally identifiable	Parameter with a unique value or a system whose parameters all have unique values
Glucagon	Hormone which raises blood glucose levels and stimulates conversion of glycogen into glucose
Gluconeogenesis	Process for synthesis of glucose from non-carbohydrates

Glucose effectiveness	Removal of glucose based only on glucose concentration
Glucose-insulin homeostatic system	System responsible for blood sugar regulation in the body
GLUT	Group of glucose transporters
Glycogen	Polymer of glucose used to store glucose in the liver
Glycogenesis	Process for creating glycogen
GSIS	Glucose-stimulated insulin secretion
Haemacel	Compound used to maintain constant volume of distribution
Han Wistar rats	Standard rat used in scientific research, see section 4.3.1
Hepatic artery	Main source of oxygenated blood into the liver
Hepatic portal vein	Main source of blood to the liver, via the gastrointestinal tract and spleen
HOMA model	Homeostatic model assessment model, see section 5.3
Hyperglycaemic	Having an elevated level of glucose
Hyperglycaemic clamp	Experiment where glucose is maintained at a high concentration for a period of time
Hyperinsulinaemic	Having an elevated level of insulin

Hypoglycaemic	Having a lowered level of glucose
IDDM	Insulin dependent diabetes mellitus
Impulse response	Output of a system when presented with a brief input signal (an impulse)
Incretins	Hormones which stimulate the release of insulin
Insulin action	Effect of insulin on a system
Insulin resistance	Level of insensitivity to insulin
Insulin sensitivity	Level of effect insulin has on glucose
Islets of Langerhans	Groups of cells in the pancreas where β-cells reside
Interstitial insulin	Insulin which is not in the blood
IVGTT	Intravenous glucose tolerance test
Krebs cycle	Part of the process for converting ADP into ATP in mitochondria (also known as citric acid cycle or tricarboxylic acid cycle)
Leptin	Hormone responsible for limiting appetite
Lipids	Group of molecules which allow energy to be stored; includes fats and fatty acids
Locally identifiable	Parameter with only a finite number of possible values or system whose parameters have only a finite number of possible values
Maple	Symbolic mathematical modelling software [2]

Mathematica	Symbolic mathematical modelling software [3]
Mathematical model	Model using mathematical equations to describe a system
MATLAB	Numerical mathematical modelling software [4]
Maximum entropy method	Method for deconvolution
Michaelis-Menten kinetics	Standard model for enzyme kinetics
Minimal Model	Model of the glucose-insulin system, see Chapter 6
Nelder-Mead algorithm	Optimisation algorithm
NHS	National Health Service
NIDDM	Non-insulin dependent diabetes mellitus
Observable	System (or part of a system) whose state can be reconstructed from observation of its outputs
ODE	Ordinary differential equation
OGTT	Oral glucose tolerance test
OLS	Ordinary least squares
ORC	Observability rank criterion
Parameter	Variable within a mathematical model
Parameter estimation	Process of determining values of variables within a mathematical model
Pharmacodynamics	Study of action which drugs have on a system

Pharmacokinetics	Study of the profile of drugs within a system
PID (controller)	Proportional-Integral-Derivative (controller)
PKPD	Pharmacokinetic pharmacodynamic
Plasma glucose	Glucose measurement taken from blood plasma
Plasma insulin	Insulin measurement taken from blood plasma
Proinsulin	Form in which insulin is stored, attached to C-peptide
p value	Probability of an event occurring due to random chance (usually based on Student's t distribution)
Quasi-Newton algorithm	Optimisation algorithm
Residual	Output from objective function (e.g. generalised least squares) when fitting a mathematical model
RRP	Readily releasable pool (of insulin)
Runge-Kutta algorithm	Algorithm for solving ordinary differential equations
Sensitivity analysis	Method for determining a system's response to a change in parameter values
SF	Stiffness factor
Steady state	State to which a system will return after perturbation; equivalent to basal level in biological terms

Stiffness	Measure for how dynamic (or otherwise) a system is
Stochastic	System whose response is not uniquely determined by the input and parameters as it has a random component
Structural identifiability	Analytical test to determine whether, given perfect, noise-free, continuous observations from an experiment, model parameters can be meaningfully determined
Substrate	Substance on which an enzyme acts
TCA cycle	Tricarboxylic acid cycle (also known as Krebs cycle or citric acid cycle)
Type 1 diabetes	Diabetes characterised by an auto-immune disorder causing loss of β-cells
Type 2 diabetes	Diabetes characterised by impaired β-cell function (though not due to an autoimmune disease as in type 1 diabetes) and reduced insulin sensitivity
UN	United Nations
Unidentifiable	Parameter with an infinite number of possible values or a system with at least one parameter with infinite possible values
Uppsala model	Model of the glucose-insulin system developed by a group based in Uppsala, see section 5.8
Volume of distribution	Size of a compartment in a compartmental model

WHO	World Health Organisation
WinNonLin	Numerical mathematical modelling software [5]
WLS	Weighted least squares
ZDF rat	Zucker diabetic fatty rat; model for subjects entering type 2 diabetes, see section 4.3.3
Zucker rat	Rat deficient in leptin receptors which is a good model for type 2 diabetes, see section 4.3.2

Chapter 1: Introduction

1.1 Aims

The primary aim of this work is to develop, using data obtained from rat models, an integrated mathematical model of glycaemic control that predicts both short-term and long-term glucose regulation [6]. It is an additional aim of this thesis that it should be understandable by non-specialists. This will ensure that any person with an interest, regardless of scientific background, can understand the work.

1.2 Objectives

- To review and evaluate the different mathematical models of glycaemic control.
- To modify/develop existing mathematical models and determine how existing glucose and insulin data from animal (rat and mouse) studies fit.
- To apply the new model to the evaluation of glucose stimulated insulin secretion using new data.
- To develop an integrated desktop utility for modelling and analysing glycaemic control and insulin secretion in animal models of diabetes.
- To develop methods for determining pancreatic degeneration and function from measurable, but indirect, parameters such as glucose, C-peptide and insulin levels.

- To include in the model physiological control parameters that address counter-regulatory systems, such as lipid levels and β-cell mass.
- To apply the model to the design of future studies evaluating pancreatic changes and effects on glycaemic control [6].

1.3 Justification

Diabetes is a huge and growing problem throughout the world. 171 million people suffer from it worldwide; this is estimated to double by 2030 [7]. In 2008, 2.3 million people in the UK had diabetes, and it is expected to rise to 4 million by 2025. Diabetes in the UK costs an estimated 10% of total NHS costs [8].

Mathematical modelling can be used to help understand glucose regulation in health and diabetes. Drug development speed can be increased by identifying key pathways that will have the greatest effect on improving glucose control. Robust and well-validated models can potentially predict experimental outcomes without the need for further experiments to be performed, making processes cheaper and faster. They can also be used to analyse experimental data in order to gain more benefit from the experiments as well as helping to improve the design of future experiments. Thus modelling can also help in replacing, reducing and refining animal testing.

Mathematical modelling involves equations that can reproduce and predict how a system will behave. To model the complex glucose and insulin system,

including feedback and non-linearities, with few data points is a challenging task. The glucose and insulin system can be looked at both in the long term (days, weeks and months) and the short term (hours and minutes); to combine these in one model and create a complete model of the glucose and insulin system is clearly a complicated and non-trivial task.

1.4 Thesis layout

Background information on mathematical modelling is provided in Chapter 2 and the biology of the glucose-insulin system is detailed in Chapter 3. Methods employed for data collection and the data used to create and validate the models created by the author of this thesis are introduced in Chapter 4. A selection of existing models of the glucose and insulin system is presented and critiqued in Chapter 5 to give an overview of the field as it stands. Chapter 6 : Minimal Model contains details of the most widely-used model in the field and new analysis of the Minimal Model performed by the author of this thesis. Chapter 7 presents the author's deconvolution of C-peptide concentrations to obtain insulin concentrations which were used to help design the model presented in Chapter 8, which is for short-term modelling of the glucose-insulin system. It is developed in Chapter 9 to additionally model long-term aspects of the glucose-insulin system. The software tool produced by the author is explained in Chapter 10. Figure 1.1 shows the relationship between chapters.

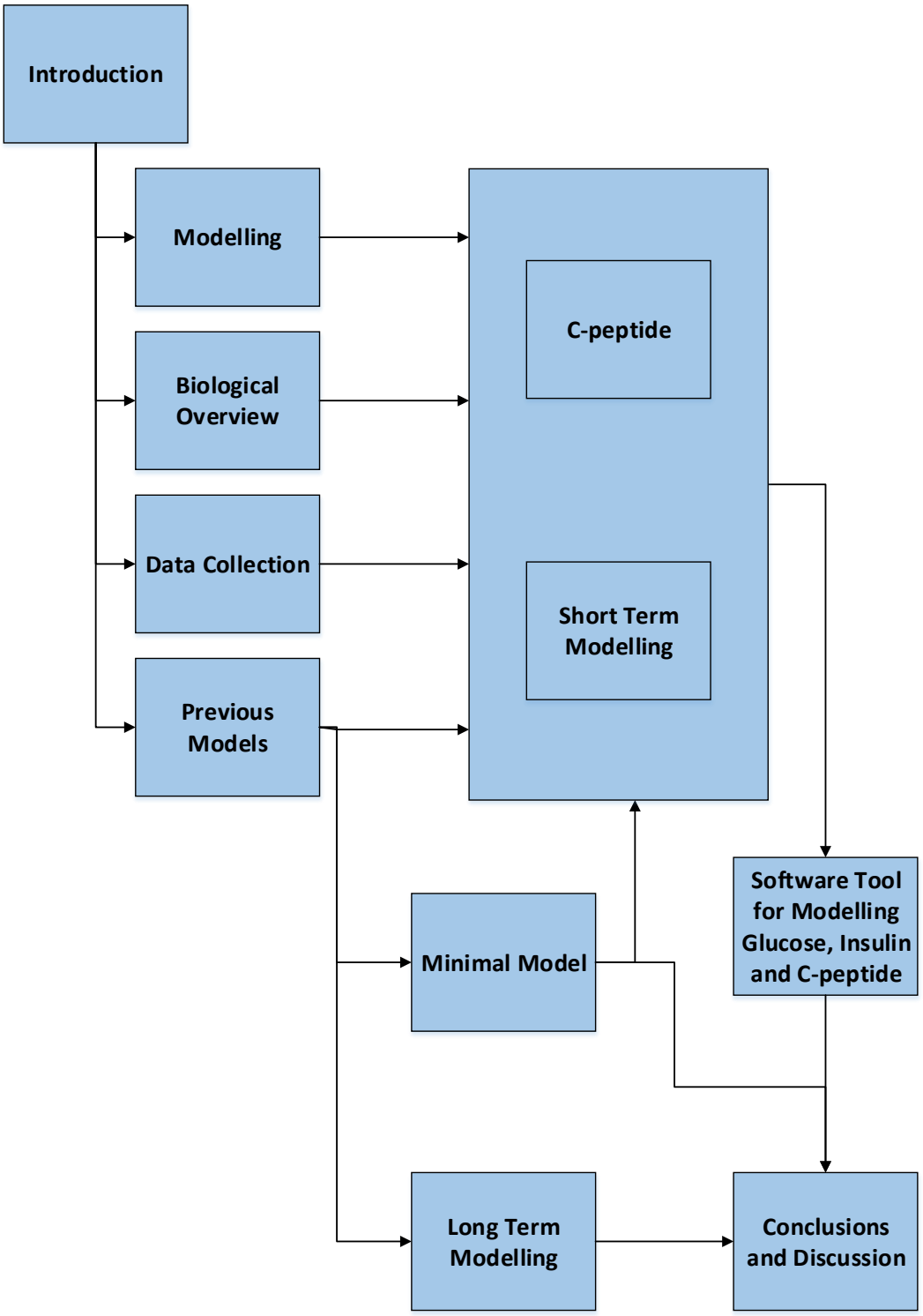

Figure 1.1 - Overview of chapters

Chapter 2: Modelling

This chapter introduces all the basic concepts of mathematical modelling and approaches to modelling that will be used and examined in the rest of this thesis. These include strategies for building models, structural identifiability analysis, model simulation, parameter estimation and sensitivity analysis.

2.1 Introduction

A mathematical model is a representation of a system. Mathematical models are invariably simplified versions of the actual physical processes modelled and thus are approximations of the systems they represent. Mathematical models are useful because they make systems easier to study. For example they may allow situations which cannot be created in reality to be studied, outcomes to be predicted without experiments being carried out and situations to be analysed more clearly as mathematical variables can be controlled more easily.

This thesis considers mathematical models of biological systems, specifically the glucose-insulin homeostatic system and other closely related systems. Two types of models are discussed in this thesis, animal models and mathematical models. A few are animal/biological models, where one animal (commonly the rat) is used as a substitute for a human. Most are mathematical models, that is mathematical descriptions of the system. The models which the author has developed and presented in this thesis are mathematical models.[9-11]

2.2 Modelling approach

In order to create a mechanistic mathematical model, the system must be represented by a set of equations. There are different ways in which this may be approached, though all tend to follow a similar approach which involves gathering information about the system, generating a model (or models) and validation.

The approach adopted in this thesis is based on approaches from several sources [9-11].

Figure 2.1 is a flowchart giving an overview of this approach; each stage is explained below.

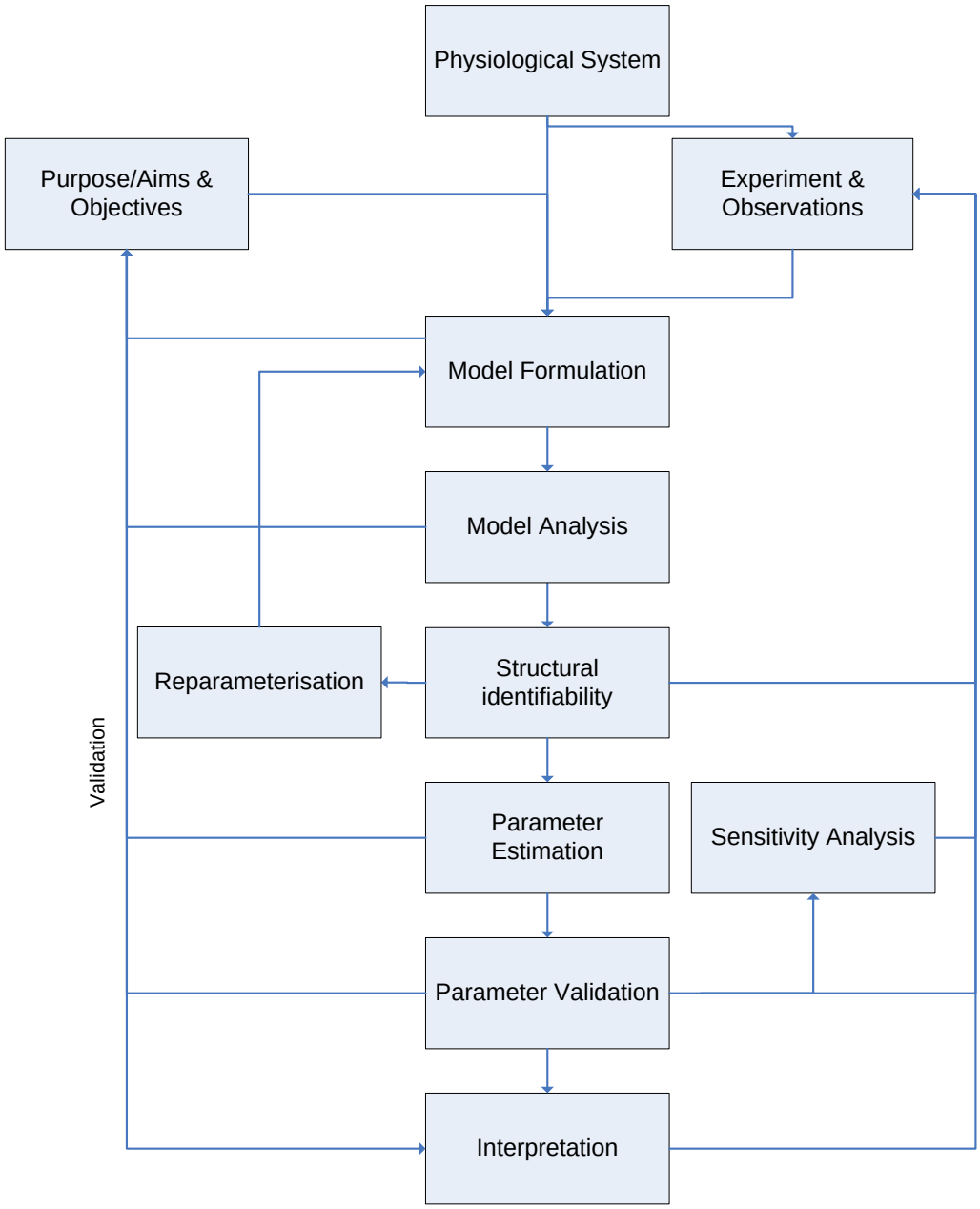

Figure 2.1: Flowchart of modelling approach adopted in this thesis

2.2.1 Physiological System

In creating a mathematical model, it is necessary to consider what is being modelled: data or the physical system itself [10]? In the first case, equations are based purely on inputs and outputs with no consideration for the mechanisms involved in the system, a numeric/descriptive model, and are essentially a curve-fitting exercise. In the second case, equations are based on information about how the system works (i.e. physical, chemical or biological laws), which ensures that all parts of the model are relevant and justifiable and is necessary to make the model robust and applicable across a variety of situations.

The models developed by the author of this thesis aim to be system, rather than data-driven, models. The biology of the glucose-insulin system is discussed at length in Chapter 3 and is used to help design the models in later chapters.

2.2.2 Purpose/Aims & Objectives

A large number of factors influence the way that a model is designed. It is important at the outset to ensure that the purpose of the model is clearly defined and that the desired outputs from the model are specified. The specific demands on this model are discussed in Chapter 5, Chapter 8 and Chapter 9.

2.2.3 Experiments & Observations

Knowing the limitations of the experimental environment helps to ensure that a model is appropriate for its purpose. For example, a model with a large number of parameters will possibly require more data and other types of measurements than can be gathered from available experiments. It may therefore be necessary to limit

the number of parameters in a model based on the potentially available experimental data. This is discussed further in the section on Structural Identifiability below.

2.2.4 Model Formulation

Once information about the system has been gathered, a model can be formulated. Where physical or biological laws related to the system are known, well accepted equations can be used; for example, laws governing enzyme kinetics are described by the Michaelis-Menten equation described in the Michaelis-Menten kinetics section below. For parts of the system where laws are unknown, numerically-derived equations based on data can be used.

This is the stage where decisions must be made about the form of the model; further detail about some of these decisions is given in the Model form section below.

2.2.5 Model Analysis

Depending on the model and the system being modelled, it is important to check that the model's behaviour matches the underlying system as well as passes mathematical tests to ensure the resulting parameters are valid. An example of this is that if the system returns to a steady state the model should also return to that steady state. It is good practice therefore to analyse the model's properties, in particular steady state analysis, to ensure that the model accurately represents the system and is stable [12-14]. Further tests, such as structural and sensitivity analyses, can be performed.

2.2.6 Structural Identifiability Analysis

Structural identifiability analysis plays an important role in testing whether a model is appropriate, in a parametric sense, for a given experiment. It is a test to investigate whether, given perfect, noise-free, continuous observations from an experiment, model parameters can be meaningfully determined. This is important because an unidentifiable parameter has an infinite number of possible values which will all produce the same model output, rendering it meaningless. If any model parameters are unidentifiable, action to resolve this is needed; whether through obtaining the parameter value from another source (e.g. via the literature on separate, external experiments), re-parameterising the model such that it is "lumped" into a reduced set of identifiable parameters or redesigning the experiment to provide more observations from other parts of the system. Methods of determining structural identifiability are described in Structural identifiability techniques below [14-19].

2.2.7 Parameter Estimation

Structural identifiability is a necessary precursor to parameter estimation (or parameter fitting) to ensure that any unidentifiable parameters have been appropriately reworked. Parameter estimation is the process of taking the postulated model and the experimental data and determining unknown model parameter values. Some parameters can be determined via alternative methods to parameter estimation; for example in a model of friction on a car wheel, gravitational acceleration need not be found from experimental data. In biological systems the majority of parameters are not documented in the literature or easily

obtainable from other experiments so most, or all, will need to be determined via parameter estimation. A method of parameter estimation is described in the Parameter estimation section below [10, 11, 18, 20-22].

2.2.8 Parameter Validation

As part of parameter estimation, it is important to assess the confidence in the fitted parameter values as structural identifiability only tests the structure of the model, rather than the measurements given to the fitting process. If there is low confidence in the parameter values estimated, then it is necessary to redesign either the experiment or the model. This topic is explained in detail in Chapter 10, as it is important for users of the tool to understand how reliant they can be on the parameter values generated.

2.2.9 Sensitivity Analysis

Sensitivity analysis involves measuring how sensitive the model output is to changes in parameter values. This is useful in helping redesign experiments and models when there is low confidence in the parameter values as it can locate dynamic phases of the model which are key in obtaining higher confidence. This is described in detail later in this chapter [11, 20, 23, 24].

2.2.10 Interpretation

Analysis and prediction are strongly linked to the model purpose as they are the primary reason for the development of a mechanistic model. In this case, the model has been designed largely to enable examination of the glucose-insulin system which allows for analysis of experiments, such as an IVGTT(Intravenous Glucose

Tolerance Test), and prediction of future experimental outcomes to this and other forms of intervention.

2.3 Model form

2.3.1 Linear and non-linear models

A linear model is one where the output is directly proportional to the input, whereas a non-linear model does not have output directly proportional to the input. A linear model, such as the model of C-peptide kinetics in this thesis (see Chapter 7), will be structurally simple in a mathematical sense but may not contain adequate dynamics to model some systems. A non-linear model, such as the model of glucose and insulin kinetics in this thesis Chapter 8, may provide a more accurate representation of a system, but will be more complex in structure.

2.3.2 General model form for equations

The standard control system state space form for representing mathematical models is as follows in equation 2.1:

$$\begin{aligned} \dot{x}(t,p) &= f(x(t,p),p) + u(t)g(x(t,p),p) \\ y(t,p) &= h(x(t,p),p) \\ x(0,p) &= x_0(p) \end{aligned} \qquad 2.1$$

where $t \geq 0$ is time, p is a vector of the model parameters $\in \mathbb{R}^p$ (a real number vector of size *p*), x is the state vector $\in \mathbb{R}^n$, y is the vector of observations $\in \mathbb{R}^m$ and u is the input to the system. In a non-linear model f is the co-ordinate function that represents the dynamics of the system, g is a function applied to states that affects the inputs and h is a function of the states; in a linear model, f, g and h are a matrix of scalars multiplied by the states [25].

Linear models have an exact analytical solution whereas very few non-linear models have known analytical solutions. Therefore when solving non-linear models numerical methods are often required. This is explained in section 2.5, Simulation.

2.3.3 Compartmental modelling

Compartmental models are used extensively in the modelling of biological systems [14]. In this type of model systems are represented by a finite set of subsystems, or "compartments", with flows linking those parts of the system which interact (see Figure 2.2). How the system is divided into compartments depends on factors such as the scale of the system and purpose of the model; for example a simple model could use a single compartment to represent all of the blood in the human body, whereas a more complex model might use one compartment per organ (such as the PBPK model in [26]).

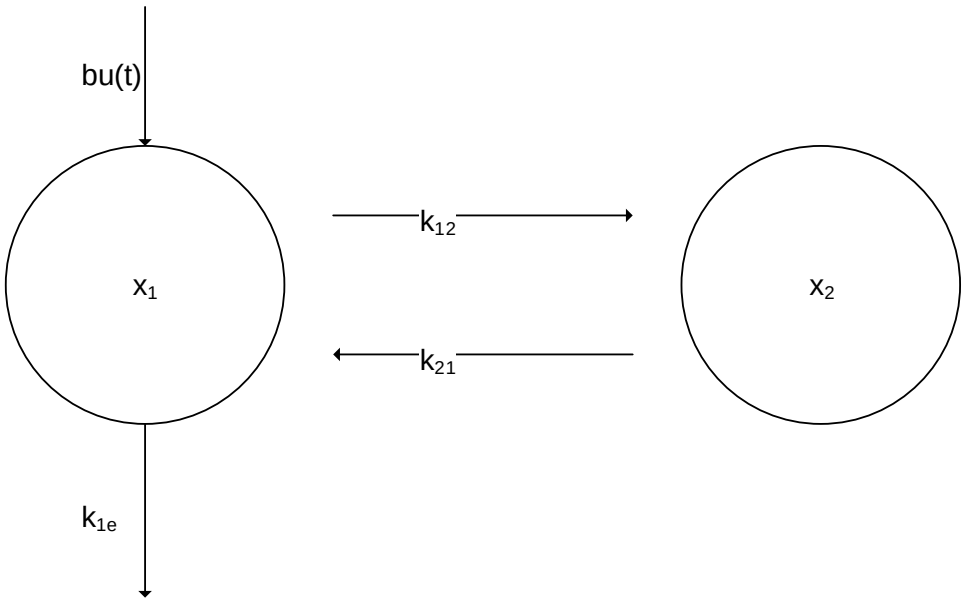

Figure 2.2: Example compartmental model

The equations defining the compartmental model shown in Figure 2.2 are given in equation 2.2.

$$\begin{aligned} \dot{x}(t,p) &= \begin{bmatrix} -k_{12} - k_{1e} & -k_{21} \\ k_{12} & k_{21} \end{bmatrix} \begin{bmatrix} x_1 \\ x_2 \end{bmatrix} + \begin{bmatrix} b \\ 0 \end{bmatrix} u(t) \\ y(t,p) &= [1 \quad 0] \begin{bmatrix} x_1 \\ x_2 \end{bmatrix} \\ x(0,p) &= x_0(p) \end{aligned} \qquad 2.2$$

where x_1 and x_2 are state variables representing concentration in compartments 1 and 2 respectively, x_1 is the only observable state (shown by the matrix in the equation for y), y is the output function, k_{12} is the flow rate from compartment 1 to compartment 2, k_{21} is the flow rate from compartment 2 to compartment 1, k_{1e} is the extraction rate from compartment 1, b is the input gain (bioavailability/volume of distribution) and u is the input to compartment 1 [14].

In biological system modelling, it is often the case that each compartment represents a concentration of a substance or quantity of a substance; this is the case in the models developed by the author and presented in this thesis as most of the data available are in the form of concentrations (e.g. glucose concentration in blood) or quantities (e.g. quantity of glucose in the subject). The substance in each compartment is assumed to be evenly distributed within the compartment, meaning that the concentration at any location in the compartment is assumed to be the same as at the sampling site (i.e. sample concentrations are representative of concentrations throughout the compartment). With this assumption in mind, the volume of distribution of a compartment is the volume in the compartment over which a substance is (evenly) distributed, i.e. the size of the compartment [9, 14].

2.3.3.1 Michaelis-Menten kinetics

Michaelis-Menten kinetics are an approximation for substrate-only enzyme kinetics, describing the reaction rate as substrate and enzyme interact. The Michaelis-Menten equation is given by equation 2.3, below:

$$v(t) = \frac{v_{max} S(t)}{K_M + S(t)} \qquad 2.3$$

where v is reaction rate, v_{max} is the maximum theoretical reaction rate, S is substrate concentration and K_M is the Michaelis-Menten constant, i.e. the substrate concentration at which v is at 50% of v_{max}.

A key feature of this equation is that it reaches a saturation level which asymptotically approaches v_{max}, as shown in Figure 2.3.

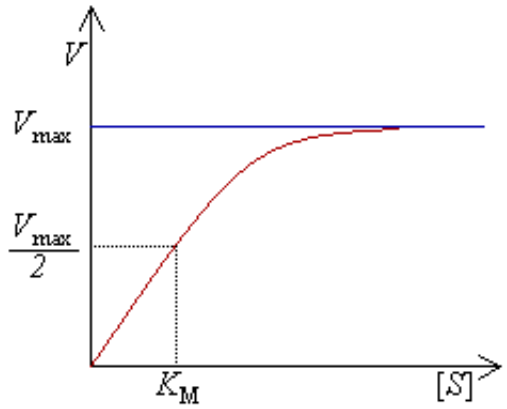

Figure 2.3: Michaelis-Menten equation plotted with concentration of substrate along x-axis and reaction rate along y-axis

The Michaelis-Menten equation is more widely applicable in situations where processes saturate, for example certain predator-prey relationships where the number of species saturate [27]. It is used in this thesis for clearance rates of glucose and C-peptide, as explained in Chapter 7.

2.4 Structural identifiability techniques

A mathematical model is said to be "structurally identifiable" if, given a perfect, noise-free, continuous set of observations, all the parameters in the system can be uniquely determined [15, 17, 19]. If a model is unidentifiable there will be an infinite number of possible combinations of values for unidentifiable parameters that will produce the same output, making these parameter values meaningless in a practical context.

In biological systems the data is far from noise-free, so a structurally identifiable model does not guarantee that these parameters will be meaningful. Identifiability ensures that the model has structurally meaningful parameters and, with the right conditions, uniquely identifiable parameters. This test should be seen as a precursor to having a sound mathematical model. If the model is not structurally identifiable, the unidentifiable parameters are meaningless.

Mathematically, structural identifiability can be defined as follows. Given the model, from equation 2.1, and a parameter value $p \in \Omega$ where Ω is an open set, $\Omega \subset \mathbb{R}^q$, of feasible values, find all parameter values $\hat{p} \in \Omega$ and the corresponding models of the form:

$$\begin{aligned} \dot{\hat{x}}(t,\hat{p}) &= f(\hat{x}(t,\hat{p}),\hat{p}) + u(t)g(\hat{x}(t,\hat{p}),\hat{p}) \\ y(t,\hat{p}) &= h(\hat{x}(t,\hat{p}),\hat{p}) \\ \hat{x}(0,\hat{p}) &= \widehat{x_0}(\hat{p}) \end{aligned} \qquad 2.4$$

such that:

$$y(t,p) = y(t,\hat{p}) \; \forall \; t \geq 0 \qquad 2.5$$

Individual parameters can be classed as unidentifiable, locally identifiable or globally identifiable. A parameter is globally identifiable if it has a unique value; it is locally identifiable if it can take its value from only a finite set of possible values. For an entire model to be globally identifiable, all parameters must be globally identifiable. For a model to be locally identifiable, all parameters must be either globally or locally identifiable with at least one parameter locally identifiable. If one or more parameters are unidentifiable then the entire model is unidentifiable.

There are several methods of determining the structural identifiability of a model. The Laplace transform approach, which involves considering the Laplace transform of the model equations, can only be applied to linear models and is explained in section 2.4.1 below. The Taylor series approach involves calculating the Taylor series coefficients of the model observations; this can be applied to both linear and non-linear models and is explained in further detail in section 2.4.2 below. The similarity transformation approach has two methods: one for linear models and one for non-linear models which is detailed further in section 2.4.3 below. The Lie-symmetry approach involves a similar mathematical approach to the similarity transformation approach, but has the advantage that it can be implemented easily . It is discussed further in section 2.4.4 below.

2.4.1 Laplace transform approach

The Laplace transform approach is simple, but appropriate only for linear systems [28]. It involves obtaining Laplace transforms of the model equations which are

then rearranged to find the system transfer function, i.e. the relationship between the input and output of the system. The coefficient of each term in the transfer function is theoretically measurable, meaning that if a single solution can be obtained for the parameters from these coefficients the parameters are measurable and unique [9, 14].

2.4.1.1 Method

- Ensure the model equations are in the standard control system state space form given in equation 2.1; as the system must be linear, f, g and h will be matrices multiplied by the states.

- Obtain Laplace transforms of the model equations, such that :

$$sX(s) = F(p)X(s) + G(p)(U(s)$$
$$Y(s) = H(p)X(s) \qquad 2.6$$

- Rearrange and combine the Laplace transforms to obtain a relationship between the input and output:

$$Y(s) = H(p)X(s) = H(p)\big(sI_n - F(p)\big)^{-1}G(p)U(s) \qquad 2.7$$

- Use equation 2.7 to identify the transfer function, $T(s)$:

where
$$Y(s) = T(s)U(s)$$
$$T(s) = H(p)\big(sI_n - F(p)\big)^{-1}G(p) \qquad 2.8$$

- Assume that coefficients of the powers of s in the transfer function, $T(s)$, are known. Any coefficients which consist only of a single parameter are identifiable however any coefficients which consist of a combination of two or more

parameters are unidentifiable on their own. The analysis then entails determining the solution set for the parameters from these coefficients.

2.4.2 Taylor series approach

The Taylor series approach is appropriate for both linear and non-linear systems. It involves successive differentiation of the output function with respect to time to obtain a Taylor series expansion of the model output, of the form in equation 2.9, about a known time point (generally t = 0).

$$y_i(t,p) = y_i(0,p) + y_i'(0,p) + \cdots + y_i^{(k)}(0,p)\frac{t^k}{k!} + \cdots \qquad 2.9$$

where $y_i^{(k)}(0,p) = \left.\frac{d^k y_i}{dt^k}\right|_{t=0}$ [22].

The coefficient of each term in the expansion is theoretically measurable, meaning that if a single solution can be obtained for the parameters from these coefficients the parameters are measurable and unique [19].

For linear systems with n parameters and no input (or a single impulse input) at most $2n$-1 successive differentiations are needed [9]. For general non-linear systems, such as the ones in this thesis, there is no strict upper bound for the number of successive differentiations. This means that this approach can only prove a system is identifiable, not that it is unidentifiable.

2.4.2.1 Method

- Ensure the model equations are in the standard control system state space form given in equation 2.1.

- Repeat the following steps until all parameters have been uniquely determined or solving to find parameters becomes intractable:

    - Successively differentiate $y(t,p)$ to obtain higher derivative than the previous iteration (i.e. $y'(t,p)$ in the first iteration, then $y''(t,p)$, etc.).

    - Evaluate this result at a known time point (e.g. t = 0) by substituting identifiable parameters already known from previous iterations.

    - Solve for p in $y^k(0,p) = y^k(0,\hat{p})$, where $p_1 = \widehat{p_1}$, $p_2 = \widehat{p_2}$, ..., $p_n = \widehat{p_n}$.

If the system of equations is solvable for a parameter, p_i, then the parameter is globally structurally identifiable. If p_i cannot be solved for then the parameter may or may not be unidentifiable; this means that the Taylor series approach cannot be used as a test for unidentifiability.

2.4.3 Similarity transformation approach

The similarity transformation approach essentially involves using a smooth, infinitely differentiated mapping to connect the state trajectories (the input/output behaviour) of two identical models. This is done by creating a smooth mapping, λ defined in equation 2.16, between the two models using terms obtained from the observable function y, see equation 2.4 This mapping is a link between the state trajectories of each model and, hence, the parameters in the models [17].

All of the models examined in this thesis using this method are uncontrolled, i.e. have no inputs or the inputs do not affect the output, therefore this technique is applicable in all of these cases [17].

In order for this method to be valid the model must satisfy the Observability Rank Criterion (ORC), described below.

2.4.3.1 Observability Rank Criterion

A system is said to be observable if all the possible initial states of the system can be observed, i.e. reconstructed from the observation. Systems that do not meet this criterion are said to be unobservable [19, 25].

The Observability Rank Criterion (ORC) is a test for observability. Consider a linear model of the form:

$$\begin{aligned} \dot{x} &= Ax + bu \\ y &= Cx \\ x(0) &= x_0 \end{aligned} \qquad 2.10$$

The observability matrix, Q_0, for this model is defined in equation 2.11. The model is observable if and only if the rank of Q_0 is n, i.e. the number of states.

$$Q_0 = \begin{bmatrix} C \\ CA \\ CA^2 \\ \vdots \\ CA^{n-1} \end{bmatrix} \qquad 2.11$$

For non-linear models, the ORC is defined slightly differently [17]. Consider a non-linear model of the form given in equation 2.1. The definition of Lie derivatives for the function *h* is (Lie derivatives are the change in *h* along the vector field of *f*):

$$L_{f_1} h(x,p) = \frac{\partial h(x,p)}{\partial x} \cdot f(x,p) \qquad 2.12$$

then successive Lie derivatives are found:

$$L_{f_n}h(x,p) = \frac{\partial L_{f_{n-1}}h(x,p)}{\partial x} \cdot f(x,p) \qquad 2.13$$

The observability matrix, Q_0, is then defined as:

$$Q_0 = \begin{bmatrix} h(x_0,p) \\ L_{f_1}h(x_0,p) \\ L_{f_2}h(x_0,p) \\ \vdots \\ L_{f_n}h(x_0,p) \end{bmatrix} \qquad 2.14$$

The model is again observable if and only if the rank of Q_0 is n [29].

2.4.3.2 Method

Consider the following theorem from [25]:

Assume that the model of equation 2.4 *is locally reduced at* $x_0(p)$ *for all* $p \in \Omega$. *Consider the parameter values* $p, \tilde{p} \in \Omega$p *an open neighbourhood* V *of* $x_0(\tilde{p})$ *in* M, *and any analytical mapping* $\lambda: V \to R^n$ *defined on* $V \subset R^n$ *such that*:

(i) $$Rank\,\frac{\delta\lambda(\tilde{x})}{\delta\tilde{x}}(t,p) = n \; for \; all \; \tilde{x} \in V \qquad 2.15$$

(ii) $$\lambda\big(x_0,(\tilde{p})\big) = x_0(p)$$

(iii) $$\mathrm{f}(\lambda\big(x_0,(p)\big) = \frac{\delta\lambda}{\delta\tilde{x}}(\tilde{x})\mathrm{f}(\tilde{x},\tilde{p})$$

$$\mathrm{g}(\lambda\big(x_0,(p)\big) = \frac{\delta\lambda}{\delta\tilde{x}}(\tilde{x})\mathrm{f}(\tilde{x},\tilde{p})$$

$$\mathrm{h}(\lambda\big(x_0,(p)\big) = h(\tilde{x},\tilde{p})$$

for all $\tilde{x} \in V$. *Then there exists* $t_1 > 0$ *such that* equation 2.4 *is globally identifiable at* p *in the experiments* $(x_0(p), U\,[0,t_1])$ *if and only if conditions (i), (ii), and (iii) imply* $\tilde{p} = p$.

- Ensure that the model equations are in the standard control system state form given in equation 2.1.
- Check the model fulfils the Observability Rank Criterion (ORC), detailed in the Observability Rank Criterion section above; if it does not, this technique will not be applicable.
- Select a candidate matrix, *H*, of smooth functions, μ.
- A good starting point will be Q_0 from the ORC, however it may be possible to select other μ to simplify computation, as long as the resulting matrix H has rank n.
- Determine the smooth mapping, λ, by considering:

$$H_p\big(\lambda(x)\big) = H_{\hat{p}}(x) \qquad 2.16$$

Where $H_{\hat{p}}(x)$ is the candidate matrix with $p_1 = \widehat{p_1}$, $p_2 = \widehat{p_2}$, ..., $p_n = \widehat{p_n}$.

- Solve for λ to find p in terms of $\hat{p}$:

$$f\big(\lambda\big(x(t,\hat{p})\big),p\big) = \frac{\partial\lambda}{\partial x} f(x(t,\hat{p}),\hat{p}) \qquad 2.17$$

If, from this system of equations, a parameter, p_i, can be directly equated to $\widehat{p_\iota}$ then the parameter is globally structurally identifiable.

2.4.4 Lie-symmetry approach

The Lie-symmetry approach uses a similar mathematical approach to the non-linear similarity transformation approach described above, as it uses Lie algebra. It has the advantage over other algorithms in that it is more procedural in nature and therefore can be implemented easily without full understanding of the deep

mathematical theory behind it, so for a full explanation of the mathematics see [15]. It is important to note however that this method proves only local structural identifiability - it cannot prove whether a model is globally structurally identifiable or unidentifiable. This method is employed in Chapter 8 and the analysis of the short-term model with this approach is included in Appendix 4.

2.4.4.1 Method

- Ensure the model equations are in the standard control system state space form given in equation 2.1.

- Check the model fulfils the Observability Rank Criterion, detailed in the Observability Rank Criterion section above; if it does not, this technique will not be applicable.

- Find the determining equations for the model; this can be done easily using the Lie symmetries package in Mathematica.

- Solve the determining equations to obtain equations for the symmetries of the differential equations, representing perturbations in time, the states and the parameters.

- If it can be seen, from these equations, that there are no non-trivial transformations that are time-invariant and preserve the initial conditions, then the model is at least locally identifiable.

2.5 Simulation

Solving Ordinary Differential Equations (ODEs) is essential for mathematical modelling as it allows model equations to be solved using parameter values to produce an output that can be compared to real output of the system being studied, i.e. it allows the system to be simulated. In the case of linear systems, there are exact analytical solutions to the ODEs, which make simulation relatively simple and generally computationally inexpensive. As most models presented in this thesis are non-linear, however it is not useful to cover solving linear ODEs here. Very few non-linear differential equations have known analytical solutions, and this is also true for all of the models presented in this thesis. This means that the only way to solve these models is by employing numerical methods.

There are many different methods for solving a model numerically. The main factors in selecting an appropriate algorithm are speed of computation, accuracy and ability to deal with stiff systems. A stiff system is a system where there is a large range of timescales; see the Stiffness section below. The algorithms used in this thesis are Runge-Kutta and Gear's Stiff.

An explicit fourth/fifth order Runge-Kutta method is implemented in MATLAB under `ode45`. This was used when the problem was non-stiff (i.e. for short-term modelling) and was useful as it had short computation time. When the problems were stiffer, a modified second/third order Runge-Kutta algorithm – `ode23tb` – was used as, although it was slower, it performed simulations in an acceptable time frame, usually less than a second [4].

The Gear's Stiff algorithm is implemented in acslX and is appropriate for stiff systems – as well as non-stiff systems [30, 31]. From experimental runs on the model presented in Chapter 8 it was seen to execute more quickly than MATLAB's ODE solvers.

The algorithms have an acceptable level of accuracy for this purpose with a tolerance of 0.1% [4] which is at least an order of magnitude lower than the experimental error in the data sets (see Chapter 4).

2.5.1 Stiffness

In general, the stiffness of a system is a measure of the range of time scales the whole system operates on. This usually means that some parts of the model may change over a period of seconds or minutes (fast variables) while others change over a period of hours or days (slow variables). The wider the range of these timescales, the stiffer the system. The stiffness of a system is important when making choices such as selection of an appropriate numerical ODE solver [30, 31].

A measure of the stiffness of a system is given by the stiffness factor. To find the stiffness factor of a non-linear system, it is necessary to linearise the system at a given time point (often t = 0, to see starting conditions of the model) by creating a Jacobian matrix:

$$A = \frac{\partial f(x,p)}{\partial x} = \begin{bmatrix} \frac{\partial f_1}{\partial x_1} & \cdots & \frac{\partial f_1}{\partial x_n} \\ \vdots & \ddots & \vdots \\ \frac{\partial f_n}{\partial x_1} & \cdots & \frac{\partial f_n}{\partial x_n} \end{bmatrix} \qquad 2.18$$

The eigenvalues, λ, of this matrix can then be found by solving:

$$\det(A - \lambda I) = 0. \qquad 2.19$$

The stiffness factor is then defined as:

$$\mathrm{SF} = \frac{\max_{\mathrm{i}} |\mathrm{Re}(\lambda_{\mathrm{i}})|}{\min_{\mathrm{i}} |\mathrm{Re}(\lambda_{\mathrm{i}})|} \qquad 2.20$$

Stiffness factors are normally provided as orders of magnitude, e.g. $O(10^6)$. Models where the stiffness is greater than $O(10^2)$ are normally considered "stiff" [9, 32].

2.6 Parameter estimation methods

In order to obtain estimates for model parameters from real data it is necessary to "fit" the model to the data. This is performed using a technique called parameter estimation [10, 11, 18, 20-22]. The stages in this process are:

1. An initial estimate for each of the unknown parameters is taken; these may be taken from known physiological values, graph peeling or from knowledge of the expected order of magnitude for the parameter. The importance of how close the initial guess is to the real value is dependent on the model and the real parameter (i.e. the actual physiological parameter).

2. The model is simulated with the chosen parameter estimates.

3. The residuals are calculated. These are a measure of the error between the simulated model output and the real data which are explained in the Least squares residual method section, the method of determining residuals used in this thesis, below.

4. Then an optimisation algorithm is used to calculate the next attempted value.

5. Steps 2-4 are repeated until the optimisation algorithm considers the residuals to have reached a minimum (or maximum depending on the method used).

2.6.1 Least squares residual method

Residuals are the error between the real data and model output, as shown graphically in Figure 2.4.

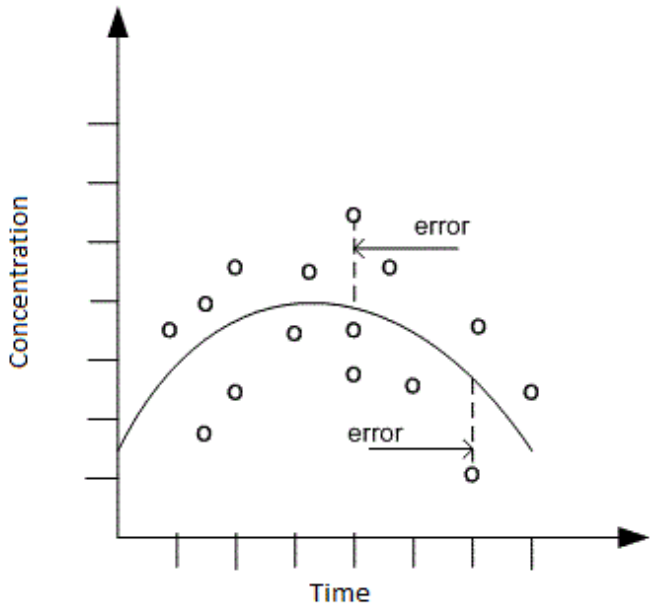

Figure 2.4: Non-linear residuals [33]

The least squares residual method involves taking the difference between the real and simulated data at each time point, squaring the difference to remove any negative values then summing the values across all time points and dividing by the number of time points to normalise the value. This assumes the data are normally distributed with the model predicting the mean. This is known as Ordinary Least Squares (OLS) and is given by:

$$E = \sum_{i=0}^{n} (d_i - \overline{d}_i)^2 \qquad 2.21$$

where E is the residual, $\boldsymbol{d} = (d_1 \ldots d_n)$ are the real data points and $\overline{\boldsymbol{d}} = (\overline{d}_1, \ldots \overline{d}_n)$ are the simulated data points.

If all the data are of a similar order of magnitude, OLS will generally provide acceptable results. However with data of different magnitudes (e.g. glucose and insulin) it is undesirable for any data set to have an unfair bias on the parameter fit due to the larger magnitude of its values as variance is likely to change with the magnitude of the data. Therefore a Weighted Least Squares (WLS) method may be used instead. There are two options for weighting each time point: based on the real data value or the simulated data value; in either case, the change is then relative rather than absolute. To weight a given time point, the chosen value can be squared to provide a greater penalty for moving further away from it. For most of the modelling in this thesis, it is assumed that the model output is correct and the real data are noisy and have other influencing factors. Therefore a Generalised Least Squares (GLS) method, with the weighting based on the simulated data values as shown in equation 2.22, is used [11].

$$E = \sum_{i=0}^{n} \frac{(x - y_i)^2}{{y_i}^2} \qquad 2.22$$

where x are the real data, y_i are the simulated model data at time point i. ${y_i}^2$is therefore acting as the weighting. The aim is to get to the global minimum which is also the structurally identifiable set of unique parameters. However, due to the noisy environment, this is not guaranteed.

2.6.2 Optimisation algorithms

An optimisation algorithm, in this context, is a method of updating parameter estimates to try to minimise (or maximise) residuals. There are many different optimisation algorithms, however the main ones used in this thesis are the Nelder-Mead [34] and Quasi-Newton [35] algorithms. The Nelder-Mead algorithm is implemented in MATLAB as the routine `fminsearch` and the Quasi-Newton algorithm is the default algorithm for the routine `fminunc`. The choice of which to use depends on several factors, for example the Nelder-Mead algorithm is generally more stable than the Quasi-Newton algorithm, however it has the drawback that it often settles in local minima/maxima rather than global minima/maxima. When using the Nelder-Mead algorithm, it is therefore important to have initial estimates which are as close as possible to the global minimum/maximum [36].

2.6.3 Statistical analysis

As a measure of how meaningful a parameter value is, it is useful to have statistical confidence values for the parameter estimates. These can be obtained from the covariance matrix of the fitted parameters, which can be estimated from the optimisation algorithm in MATLAB. To do this it is necessary to obtain the Hessian matrix, an estimate of which is optionally produced by `fminunc` in MATLAB using the BFGS (Broyden-Fletcher-Goldfarb-Shanno) algorithm [30]. The covariance matrix can then be calculated as:

$$C(\hat{p}) = \frac{2}{N - n_p} E(\hat{p}) H(\hat{p})^{-1} \qquad 2.23$$

where $\hat{p}$ is the set of parameter estimates, N is the number of time points, n is the number of parameters fitted, E is the output from the residual function and H is the Hessian matrix.

Individual parameter confidence values can then be obtained as:

$$\delta_i = \pm t_{N-n_p}^{1-\left(\frac{\alpha}{2}\right)} \sqrt{C_{ii}} \qquad 2.24$$

for $i = 1, \ldots, n_p$ where $t_{N-n_p}^{1-\left(\frac{\alpha}{2}\right)}$ is a two-tailed Student's t distribution for confidence level α and N-n_p degrees of freedom [21].

The package acslX, which was used for parameter fitting in part of this thesis, uses a similar method for calculating confidence values automatically [31].

2.7 Sensitivity analysis

This is the process of finding out what the most "important" parameters in a model are. In this case, “important” refers to the parameters which have the greatest effect on the model output, i.e. those to which the model is most sensitive. This is not only model-dependent, but also dependent on the parameters, initial conditions and system input. When performing a sensitivity analysis nominal/mean parameter values are used. In the context of a biological system, an experiment is performed and the system is examined over the duration of the experiment [23, 37].

Sensitivity analysis is also useful for determining which parameters are sensitive to change and at which time points. Time points where a large number of parameters

are particularly sensitive are good choices for increased sampling to ensure a good parameter estimate [23, 38].

There are several ways of looking at sensitivity. The simplest method is to vary each parameter (either independently or as part of a group) to see the effect on the resulting model output.

A more complex method used in this thesis involves examining the sensitivity matrix, $S(t, p)$ given in equation 2.25. This is a set of Jacobian matrices of the model with respect to the model parameters and time points, i.e. one matrix per model state. These matrices contain actual parameter values which can be examined, or plotted graphically against time, to show which have the greatest effect at each time point.

$$S(t,p) = \begin{pmatrix} \frac{\partial x(t_1,p)}{\partial p_1} & \cdots & \frac{\partial x(t_1,p)}{\partial p_n} \\ \vdots & \ddots & \vdots \\ \frac{\partial x(t_m,p)}{\partial p_1} & \cdots & \frac{\partial x(t_m,p)}{\partial p_n} \end{pmatrix} \qquad 2.25$$

where $t = (t_1, \ldots, t_m)$ is a vector of time points, $p = (p_1, \ldots, p_n)$ is a vector of all parameters, and x is a scalar output of the state.

If it is not possible to compute $S(t,p)$ analytically, equation 2.26 may be solved to compute sensitivity values numerically [23, 37] using:

$$\begin{aligned} \frac{dS(t,p)}{dt} &= \frac{\partial}{\partial x} f(x(t,p),p)S(p) + \frac{\partial}{\partial p} f(x(t,p),p) \\ S_0(p) &= \frac{\partial x_0(p)}{\partial p} \end{aligned} \qquad 2.26$$

This matrix shows absolute sensitivities, therefore it is useful to normalise the sensitivity matrix to form a matrix of relative sensitivities, S_r. This is done by multiplying by the parameter vector, p, and dividing by the state, x_k, to give:

$$S_r(t,p) = S(t,p)\begin{pmatrix} p_1/x_k(t,p) \\ \vdots \\ p_n/x_k(t,p) \end{pmatrix} \qquad 2.27$$

In order to compute this matrix it is necessary to differentiate the model equations. This can be a laborious process so it is useful to have a way of producing these matrices automatically. This can be achieved through automatic differentiation which is explained fully in Chapter 8. Essentially, instead of creating a sensitivity matrix which contains parameters and a specific set of time points, as in equation 2.25, it is possible to create a time-dependent matrix which contains states and parameters. This matrix, shown in equation 2.28, is a set of ODEs which can be solved alongside the model equations, $x(t, p)$, making it easy to calculate sensitivities if a new experiment is presented to the model.

$$S(t,p) = \begin{pmatrix} \dfrac{\partial x_1(t,p)}{\partial p_1} & \cdots & \dfrac{\partial x_1(t,p)}{\partial p_n} \\ \vdots & \ddots & \vdots \\ \dfrac{\partial x_n(t,p)}{\partial p_1} & \cdots & \dfrac{\partial x_n(t,p)}{\partial p_n} \end{pmatrix} \qquad 2.28$$

where t is now the current time point (during the model simulation) and is therefore a scalar, rather than a vector.

2.8 Summary

The process and methods that have been described in this chapter are used throughout this thesis to help model the dynamics of the glucose-insulin system.

There are many other techniques and methodologies which may be useful; those presented here were selected based on the author's engineering background and knowledge and understanding of the techniques.

Chapter 3: Biological Overview

This chapter discusses the components of the glucose and insulin homeostatic system. The aim of this chapter is to provide an introduction to the system as a whole in the context of being able to mathematically model the process. There are many factors affecting this biological system; these factors and their importance are discussed.

3.1 Introduction

The glucose and insulin homeostatic system is complex, involving many organs including the liver, pancreas and kidneys. Glucose has critical importance to the body, as it is used by every cell and is the primary source of energy for the central nervous system (CNS). If the glucose level goes too low (hypoglycaemia) it can lead to coma and death, however glucose is also toxic and if it rises too high (hyperglycaemia) this can lead to long-term damage. Insulin regulates glucose uptake in many different tissues, including the liver, adipose (fat) tissue, and skeletal muscle [39-47].

3.2 Glucose

Glucose is a monosaccharide, i.e. it consists of one sugar group (Figure 3.1), and is one of the most important molecules in biology [48].

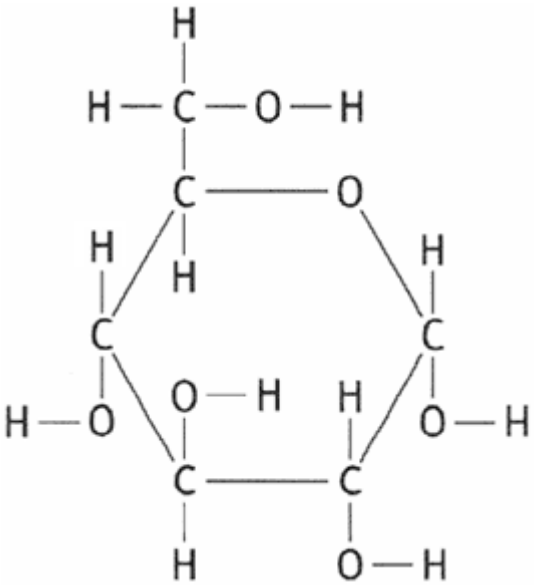

Figure 3.1: Glucose molecule [49]

Glucose is important for several reasons:

- it can be used to produce energy very quickly for cells to use [48, 50];
- it can be mobilised very quickly from glycogen, a polymer of the monosaccharide, in the liver [43, 48, 50];
- it is created and used by most organisms, therefore is abundant in plants and animals and consequently it can be obtained as a food source very easily [48, 50];
- it can be used as an energy source in the absence of oxygen; (anaerobically), as well as in the presence of oxygen (aerobically) [48];
- it can be built up into other molecules for storage (energy) and structures (e.g. starch) [48].

3.2.1 Respiration

Glucose is utilised by the same mechanism in most cells - respiration - therefore it is important to understand the basics of this mechanism.

Energy required in cells is derived from exothermic hydrolysis of adenosine triphosphate (ATP) to adenosine diphosphate (ADP) and inorganic phosphate (P_i).This means that ATP is the unit of energy in a cell; the more ATP there is (or more specifically the higher the ATP/ADP ratio) the more energy is in the cell. When ATP is hydrolysed to ADP, heat energy is produced. The reverse process - where ADP is converted to ATP to produce stored energy - is known as mitochondrial respiration, or in some fields metabolism [48].

The basic inputs for respiration are oxygen (O_2) and glucose and the outputs are kinetic energy and carbon dioxide (CO_2). Transporters drive active uptake of glucose into the cell (discussed in Glucose transporters below). Glucose is converted to pyruvate via the glycolytic pathway before entering the mitochondria and producing two molecules of ATP; mitochondria are organelles (cellular subunits) which produce ATP in the process. Pyruvate is converted to acetyle coenzyme A which then enters the citric acid cycle (CAC), also known as the tricarboxylic acid cycle (TCA cycle) or the Krebs cycle where a further 34 molecules of ATP are generated per molecule of glucose [43, 48, 51]. This process is shown in Figure 3.2 below.

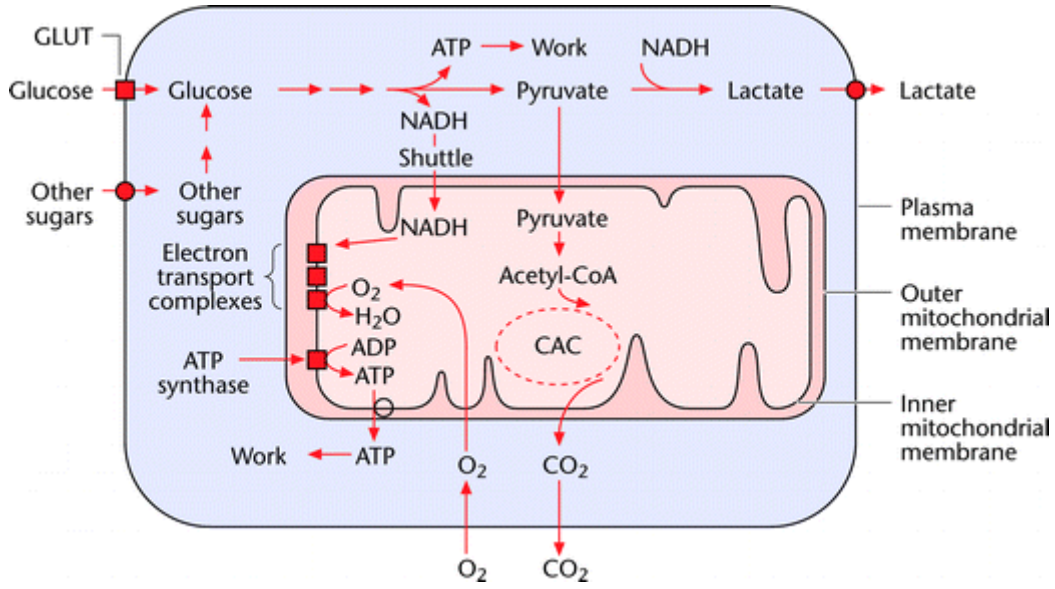

Figure 3.2: Diagram of respiration [52]

3.2.2 Uses in humans

In humans, a critical and main use for glucose is in the CNS as it requires a rapid source of energy due to its fluctuating demands. Nerve cells require a large

amount of energy to function, so are specially adapted to utilise glucose at a greater rate, e.g. increased mitochondrial density[45]. The CNS uses around 45-60% of glucose in the body, in an overnight fasted state [46].

Skeletal muscles are another big user of glucose in the human body. Depending on exercise the muscles use approximately 15-20% of the glucose being used at that time, in an overnight fasted state[46]. When not contracting, skeletal muscles mainly use energy from lipids in the blood. These contain higher amounts of energy than glucose but take longer to process as they require more oxygen to generate ATP. Fat utilisation hits its peak contribution to muscle ATP generation when energy requirement is at 40% of the maximum possible, i.e. moderate exercise. When exercise increases, more glucose is used to support muscle function[53].

Other major users of glucose in the body include the kidneys at 10-15%, blood cells at 5-10% and other tissue (including fat) 5-10%, in an overnight fasted state[46].

3.3 β-cells

The pancreas contains a group of cells that produce hormones (endocrine cells), which are located in the islets of Langerhans. These were found in 1869 by Paul Langerhans [54]. They make up about 1-2% of the pancreas and weigh about 1g to 1.5g in a normal human. The islets contain several different types of cells, including α- and β-cells [46].

3.3.1 Glucagon

α-cells make about 30% of the islets of Langerhans [55] and produce glucagon. The function of glucagon is to raise blood glucose levels [42]. Its main place of action is the liver, where it stimulates glycogenolysis which is the process of turning glycogen into glucose [53].

3.3.2 Insulin

3.3.2.1 Creation of insulin

β-cells make up about 60% of the islets of Langerhans and produce insulin, which lowers blood glucose levels [42, 55]. Insulin is actually produced as proinsulin, which consists of C-peptide attached to insulin. Proinsulin is inactive and does not lower blood glucose.

3.3.2.2 C-peptide

When proinsulin is activated, C-peptide is cleaved from it using carboxypeptidase and a series of prohormone convertases [54, 56]. This causes C-peptide and insulin to be released into the hepatic portal vein in equal molar quantities.

An important feature of C-peptide is that it is cleared by the kidneys and not by the liver, like insulin. All secreted C-peptide can therefore be assumed to reach systemic circulation [57-61].

3.3.2.3 Secretion of insulin

Glucose enters β-cells via transporters passively (see Glucose transporters below) and therefore the level of glucose in β-cells is proportional to the blood glucose level [42].

In a β-cell these reactions occur as shown in Figure 3.3 and are explained as follows [54, 62]:

- Glucose enters the β-cell via GLUT2 (see Glucose transporters below).
- Respiration occurs, converting glucose to ATP.
- ATP closes K_{ATP} gates which allows potassium (K) out of the β-cell. This creates a negative charge in the β-cell and depolarises the membrane.
- Depolarisation of the membrane causes the sodium channel to open, allowing calcium ions into the β-cell.
- Calcium entering the β-cell releases calcium stored in the endoplasmic reticulum (small tubes inside cells).
- Calcium releases the insulin stored in the β-cell.

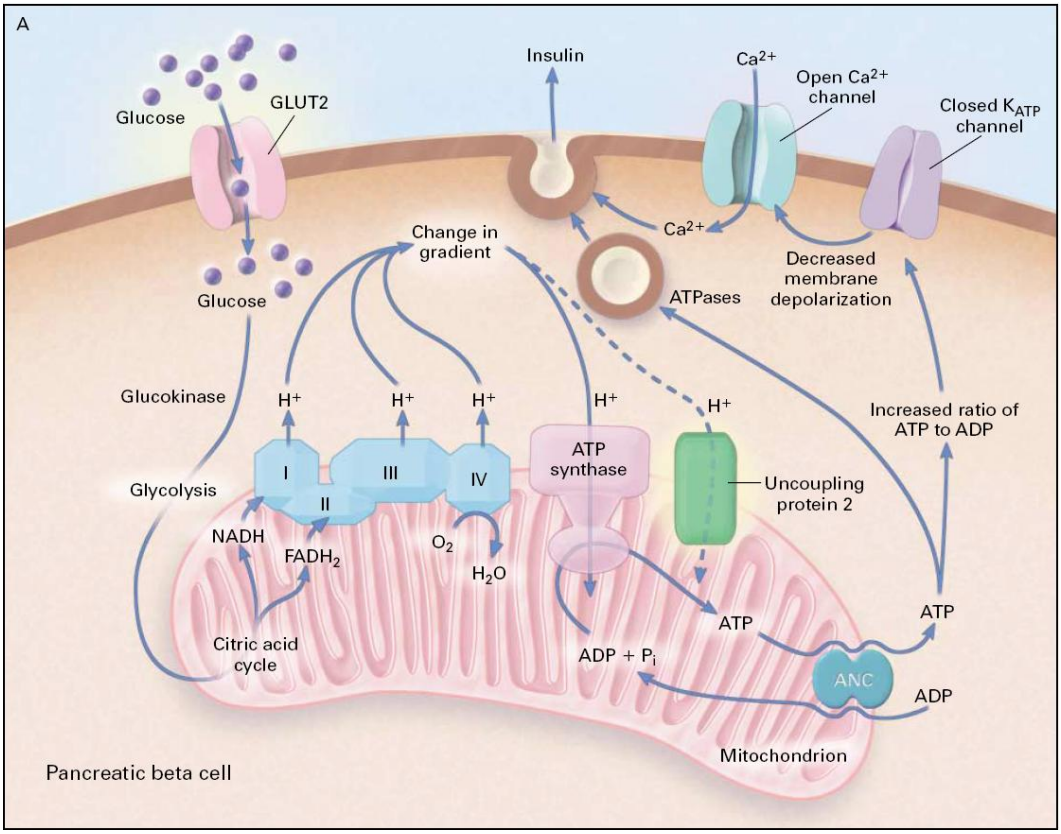

Figure 3.3: Diagram showing how glucose potentiates insulin release [62].

Incretins

Although insulin release is mainly stimulated by glucose, other mechanisms for stimulating insulin release exist. Incretins stimulate insulin release by activating a receptor on the β-cell which opens the calcium gates of the β-cell. This allows calcium into the β-cell, which triggers the release of insulin [63].

One example of an incretin is GLP-1 [63], which is released from the gut and activates the GLP-1 receptor on the β-cell [41].

3.3.2.4 Storage of insulin

There are a lot of uncertainties in our knowledge around the storage of insulin, in particular concerning the quantity of insulin stored [42, 62, 64].

Insulin is stored and transported within β-cells in granules. These granules are stored in various places in the β-cell, though where exactly and how they move is uncertain. Energy (ATP) is required to move the granules from where proinsulin is created to the membrane and then to dock them to the membrane. When the insulin is required, energy is also needed to cleave the insulin and C-peptide from the pro-insulin molecule and to release the insulin into the blood.

The Rorsman & Renström review [42] states that there could be four states of insulin:

- undocked (stored in the cytoplasm): ~73%;
- almost docked: ~20%;
- docked: ~6%;
- "Rapid Release Pool" (RRP): ~<1%.

This means that glucose stimulation can cause different levels of response. The RRP consists of a small number of granules attached to the β-cell membrane which can be released very quickly. Rorsman & Renström [42] believe that the fast release of insulin from the RRP could be what causes a high peak of insulin secretion immediately following a glucose stimulus, known as the first-phase

response. The second-phase response is thought to be created by mobilisation of the undocked and almost docked granules [42, 65, 66].

3.4 Disposal of glucose

3.4.1 Glucose transporters

There are 4 main passive transporters of glucose, commonly known as GLUTs [54, 67, 68].

GLUT 1 is responsible for low levels of glucose uptake to maintain respiration in all cells. Expression of this transporter is reduced when there are increased levels of glucose. It exhibits Michaelis-Menten type kinetics [48, 54].

GLUT2 is expressed in the pancreas, liver, hypothalamus, small intestine and kidneys. It is a high capacity transporter of glucose and is often referred to as the glucose-sensing transporter. In the pancreas, it transports glucose into β-cells without requiring insulin to be present, which allows the β-cells to sense the level of glucose and respond with a corresponding quantity of insulin. In the liver, it allows the flow of glucose in and out of the hepatic cells [48] .

GLUT3 is expressed mainly in neurons and, like GLUT1 and GLUT2, operates independently of insulin [48, 54].

GLUT4 is an insulin-dependent transporter and is expressed in adipose tissue and skeletal muscle tissue. It is the main controlling mechanism for glucose outside the liver. It is very important in modelling the glucose and insulin system because of its large role in glucose uptake and insulin-dependence [69, 70].

3.4.2 Insulin sensitivity and resistance

Insulin sensitivity is the effect of insulin on the disposal of glucose; higher insulin sensitivity means that more glucose will be disposed of with the same amount of insulin. The main transporter involved in this is GLUT4. Insulin resistance applies to the same process, but higher insulin resistance means that less glucose will be disposed of with the same amount of insulin. Therefore being less insulin-sensitive and more insulin-resistant are equivalent; conversely, more insulin-sensitive is equivalent to less insulin-resistant.[41]

3.4.3 Liver

Glucose enters the hepatic cells via GLUT2. Here it is converted into glycogen by glycogenesis, which is the largest glucose uptake mechanism dependent on insulin. Glycogen can be quickly converted back to glucose when required [43].

The portal vein comes from the gut and the pancreas into the liver; this means that glucose is absorbed from the gut and then is transported to the liver. As most sampling of blood glucose occurs after the liver, there is a "first pass" effect on the glucose as some of it is removed by hepatic extraction (approximately 13% is retained by the liver in rats) as described above [71]. A similar action occurs with insulin clearance in the liver [57].

3.4.4 Skeletal muscle

GLUT4 is the main transporter of glucose into skeletal muscle tissue. It is activated by insulin receptors. This means that an increase in insulin will increase the amount of glucose entering the cells, causing an increase in glucose

utilisation [48, 69]. Glucose is utilised through respiration in skeletal muscle cells as well as being stored as glycogen. As there is a large amount of skeletal muscle, this is a major mechanism of glucose disposal.

3.4.5 Adipose

GLUT4 also transports glucose into adipose tissue. Here it is converted into fatty acids which can be stored in the adipose tissue as triglycerides. The storage of fatty acids will, in general, mean that the adipose tissues become larger. The important thing to note here is that, unlike glycogen, fatty acids cannot later be converted back into glucose [48]. Increased triglyceride concentration will decrease the insulin sensitivity of the adipose tissue, which means less glucose and fatty acids can be taken in by the adipose, thus increasing circulating fatty acids [69].

3.4.6 Blood flow

The amount of blood flowing though the gut, that is through the hepatic arteries and hepatic portal vein, can vary [72, 73] from 14.60 14.60 ± 0.96 ml/min to 27.35 ± 1.82 ml/min between fasted and fed rats [74]. It is hypothesised that gut blood flow plays an important role in disposal and absorption of glucose and clearance of insulin (see Chapter 7 for further details).

3.5 Lipids

Lipids are a store of energy and therefore have the same capability as glucose in increasing the ATP/ADP ratio. However they have a different rate of utilisation and insulin secretion profile to that of glucose [75].

3.5.1 Lipid effects on insulin sensitivity

In the short term, high levels of lipids have the effect of lowering insulin sensitivity, which can be seen as an inhibitory effect of lipids on glucose uptake via GLUT4 [41, 69].

3.5.2 Lipid effects on insulin secretion

In the long term, high levels of lipids have a toxic effect on β-cells. This causes a cycle, as insulin lowers lipid levels and as β-cells become damaged they cannot produce enough insulin to lower the lipid levels. This means that the lipid levels remain high and cause further damage, and so on [69, 70].

3.5.3 Insulin effect on lipids

It is known that increased insulin levels increase uptake of fatty acids into tissue. For more detail, see [69].

3.6 Diabetes

Diabetes mellitus – commonly referred to simply as diabetes – is a huge problem worldwide and it is growing. The World Health Organisation states the following:

"Diabetes is a major threat to global public health that is rapidly getting worse, and the biggest impact is on adults of working age in developing countries. At least 171 million people worldwide have diabetes. This figure is likely to more than double by 2030 to reach 366 million." [7].

This means that it is one of the fastest growing diseases in the world. They also note that diabetes is a life-threatening condition and that "worldwide, 3.2 million deaths are attributable to diabetes every year" [76].

The UN also recognise the impact of diabetes and have a resolution on the disease; this includes designating World Diabetes Day (14th November) as a UN Day and inviting member states and organisations to observe it each year as well as "[encouraging] Member States to develop national policies for the prevention, treatment and care of diabetes" [77].

Diabetes is a disease which occurs when a person is unable to control their blood glucose level. The WHO defines diabetes – as opposed to the related problems of impaired glucose tolerance and impaired fasting glucose – as shown in Table 3.1.

The following Table summarises the 2006 WHO recommendations for the diagnostic criteria for diabetes and intermediate hyperglycaemia.

Diabetes	
Fasting plasma glucose	≥7.0mmol/l (126mg/dl)
2–h plasma glucose*	**or** ≥11.1mmol/l (200mg/dl)
Impaired Glucose Tolerance (IGT)	
Fasting plasma glucose	<7.0mmol/l (126mg/dl)
2–h plasma glucose*	**and** ≥7.8 and <11.1mmol/l (140mg/dl and 200mg/dl)
Impaired Fasting Glucose (IFG)	
Fasting plasma glucose	6.1 to 6.9mmol/l (110mg/dl to 125mg/dl)
2–h plasma glucose*	**and (if measured)** <7.8mmol/l (140mg/dl)

* Venous plasma glucose 2–h after ingestion of 75g oral glucose load

* If 2–h plasma glucose is not measured, status is uncertain as diabetes or IGT cannot be excluded

Table 3.1: WHO recommendations for diagnostic criteria for diabetes [7].

There are 3 main types of diabetes which are distinguished based on cause, not severity [7, 54].

3.6.1 Type 1

Type 1 diabetes is thought to be caused by an autoimmune disease which leads to destruction of insulin-producing β-cells in the islets of Langerhans [54]. This means that the individual cannot produce insulin to regulate their blood glucose

levels. It is also known as “Juvenile Diabetes” as the disease usually occurs in childhood, and most children with diabetes are Type 1 diabetics.

3.6.1.1 Treatment

Type 1 diabetes is most often treated through regular subcutaneous insulin injections, though insulin pumps may also be used, leading to the alternative name of IDDM (Insulin-Dependent Diabetes Mellitus), and must be continued throughout the person’s life as there is currently no widely-used cure. Pancreas or islet cell transplants may be used but there are many limitations, including a lack of donors, very serious potential complications (as with any transplant) and the need for immunosuppressants post-transplant both to avoid rejection of the organ and to prevent a relapse of Type 1 diabetes. For these reasons, transplants are rarely used and tend to be reserved for extremely severe cases [78].

A CGM (Continuous Glucose Monitor) is a device implanted subcutaneously which automatically measures blood glucose levels at regular intervals (e.g. every 1 or 5 minutes). With this development, trials have commenced to try and link a CGM to an insulin pump and other trials including both an insulin pump and a glucagon pump to produce an artificial pancreas [79]. The research has fallen into two groups: reactive controllers and model-based predictive controllers. The leading reactive controller is a PID (proportional-integral-derivative) controller, discussed in Chapter 8. The model-based predictive controllers use mathematical models to predict future glucose levels, based on current and previous measurements, and hence the insulin required at a given future time-point, to

control insulin release. There are several groups working on this second type of controller using a range of different methods; many of them are funded by the JDRF (Juvenile Diabetes Research Foundation) [80, 81].

3.6.2 Type 2

Type 2 diabetes is characterised by impaired β-cell function (though not due to an autoimmune disease as in Type 1 diabetes) and reduced insulin sensitivity. This means that Type 2 diabetics may produce some insulin, but it will be insufficient to regulate blood glucose levels effectively. It is important to note that reduced insulin sensitivity alone is not sufficient to cause Type 2 diabetes as, in the majority of cases, the pancreas is capable of adapting to changes in insulin sensitivity, unless its function is also impaired. It is unclear, however, whether the reduction in insulin sensitivity precedes, follows or is concurrent with impaired β-cell function or what the causes of either are. Insulin sensitivity is linked to free fatty acid levels (see section 3.5 Lipids), however there may be other causes. β-cell function is a combination of the number of β-cells (β-cell mass) and the secretory capacity of a β-cell; as it is difficult (or not currently possible) to determine in a Type 2 diabetic whether the mass or the capacity has been reduced, in this thesis the general term “β-cell function” will be used to refer to the overall combination of these factors. Reduction in β-cell function is often attributed to glycolipid toxicity, i.e. the damaging action of glucose and/or lipids on β-cells. This is a major problem in Type 2 diabetics as insulin cannot control the level of glucose and lipids, which results in further reductions in insulin secretion.

3.6.2.1 Treatment

Treatment ranges from diet and exercise regimes to drug and insulin therapy like that for a Type 1 diabetic; however insulin therapy is used in only a small minority of cases, leading to the alternative name NIDDM (Non-Insulin-Dependent Diabetes Mellitus). Type 2 diabetes is generally found in older patients (i.e. those over 40 years old) and, as such, is sometimes also known as adult-onset diabetes. Recently, there has been a rise in diagnoses of Type 2 diabetes in children which can be directly related to increasing childhood obesity, as obesity is a major risk factor for diabetes. Other risk factors include lack of exercise and excessive alcohol consumption; as a result Type 2 diabetes is often considered to be "preventable" by adopting a healthy lifestyle [41, 54, 78].

3.6.3 Gestational diabetes

The final recognisable type of diabetes occurs in pregnant women who have not been previously diagnosed with diabetes, but who have elevated blood glucose levels during their pregnancy. The cause is currently unknown, but it generally disappears after the baby's birth and is usually managed through changes to diet and exercise [54].

3.6.4 Implications of diabetes

Glucose being a potentially toxic substance has meant that animals have evolved very fine levels of glucose control. This level of control is important firstly due to glucose providing the main source of energy to the CNS and secondly to ensure non-toxic levels of glucose are maintained [54, 70, 82].

3.6.4.1 Short term

In the short term, the danger mainly lies with hypoglycaemia (low blood sugar levels), which could be classed as below 3 mmol l^{-1}. Glucose is essential for the CNS and reductions in the level of glucose can cause drowsiness and confusion. A large reduction in the amount of glucose can lead to diabetic coma, which can cause prolonged seizures, brain damage and death [54].

If a person has other conditions, this can lead to further complications if blood sugar becomes low. It can cause heart attacks, strokes and exacerbate cardiac problems. If the person is diabetic and has eye problems, it can lead to retinal haemorrhaging and subsequent blindness [54].

3.6.4.2 Long term

In the long term, the main problems occur from vascular disease caused by chronically high levels of blood glucose, hyperglycaemia. It is thought due to the loss of endothelial cell function this can lead to the thickening and weakening of the smooth muscle cells of the vascular wall. However the exact mechanisms by which this damage occurs are unknown [45, 54]. For this reason, although modelling of diabetes could eventually help to allow tighter control of glucose levels, the effect this would have on complications is unknown.

Microvascular damage

Microvascular damage – where small blood vessels are damaged – can lead to heart disease, poor eyesight or blindness, kidney damage and loss of sensation in the affected areas.

Diabetic cardiomyopathy is a form of heart disease where the heart muscle itself begins to fail, potentially leading to arrhythmia or death [41, 54, 70].

Diabetic retinopathy (retina damage) occurs when the retinal blood vessels become damaged due to sustained hyperglycaemia. Over time this leads to lack of blood in the retina, causing new blood vessels to grow in the vitreous humour (the clear fluid that fills the eye). These, in turn, burst and bleed into the eye, causing further damage to the retina [54, 70].

Diabetic nephropathy (kidney damage) occurs when the capillaries in the kidneys where blood filtration occurs harden and lose functionality due to high blood glucose levels. Additionally, tubular cells in the kidneys are damaged, leading to poor reabsorption of amino acids, glucose and albumin which creates water balance problems, Diabetes Insipidus. Importantly, this means less glucose is reabsorbed into the body, however diabetics at this stage have very poor glycaemic control. The risk of diabetic nephropathy is increased with high blood pressure and high cholesterol. Over a long period of time (15 years or more) diabetics can end up with kidney failure and may require dialysis or kidney transplant [54, 70].

Diabetic neuropathy (nerve damage resulting in loss of sensation) may occur in the short term and be reversible; however long-term hyperglycaemia leads to irreversible neuropathy. The elevated glucose levels result in long nerves dying back, causing sensation to be lost in the extremities; feet are at particularly high risk. The neuropathy can also cause paralysis and pain [54].

Macrovascular damage

Macrovascular damage is caused when proteins in arterial walls are degraded, causing the walls to become thicker. This leads to circulation difficulties and cardiovascular disease – including angina, heart attacks and stroke – which is the most common cause of death in diabetics. Direct risk factors are not strongly established, however there are known mechanisms by which both hyperglycaemia and hyperinsulinaemia could cause macrovascular disease [54].

Other effects

Diabetic foot is a combination of microvascular and macrovascular damage, including poor circulation and neuropathy. This causes loss of sensation, poor motor control, ulceration and callusing. These problems can lead to infection, which may result in the need for amputation [54, 70].

Another important long-term effect of hyperglycaemia is hypertension (raised blood pressure). It is “up to twice as common in diabetes as in the general population, and affects some 10-30% of Type 1 and 30-50% of Type 2 diabetic patients” [54]. In Type 2 diabetics, it is linked to insulin resistance and

hyperinsulinaemia; this is thought to be because insulin stimulates the growth of vascular smooth muscle [83].

3.7 Discussion

The biological system for glucose homeostasis is complex with many factors involved. It is important to focus on the critical factors that affect the system to enable identification of key components for modelling. The glucose homeostatic system is very finely controlled due to the necessity for glucose in the body and damage that can be caused if glucose is not maintained at the correct level.

Chapter 4: Data Collection

4.1 Introduction

This chapter introduces the tests that were performed at AstraZeneca, Alderley Park, Cheshire, UK and elsewhere to collect data on glucose and insulin homeostasis. It explains the methods behind the data measurement and collection and discusses the limitations of and difficulties with collecting such data.

4.2 Animal experiments

All animal experiments in the UK are carried out only when no alternative can be found and only when it is essential for scientific understanding, medical progress and protecting people, animals and/or the environment [84, 85]. Whenever possible, AstraZeneca and other facilities that use animals try to replace, reduce and refine animal work. This is known as the "three Rs" of animal work. Replacement means finding alternatives where possible; reduction means minimising the number of experiments carried out and refinement means designing experiments to minimise stress and the number of procedures, to improve animal welfare and maximise informative data. Modelling can play an important role in all of these by attempting to predict outcomes from experiments – thus reducing the need for animal work – and designing better experiments.

AstraZeneca complies with Home Office regulations as well as its own internal ethical review procedures [86-88]. The Animals (Scientific Procedures) Act 1986 is based on a number of historical acts focusing on animal protection and procedures involving animals, including the Cruelty to Animals Act 1876 and Protection of Animals Act 1911. It falls under the jurisdiction of Home Office Inspectors. It stipulates that animal studies can only be performed by trained personnel who hold a Personal Licence, i.e. are endorsed as competent by the Home Secretary on the recommendation of a Project Licence Holder. Personal Licence holders must work under the guidance of a Project Licence Holder within

a specific “project”, which must have a Project Licence. This Project Licence includes a 5-year work plan with aims, scientific plans, details of models and techniques used and an outline of control measures to maintain animal welfare. In addition, the site where the animal work is undertaken must have a Certificate of Designation which states that the available facilities are suitable and that it meets the recommended guidelines with an infrastructure of veterinary care, husbandry and animal welfare trained staff to support the studies. The site or project may be inspected by Home Office Inspectors at any time and animal usage statistics must be submitted to the Home Office annually [84]. Additionally AstraZeneca has rigorous procedures for the prevention, detection and monitoring of abnormal occurrences which may affect animal welfare.

4.3 Species used to gather data for this thesis

4.3.1 Han Wistar rats

Han Wistar rats are bred for research and have no complications (i.e. have no genetic or other medical problems). As such, they are a standard species used in laboratories across the world as models of normal, healthy animals[89].

4.3.2 Zucker rats

Zucker rats are deficient in leptin receptors [90-92]. This anomaly was noticed when it was discovered that these rats had an unusually high glucose level. There are two types of Zucker rat, the lean Zucker and the obese Zucker. The obese gene is recessive. Subsequently colonies were selectively bred to maintain this particular phenotype. Leptin is a hormone which is usually released from

adipocytes (fat cells) and reduces appetite. This means that these animals constantly eat as long as food is available and, as a result, they become overweight and both hyperglycaemic and hyperinsulinaemic. The animals are hyperinsulinaemic in an attempt to control their high levels of glucose. Due to them having high levels of lipids they are insulin resistant therefore insulin has little effect. This makes them a good animal model for Type 2 diabetes.

With a restricted intake of food, their glucose and insulin profile can remain close to that of a normal rat. The intake of food can be controlled by having a restricted time window in which food is available. Zucker (obese/fatty) rats were used in these experiments.

Leptin receptor deficiency can also affect humans and is very severe, where they constantly seek out and consume food [93, 94].

4.3.3 ZDF (Zucker Diabetic Fatty) rats

ZDF rats are from the same strain as Zucker rats [95], but with a more severe problem. They are unable to maintain a high level of insulin production and release in order to overcome the insulin resistance; the exact cause of the inability to produce insulin is unknown. Without intervention, a ZDF rat will suffer from β-cell failure and therefore failure to control glucose levels, ultimately leading to severe hyperglycaemia and subsequent death. Therefore, one of the hypotheses as to why ZDF rats are more severely diabetic is that they have faulty β-cells [95].

These animals are used as a model of subjects entering Type 2 diabetes and progressing through the disease. Both Zucker and ZDF rats are used in acute and chronic studies.

4.3.4 C57BL/6J Mice

AstraZeneca uses C57BL/6J mice as it is the most widely-used strain in research and can be used for diet-induced obesity experiments [96]. The mice in the studies used different diets in order to model, in animals, different diabetic conditions. Data was collected over a period of days to show disease progression.

4.4 Tests used to generate data modelled in this thesis

4.4.1 IntraVenous Glucose Tolerance Test

The intravenous glucose tolerance test (IVGTT) is a test for β-cell function [97]. It involves giving a bolus of glucose and measuring the resulting glucose and insulin concentrations in blood samples taken at frequent intervals. The insulin concentration measured is considered to be the quantity of insulin produced and the amount of glucose in the blood is seen as a measure of how effective the insulin is at removing glucose. The standard protocol for performing such a test (in both humans and animals) is represented in Figure 4.1 and explained here:

- A period of fasting before the experiment (at AstraZeneca this is usually 4 hours, however some studies examined in this thesis involve fasts of up to 16 hours);

- Animals are weighed and anaesthetised with an intra-peritoneal injection of sodium-thiobutabarbitol;
- Fasting levels of glucose and insulin are measured;
- Glucose is injected into the subject (at AstraZeneca, this usually ranges between 0.2 and 2g/kg of lean body mass of rat);
- For rats, measurements are taken at 1, 2, 5, 10, 15, 20 and 30 minutes after the glucose is injected; in a human, this period is longer – usually up to 120 minutes – as insulin and glucose are not cleared as quickly in humans due to a slower heart-rate and other factors.
- 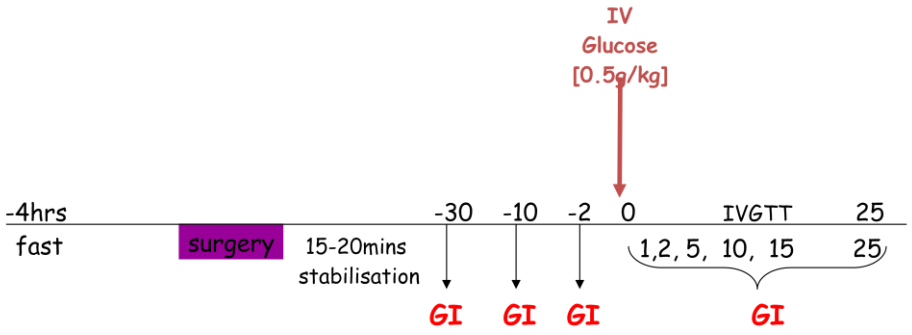

Figure 4.1: Example IVGTT protocol ***[86]***

This type of study is very intensive and usually requires one or two scientists working constantly on a small number of animals. The number of data points which can be obtained is limited by blood sample volumes that can be taken following the Home Office guidelines.

There are many different ways of assessing the results from an IVGTT. Sometimes the AUC (Area Under the Curve) from baseline or the whole AUC is used as a measure of function. Alternatively AIR (Acute Insulin Response) and

disposition index may be used [40, 98] and possibly the Minimal Model, see Chapter 6.

AIR (Acute Insulin Response) – is the area under the curve for the first 8 minutes of an insulin profile in humans. In rats it is sometimes taken as either 3, 5 or 10 minutes [99]. This is a measure of how much of a first-phase response the pancreas provides.

Using a measure of insulin sensitivity, which can be a measure from the Minimal Model or other means such as a clamp study, it is possible to define the disposition index as follows:

$$\text{Disposition Index} = \text{AIR} \times \text{Insulin Sensitivity Index} \qquad 4.1$$

The disposition index is a measure of insulin secretion in relation to insulin sensitivity, which indicates how well the subject/animal is maintaining its glucose level. If the disposition index remains the same from one occasion to another it means that the insulin secretion of the subject relative to the insulin sensitivity remains basically constant and, therefore, the subject is not losing the ability of insulin to control blood glucose disposal. This does not necessarily mean that insulin sensitivity and insulin secretion have remained constant as, if insulin sensitivity decreases and insulin secretion increases, the disposition index will remain unchanged and glucose control is maintained [100].

4.4.2 Oral Glucose Tolerance Test

The Oral Glucose Tolerance Test (OGTT) is used to measure regulation of blood glucose and can also be used to test insulin secretion. It can be used as a test for diabetes [7]. It is considered to be less artificial than other tests as it mimics more normal glucose intake [101]. AstraZeneca use it when a large number of animals is required for a study as it is less invasive and time consuming than either an IVGTT or a hyperglycaemic clamp experiment. The standard protocol for performing such a test (in both humans and animals) is:

- Fasting for 4 hours before the experiment;
- Animals were dosed with 2g of glucose per kilogram of body mass (2% glucose solution at 10ml/kg);
- Blood glucose measurements were taken using a Roche Accuchek® instrument and 5µl whole blood samples with an ELISA assay for insulin at 0, 15, 30, 45, 60, 75 and 90 minutes after the glucose was administered.

The limitations on the number of samples taken are due to the blood volume sampling limits and the timing of the blood sampling. A typical situation would involve one scientist dosing, then another two scientists involved with sampling at each interval. These three scientists would each sample blood from one animal every minute. Therefore with three scientists a maximum of thirty animals could be studied [102].

4.4.3 Hyperglycaemic clamp

This experiment is known as the gold standard for testing β-cell function [103] and can also be used for insulin sensitivity [104]. The idea of clamping is that the glucose and insulin levels are at a steady state and are therefore not affected by the dynamics of the system. A hyperglycaemic clamp involves infusing glucose into a subject to create a steady state of glucose which is higher than the subject's usual basal level. Depending on the experiment, this is either a certain, set level of glucose (e.g. 11mmol) or a set amount above that subject's basal level (e.g. 6mmol above a basal level of 5.5mmol, giving 11.5mmol). This glucose level is maintained and when the insulin level is thought to have stabilised, usually after approximately 60 minutes, the ratio between the insulin level and the infused rate of glucose at steady state is said to be the insulin sensitivity.

The clamping experiment data used in this thesis are from hyperglycaemic clamps. This usually involves the following preparation:

- Animals were fasted at 16:00 the day before the experiment in a clean cage with no access to food but with access to water;
- At 08:00 on the day of the experiment, animals were weighed and anaesthetised with an intra-peritoneal injection of sodium-thiobutabarbitol;
- Four catheters were placed in the jugular vein for infusions of glucose, compound, haemacel (to stabilise the volume of distribution in the subject) and top-ups of anaesthetic;

- A further catheter was placed in the left carotid artery for blood sampling and recording arterial blood pressure;
- Body temperature was maintained at 37.5˚C and 45 minutes was allowed after surgery for stabilisation.

Two types of glucose measurement are taken in hyperglycaemic clamps - one which is quick and provides near-instant feedback and another which is slower but more accurate - which will be referred to as blood glucose and plasma glucose, respectively. For the data used in this thesis, blood glucose measurements were taken by a Roche Accuchek® using 10μl of blood and obtained in a few seconds. Plasma glucose was measured using 300μl of blood and took longer to sample as plasma had to be spun off. After each plasma glucose sample, insulin and C-peptide measurements are also taken. Figure 4.2 shows the protocol for the hyperglycaemic clamp.

Before the clamp is initiated, a plasma sample is taken for basal levels of glucose, insulin and C-peptide. At time zero, glucose is usually infused at 375mg kg^{-1} min^{-1} for 1 minute. The infusion rate is then lowered and blood glucose values are used to clamp the glucose at the required level. Blood glucose is sampled roughly every minute during this initial period. When the clamp has been maintained at a constant level of glucose between 70 and 90 minutes of the experiment, this is considered to be “steady state”; this is where standard analysis of this experiment is performed, such as the disposition index. Just before the end of the experiment 200ug/kg arginine is dosed, in order to release all of the insulin

left in the β-cells, as a measure of the total insulin that could be secreted. At the end of the experiment the animals are culled.

Knowledge of this procedure is important for the modelling. For example, at the start of the clamp there is as a "375mg kg^{-1} primer" which could be misinterpreted as being a bolus injection rather than an infusion; this has implications for how the input function for the model is described.

It is also important to understand the limitations of such an experiment. So many of the data collected in this experiment are dependent on the blood volumes of the samples; for example, it is not possible to get as many insulin measurements as glucose measurements since insulin measurements require 300μl of blood compared to the 10μl required for glucose measurements [86]. Hyperglycaemic clamps are also very labour intensive and require one or two scientists per subject.

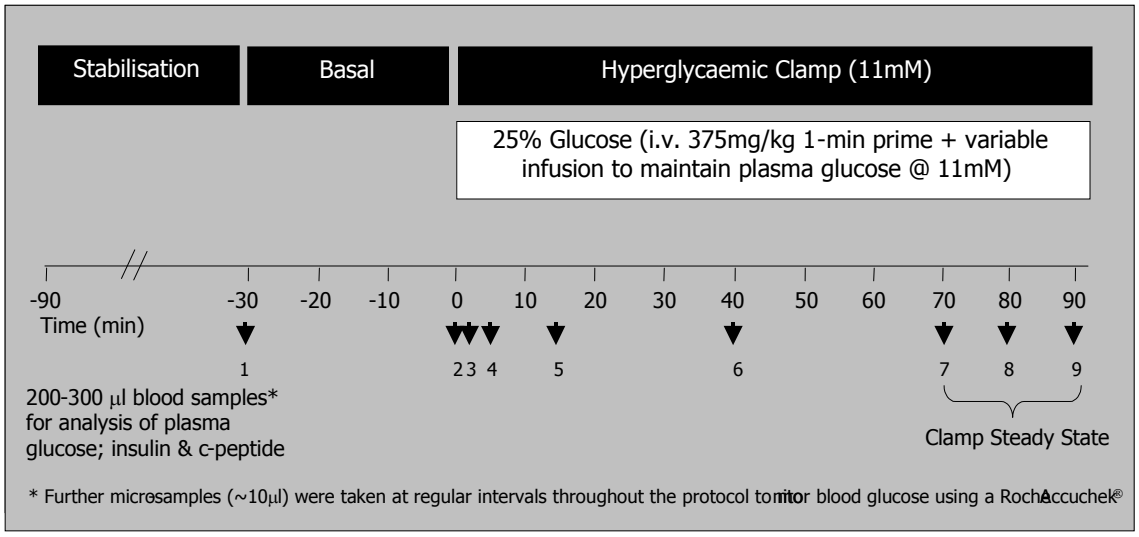

Figure 4.2: Protocol for hyperglycaemic clamp experiment

4.4.4 C-peptide intravenous experiment

Unlike the other tests described here, this test was performed specifically for the purpose of modelling. This will be described in more detail in Chapter 7. This test involved injecting human C-peptide into anaesthetised Han Wistar rats. Injected C-peptide has the same kinetic characteristics as the endogenous C-peptide but can be distinguished from the endogenous C-peptide in the assay which distinguishes between human and rodent C-peptide. It is important to note here that it requires similar sample sizes to insulin and is therefore sampled only infrequently [105].

4.4.5 Chronic study

Data for long-term modelling in Chapter 9 were obtained from studies performed over an extended period of time, in this case 40 days. These studies consist of feeding animals on particular diets and restricting when the animals can feed, generally to a 4-hour window, outside which food is removed from the cage. On selected days, profiles of glucose and insulin are taken in a similar way to OGTTs but with measurements taken over a 24-48 hour period. An example protocol is shown in Figure 4.3:

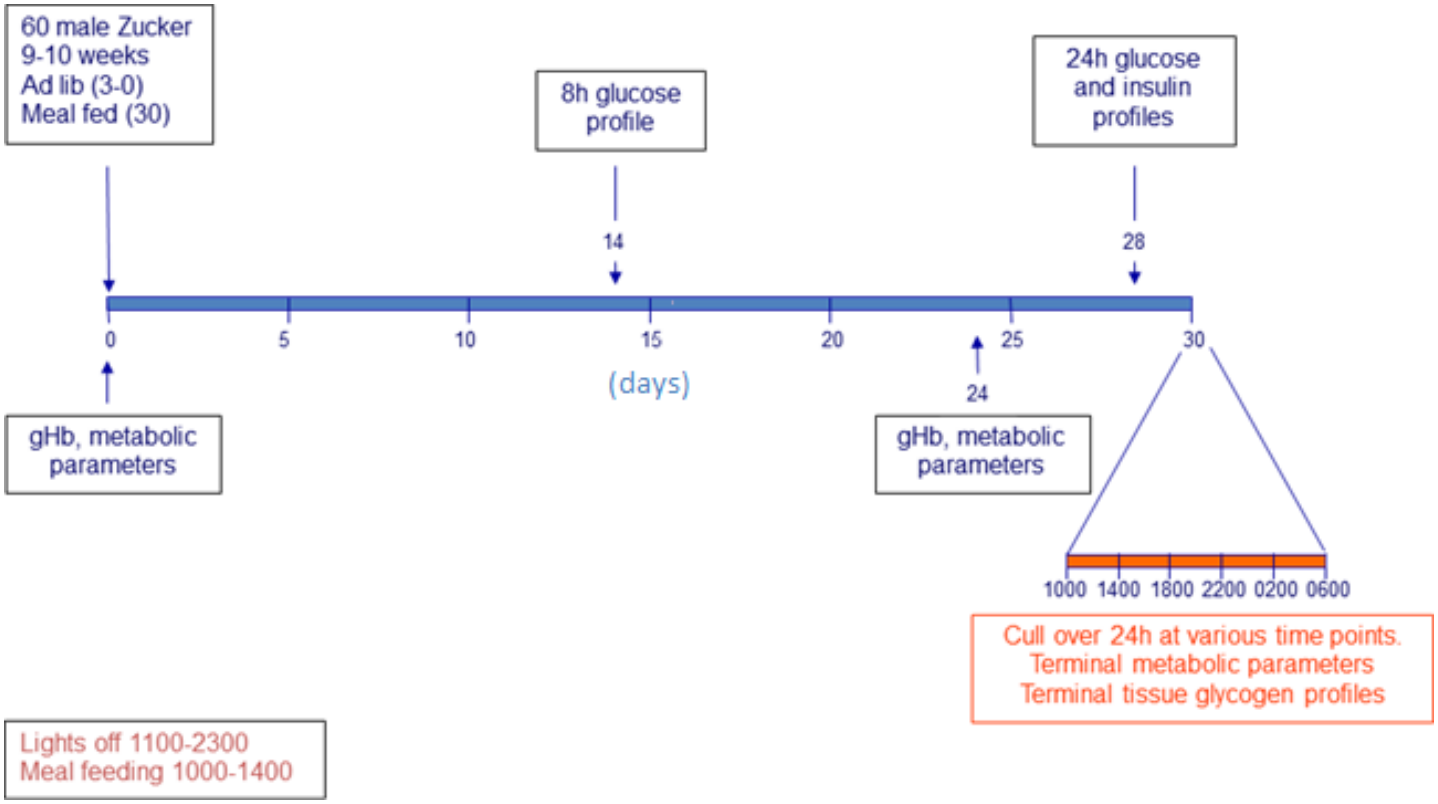

Figure 4.3: Example protocol for a chronic C-peptide study [86]

4.4.6 Summary

The following table summarises the main points about each test described above.

Test	Primary Result	Secondary Result	Limitations
IVGTT	β-cell function	Insulin sensitivity (from modelling)	• Intensive • Only practical with small number of subjects
OGTT	Glucose regulation		• Small number of data points
Hyperglycaemic clamp	β-cell function	Insulin sensitivity	• Intensive • Only practical with small number of subjects
C-peptide intravenous experiment	C-peptide kinetics		• Intensive • Only practical with small number of subjects
Chronic study	Disease progression	Any obtained from incorporated experiments (e.g. OGTT)	• Extended period of time required

Table 4.1: Summary of tests described in this chapter

4.5 Sampling and assays

As mentioned with the hyperglycaemic clamps, glucose samples can be measured in two different ways: either with a small sample with an Accuchek® [106] or with a larger sample from blood plasma and a glucose analyser. The measurements from the glucose analyser are considered to be more accurate so the blood glucose measurements are often corrected or calibrated using the plasma glucose measurements.

C-peptide and insulin are measured using Millipore and Mercodia ELISA (Enzyme-Linked Immunosorbent Assay) kits [107, 108]. These assays have a non-linear response to the substances put in them, therefore when performing these assays a known quantity (standard) of the substance is run at the same time as the sample to generate standard curves (see example in Figure 4.4). The scientists often aim to dilute the unknown plasma samples so that the results will end up on the linear part of the standard curve. When this is not possible, a polynomial is frequently employed to describe the curve, which is then used to reference the measurement from the kit to the corresponding amount of that substance; however this may reduce the accuracy of the assay so it is avoided where possible.

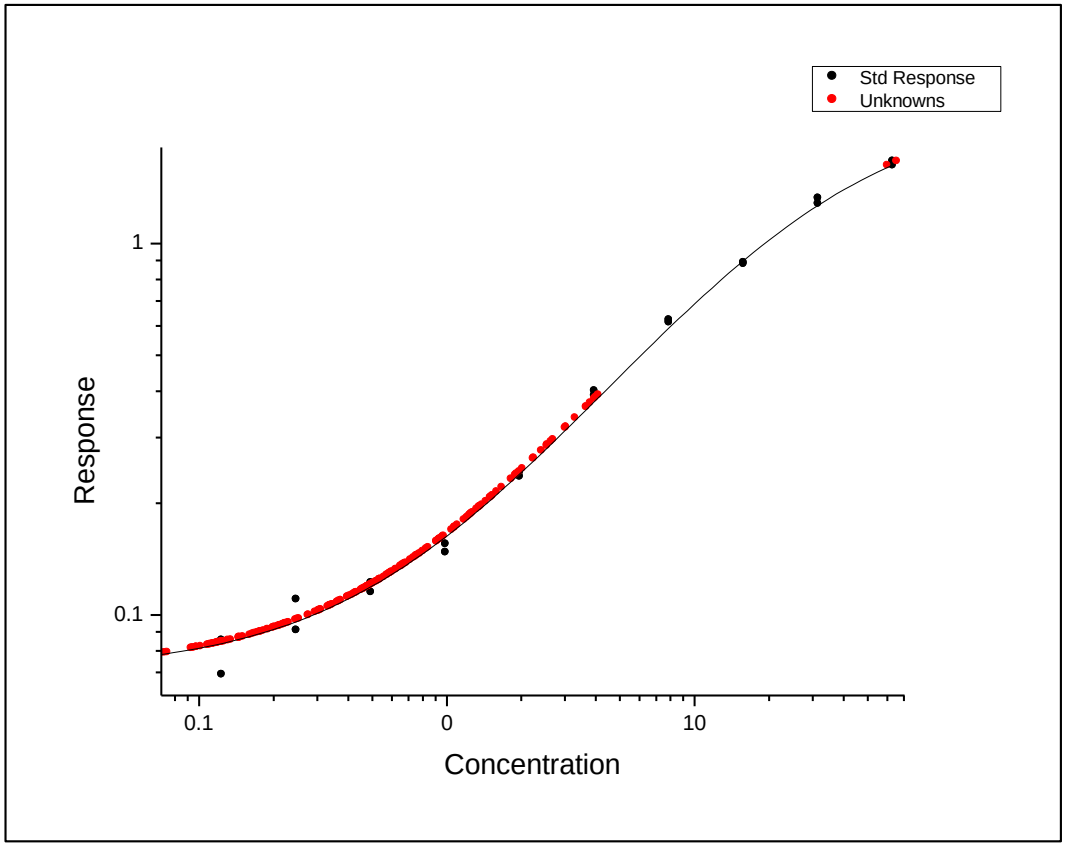

Figure 4.4: Example of a standard curve on a log-log scale for an ELISA assay ***[86]***

All these assays have different degrees of accuracy (see Table 4.2). AstraZeneca uses a range of assays to perform measurements. The Accuchek® device, used for blood glucose measurements, has a higher accuracy at high glucose levels than at low glucose levels [106]. Plasma glucose is measured using a Yellow Springs Glucose Analyser and insulin and C-peptide are measured using ELISA kits.

Assay	Accuracy
Accuchek®	58.5% of samples within 5% or 0.28mmol/l of reference value 99.3% of samples within 20% of reference value [108, 109]
Yellow Springs Glucose Analyser	To at least 5.8%
ELISA kits	To at least 6.8% for C-peptide To at least 3.8% for insulin[108]

Table 4.2: Assay accuracies

Although the assays have the stated accuracies, there are other sources of error which may result in errors in the final measurements; these include inaccuracies in pipetting volumes and a "freeze-thaw" effect (where the sample has been frozen and then thawed later which may degrade the sample, which is particularly relevant for C-peptide and insulin). However all practical steps are taken to minimise these types of errors, such as using mechanical pipetting and avoiding freezing samples where possible [86].

The standard curve and the level of quantification means that errors may not always be proportional to the sample value. It is important to take all these issues into consideration when modelling.

4.6 Data sets

A variety of data sets from several sources are used in this thesis. A list of data sets and sources is provided in Table 4.3 below; the first is also detailed fully in Chapter 7. *n* denotes the number of animals in each group.

Name	**Experiment Type**	**Lead AstraZeneca Scientist**
RuthCPeptide	C Peptide Intravenous Injection	Ruth MacDonald
	Anaesthetised - Han Wistar rats 6nmol/ml (*n*=3),3nmol/ml (*n*=3),0.8nmol/ml (*n*=2) Measurements taken at 0, 1, 2, 5, 10, 15, 20, 25 and 30 minutes C Peptide Measured	
RuthClamp	Hyperglycaemic Clamp	Ruth MacDonald
	Anaesthetised - Han Wistar rats Fed (*n*=5), 4 Hour Fast (*n*=4),8 Hour fast (*n*=4) Measurements detailed in RuthCPeptide above	
AliceIVGTT	IVGTT	Alice Yu
	Anaesthetised - Han Wistar rats Fed (*n*=5), 4 Hour Fast (*n*=4),8 Hour fast (*n*=4) Measurements detailed in RuthCPeptide above	
AmieIVGTT	IVGTT	Dr Amie Gyte
	Anaesthetised - Han Wistar rats Fed (*n*=7) 0.2 (*n*=3) 0.5 g/kg(*n*=3) 1g/kg (*n*=1) Glucose dose Measurement times -10, 0 ,1, 2, 5, 10,15,25 Plasma Glucose, Plasma Insulin, Plasma C-peptide	
GeorgiaIVGTT	IVGTT [102]	Dr Georgia Frangiousdakis
	Conscious - Han Wistar rats 4 Hour Fast (*n*=18)	

Name	Experiment Type	Lead AstraZeneca Scientist
	0 (*n*=8) 0.5 g/kg (*n*=6) 1g/kg (*n*=4) Glucose dose Measurement times -10, 0 ,1, 2, 5, 10,15,25 Plasma Glucose, Plasma Insulin, Plasma C-peptide	
StevenOGTT	OGTT	Dr Steven Wang
	Conscious - C57BL/6J mice (*n*=20) 2g/kg 4 days of profiles for each over 8 days. Measurements at 0, 15, 30, 45, 60, 75 and 90 Blood Glucose, Plasma Insulin	
JoChronic	Chronic	Jo Teague
	Conscious - Zucker and ZDF rats 38 Days - 4 hours Meal Feed Zucker (*n*=30), Adlib Zucker (*n*=30), Ad lib Obese ZDF (*n*=10), Meal fed Obese ZDF (*n*=32) Measurements at 0,2,4,6,8,12,16,20,24 hrs on days 3,13,16,27,37 Blood Glucose, Plasma Insulin	

Table 4.3: Data Collection – data sets

Chapter 5: Previous Models

This chapter is a review of the details of previously developed mathematical models of the glucose-insulin system. This provides context for the model detailed in this thesis and indicates where some useful ideas for elements of the model have originated. The models described are detailed in chronological order, beginning in 1961 with a very simple, linear system and continuing, over the last 45 years, to a recent development from Swedish modellers.

5.1 Bolie Model

In 1961, Bolie created one of the first (if not the first) mathematical models of the glucose-insulin system, using dog data [110]. Due to the limited ability at the time to simulate complex models, it was necessarily very simple in nature (see Figure 5.1 below).

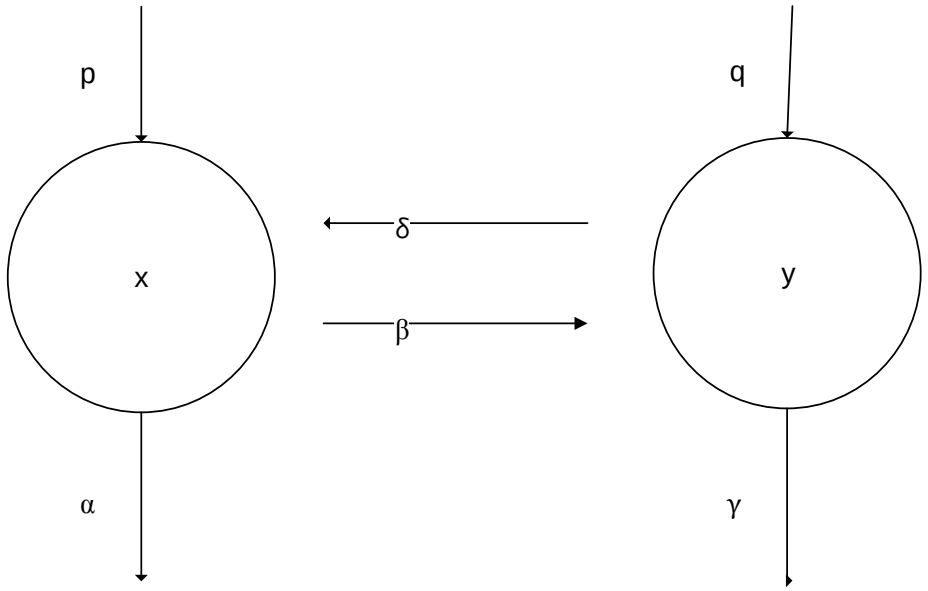

Figure 5.1: Conceptual diagram of the Bolie Model

It had only two compartments, one for glucose (*y*) and one for insulin (*x*). It consists of a pair of first-order differential equations which comprise a second-order system:

$$\frac{dx}{dt} = p - \alpha x + \beta y$$
$$\frac{dy}{dt} = q - \gamma x - \delta y \qquad 5.1$$

where *x* is insulin concentration; *y* is glucose concentration; α, β, γ and δ are "regulatory coefficients" which, when multiplied by volume of distribution, represent insulin clearance, glucose-stimulated insulin secretion, insulin sensitivity and glucose effectiveness respectively; *p* is rate of insulin injection divided by volume of distribution and *q* is rate of glucose injection divided by volume of distribution (see Chapter 2).

The model was simulated using an analogue computer (see Figure 5.2 below).

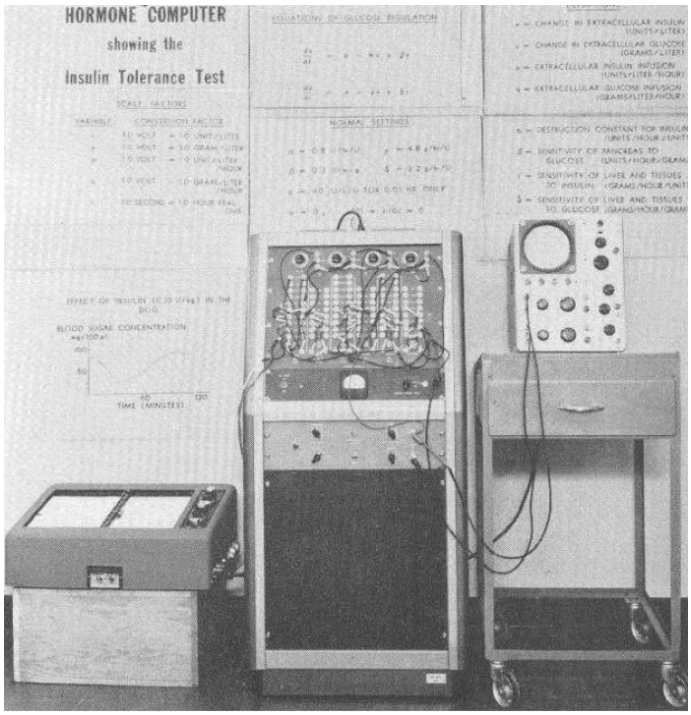

Figure 5.2: Bolie Glucose Insulin Analogue Computer ***[110]***

The main drawback of this model was that it was linear, and therefore both glucose and insulin levels could become negative - a physiologically impossible situation. In developing this model, Bolie noted a key point: that the glucose and

insulin system is critically damped and therefore returns to a steady state quickly and efficiently [110].

5.2 Minimal Model

The Minimal Model was created in 1979 by Bergman & Cobelli [111, 112] and has been referenced in over 900 papers in 2009 to date [40]. It is so-called because it was designed to comprise the smallest number of parameters possible while adequately representing the glucose-insulin system. It is now widely accepted as a three-state model with parameters for insulin sensitivity and glucose effectiveness, and a delay compartment for insulin action. In terms of limitations, the Minimal Model is only valid for IVGTTs and there are also mechanistic issues - for example, no first-phase insulin secretion - and structural issues with the model - for example, it does not return correctly to a steady state [113].

As the Minimal Model is such an important model in this field it is discussed in detail in Chapter 6.

5.3 HOMA Model

In 1985, Matthews, et al. developed another model of the glucose-insulin system known as the HOMA (Homeostatic Model Assessment) model [114, 115]. This takes fasting (i.e. steady-state) values of glucose and insulin and uses them to produce output in the form of a graph, from which estimates of β-cell function and insulin sensitivity can be obtained. It is a very simple model, consisting of

only two simple equations 5.2 which are derived from the underlying physiology of the glucose-insulin system shown in Figure 5.3.

$$HOMA1_{IR} = (FPI \times FPG)/22.5$$

$$HOMA1_{\%B} = (20 \times FPI)/(FPG - 3.5) \qquad 5.2$$

where $HOMA1_{IR}$ is insulin resistance, $HOMA1_{\%B}$ is β-cell function, *FPI* is fasting plasma insulin and *FPG* is fasting plasma glucose.

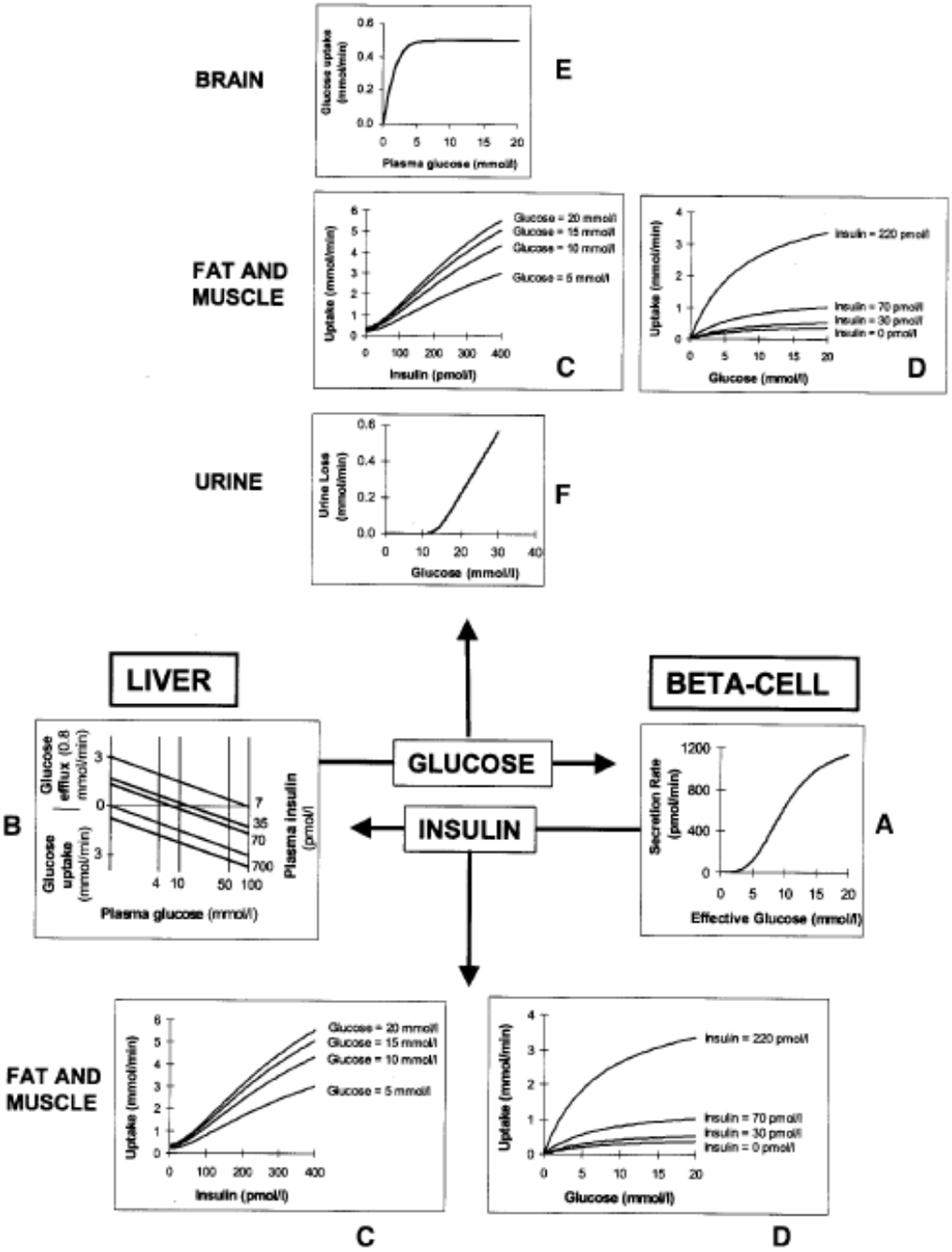

*The underlying physiological basis of the HOMA model. The feedback loop between the liver and the β-cell is central to the model. Plasma glucose concentration in the basal state is regulated by hepatic glucose output, which is insulin dependent (*B*). Insulin concentration is dependent on β-cell response to glucose (*A*). Insulin signals glucose uptake in fat and muscle (*C *and* D*). Glucose disposal is modelled in brain (*E*) and kidney (*F*)as being dependent only on glucose, and in fat and muscle as being dependent on glucose and insulin concentrations (*C *and* D*).*

Figure 5.3: Physiological basis of the HOMA model ***[116]***

The model was updated in 1996 – to produce the HOMA2 model – which uses non-linear solutions to produce a more accurate output graph shown in Figure 5.4, but results in more complex equations [116].

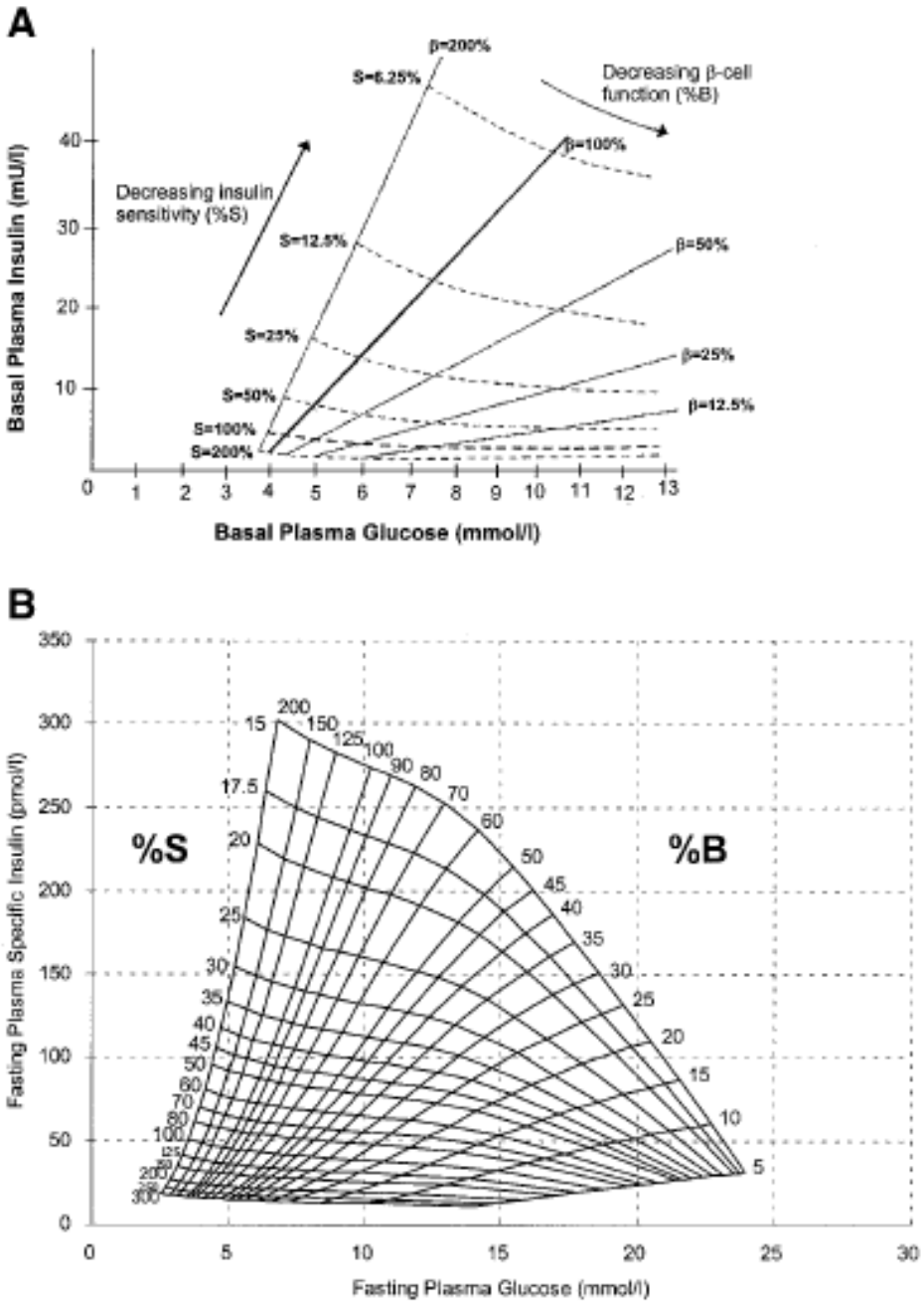

Figure 5.4: A: HOMA from 1985 B: HOMA2 from 1996 where S is insulin sensitivity and B/β is β-Cell function *[116]*

The authors note that both models have been widely misused. For example, the models have been validated only against humans, by testing for correlation between model output for insulin resistance and euglycaemic clamp data, and model output for β-cell function and hyperglycaemic clamp data; however the models have been applied to animal data without validation [116].

A key limitation of these models is that they do not model the system dynamically and provide only insulin sensitivity and β-cell function estimates. However, the fact that the models use only steady-state values acknowledges that these are an indication of the state of a subject. In turn, the model shows that the interplay between insulin secretion and glucose disposal produces different steady-state values, which is an important concept in dynamic models.

5.4 AIDA Model

The AIDA model was developed in 1992 by Lehmann & Deutsch for the purpose of educating Type 1 diabetes patients about how best to manage their condition [117, 118]. It has a large number of parameters, including body-weight and meal size (see Figure 5.5).

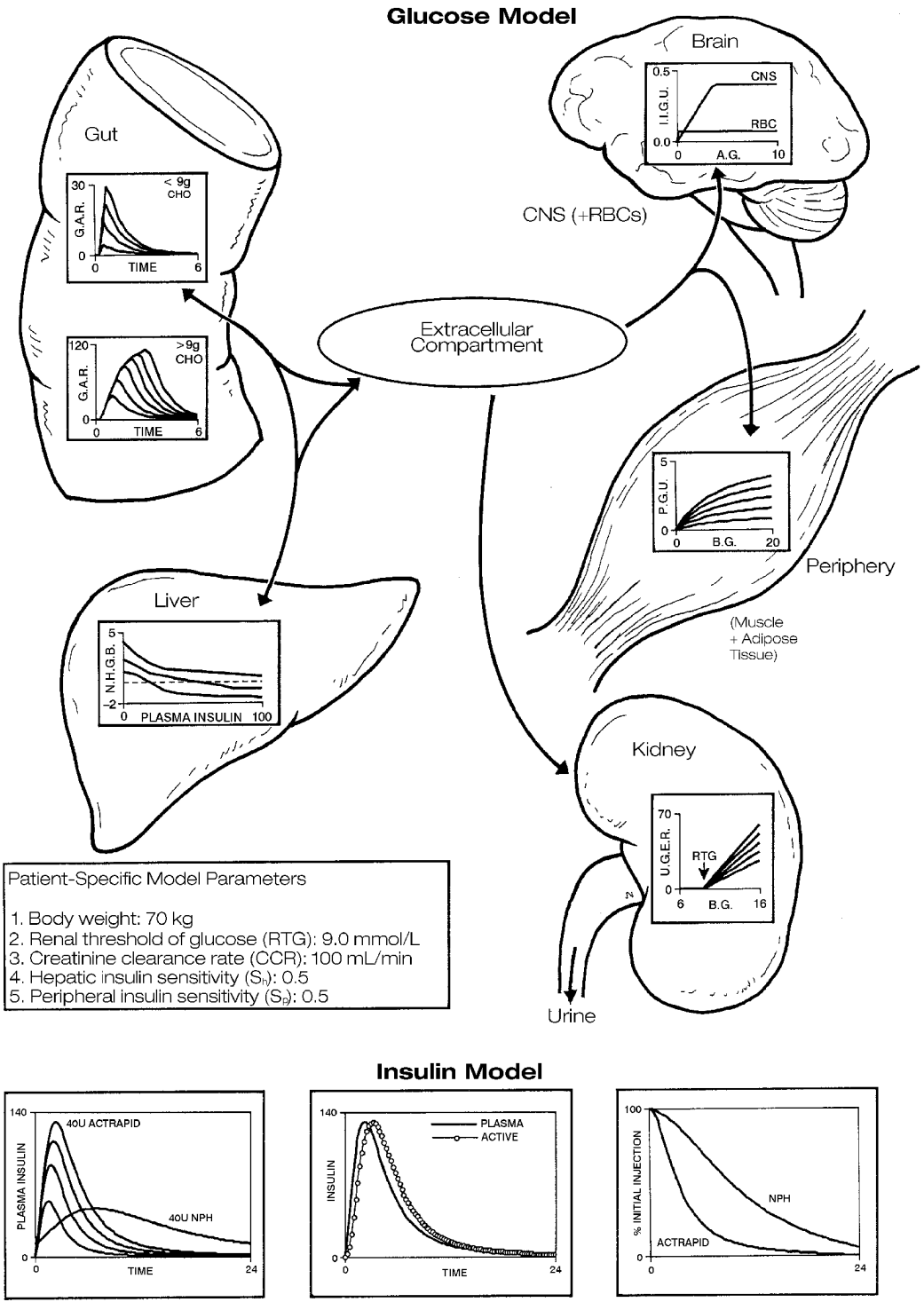

Figure 5.5: AIDA Model Diagram [117]

Parameters can be adjusted and simulations performed through a web interface, and there is also a free downloadable tool which performs basic parameter estimation. As there are a large number of parameters, example parameter sets which can be adjusted slightly to fit an individual are also provided. The output is in the form of graphs showing blood glucose and plasma insulin over the course of a day (see Figure 5.6 below).

Figure 5.6: Screenshot of AIDA model software tool with demo subject

This model has a large number of different factors which contribute to the output, including compartments for insulin, insulin action, different types of insulin (short- or long-acting), gut absorption, carbohydrate ingestion rate and renal clearance. Most of these factors are based on previously known

physiological values. The model is specifically for Type 1 diabetes patients, who do not produce insulin, and therefore does not have any insulin secretion terms; the only insulin included in the model comes from insulin injections (which are used for treatment).

This model is interesting for two reasons: it includes more complex features of the glucose-insulin system which others do not (e.g. renal clearance), and its aim as a freely-available modelling tool to help Type 1 diabetes patients is also different to other models, which are generally aimed at clinicians and other modellers.

5.5 β-Cell Mass Model

The β-Cell Mass Model is one of very few attempts to model the glucose-insulin system in the longer term [119]. It was created by Topp, et al. in 2000 to help predict the aetiology of diabetes, i.e. over weeks and months rather than hours, and to explain self-regulation of the glucose-insulin system using β-cell mass. Although not validated against real data, the parameters in the model were taken from physiological values or the literature on previous models. The model sets up the glucose-insulin system in an elegant three state mathematical model.

There are many aspects of the β-cell mass model which are relevant to the model presented in this thesis so it is examined in greater detail in Chapter 9.

5.6 Picchini Clamp Model

This model was created in 2005 by Picchini, et al. to mathematically model the response to a euglycaemic-hyperinsulinaemic clamp experiment [120, 121]. The model was validated using human data. A stochastic approach to modelling was used as it was found that the model itself was unable to explain the apparent randomness in the data. The deterministic part of the model contains two state variables: glucose and insulin concentrations. The glucose state contains glucose effectiveness and insulin sensitivity; the insulin state includes proportional secretion of insulin and hepatic glucose output, see Figure 5.7. The stochastic element of the system was applied to the insulin-sensitive parts of the model, i.e. the hepatic glucose output and insulin sensitivity. It was modelled using a Wiener process (also called Brownian motion) which is a continuous-time stochastic model describing the random movement of particles. This can be seen in the equation 5.3:

$$dG(t) = \left[\frac{(T_{gx}(t-\tau_g) + T_{gh}(t))}{V_g} - T_{xg}\frac{G(t)}{0.1+G(t)} - K_{xgI}G(t)I(t)\right]dt + \sigma G(t)I(t)dW(t) \qquad 5.3$$

$$T_{gh}(t) = T_{ghmax}\exp(-\lambda G(t)I(t))$$

with $G(0) = G_b, I(0) = I_b$ and $T_{gh}(0) = T_{ghb} = T_{ghmax}\exp(-\lambda G_b I_b)$. T_{gx}, T_{ix} are input state variables, V_i, V_g are volumes of distributions. K_{xgI} varies randomly

as $K_{xgI} - \xi(t)$, where $\xi(\cdot)$is Gaussian white-noise process. Then the system noise is $\xi(t)dt$ can be written as $\sigma dW(t)$ [120].

The Picchini et al. model is important because it relatively successfully models glucose and insulin concentrations in a subject undergoing a euglycaemic-hyperinsulinaemic clamp experiment; however it is not applicable in other situations. The stochastic approach is also interesting and was chosen by Picchini because the subjects were conscious and therefore their utilisation of glucose varied somewhat randomly over time. A stochastic approach is useful when there is a lot of random variation and it provides a quantification of the randomness in the system; however if there is little variation in individual subjects a stochastic approach is not applicable. Additionally, stochastic models take longer to simulate than deterministic models as they generally require the model to be simulated repeatedly with different random seeds.

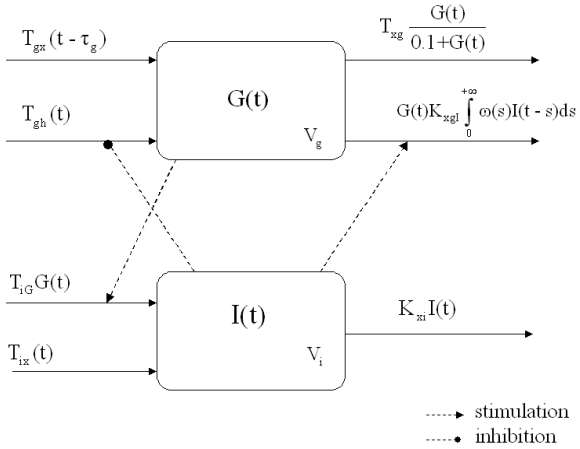

G_b [mM]	basal glycemia
I_b [pM]	basal insulinemia
T_{xg} [mM / min]	maximal insulin-independent rate constant for glucose tissue uptake
K_{xgl} [min^{-1}/pM]	insulin-dependent apparent first-order rate constant for glucose tissue uptake at insulinemia I
K_{xi} [min^{-1}]	apparent first-order rate constant for insulin removal from plasma
T_{iG} [pM/min/mM]	apparent zero-order net insulin synthesis rate at unit glycemia (after liver first-pass effect)
T_{ixb} [pmol/min/kgBW]	basal insulin infusion rate, which is given by the measured value of T_{ix} at time zero according to [18]
T_{ghmax} [mmol/min/kgBW]	maximal Hepatic Glucose Output at zero glycemia, zero insulinemia
T_{ghb} [mmol/min/kgBW]	basal value of T_{gh}
V_g [L/kgBW]	volume of distribution for glucose
V_i [L/kgBW]	volume of distribution for insulin
α [#]	time constant for the insulin delay kernel $\omega(\cdot)$
τ_g [min]	discrete (distributional) delay of the change in glycemia following glucose infusion
λ [$mM^{-1}pM^{-1}$]	rate constant for Hepatic Glucose Output decrease with increase of glycemia and insulinemia
ρ [#]	average delay of insulin effect

Figure 5.7: Schematic representation of the Picchini clamp model [121]

5.7 Cobelli Model

Cobelli began work on model-based predictive control in order to create an artificial pancreas [122]. In order to do this, a meal simulation model of the glucose-insulin system was developed, with first-phase insulin response based on Andrea Mari's work [123] and second-phase insulin response and insulin effect compartment from the Minimal Model [111, 112]. The model has two compartments for glucose and two for insulin (plasma and periphery), piecewise functions simulating insulin secretion (i.e. separate equations for different phases of insulin secretion) and non-linear Michaelis-Menten kinetics for glucose disposal (see Figure 5.8). It also includes renal extraction of glucose and hepatic insulin clearance.

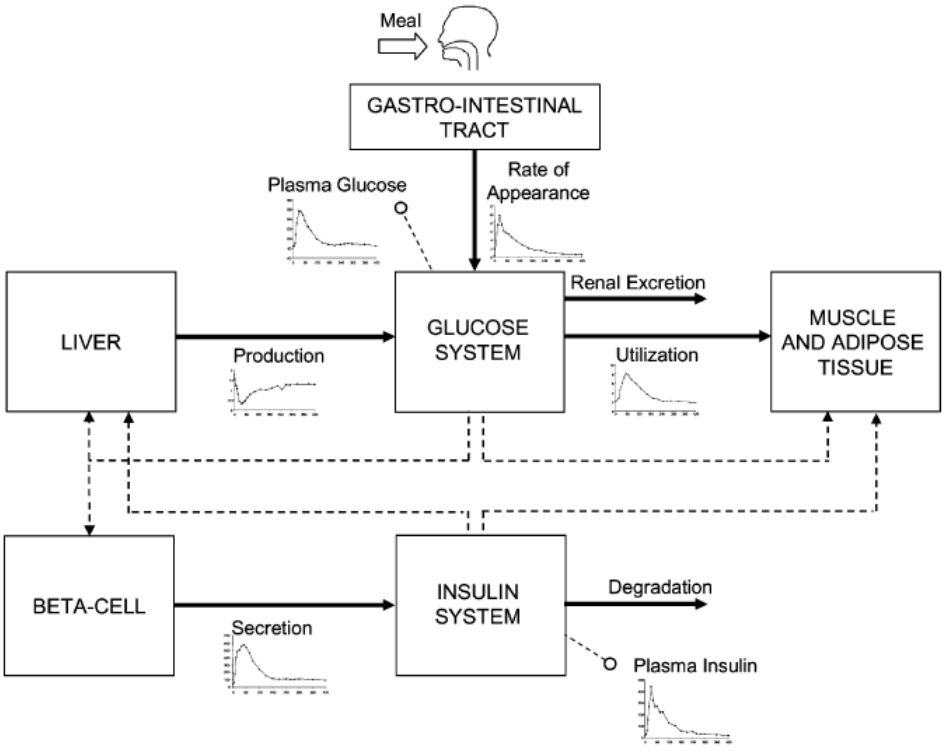

Figure 5.8: Conceptual diagram of the Cobelli model [122]

This model was important in the field of glucose-insulin system modelling because it was used to validate, in simulation, a model-based predictive controller for the artificial pancreas [80]. It was used to investigate the effects of the controller on simulated patients. On the basis of this, approval was granted by the FDA (Food and Drug Administration; regulatory authority for drugs in the USA) to begin human testing with the artificial pancreas with the caveat that a clinician would have to approve the insulin infusion [81].

The Cobelli model was developed into a software tool called GIM (Glucose Insulin Model) using MATLAB [124]. GIM also shows the effect of a PID controller on the glucose-insulin system, which is particularly relevant to this thesis.

A key limitation of the Cobelli model is that it is relatively complex, compared to other models described here. It also has set values for parameters including basal levels of glucose which define the piecewise function for insulin secretion and therefore may not mechanistically truly reflect insulin secretion.

5.8 Uppsala Model

This model was developed in Mats Karlsson's group at Uppsala University, primarily by Hanna Silber. It was first published in 2007 [125] and there have since been several follow-up papers [126-128]. The authors used a population approach to modelling the system and the structure was compartmental. The model included two glucose compartments (plasma and periphery) and a single insulin compartment. It also had "effect" compartments for glucose

effectiveness, glucose effect on insulin secretion, insulin effect on glucose disposal and first-phase insulin secretion based on glucose dose, see Figure 5.9. It used a fitted forcing function for glucose absorption in an OGTT which was called the “flexible input model”; for this, twelve time periods were specified, each of which could have a different absorption rate of glucose into the blood plasma. The model was validated using human data from OGTTs and IVGTTs.

This modelling strategy considered the system in a more mechanistic way than previous models to take account of the interplay between biological processes and to help hypothesis testing [129]. This is an aspect of modelling which has been incorporated into the model presented in this thesis in Chapter 7. Additionally, as the model is pharmacology-based, mass is not lost through the model and it maintains mass balance. However, it is a complex, multi-state model which requires more data than most other models to fit certain elements and parameters such as glucose absorption in the OGTT setting [129]. As there is an abundance of data for human IVGTTs and OGTTs, which are what this model was designed for, this is reasonable but for animal models this is not so practical and a more minimal model is required.

The equations are quite lengthy. Figure 5.9 gives an overview of the model for the full equations, see papers [125-129].

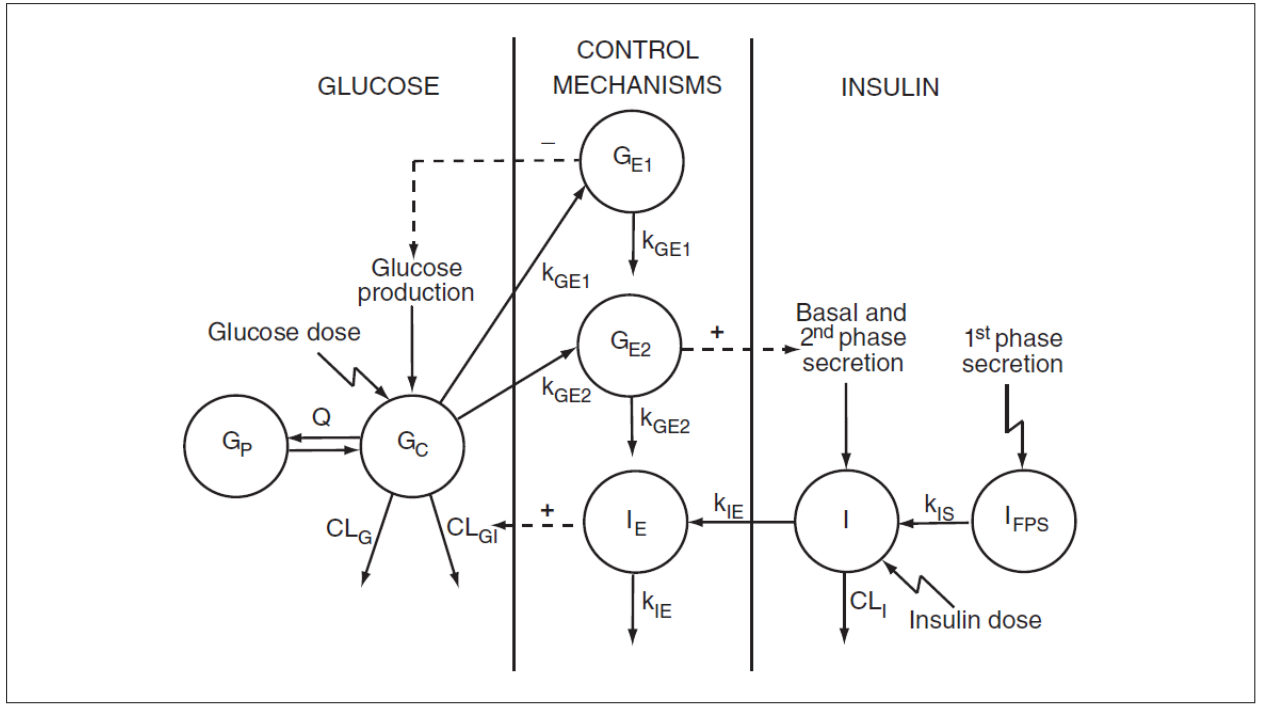

Figure 1. Schematic presentation of the integrated model including total glucose, insulin, and regulation of glucose production, second-phase insulin secretion, and glucose elimination. Full arrows indicate flows, and broken arrows indicate control mechanisms. G_C and G_P, central and peripheral compartments of glucose; G_{E1} and G_{E2}, effect compartments for control of glucose production and insulin secretion; I, insulin disposition compartment; I_{FPS}, delay compartment for the first-phase insulin secretion; I_E, effect compartment for control of glucose elimination; Q, CL_G, and CL_{GI}, clearance parameters of the glucose model; CL_I and k_{IS}, parameters of the insulin model; k_{GE1}, k_{GE2}, and k_{IE}, rate constants for the effect compartments.

Figure 5.9: Schematic representation of the Uppsala model [125]

5.9 Summary

The following table summarises the main points about each model described above.

Model	Structure	Timescale	Main positive attributes	Main negative attributes
Bolie	Linear two-state	Hours	• Simple. • Linear.	• Potential for physiologically impossible outputs.
Minimal	Non-linear three-state	Hours	• Small number of parameters. • Well-established.	• Only valid for IVGTT. • Mechanistic and structural issues. • Not physiologically-based.
HOMA	Two non-dynamic equations	Instantaneous	• Simple. • Small number of measurements required. • Physiologically-based.	• Non-dynamic. • Only estimates insulin sensitivity and β-cell function.
AIDA	Non-linear multi-state	Hours/days	• Includes complex features, e.g. renal clearance. • Physiologically-based.	• Only relevant for Type 1 diabetes patients.
β-cell mass	Non-linear three-state	Weeks/months/ years	• Suitable for long-term modelling. • Physiologically-based.	• No short-term aspects incorporated.
Picchini Clamp	Stochastic non-linear two-state	Hours	• May be appropriate for large variations in glucose levels in subjects, where deterministic modelling fails. • Physiologically-based.	• Inappropriate where there is no random variation in glucose levels. • Longer simulation time compared to deterministic models.

Model	Structure	Timescale	Main positive attributes	Main negative attributes
Cobelli	Non-linear multi-state	Hours	• Includes complex features, e.g. hepatic insulin clearance.	• Relatively complex. • Not entirely physiologically-based.
Uppsala	Non-linear multi-state	Hours	• Physiologically- and pharmacology-based.	• Complex. • Requires a large amount of data.

Table 5.1: Summary of models presented in this chapter

Several of these models are not physiologically-based, meaning that they work only in the situation they were specifically designed for - for example, the Minimal Model works only for IVGTTs and is invalid for OGTTs and clamp experiments. Such models are not true models of the system and model only the specific test; it is therefore important that a model of the glucose-insulin system should be physiologically-based. Table 5.1 also shows that there is no single model which is appropriate for use in both short- and long-term modelling of the glucose-insulin system. Finally, especially for animal modelling where data points tend to be sparse, a simple, but dynamic, model is required. For these reasons, it appears that there is a need for a model of the glucose-insulin system which is physiologically-based, incorporates short- and long-term aspects of the system and which is both simple and dynamic. The model presented in this thesis in Chapter 8 and Chapter 9 aims to fulfil all of these criteria.

Chapter 6: Minimal Model

This chapter is concerned with the structural identifiability of the Minimal Model and parameter estimates for Han Wistar rats using (AliceIVGTT) data. It shows the Minimal Model is structurally identifiable with insulin and glucose as observables, as well as with only glucose as an observable under certain assumptions. It also shows the results of the parameter fitting performed using MATLAB on actual experimental data from IVGTT on fasted and non-fasted anaesthetised Han Wistar rats, including consideration of the sensitivity of each of the parameters. The results show a reasonable fit using both glucose and insulin, however the model fails to produce physiologically relevant insulin parameters when using only glucose as an observable.

6.1 Introduction

The Minimal Model was developed by Bergman and Cobelli in 1979 (see [111, 112]) , however it is still the most widely-used mathematical model in this field; this 2007 article states that there have been 900 citations, as of 2009, in the literature relating to the Minimal Model [40]. The authors compared seven candidates for the glucose part of the system model and attempted parameter fitting, selecting the one they considered the most appropriate in terms of identifiability (meaning parameter estimation), meaningfulness of parameters and "goodness" of fit: the Minimal Model. Its name comes from its minimal approach, which the authors define as being "the simplest mathematical representation able to account for glucose disappearance kinetics"[112] .

Two computer programs have been written to perform the modelling and simulation automatically [130, 131]. These programs apply a technique whereby they use the glucose levels as a forcing function on the insulin and fit only the insulin data, then the glucose data are fitted using the insulin as a forcing function. This means that the model is never fully coupled, hence insulin and glucose never directly interact in the model; this could thus be viewed as the application of two separate models.

6.1.1 Intended Use

This model is designed to be used in one situation: by an IVGTT, which tests β-cell function (insulin secretion capacity). An injection of glucose stimulates the

release of insulin, which is then measured to determine the β-cell function. This paradigm is sometimes referred to as GSIS (Glucose Stimulated Insulin Secretion) [132].

Prior to an IVGTT experiment, the subject is normally fasted so they are at basal glucose and insulin levels; in humans, this fasting is generally overnight for 12 hours [112]. When glucose and insulin levels are measured after glucose injection, changes will be purely the result of the injection and the endogenous levels, not of meals before the experiment.

6.1.2 Description

The Minimal Model is a three-compartment model two of which are insulin compartments - plasma and interstitial - and the other is a glucose compartment. The plasma insulin and glucose compartments are where insulin and glucose respectively are measured (i.e. in the periphery). The interstitial insulin compartment simulates the delay between insulin secretion and the effect on glucose levels.

Figure 6.1 shows these compartments and how they are connected.

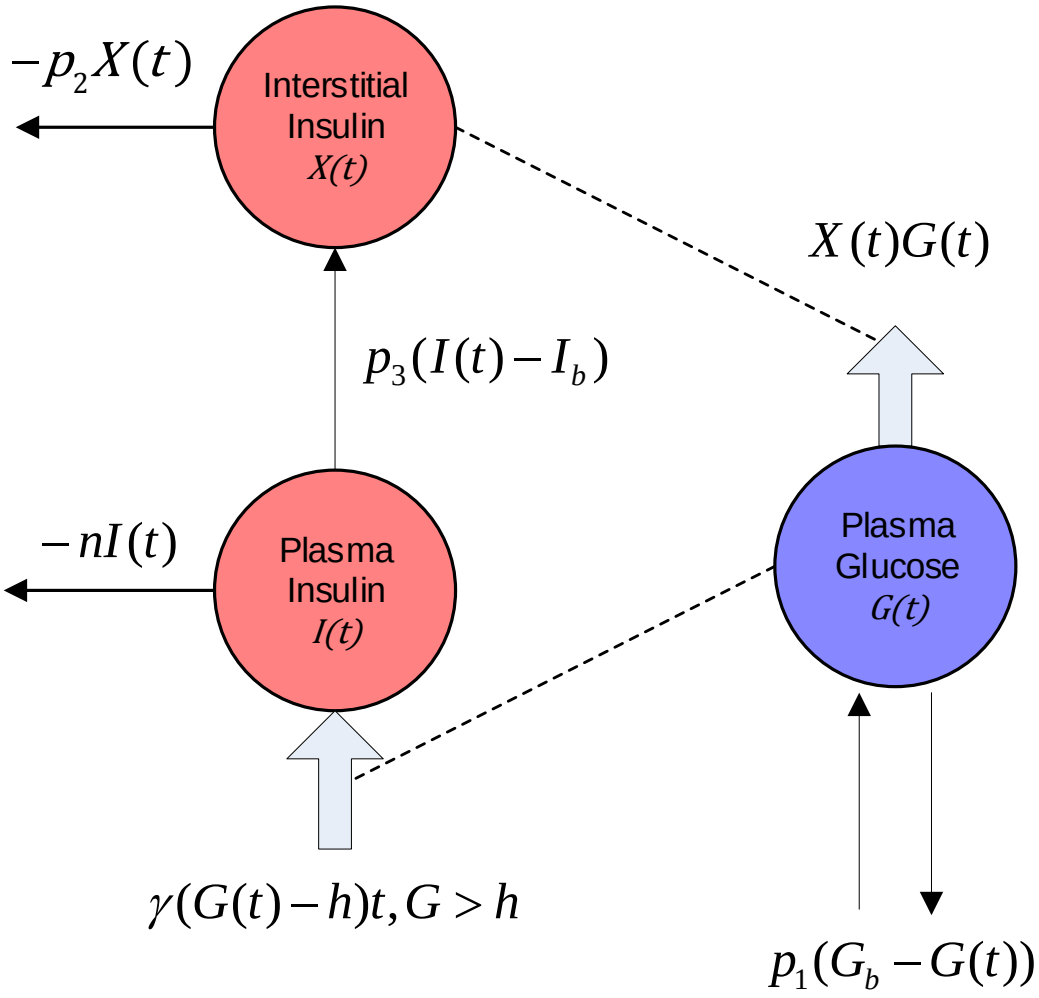

Figure 6.1: Minimal Model structure

The Minimal Model can produce results for insulin sensitivity, glucose effectiveness and insulin and glucose clearance. It can also be used to calculate the delay of insulin effect.

6.1.3 Equations

The Minimal Model is defined with the following equations:

$$\frac{dX(t)}{dt} = p_3(I(t) - I_b) - p_2X(t) \qquad 6.1$$

$$\frac{dG(t)}{dt} = X(t)G(t) + p_1(G_b - G(t)) \qquad 6.2$$

$$\frac{dI(t)}{dt} = \begin{cases} \gamma(G(t) - h)t - nI(t) & G \geq h \\ -nI(t) & G < h \end{cases} \qquad 6.3$$

where:

$G(t)$	plasma glucose
$I(t)$	plasma insulin
$X(t)$	interstitial insulin
p_1	glucose effectiveness (removal of glucose based on only glucose concentration)
p_2	clearance of interstitial insulin
p_3	insulin kinetic into the interstitial insulin compartment from the plasma insulin compartment
γ	secretion rate of the second phase of insulin
n	clearance rate of insulin
h	threshold value for insulin release.

Table 6.1: Parameters in the Minimal Model

The Minimal Model in standard control system state form, as defined in Chapter 2 , is given in equations 2.1, 6.2 and 6.3. Note that h used in the standard model

from Chapter 2, has been replaced by a *c* to avoid confusion with the h already used in equation 6.3 above.

$$\dot{x}(t,p) = \begin{cases} \begin{bmatrix} p_3(x_3(t,p) - I_b) - p_2 x_1(t,p) \\ -x_2(t,p)x_1(t,p) + p_1(x_2(t,p) - G_b) \\ \gamma(x_2(t,p) - h)t - nx_3(t,p) \end{bmatrix} & \mathrm{x}_2 \geq \mathrm{h} \\ \begin{bmatrix} p_3(x_3(t,p) - I_b) - p_2 x_1(t,p) \\ -x_2(t,p)x_1(t,p) + p_1(x_2(t,p) - G_b) \\ -nx_3(t,p) \end{bmatrix} & x_2 < h \end{cases} \qquad 6.4$$

$$g(x(t,p),p) = 0$$

$$C = \begin{bmatrix} 0 & 1 & 0 \\ 0 & 0 & 1 \end{bmatrix}$$

$$y = Cx(t,p)$$

$$x(0,t) = [0 \quad G_0 \quad I_0]$$

where $$x = (x_1, x_2, x_3) = (X, G, I)$$

The bolus glucose injection is the initial state of the glucose compartment therefore G_0 is the peak of the glucose profile. I_o is the first-phase insulin secretion, as the Minimal Model does not have a term for this.

To remove potential problems with symbolic tools and to fit in with the similarity transformation approach to structural identifiability, the t term in equation 6.4 is replaced by a fourth state, x_4, which simulates a ramp function. The "time" state is known and therefore seen as being observable. This produces equations 6.5.

$$\dot{x}(t,p) = \begin{cases} \begin{bmatrix} p_3(x_3(t,p) - I_b) - p_2 x_1(t,p) \\ -x_2(t,p)x_1(t,p) + p_1(x_2(t,p) - G_b) \\ \gamma(x_2(t,p) - h)x_4 - nx_3(t,p) \\ 1 \end{bmatrix} & x_2 \geq h \\ \begin{bmatrix} p_3(x_3(t,p) - I_b) - p_2 x_1(t,p) \\ -x_2(t,p)x_1(t,p) + p_1(x_2(t,p) - G_b) \\ -nx_3(t,p) \\ 1 \end{bmatrix} & x_2 < h \end{cases} \qquad 6.5$$

$$g(x(t,p),p) = 0$$
$$c = \begin{bmatrix} 0 & 1 & 0 & 0 \\ 0 & 0 & 1 & 0 \\ 0 & 0 & 0 & 1 \end{bmatrix}$$
$$y = cx(t,p)$$
$$x(0,t) = [0 \quad G_0 \quad I_0 \quad 0]$$

6.1.4 Improvements

Various approaches have been used in attempts to improve the model, which have achieved limited success in different situations. One example is the alteration of the time term to an integral term [113]. This removes the problem of having the insulin level increasing with time if plasma glucose (G) is greater than the threshold value for insulin release (h) as it integrates the glucose over a set amount of time causing a build-up.

6.2 Structural identifiability analysis of the Minimal Model

A full explanation of the methods for determining structural identifiability can be seen in Chapter 2 [17, 19]. Here, the Taylor series and similarity transformation approaches are applied to the Minimal Model to determine whether or not it is structurally identifiable.

6.2.1 Taylor series approach

6.2.1.1 Glucose and insulin as observables

Here we examine the Minimal Model with both glucose and insulin as observable functions. The unknown parameters, from equation 6.5, are p_1, p_2, p_3, γ, n and h. The known parameters, also from equation 6.5, are I_b, I_0, G_b and G_0.

It can be done by successively differentiating both glucose and insulin then using both of these sets of equations as this produces simpler equations than looking at each separately. The analysis was initially performed using Mathematica, see Appendix 2, to produce the following coefficients of derivatives, y_1 is glucose and $y_2$is insulin:

$$\begin{aligned} y_1(0) &= G_0 \\ y_1'(0) &= (G_b - G_0)p_1 \\ y_1''(0) &= -(G_b - G_0)p_1^2 + G_0(-I_b + I_0)p_3 \\ y_1'''(0) &= 2(G_b - G_0)(I_b + I_0)p_1p_3 - p_1(-(G_b - G_0)p_1^2 \\ &\quad + G_0(-I_0np_3 - (-I_b + I_0)p_2p_3) \end{aligned} \qquad 6.6$$

$$\begin{aligned} y_3(0) &= I_0 \\ y_3'(0) &= -I_0n \\ y_3''(0) &= \gamma(G_0 - h) + I_on^2 \\ y_3'''(0) &= -n(\gamma(G_0 - h) + I_0n^2) + 2\gamma(G_b - G_0)p_1 \end{aligned} \qquad 6.7$$

Mathematica solved this system of eight equations: the first four coefficients for both observations of glucose and insulin to yield unique solutions for p_1, p_2, p_3, γ, n and h. This proves the Minimal Model is globally structurally identifiable with glucose and insulin as observables and under the assumption that G_b and I_b are both known.

6.2.1.2 Glucose as the only observable

Here we consider the Minimal Model with glucose as the only observable function, i.e. $y = y_1$ which is glucose. To reflect this, c, from equation 6.5, must be replaced by:

$$c = \begin{bmatrix} 0 & 1 & 0 & 0 \\ 0 & 0 & 0 & 1 \end{bmatrix} \qquad 6.8$$

Again the unknown parameters, from equation 6.5, are p_1, p_2, p_3, γ, n and h. The assumed known parameters, also from equation 6.5, are I_b, I_0, G_b and G_0.

In this case, Mathematica was unable to produce a unique solution for the parameters, even when using 10 equations, see Appendix 2. Maple produced some solutions after 9 differentiations but not beyond that, also in Appendix 2. This suggests that, although both were ultimately unsuccessful, Maple was better than Mathematica at dealing with the complexity of differential equations in this situation; however this does not necessarily mean that it will be better for other problems of similar complexity.

As neither Mathematica nor Maple were able to obtain full solutions with a reasonable number of Taylor series coefficients, the problem was considered to be computationally intractable. The lack of solutions meant it was not possible to prove the identifiability of the system one way or the other using this technique, so a different approach was required to determine if the system was or was not structurally identifiable conclusively. For this reason, the similarity transformation approach was also applied and is detailed below.

6.2.2 Similarity transformation approach

6.2.2.1 Glucose as the only observable

Here we again consider the Minimal Model with glucose as the only observable function. As with the Taylor series approach above, c, from equation 6.5, must be replaced by:

$$c = \begin{bmatrix} 0 & 1 & 0 & 0 \\ 0 & 0 & 0 & 1 \end{bmatrix} \qquad 6.9$$

Again the unknown parameters, from equation 6.5, are p_1, p_2, p_3, γ, n and h. The known parameters, also from equation 6.5, are I_b, I_0, G_b and G_0.

The method for applying the Similarity Transformation Approach is described in Chapter 2. See Appendix 2 for the Mathematica implementation of the method.

As I_b and G_b are not known from the glucose and insulin observables, it is assumed that they will not be identifiable with glucose as the only observable.

With this in mind, the candidate smooth functions, μ, were chosen as follows to ensure simple computation (as described in Chapter 2):

$$\begin{aligned} \mu_1 &= x_2\,(glucose) \\ \mu_2 &= x_4\,(time) \\ \mu_3 &= \frac{d\mu_1}{dx} f(x,p) \\ \mu_4 &= \frac{d\mu_3}{dx} f(x,p) \end{aligned} \qquad 6.10$$

After checking the model fulfils the Observability Rank Criterion (ORC) for non-zero x, the candidate vector, H, is therefore:

$$H(p) = \begin{bmatrix} x_2 \\ x_4 \\ p_1(G_b - x_2) - x_1 x_2 \\ (-p_1 - x_1)(p_1(G_b - x_2) - x_2\big(-p_2 x_1 + p_3(-I_b + x_3)\big) \end{bmatrix} \qquad 6.11$$

The smooth mapping can be found by using the equation:

$$f\left(\lambda\left(x(t,\hat{p})\right),p\right)=\frac{\partial\lambda}{\partial x}f(x(t,\hat{p}),\hat{p}) \qquad 6.12$$

and rearranging it so it is equal to zero, then solving it. This gives the smooth mapping which is quite complex so it would be useful to simplify it. Evaluating at t = 0, γ and n cannot be zero, therefore there is only one valid solution. See Appendix 2 for the analysis for this model and the extraction of coefficients. The result is therefore that the model is structurally globally identifiable even with glucose as the only observable. This means that unique parameter values can be obtained from only glucose measurements, providing basal levels of glucose(G(0)) and insulin I(0) are known. In turn, this means it is possible, in theory to estimate parameters for the model using only glucose measurements and therefore to simulate insulin levels without direct measurements.

6.3 Stiffness of the Minimal Model

The idea of the stiffness of a system is introduced in Chapter 2. It is a measure of the range of timescales that a system operates in. Here we examine the stiffness of the Minimal Model using the method described in Chapter 2.

The Jacobian matrix, A as specified in equation 6.13, for the Minimal Model evaluated at time t = 0 is:

$$A=\begin{bmatrix}-p_2 & 0 & p_3 & 0\\ -G_0 & -p_1 & 0 & 0\\ 0 & 0 & -n & \gamma(G_0-h)\\ 0 & 0 & 0 & 0\end{bmatrix} \qquad 6.13$$

The corresponding eigenvalues are 0, $-n$, $-p_1$ and $-p_2$. These have average absolute values of 0, 0.10, 0.08 and 0.02 respectively, using values from [111]; however, for the purposes of stiffness, a zero eigenvalue is treated as $O(10^0)$ or one [9, 32] so the values will be treated as 1, 0.10, 0.08 and 0.02. Therefore the stiffness factor, SF as defined in equation 6.14 is:

$$SF = \frac{1}{0.02} = 50 \qquad 6.14$$

The stiffness factor is therefore $O(10^1)$ and hence the model can be considered non-stiff.

As an additional note, the Minimal Model has a discontinuity when G drops below h. As shown in equation 6.3, at this point the term $\gamma(G_0 - h)$ is not included in the model, which gives the Jacobian matrix as:

$$A = \begin{bmatrix} -p_2 & 0 & p_3 & 0 \\ -G_0 & -p_1 & 0 & 0 \\ 0 & 0 & -n & 0 \\ 0 & 0 & 0 & 0 \end{bmatrix} \qquad 6.15$$

As this term does not affect the eigenvalues, the stiffness is therefore not affected by the discontinuity.

6.4 Parameter fitting

6.4.1 Data

The data set used for parameter fitting was (AliceIVGTT) in Chapter 4. The data were obtained from anaesthetised Han Wistar rats (fed, fasted for 8 hours or 16

hours over-night) which were given a bolus injection of glucose (0.5 or 0.375mg/kg). Readings were taken at 1, 2, 5, 10, 15 and 25 minutes after the injection of glucose.

The data were transferred from the original spreadsheet format to a Microsoft Access database format. This made it easier to import into MATLAB and other packages as required for analysis.

6.4.2 Model function

As the Minimal Model is not stiff ($O(10^1)$) as shown above there is no requirement for an ODE solver that will solve stiff systems. Therefore, MATLAB's `ode45` solver was used (Chapter 2).

6.4.3 Error function

The error function is an important component in fitting as it determines how the fitting function "sees" the data. Therefore the better the error function is, the quicker and more accurate the fit will be.

The error function used was based on a weighted least squares method (Chapter 2) and is given in equation 6.16.

$$E = \sum_{i=0}^{n_g} \left(\frac{g_i - y_i}{g_i} \right)^2 + \sum_{j=0}^{n_i} \left(\frac{i_j - k_j}{i_j} \right)^2 \qquad 6.16$$

where g_i is the glucose data,$y_i$is glucose simulated, $i_j$is insulin data and k_j is the simulated insulin data As the glucose and insulin values were sometimes different in magnitude it was important to consider relative, rather than absolute, errors to avoid larger values disproportionately affecting the error function and therefore the parameter fit. Therefore, the output from the model function was weighted on the real data points in order to give glucose and insulin equal weighting in the fitting process.

6.4.4 Fitting function

The fitting function used was MATLAB's standard `fminsearch`, which is an implementation of the Nelder-Mead Simplex method. The function options were altered to reduce error tolerance of the results.

The Minimal Model only works with the initial value set at the peak insulin value hence, when fitting the data. With the data used, there is a value at time zero which is before the glucose bolus has had chance to affect the system hence it was necessary to remove the data point at time zero as the insulin peak had not yet been reached.

6.5 Results

6.5.1 Glucose and insulin as observables

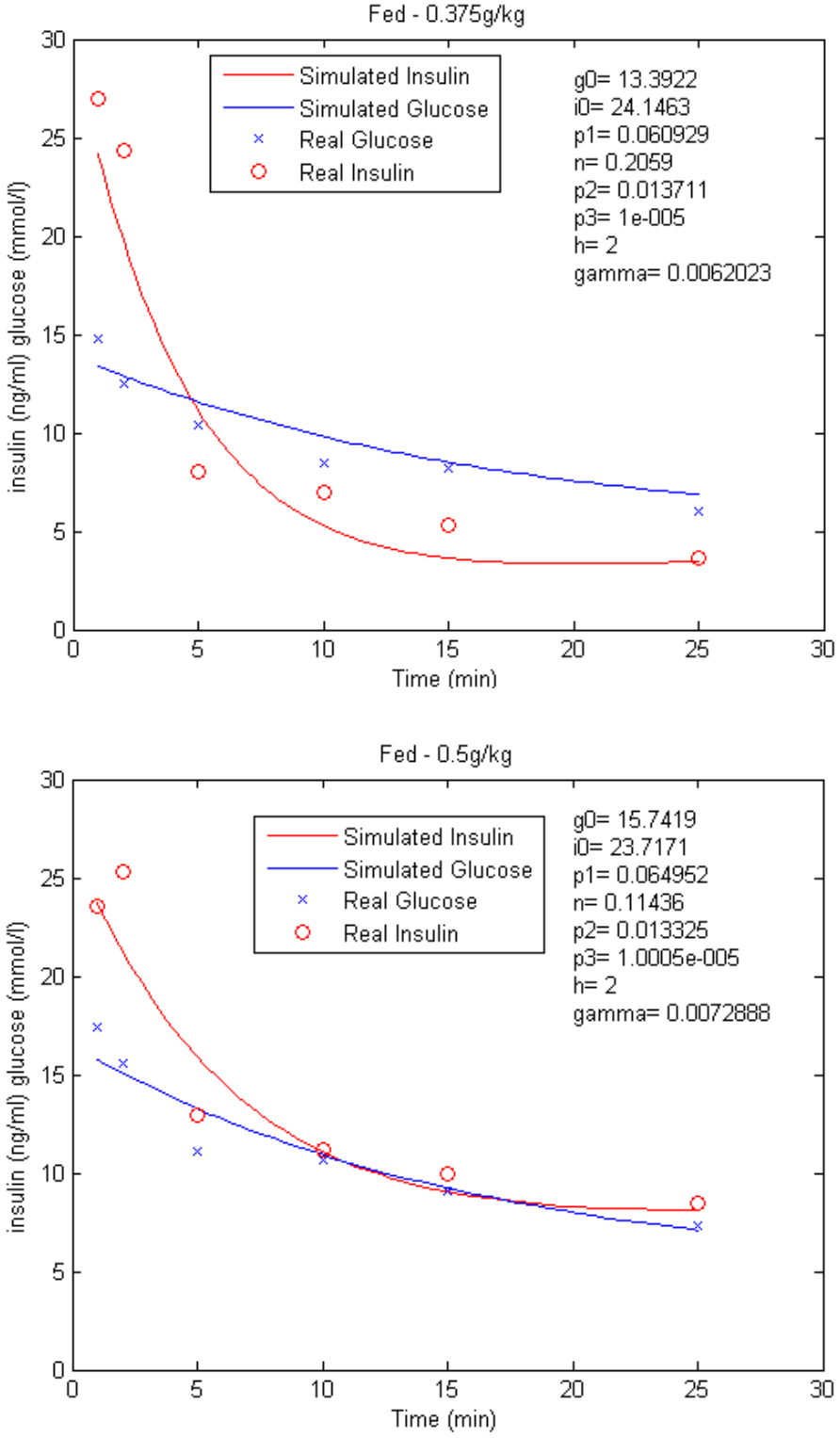

Figure 6.2: Examples of Minimal Model parameter fits

Group	g_0 (mmol/l)	i_0 (ng/ml)	p_1 (min-1)	n (min-1)	p_2 (min-1)	p_3 (min-1)	h (mmol/l)	γ (min-1)	Residual	Insulin sensitivity
8 Hour Fasted - 0.5g/kg StdDev	0.80	7.87	0.0156	0.0485	0.0233	0.0000076	6.57	0.00202	0.20	1.3819
8 Hour Fasted - 0.5g/kg Average	14.22	9.90	0.0876	0.0663	0.0154	0.0000194	8.65	0.00522	1.34	0.8010
Fed - 0.375g/kg StdDev	0.53	4.80	0.0193	0.0373	0.0064	0.0000033	0.00	0.00111	1.88	0.8303
Fed - 0.375g/kg Average	13.16	19.82	0.0792	0.1673	0.0054	0.0000117	2.00	0.00606	4.60	0.4202
Fed - 0.5g/kg StdDev	0.27	3.02	0.0278	0.0245	0.0075	0.0000164	1.05	0.00677	0.62	2.2161
Fed - 0.5g/kg Average	15.76	22.34	0.0959	0.1382	0.0047	0.0000195	3.05	0.01359	2.83	1.2876
O/N fast - 0.5g/kg StdDev	2.49	2.23	0.0064	0.0468	0.0163	0.0000021	1.66	0.00567	1.51	0.0037
O/N fast - 0.5g/kg Average	13.80	6.40	0.0925	0.1050	0.0183	0.0000110	4.75	0.00598	1.99	0.0025
Grand StdDev	1.60	8.08	0.0172	0.0527	0.0142	0.0000084	3.72	0.00515	1.76	1.2023
Grand Average	14.13	14.40	0.0884	0.1216	0.0110	0.0000148	4.44	0.00747	2.78	0.5683

Table 6.2: Parameter Fitting Results (Groups)

Group	g_0 (mmol/l)	i_0 (ng/ml)	p_1 (min-1)	n (min-1)	p_2 (min-1)	p_3 (min-1)	h (mmol/l)	γ (min-1)	Residual	SI - Insulin sensitivity
Fed Average	14.3	20.9	0.0863	0.155	0.0051	0.000015	2.45	0.00929	3.84	0.345
Fed StdDev	1.45	4.05	0.0229	0.0337	0.0063	1.06E-05	0.83	0.00566	1.67	0.905
Fasted Average	14.0	7.9	0.0904	0.0884	0.017	1.46E-05	6.42	0.00565	1.71	0.568
Fasted StdDev	1.84	5.16	0.0104	0.048	0.0178	6.42E-06	4.48	0.0042	1.13	1.2
Grand Average	14.1	14.4	0.0884	0.122	0.011	1.48E-05	4.44	0.00747	2.78	0.345
Grand StdDev	1.6	8.08	0.0172	0.0527	0.0142	8.44E-06	3.72	0.00515	1.76	0.905
T-Test (Two Tailed homoscedastic)	0.748	0.0002	0.676	0.0125	0.134	0.935	0.0582	0.2		0.5

Table 6.3: Parameter Fitting Results (fasted and fed groups)

Recall from the Structural identifiability analysis of the Minimal Model section above, the unknown parameters were p_1, p_2, p_3, γ, n and h. See Table 6.2 and Table 6.3.

p_1 (glucose effectiveness). The value obtained across the whole group was indeed consistent at 0.088 min^{-1} (SD 0.017), showing little variation in comparison to other parameters, indicating that other factors created the different insulin and glucose profiles. However, the magnitude of this value means that it does play a part in the dominant glucose disposal.

6.5.1.1 Glucose

G_0 (initial glucose concentration). This is fitted to the first data point. A point of contention here is that if the peak was missing when sampling the data, this value would be incorrect.

A way to improve this would be to use the quantity of glucose injected with the volume of distribution to obtain an estimate for the total quantity of glucose.

6.5.1.2 Insulin

I_0 (initial insulin concentration). Little variation within groups and this is fitted to the first data point. It may have missed the peak due to no instantaneous measuring. The same problem arises as it may be missing the peak. The insulin secretion in fasted animals is far lower than in fed animals.

n (clearance rate of insulin). This varied between fed and fasted animals, being higher in the fed animals than in the fasted animals. This is an interesting observation, that will be gone into in more depth in Chapter 7.

h (threshold level at which insulin is secreted ; i.e. insulin is secreted only if the glucose is above this level). Most of the subjects did not reach basal levels so they may not have reached this threshold. *h* also has a effect on insulin secretion, that is the smaller the value of *h* the greater the insulin secretion.

γ (secretion rate of insulin). This was not statistically different between groups (see Table 6.3).

6.5.1.3 Interstitial insulin dynamics

p_2, p_3 (clearance rate of insulin and insulin kinetic into the interstitial compartment from the plasma insulin compartment). The lack of data points could account for the large variation in values seen for these two parameters. p_2 and p_3 are used to create the Insulin Sensitivity, *SI*, however with the large variation in these fitted parameter values it is not possible to achieve a reliable *SI* value.

This is not as expected as the purpose of insulin is to affect glucose, however this was not seen. This may be a problem with applying the model to an IVGTT, a problem with the parameter fit (i.e. that the minimum is local and not global) or

a problem with the model more generally. It is therefore important to clarify this matter by checking a sensitivity analysis (see section 2.7).

6.5.2 Glucose as the only observable

To simulate having glucose as the only observable was simply a matter of removing insulin from the error function. This effectively means that the optimisation technique cannot "see" the insulin, but the model will still produce the predicted insulin output for inspection.

However, this did not predict any realistic insulin results as neither the shape of the curve or the values were close, showing that it is necessary to have the insulin data in order to achieve a good model fit. The problem lies in the fact that the p_2 and p_3 parameters are sensitive to the number of glucose data points available.

An additional problem is that it may not be possible to obtain an accurate view of insulin from this test by looking only at glucose measurements. This is likely to be due to the level of insulin in the rats at the start of the experiment making very little difference to glucose decay, as it has reached saturation and glucose effectiveness is playing the main role in removing glucose.

Even though the model was structurally identifiable in this situation, this does not prove that it is necessarily possible. If the model had been structurally unidentifiable, the parameters would not have had a unique solution and,

therefore, they would have been meaningless and the insulin output may have been incorrect.

6.6 Sensitivity Analysis

The sensitivity analysis was performed in Berkley Madonna [1] using a basic technique of taking the average of fitted parameters then modelling with parameter values an order of magnitude smaller and an order of magnitude larger. This should ensure that the whole range of likely values is covered and gives an idea of how accurate the parameters will be from visual inspection if they change subtly.

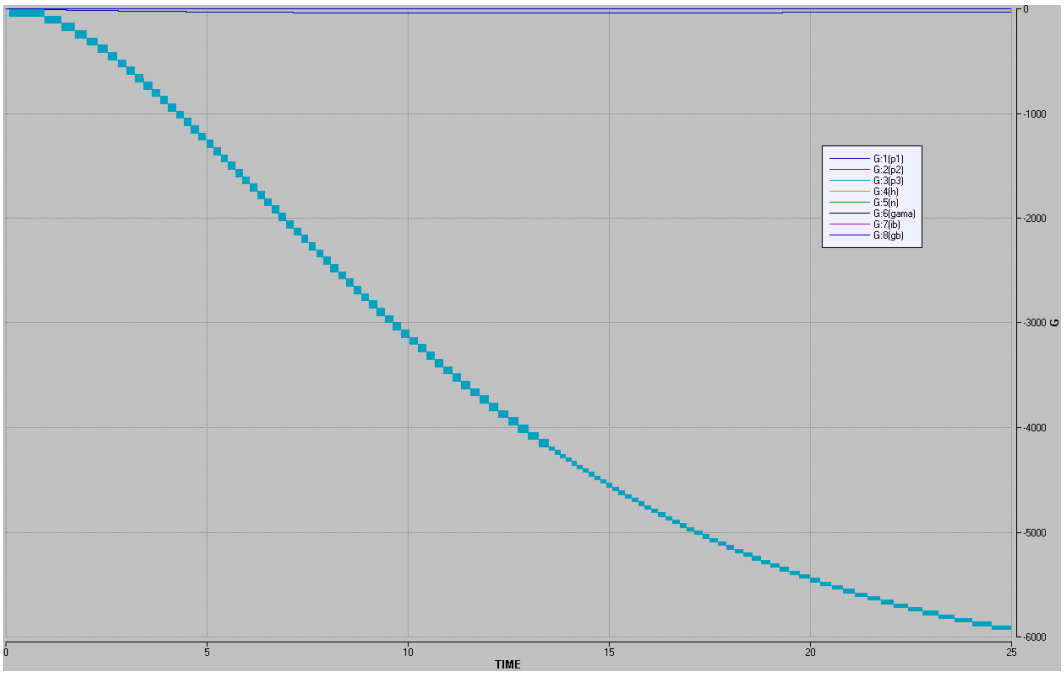

Figure 6.3: Relative sensitivity analysis of glucose with all parameters (time in minutes)

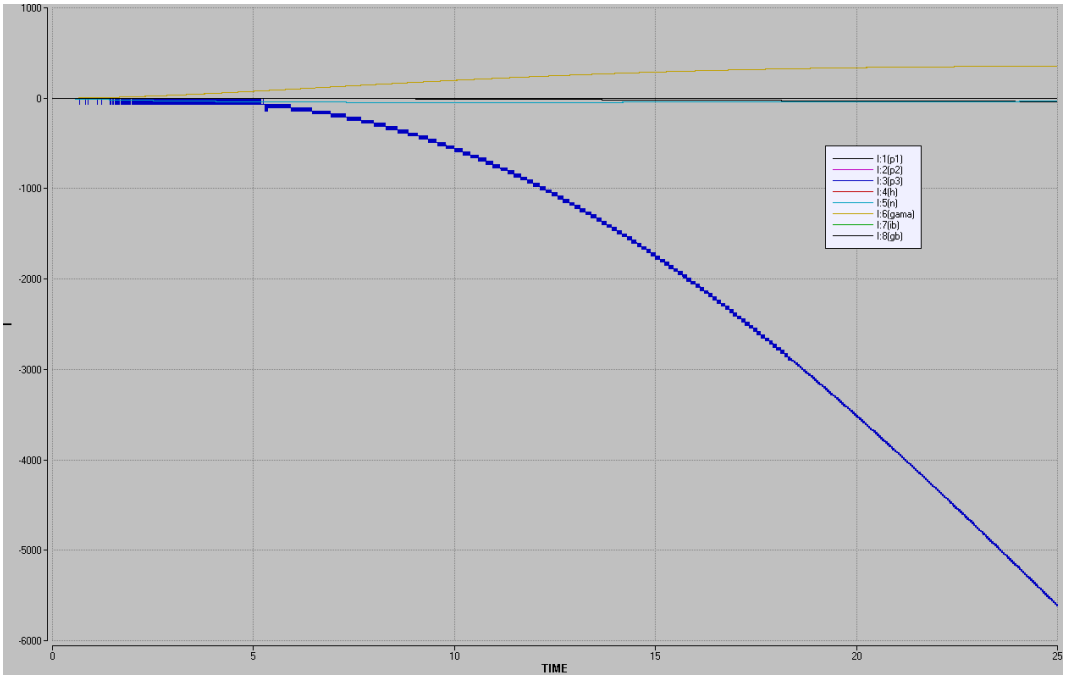

Figure 6.4: Relative sensitivity analysis of insulin with all parameters(time in minutes)

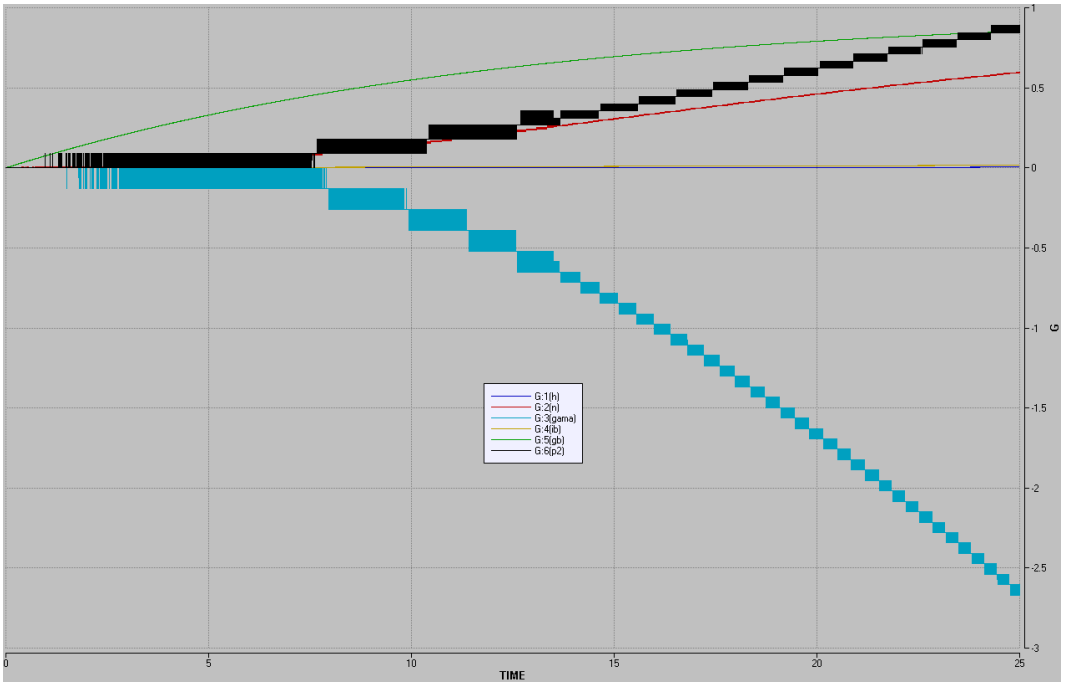

Figure 6.5: Relative sensitivity analysis of glucose with all parameters except p1 & p3(time in minutes)

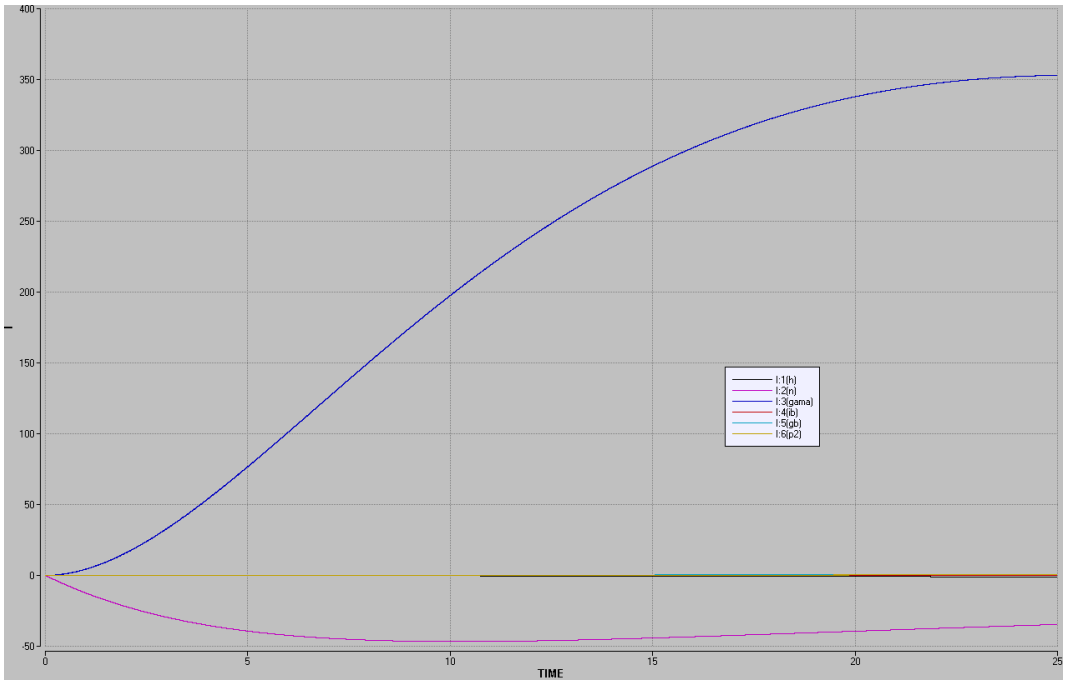

Figure 6.6: Relative sensitivity analysis of insulin with all parameters except p1 & p3(time in minutes)

Figure 6.2 – Figure 6.6 show the results from relative sensitivity analysis. The parameters have affected the different compartments as follows:

The glucose compartment is affected by G_0 as it has a clear and direct effect on the starting level of glucose. The effects are dramatic when the order of magnitude is changed. The glucose maintains an exponential decay from its starting point, however the insulin response is even more dramatic with the second phase response being altered greatly. In addition, p_1 has a large effect on glucose, though not as much as G_0, so it also effects the insulin second phase response (see Figure 6.3 and Figure 6.6).

The insulin compartment is largely affected by I_0 but only has a limited effect on glucose. This is to be expected as the insulin profile in an IVGTT test happens rapidly, plus the insulin may be at saturation. Moreover *n* and *h* have a great effect on insulin, but only a very small effect on glucose. Furthermore γ has a large effect on insulin secretion, in particular in the second phase insulin curve (see Figure 6.4 and Figure 6.6).

p_2 has almost no effect on glucose or insulin, hence its value will not be found reliably in the parameter fitting. p_3 subtly alters the glucose and, to a lesser extent, the insulin response. In order to achieve an accurate result, very accurate results from a large number of data points would be needed.

6.6.1 Conclusions

Parameters sensitive to change: G_0, p_1, I_0, h, n, γ.

Parameters less sensitive to change: p_2, p_3.

It is necessary to know the parameters that are sensitive to change as this confirms the variation in the parameter fitting results and shows that the parameters which are sensitive to change can be picked up by the parameter fitting. As small changes in parameters can make a big difference to the results, the smaller the range that the sensitive parameters can realistically range over the smaller the variation in the results.

Changes in the parameters p_2 and p_3 do not show much change in the glucose or insulin responses so obtaining highly accurate values for them is questionable. In the case of an IVGTT, the insulin may be having its maximum effect, hence the insulin profile will have only a subtle effect on the glucose dynamics. From this perspective, it is correct that these parameters are reliant on subtle changes in the glucose and insulin profiles.

This also shows why the glucose-only observations did not work very well. In this situation the model was structurally identifiable which meant that there was the possibility of finding a unique set of parameter values that would have returned the correct insulin. However, it does not guarantee it. As parameter value changes in the insulin section of the model do not affect the glucose greatly, there is effectively not enough information contained in the glucose measurements alone to be able to obtain accurate insulin results.

All of these comments relate specifically to the Minimal Model; alternative models with a different structure may produce different results and it may still be possible to obtain insulin values with glucose-only observations.

6.7 Overall Summary

6.7.1 Conclusions Between Groups

Between the fed and fasted groups the only parameters that show statistical significance are I_0 and n. This means that the first phase insulin secretion and

clearance rate of insulin are different between the 2 groups. This issue is investigated when we take into account C-peptide as detailed in Chapter 7.

6.7.2 General Conclusions

The Minimal Model has been shown to be uniquely structurally identifiable with both glucose and insulin measurements. It has also been shown to be uniquely structurally identifiable with only glucose measurements. Both of these statements have the caveat that basal insulin and glucose levels must be known; however, in the experiments where the Minimal Model is used (i.e. IVGTT) this is always the case.

Although the system is structurally identifiable with glucose measurements only, the low sensitivity of the effect of insulin on glucose causes a failure to produce realistic insulin results.

In the parameter fits performed here, the main driver for glucose disposal was glucose effectiveness. This could be attributed to several causes:

- the IVGTT may not be a good experiment to measure insulin sensitivity due to the fast rate of glucose disposal;
- the model may have fitted a local minimum where glucose effectiveness was dominant, but there could have been other local minima with high insulin sensitivity and low glucose effectiveness;

- there could be an issue with the model design as it may not be physiologically relevant.

Chapter 7: C-peptide Deconvolution and Modelling

As C-peptide and insulin are secreted in equal molar quantities, as explained in Chapter 3, insulin secretion can be calculated using deconvolution of C-peptide concentrations. Methods of deconvolution used in this thesis, and explained here, are the Maximum Entropy method and the technique employed in WinNonLin. Whereas 100% of C-peptide is observed when measuring peripherally as none is absorbed by the liver, as shown through the work deconvolving C-peptide presented in this chapter, less than 100% of insulin leaving the pancreas is observed when trying to measure peripherally after the liver. Deconvolving data from IVGTTs and hyperglycaemic clamps shows that the fraction of insulin leaving the pancreas when measured peripherally after leaving the liver can be anywhere between 7% and 58%, depending on the subject and the deconvolution method used. For example, the Maximum Entropy method produced fractions of 38% for fed animals and 19% for 8-hour fasted ($p < 0.05$) while the WinNonLin method produced values of 36% for fed animals and 16% for 8-hour fasted ($p < 0.005$). The data also show there is a variable clearance rate depending on the level of fasting of the animals; it is hypothesised in this chapter that this is down to a change in hepatic blood flow.

7.1 Introduction

Insulin is cleared primarily by the liver [133], which is fed by two blood vessels – the hepatic artery and the hepatic portal vein [134]. Hepatic blood flow is known to change for a variety of reasons, for example exercise and food intake [72]. Insulin clearance rates are also known to change, a large variety of factors affect this [103, 129, 135, 136] ; as insulin is cleared by the liver, it is hypothesised here that there is a connection between hepatic blood flow and insulin clearance rate.

In order to measure insulin concentration as it appears directly from the pancreas it is necessary to sample from the portal vein, into which the pancreas feeds [134]. This is an intricate and invasive procedure and it is therefore difficult to measure insulin secretion directly, particularly in a clinical setting [137]. Additionally, the variable rate of insulin clearance makes it complicated to model accurately; other models presented in Chapter 5 do not take into account the changes in clearance rate.

Accurate values of insulin concentration produced by the pancreas are necessary to establish insulin sensitivity [133]; without knowing how much insulin was originally present in the system, it is not possible to say accurately how much glucose is cleared per unit of insulin and therefore to calculate insulin sensitivity. Insulin sensitivity is important both for determining how effective a drug is at improving glucose uptake and for tracking disease progression in diabetic patients.

Some studies have found that the insulin clearance rate can be considered to be a constant under certain conditions. For example, Bergman found that the fraction of insulin cleared as it passes through the liver, known as the hepatic extraction ratio, is 33.4% ± 0.1 for an IVGTT and 64.5% ± 3.6 for an OGTT [59]. While this may be useful for simplifying calculations, it does not provide an explanation for what is happening mechanistically or allow us to predict what will happen in other situations.

Insulin secretion must be determined to establish the relationship between glucose concentration and insulin secretion. This has been attempted in several previous models, each with their own different approach. The Minimal Model only simulates second-phase insulin response and for the first-phase response it uses the initially measured insulin level [113]. Cobelli used a combination of the Minimal Model's approach and the derivative of glucose concentration from work by Mari to establish a relationship between glucose concentration and insulin secretion [80, 123].

In order to produce an accurate model of insulin secretion for future use in this work, it is important to have an accurate relationship between glucose and insulin

7.2 C-peptide

As explained in Chapter 3, insulin is synthesised in the ß-cells in the islets of Langerhans in the pancreas. It is held in granules as pro-insulin, an inactive form.

When pro-insulin is activated, C-peptide is cleaved from it by carboxypeptidase and a series of prohormone convertases [54]. This results in C-peptide and insulin release into the hepatic portal vein in equal molar quantities.

An important feature of C-peptide is that it is cleared by the kidneys at a constant rate [57, 138]. As C-peptide is produced at the same rate as insulin, it is possible to calculate insulin clearance from C-peptide concentration using a technique called deconvolution, which is explained in the Deconvolution section below.

7.3 Deconvolution

Convolution is a mathematical operator on two functions which produces a third, often considered to be a modification of one of the original functions. This can be viewed as "filtering" one function through another. Convolution is mathematically defined as follows:

$$y(t) = u(t) * f(t) = \int_0^\infty u(t-\tau) f(\tau) d\tau \qquad 7.1$$

where y is the output of the system, u is the input to the system, f is the system impulse response and $*$ is the convolution operator.

Deconvolution is the reverse process where, given the output, y, and usually the system impulse response, f, the input, u, can be found. This is very useful in

mathematical models of biological systems where, given the output (y) and system equations (f), deconvolution can be used to establish the input (u).

In the case presented here, the output is the measured C-peptide concentration which is deconvolved to calculate the original insulin secretion. Two methods of deconvolution are used in this thesis and described below: the Maximum Entropy technique and the technique employed in the software package WinNonLin. These were selected as they have been successfully applied to biological systems previously [139, 140] and, as results from different deconvolution can vary, using two methods allows for comparison of results.

7.3.1 Maximum Entropy

A lot of the original work using maximum entropy was based on applications in astrophysics, looking at far away objects and correcting for telescopic lenses and gravitational lensing [141, 142], but it also has noted applications in biomedical systems [143]. A review of six different deconvolution techniques applied to certain well-accepted pharmacokinetic models and data was performed by Madden, et al., which noted the advantages of certain types of deconvolution approaches over others [144].

Entropy in this context is a measure of the amount of information or uncertainty in a signal. The Maximum Entropy technique seeks to minimise assumptions about a signal, while constraining the result to the observed signal, by maximising entropy.

7.3.1.1 Method

The standard continuous measure for entropy, *S*, is:

$$S = \sum_{n=1}^{N} p_n \ln (p_n) \qquad 7.2$$

where p_n is the probability of an event occurring. This can be adapted to form a discrete measure of entropy for a piecewise step input function:

$$u(t) = \sum_{n=1}^{N} u_n I_n \qquad 7.3$$

where $I_n(t) = \begin{cases} 1 & if\ t \in [t_n, t_{n+1}) \\ 0 & elsewhere \end{cases}$ which is combined with equation 7.2 to produce:

$$x_n = \frac{u_n}{\sum f_n}$$
$$S = \sum_{n=1}^{N} x_n \ln \left(\frac{x_n}{r_n}\right) \qquad 7.4$$

where x_n is the normalised value of the input for the n^{th} sample and r_n is the base-line value of the input and is calculated using a nearest neighbour average (i.e. $(x_{n-1} + x_{n+1})/2$). The inclusion of r_n smoothes the function x to make the signal more "natural" by removing any sharp spikes. The input is considered to be always positive as a negative input function would be nonsensical biologically.

This entropy function is used as the objective function for the optimisation algorithm. The input function in 7.3 is convolved with the system equations to produce the output function. The output function is then constrained against the real data. The constraining function is the χ^2 constraining function:

$$\chi^2 = \sum_{i=1}^{N} \frac{(x_i - h_i)^2}{{\sigma_i}^2} \qquad 7.5$$

where $$E(\chi^2) = N$$

and where *E* is the expected value, *N* is the number of samples, x_i is the measurement, h_i is the predicted value and σ_i is the weighting, as this can be seen as a weighted least squares estimator (see Chapter 2).

This is fed into a constrained optimisation algorithm, in this case the MATLAB `fmincon` method, which uses a quadratic programming sub-problem coupled with calculation of the Hessian of the Lagrangian via the BFGS formula [4, 139, 145].

This Maximum Entropy implementation has been tested and used successfully by others [139, 145, 146].

7.3.2 WinNonLin

WinNonLin [5] is a tool widely used in the pharmaceutical industry for the modelling of pharmacokinetic processes and systems. It incorporates a method of deconvolution that takes a linear system for drug kinetics and calculates the

input rate to the system. This is commonly used for estimating gut absorption rates and bioavailability of a drug from IV and oral drug dose profiles. The software is designed specifically for biological systems and is accepted and approved by the FDA (Food and Drug Administration), making it very appropriate for this application.

7.3.2.1 Method

The WinNonLin method is described in detail in the documentation of WinNonLin [5]. The basic concept is explained here.

The WinNonLin deconvolution technique is an optimisation process, as is the Maximum Entropy technique; however unlike Maximum Entropy, which sets up data points and interpolates between them, it sets up an input function to the system. The input to the system is described as a piecewise linear "precursor" function of the following form:

$$f_p(t) = \sum x_j h_j(t), x \geq 0 \qquad 7.6$$

$$\text{where } h_j(t) = \begin{cases} \frac{t-T_j}{T_{j+1}-T_j} & T_j < t < T_j \\ \frac{T_{j+2}-t}{T_{j+2}-T_{j+1}} & T_{j+1} < t < T_{j+2} \\ = 0 & otherwise \end{cases}.$$

The optimisation is performed by varying the weights, x_j. $T_0 \ldots T_{j+2}$ are the time points at which observations are taken plus one point at time zero and another half way to the first point to allow for an initial peak at the start. This allows the

system to simulate a rapid absorption rate at the start, which is common in drugs being absorbed though the gut.

This function is then convolved with a "dispersion" function which acts as a smoothing function. It is a normalised decaying exponential of the form:

$$f_d = \frac{e^{-\frac{t}{\delta}}}{\delta} \qquad 7.7$$

where δ is a smoothing coefficient.

This effectively creates a smoothed curve function with *n*+2 points, where *n* is the number of data points.

The WinNonLin deconvolution method was implemented in MATLAB; this made use of MATLAB's own optimisation and simulation functions, which may be different to WinNonLin's. However, the results from the MATLAB implementation were found to be very similar to those from WinNonLin (see Deconvolution Results below). The method for finding residuals in WinNonLin is not explained in the manual, so least squares was selected as the most appropriate. The implementation of this in Appendix 3.

7.4 Data Collection

In order to apply these two methods the system model needs to be known. Most modellers use one particular C-peptide model [57], which is a linear two-compartmental model with first order clearance (Figure 7.1). From these models

we can assume this system to be linear so the impulse response is required. It is also necessary to know the parameter values for the model. This was achieved using an intravenous C-peptide injection and fitting the parameters in acslX using a PKPD toolkit developed at AstraZeneca.

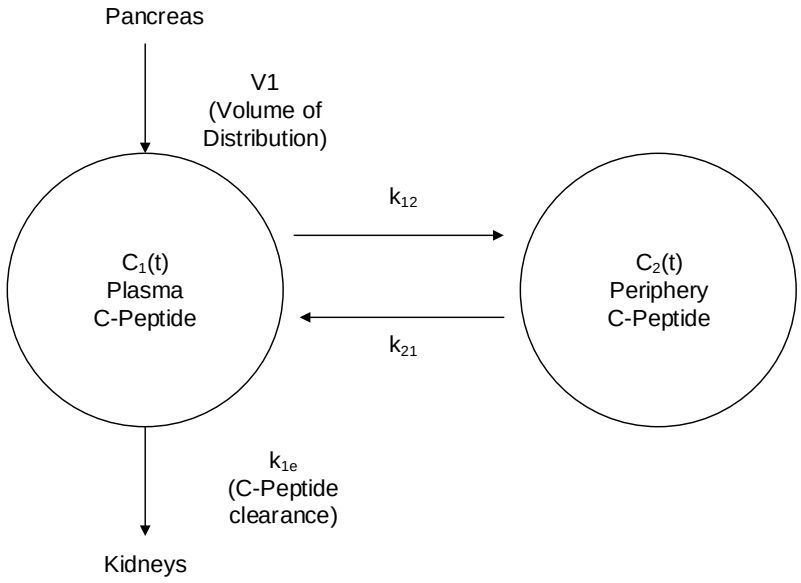

Figure 7.1: C-peptide kinetic compartmental model

Doses of 6nmol/ml (n=3),3nmol/ml (n=3),0.8nmol/ml (n=2) C-peptide were administered and measurements taken at 1, 2, 5, 10, 15, 20, 25 and 30 minutes, see (RuthCPeptide) from Chapter 4. The mean of the parameter values were used for deconvolution, see Figure 7.2 and Table 7.1.

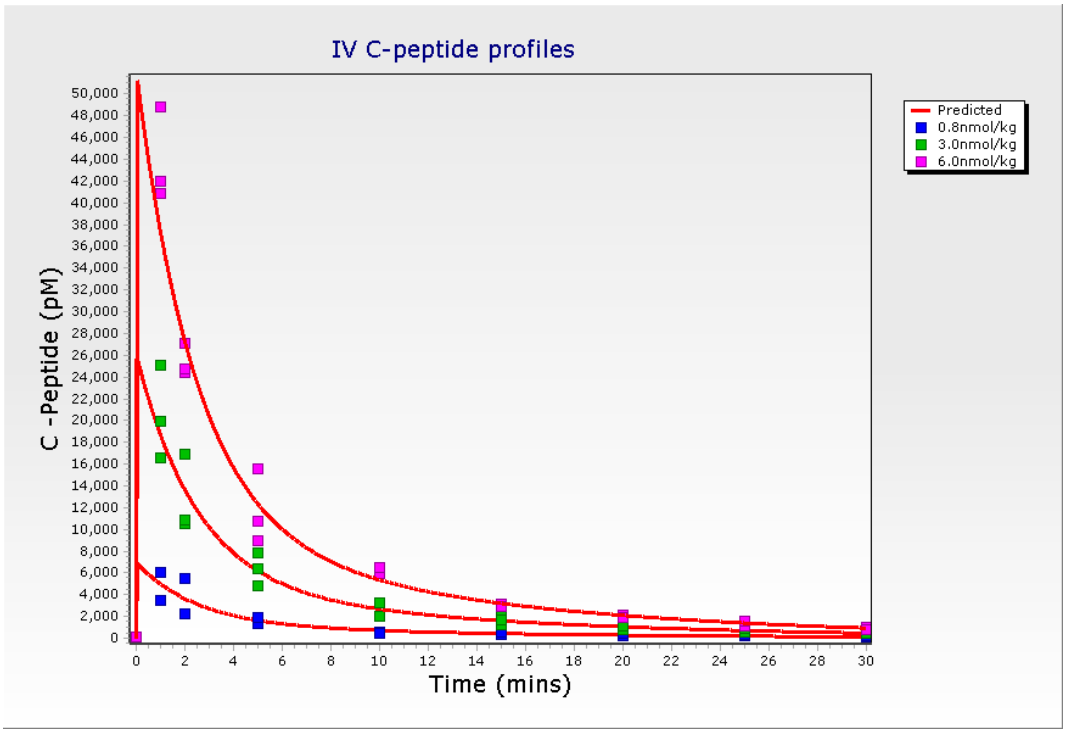

Figure 7.2: Parameter Fits of C-peptide

Parameter	Final	Std.Dev.	%Covariance
V1	0.0796	0.0038	4.75
K21	0.2540	0.0095	3.73
K12	0.3410	0.0101	2.95
KE	0.3150	0.0089	2.84

Table 7.1: C-peptide fitted kinetic parameters

The data used for deconvolution were collected from a series of different experiments: conscious and anaesthetised; ad-lib fed, 4-hour fasted and 8-hour fasted; and IVGTT and hyperglycaemic clamps. These are contained in the data sets (AliceIVGTT), (GeorgiaIVGTT) and (RuthClamp) (see Chapter 4).

7.5 Deconvolution Results

Data from these studies were deconvolved using the two techniques described above. Full results are given in Appendix 3. Presented below, in Figure 7.3 and Figure 7.4, are typical examples of deconvolution outputs for IVGTT and hyperglycaemic clamp experiments respectively.

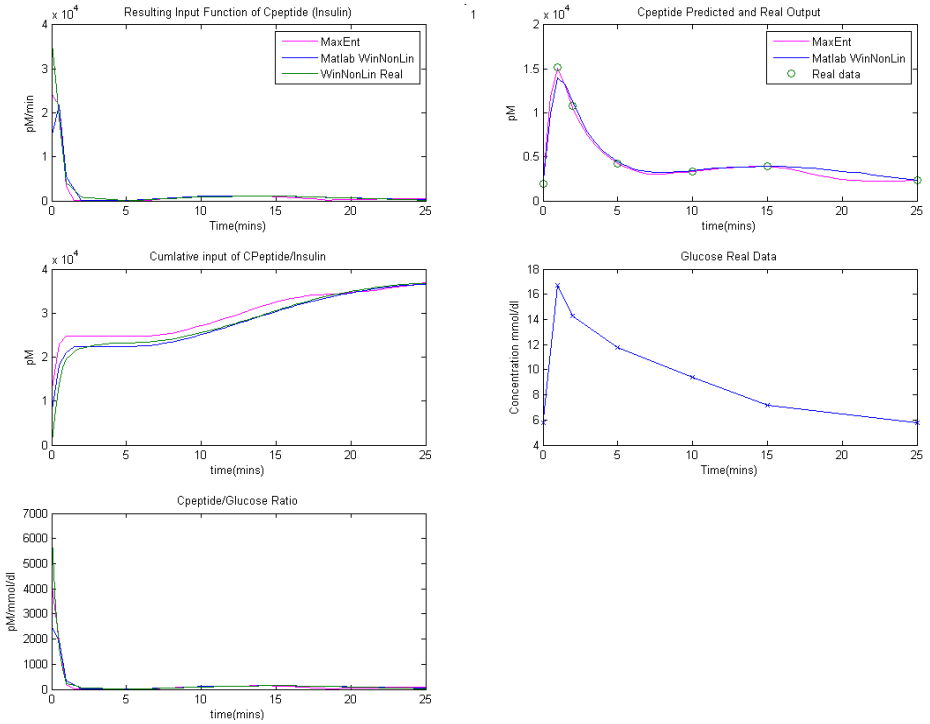

Figure 7.3: Deconvolution of IVGTT data from rat 1 in (AliceIVGTT) (fed Han Wistar rat) from the original WinNonLin method, the WinNonLin MATLAB method and the Maximum Entropy method

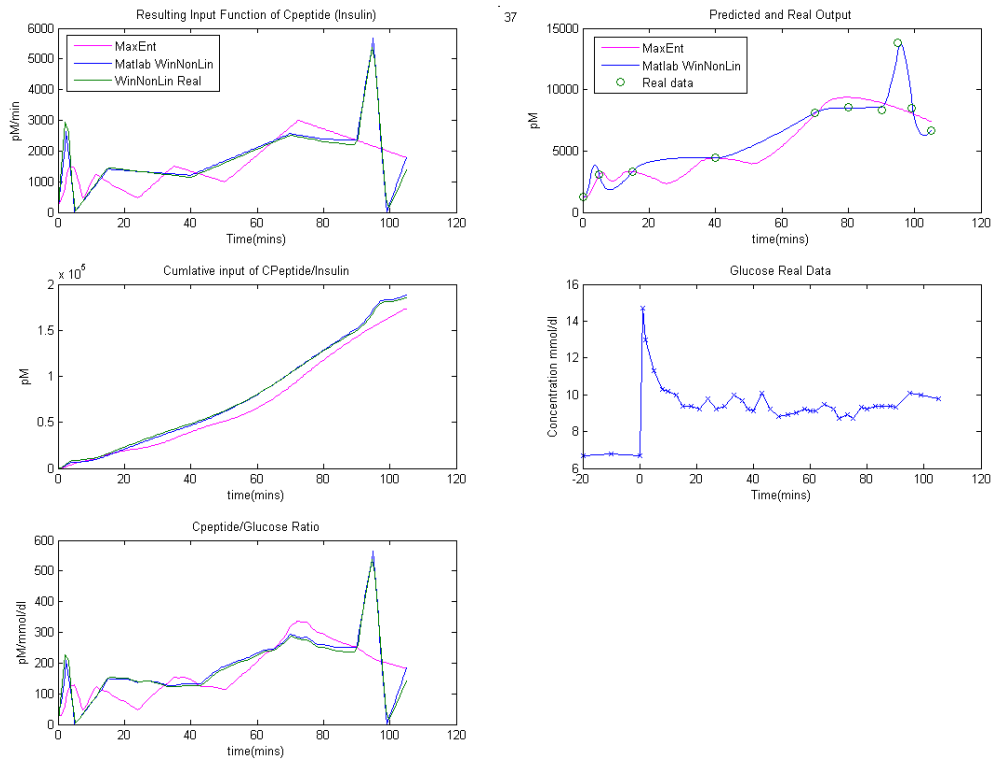

Figure 7.4: Deconvolution of hyperglycaemic clamp data from rat 37 in (RuthClamp) (fed Han Wistar rat) from the original WinNonLin method, the WinNonLin MATLAB method and the Maximum Entropy method

As the fundamental techniques used for both the WinNonLin deconvolution and the MATLAB implementation of the WinNonLin deconvolution are the same, they produce very similar results; any errors can be explained by differences in the ODE solvers and optimisation techniques used. The results from both of these are approximately identical and therefore the MATLAB implementation is used for the remainder of the data analysis.

Both the Maximum Entropy and WinNonLin techniques produce similar deconvolution outputs and also predict approximately the same level of insulin secretion. The data in Appendix 3 show that in 80% of cases WinNonLin produced higher values for insulin secretion than the Maximum Entropy technique. However, there was a maximum difference of 36% with the average difference between the values being only 8%.

Figure 7.3 and Figure 7.4 also show the glucose levels in each rat and the ratio between C-peptide (insulin secretion) and glucose concentrations. This is useful as it shows the relationship between the pancreas and glucose levels when secreting insulin. From these graphs, it is important to note that the relationship is not proportional. It also shows that a large quantity of glucose in an IVGTT does not cause saturation in insulin secretion; in fact, a larger than proportional secretion occurs.

It can also be seen, for both the IVGTT and the hyperglycaemic clamp experiments, that there is an increase in insulin secretion after sustained high

levels of glucose. This is particularly apparent for the hyperglycaemic clamp data, where glucose remains roughly constant while the ratio between glucose and insulin secretion increases. This information is used later to develop a short-term model of the glucose-insulin system.

Finally, it is clear that from around 90 minutes into the hyperglycaemic clamp there is a sudden increase in insulin secretion. This is in fact down to arginine being injected, as described in Chapter 4, and therefore has little to do with glucose concentrations.

7.6 Insulin clearance

As C-peptide is secreted in the same molar quantity as insulin, working out the C-peptide secretion rate gives the corresponding insulin secretion rate. When the IVGTT and hyperglycaemic clamp experiments were performed, plasma insulin concentrations were also measured; it is therefore possible to calculate the amount of insulin that appears and the clearance rate of insulin. This is done by fitting a simple one-compartmental model (Figure 7.5) described by the differential equation in equation 7.8.

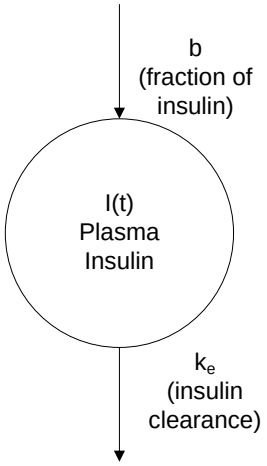

Figure 7.5: Diagram of simple insulin clearance compartmental model

$$\frac{dI(t)}{dt} = -k_e I(t) + b.u(t) \qquad 7.8$$

where I is plasma insulin, k_e is insulin clearance (min^{-1}), b is the fraction of secreted insulin that is observed after the liver in the periphery and u is the input function obtained from the C-peptide deconvolution.

This was fitted in MATLAB using MATLAB's unconstrained fitting algorithm, `fminunc` [36]. The fitting algorithm used transforms of the parameters to create upper and lower bounds [147, 148] using the following equations:

$$p(\hat{p}) = \frac{l + ue^{\hat{p}}}{1 + e^{\hat{p}}}, l < u$$

$$\hat{p} = log\left(\frac{p - l}{u - p}\right), l < u \qquad 7.9$$

where p is a parameter, $\hat{p}$ is the transpose parameter used by the optimisation algorithm, l is the lower bound and u is the upper bound.

The unconstrained fitting algorithm was selected because MATLAB's constrained fitting algorithm tended to find local minima around the constrained points. The model itself was simulated using the numerical algorithm `ode45` as this is not a stiff system. The error function used was Weighted Least Squares, as detailed in Chapter 2, with weighting based on real data. The use of Generalised Least Squares, also in Chapter 2, as the error function was attempted, however this also tended to lead to local minima; this was due to the fact that parameters a long way off from the true minima caused the value of the error function to show little difference between different incorrect values of parameters.

7.6.1 Results

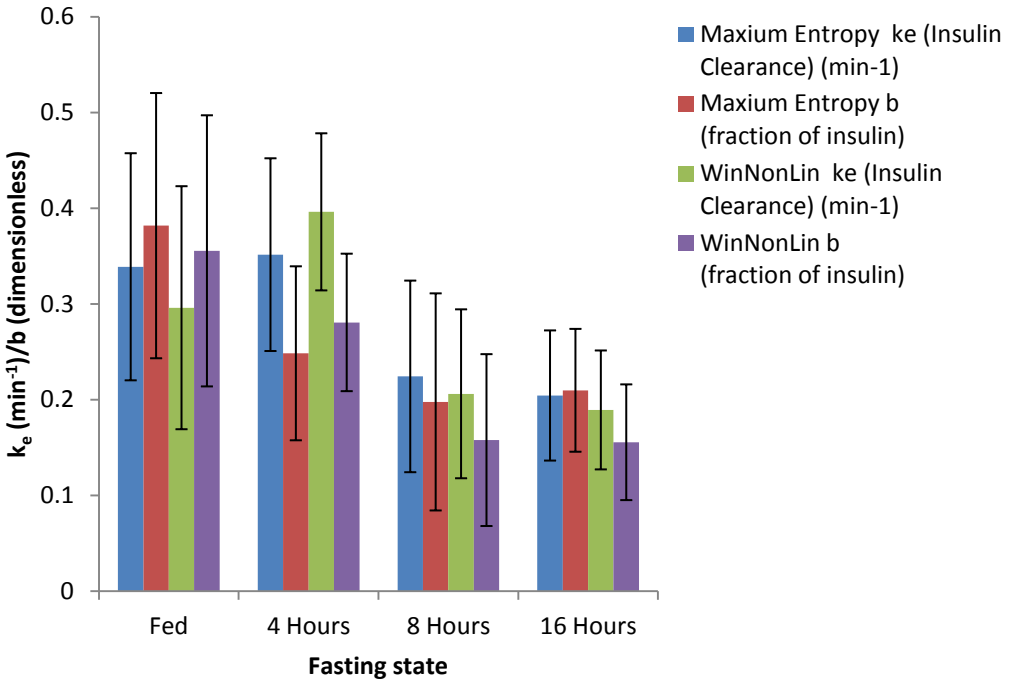

Figure 7.6: Insulin clearance (k_e) and fraction of insulin observed (b) in all rats using both Maximum Entropy and WinNonLin deconvolution techniques, grouped by fasting state with standard deviation error bars

Fasting state	Maximum Entropy		WinNonLin	
	k_e (min^{-1})	b (fraction)	k_e (min^{-1})	b (fraction)
Fed	0.34	0.38	0.30	0.36
4-hour fasted	0.35	0.25	0.40	0.28
8-hour fasted	0.22	0.20	0.21	0.16
16-hour fasted	0.20	0.21	0.19	0.16

Table 7.2: Insulin clearance (k_e) and fraction of insulin observed (b) in all rats using both Maximum Entropy and WinNonLin deconvolution techniques, grouped by fasting state

Figure 7.6 and Table 7.2 summarise the overall insulin clearance and fraction of insulin observed results obtained using both Maximum Entropy and WinNonLin deconvolution techniques on data from all data sets used here, (AliceIVGTT), (GeorgiaIVGTT) and (RuthClamp), as detailed in Chapter 4.

The full data set was analysed using a two-tailed Student's t-test (see Appendix 3). This showed that there is a statistically significant difference in the fraction of insulin observed (b) between fed and both 8-hour and 16-hour fasted rats for both the Maximum Entropy and WinNonLin methods ($p < 0.05$). There is also a statistically significant difference in insulin clearance (k_e) between 4-hour fasted and both 8-hour and 16-hour fasted rats for both Maximum Entropy ($p < 0.05$) and WinNonLin ($p < 0.005$). There is no statistically significant difference between results from Maximum Entropy and WinNonLin based on the residual function.

7.6.2 Discussion

The results in Figure 7.6 and Table 7.2 show that the fraction of insulin observed (b) is well below 100%, meaning that there is a large proportion of insulin that is not observed in the periphery. This is possibly down to the pancreas releasing insulin into the portal vein, which goes straight to the liver and is therefore cleared before it reaches the periphery where the plasma is sampled.

It can also be seen that there is a difference in the amount of insulin "lost" and the clearance rate of insulin based on the feeding state of the animals. This could

be hypothesised to be attributed to the changes in blood flow from fed to fasting states.

7.7 Modelling hepatic blood flow

7.7.1 Biology

Blood from the gut is transported to the liver via the portal vein. The circulation to the pancreas is directly from the gut so the β-cells can sense glucose levels immediately after glucose has been absorbed by the digestive system [134]. The insulin from the β-cells is fed into the portal vein. From the liver, blood flows into the rest of the body via a complex series of blood vessels and can then recirculate into the liver through the hepatic artery and portal vein. The pancreas and, therefore, the β-cells are also served by other blood vessels such as branches of the splenic artery, independent from the gut.

The blood flow in the portal vein can vary [72, 149] from 14.60± (0.96) ml/min to 27.35 (± 1.82) ml/min between fasted and fed rats [74]. This is affected by several factors, including exercise (where blood is required in areas such as muscles) and digestion (where blood is required in other areas). As described earlier, insulin is cleared by the liver; therefore it could be hypothesised that the rate of clearance changes with alterations in blood flow. This problem has been found in pharmacokinetics where a drug flows in to the liver and is cleared. As different species have different rates of blood flow, they have different rates of clearance; this has been studied in depth before [150]. With insulin there is a

first pass effect which means that the insulin is cleared without it passing into the periphery and also a standard clearance rate of insulin. However the liver may have only one intrinsic rate of clearance [151]; adding variable blood flow into the model may provide a reason for the clearance.

Knowing this, and knowing the first pass and observed clearance of insulin (from deconvolving C-peptide), it may be possible to calculate the hepatic blood flow.

7.7.2 Model

This model is a standard set of equations used by pharmacokineticists for hepatic blood flow [73, 138], given in equation 7.10; in this case, *I* is insulin, however it could also be a drug:

$$\frac{dI}{dt} = \frac{Q_h CL_{int}}{Q_h + CL_{int}} \frac{I}{V} + \left(\frac{Q_h}{Q_h + CL_{int}}\right) u(t) \qquad 7.10$$

where Q_h is hepatic blood flow, CL_{int} is intrinsic clearance rate, V is volume of distribution of insulin and u is insulin secretion rate (i.e. C-peptide secretion rate). Note that there is no volume of distribution associated with u, due to the fact that the input is already defined as a concentration.

There is a structural identifiability issue with this model which is apparent when looking at the model structure as the volume of distribution of insulin will be a ratio that is not determinable from the observables shown. This can be determined by inspection of the model or, as this model is linear, by the Laplace

transform approach to structural identifiability, see Chapter 2 [14]. Therefore it is necessary to find a value for the volume of distribution of insulin from the literature, which is known to be 0.08 l/kg [152]; this value is close to (i.e. within 10% of) the volume of distribution of C-peptide 0.0796 l/kg.

The average weights of the rats in each of the studies (Appendix 1) were:

- (AliceIVGTT): 260g
- (RuthClamp): 282g
- (GeorgiaIVGTT): 300g.

This gives an overall average weight of 280g, yielding a volume of distribution of insulin (V) of 0.0224l for the rat models used.

7.7.3 Results

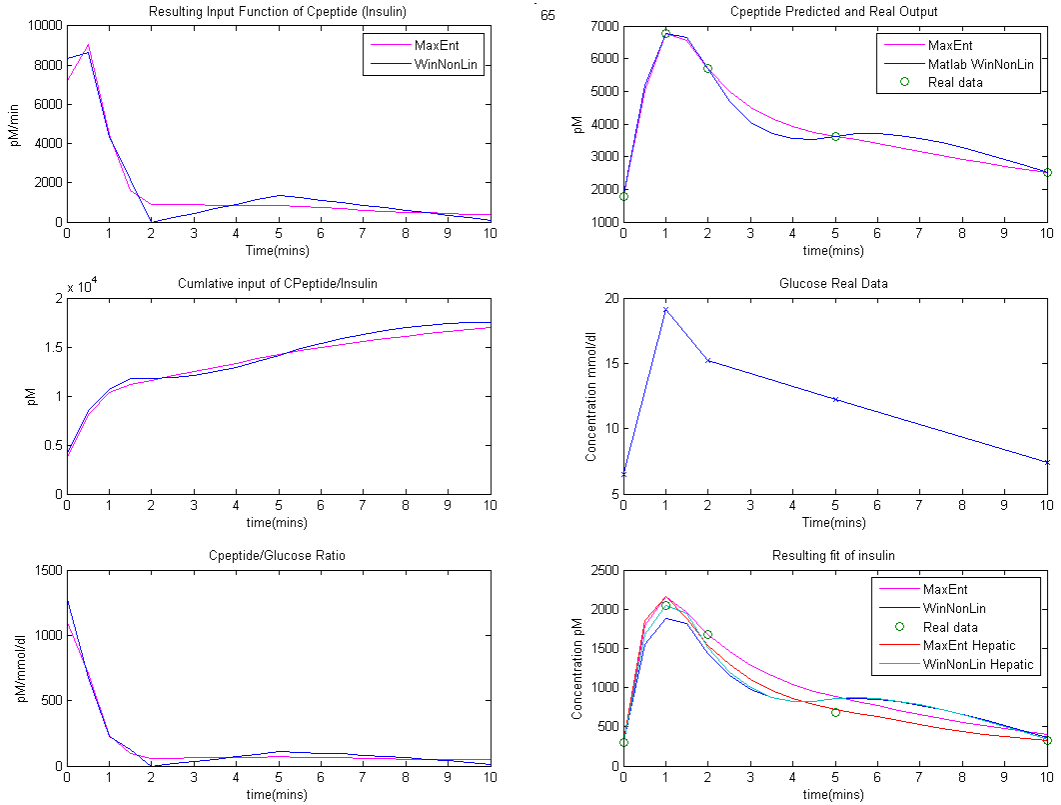

Figure 7.7: Conscious IVGTT from (GeorgiaIVGTT) ID65 - 4-hour fasted 0.5g/kg glucose bolus

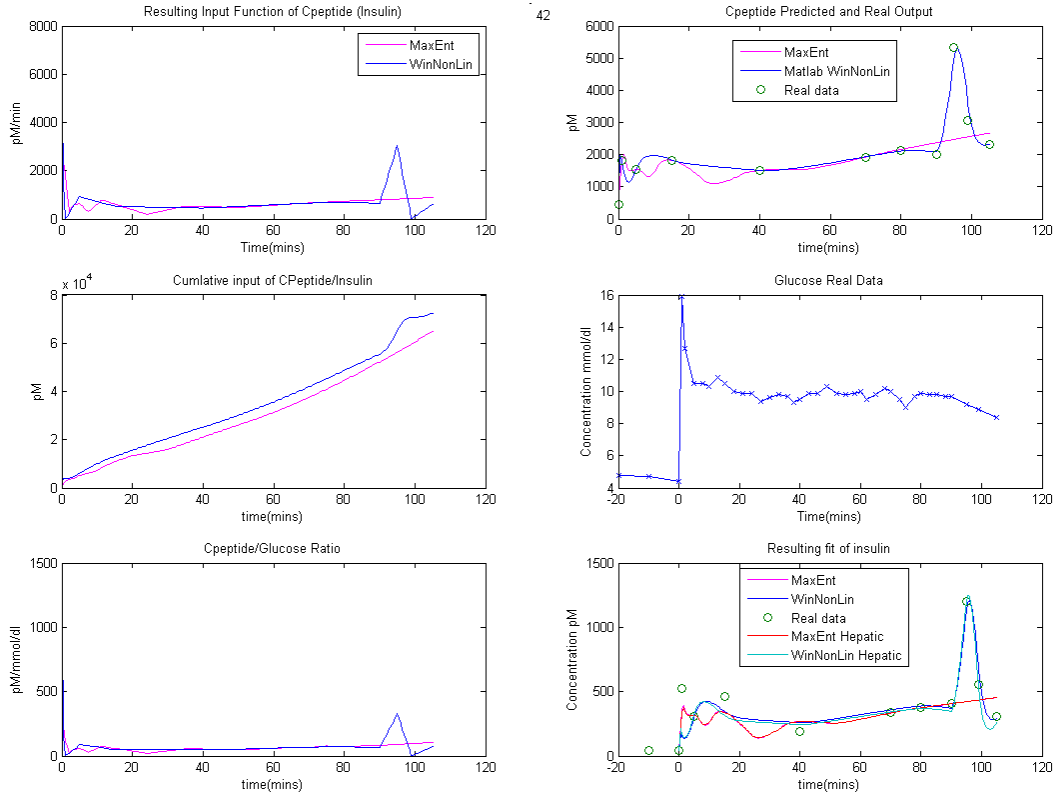

Figure 7.8: Hyperglycaemic clamp from (RuthClamp) ID 42 - 8-hour fasted

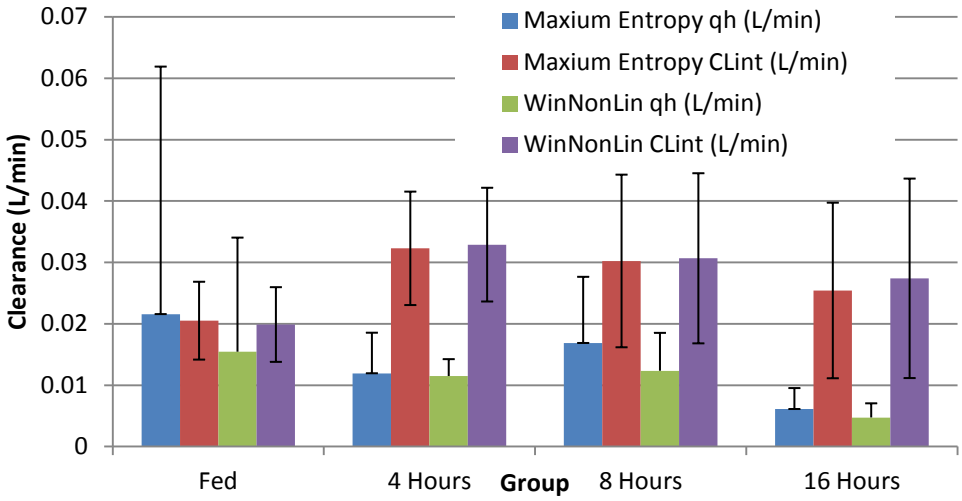

Figure 7.9: Hepatic blood flow (qh) and intrinsic clearance (CLint) in all rats using both Maximum Entropy and WinNonLin deconvolution techniques, grouped by feeding state with standard deviation error bars

	Maxium Entropy		WinNonLin	
	qh (L/min)	CLint (L/min)	qh (L/min)	qh (L/min)
Fed	0.022	0.020	0.015	0.020
4 Hours	0.012	0.032	0.011	0.033
8 Hours	0.017	0.030	0.012	0.031
16 Hours	0.006	0.025	0.005	0.027

Table 7.3: Hepatic blood flow (qh) and Instinct clearance (CLint) observed in all rats using both Maximum Entropy and WinNonLin deconvolution techniques, group by feeding state.

Although fitting to the hepatic blood flow model [73] produced similar fits to the simple insulin clearance model, see Figure 7.7 and Figure 7.8, the results for the

parameter estimates, see Table 7.3, showed considerably more variation, as seen by the standard deviation error bars in Figure 7.6 and Figure 7.9. There were fewer C-peptide results collected in the experiment than insulin ones due to the greater amount of blood needed to take C-peptide measurements. More C-peptide results may reduce variability. The hepatic blood flow model does, however, produce realistic results for the hepatic blood flow [153]. Figure 7.10 shows the hepatic blood flow for the animals at different states; the units were converted using the average weight of the animals in these studies, which was previously calculated as 280g (in section 7.7.2 above). The full results for this can be seen in Appendix 3.

Ideally, CL_{int} should remain constant as this is the liver clearance rate which should not be affected by blood flow or feeding state. However, there is a statistically significant difference in CL_{int} between fed and 4-hour fasted rats.

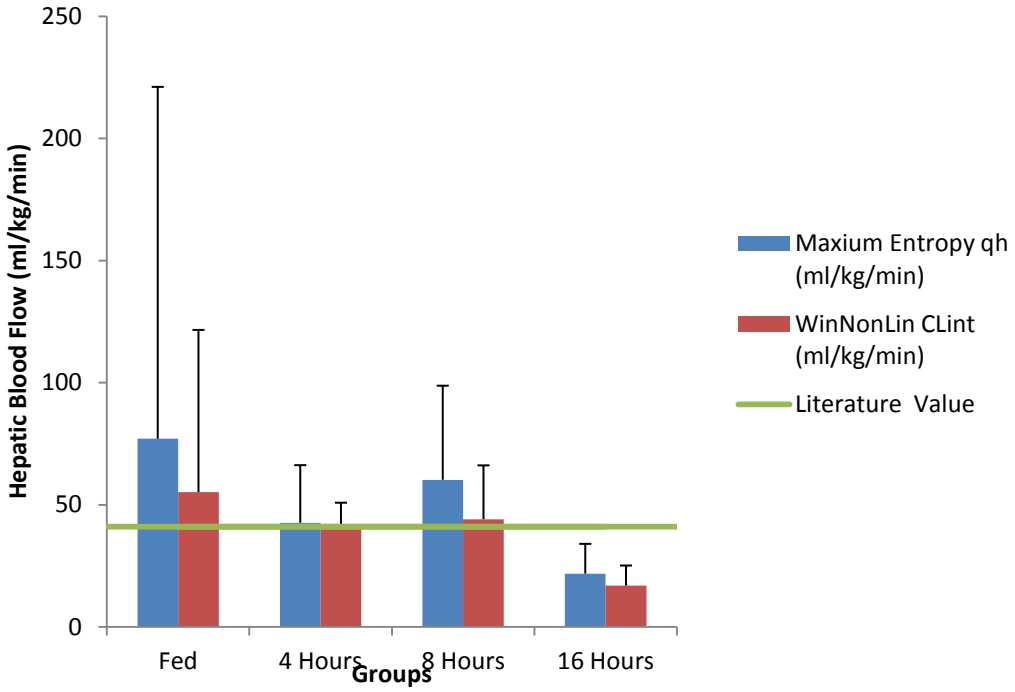

Figure 7.10: Hepatic blood flow with normalised units

7.7.4 Discussion

It is shown that there are statistically significant differences between groups of rats for hepatic blood flow. Hepatic blood flow is near the expected value, however there is a statistically significant difference between the intrinsic clearance of insulin in the 4-hour fasted animals compared to the other groups. This could be due to either of two reasons: a factor which is unaccounted for in the model or a different mechanism from that hypothesised here for hepatic clearance of insulin. It is not possible to conclude which of these it is without testing different candidate models or doing further experiments to measure insulin levels or blood flow.

In order to estimate the hepatic blood flow, deconvolution has been used to calculate a "best guess" of insulin secretion based on a small number of data points from a limited number of animal experiments. The deconvolution results had little variation across animals, however the modelled hepatic blood flow and clearance showed large variation. Pushing the data to this point is interesting, however without further experiments to actually measure blood flow – such as using the Doppler ultrasound method [73, 149] – it is not possible to fully validate this process.

From the point of view of using this approach as a tool to analyse data in the context of this thesis, being able to calculate hepatic blood flow is not as important as obtaining an accurate estimate for changes in insulin clearance.

This is because other factors, such as the activity rate and drugs, may affect the blood flow. Hence hepatic blood flow is not calculated in the software tool described in Chapter 10.

7.8 Maximum Entropy vs. WinNonLin

As noted in sections 7.6.1 and 7.7.3 above, the results from the residual functions for both the hepatic blood flow and insulin clearance models are comparable for each deconvolution technique and there is no statistically significant difference between the values each technique produces from the residual function. However there is a noticeable difference in the visual

appearance of the two sets of graphs produced; this is particularly apparent with a bolus injection of C-peptide as shown in Figure 7.11.

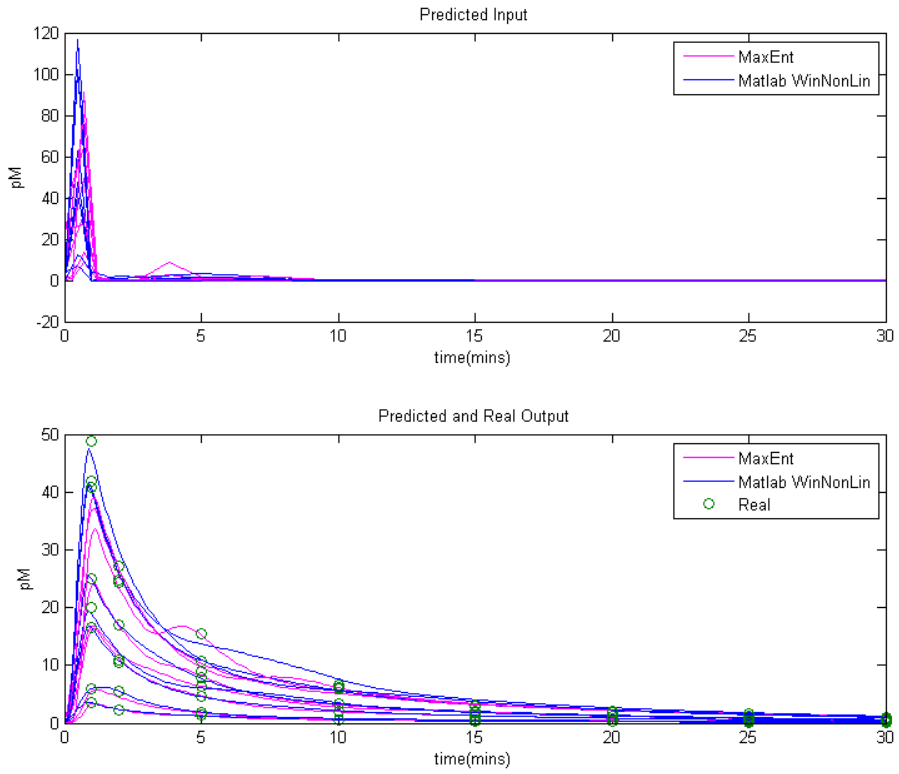

Figure 7.11: Deconvolutions of C-Peptide

As commented before, the WinNonLin technique is more prone to producing initial peaks than the Maximum Entropy technique, which employs a smoothing technique.

The WinNonLin technique is known to be correct in situations such as a bolus input of C-peptide when the data were deconvolved back to the C-peptide;

however this does not mean that the WinNonLin results correct in other situations.

The MATLAB implementations of both the WinNonLin and Maximum Entropy deconvolution techniques execute in comparable times: around 20 seconds for an individual rat on a AMD 6000+ processor. However, the WinNonLin implementation is much faster, taking only a few seconds per rat on the same processor.

7.9 Overall Summary

In this chapter, the important issue of variable insulin secretion was considered. Two methods of deconvolution were used to calculate insulin secretion; both provided reasonable predictions of insulin secretion. Both the Maximum Entropy and WinNonLin methods produced the same cumulative output of insulin, i.e. there was no statistically significant difference between the two.

The fraction of insulin observed in ad-lib fed animals was statistically significantly higher ($p < 0.05$) than the 8-hour and 16-hour fasted rats (for both the Maximum Entropy and WinNonLin methods) which shows that the state of the animal is important when considering the measurement of plasma insulin alone.

This confirms that using C-peptide as a biomarker of insulin secretion is evidently better than measuring insulin itself.

The hepatic blood flow hypothesis was partly successful as it returned realistic values for hepatic blood flow. However factors other than blood flow may be involved in insulin clearance. This process also pushed the data set to an extreme where it tried to obtain more information than is realistically possible given the limited number of data points available.

Chapter 8: Short Term Modelling

This chapter's aim is to produce a model which can simulate the glucose and insulin system accurately and is not confined to a diseased state or experiment. The attempted model will relate to the underlying biology and will fit existing data as well as predict the outcome of future experiments. In this chapter the model is produced then minimised into a simpler form and successfully fitted to OGTT (Oral Glucose Tolerance Test), IVGTT (Intra-Venous Glucose Tolerance Test) and hyperglycaemic clamp data. Sensitivity analysis is also performed on the model.

8.1 Introduction

This chapter develops a model for the regulation of glucose and insulin kinetics for short time-scales. It looks into the importance of a well-validated and robust model for short-term kinetics.

8.1.1 Purpose of the modelling

This short term modelling work is designed to achieve the following:

- To derive a mechanistically appropriate mathematical model of short-term glucose and insulin kinetics, generically applicable across experimental protocols.
- To perform parameter fits to experimental data to parameterise key aspects of the system.
    - The aim of this is to see the effect of external influences (such as drugs or disease) on the glucose-insulin system.
- To allow potential experimental outcomes to be predicted.
    - For example, knowing that a drug has an effect on a particular model parameter, it is possible to see the effect of perturbing that parameter on the system before the experiment is done (i.e. to assess parameter sensitivity).
- To test a new potential experiment to see the expected output and aiding experimental design.

- For example, by selecting appropriate time points for sampling and measurement of glucose and insulin and experiment duration for robust and accurate parameter estimation.

8.1.2 Requirements of the model

In order to create a model which improves upon existing models and create a unique new model, this model will aim to meet a list of desirable features:

- The model should be universal, rather than designed for use with a specific test or for particular situations.
  - This will mean that the model is closer (mechanistically) to the underlying physical process it is trying to mimic.
- The model does not have explicit parameters for steady state conditions (glucose and insulin basal levels are not “fixed” by a parameter).
  - This is to provide physiological reasons to explain why glucose and insulin basal levels may change, for example due to insulin sensitivity.
- The model should be stable, robust and provide realistic model outputs.
  - This includes returning to a valid steady state at the end of the experiment and producing only outputs which are physiologically possible.
- The model should be minimal in mathematical form and structure whilst incorporating all necessary components.

8.2 Model Minimisation

The Minimal Model was introduced in Chapter 6. The concept behind the Minimal Model was that it was the simplest model that could adequately explain the experimental data[113]. The Minimal Model was designed by taking a set of possible candidate models and seeing which model fitted the data best, and produced a simple model with a good fit to the available experimental data, but which was not mechanistically valid and therefore would not necessarily adequately describe new experimental data. The model is therefore not necessarily applicable to experiments other than those used for the original modelling.

Although this approach led to a model which was not mechanistically valid, it is desirable to have a model which is structurally minimal because this ensures that all parameters in the model are mathematically meaningful. This means that, when a parameter fit is performed, there will be a finite set of parameter values which will be at least mathematically valid and meaningful, even if they are not physiologically meaningful. Structural identifiability, described in Chapter 2, is a useful test for the meaningfulness of parameter values.

The challenge is therefore to create a model that has sufficient dynamics that it can reflect a large range of scenarios and situations, but which is still as minimal as possible in structure.

8.3 Model Concept

As mentioned above, it is important to keep the model minimal yet to be sufficiently dynamic to adequately explain the data and to be physiologically relevant in order for it to work under many practical situations.

Humans have defined very fine levels of system control for systems like chemical plants. The human body requires a very fine level of control over the glucose-insulin system, as described in Chapter 3. It is therefore logical to assume that the methods humans have created for obtaining fine levels of control of physical and engineering processes may be similar to those methods that have evolved in the human body. One specific type of controller produces outputs very similar to those of the pancreas, namely a PID (Proportional-Integral-Derivative) controller [12], see Figure 8.1.

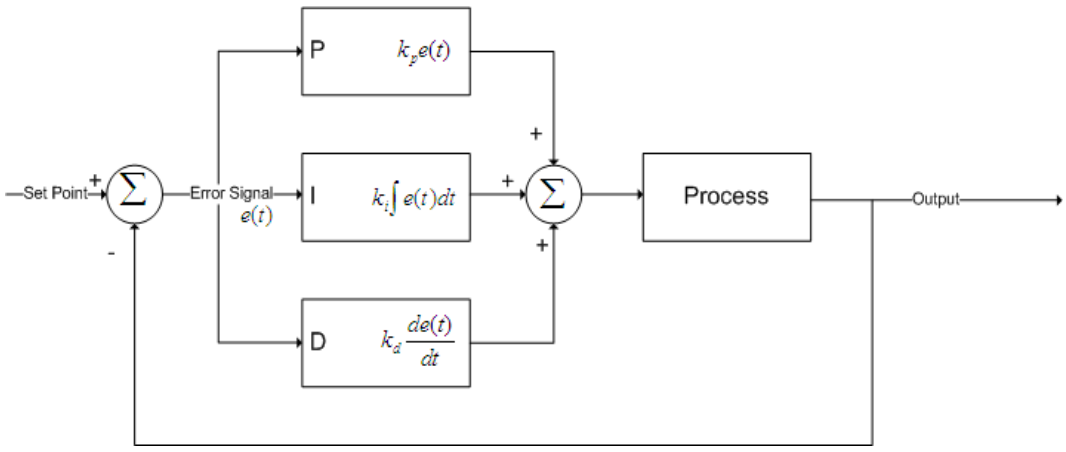

Figure 8.1: PID (Proportional-Integral-Derivative) controller

Each part of this controller can be explained as follows:

8.3.1.1 Proportional:

- In mathematical terms, this means that for every unit of plasma glucose, a fixed amount of insulin is released by the pancreas.
- This element of the controller simulates the secretion of insulin in basal conditions. The proportional aspect maintains a basal level of glucose in the system and a basal level of insulin to match it.
- In biological terms, this means that glucose enters the β-cells which, via glycolysis and oxidative phosphorylation, increases the level of ATP shown by [62]. In the proportional controller analogy, the ATP predominantly promotes granules of pro-insulin towards the membrane as described in Chapter 3.

8.3.1.2 Integral:

- In mathematical terms, this is the area under the curve (AUC) of the glucose concentration.
- This element simulates the second phase insulin response: the shoulder of insulin observed after an IVGTT[42].
- In biological terms, this is similar to the proportional control and means that an accumulation of glucose causes the β-cells to secrete an additional quantity of insulin, possibly from the readily releasable pool in β-cells [65]. This represents the amount of insulin required to remove the glucose after a meal, sugar intake or clinical challenge.

8.3.1.3 Derivative:

- In mathematical terms, this is the rate of change of glucose level.
- This element represents the first phase insulin response: the relatively high amount of insulin that is seen initially in experiments such as IVGTT.
- In biological terms, this could mean that the docked insulin granules on the cell membrane are predominantly released in a rapid response to a large increase in the amount of glucose present. It gives a measured response to sudden, large changes in concentration of glucose but has little effect when levels rise slowly [42, 66].

8.4 Model Structure and Equations

The model presented here is a three-state compartmental model. A diagrammatic representation is shown in Figure 8.2.

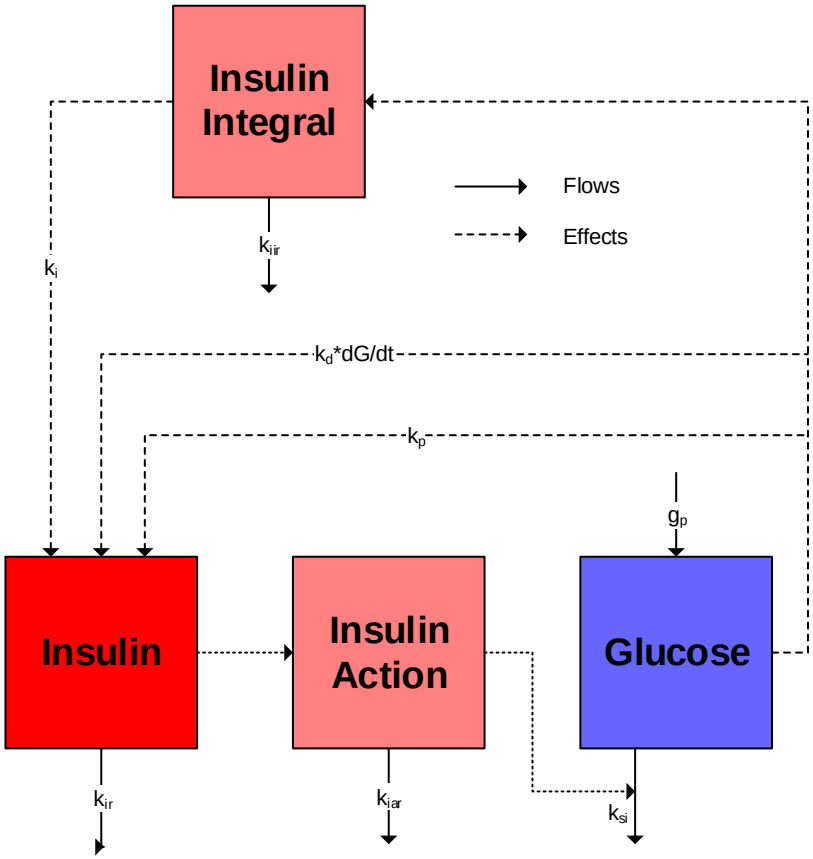

Figure 8.2: Schematic diagram of the PID model of the glucose and insulin system.

The model equations are as follows:

$$\frac{dI_i(t)}{dt} = G(t) - k_{iir}I_i \tag{8.1}$$

$$\frac{dI(t)}{dt} = k_pG(t) + k_iI_i(t) + k_d\frac{dG(t)}{dt} - k_{ir}I \tag{8.2}$$

$$\frac{dI_a(t)}{dt} = I(t) - k_{iar}I_a \tag{8.3}$$

$$\frac{dG(t)}{dt} = g_p - \big(g_r + k_{si}I_a(t)\big)G(t) \tag{8.4}$$

The model states and parameters are explained in Table 8.1 below.

Parameter	Description	Units
g_r	Glucose effectiveness	min^{-1}
g_p	Glucose production rate	mmol l^{-1} min^{-1}
k_{si}	Insulin sensitivity, insulin-dependent glucose removal	ml ng^{-1}
k_p	Proportional parameter for PID model	µg $mmol^{-1}$ min^{-1}
k_i	Integral parameter for PID model	µg $mmol^{-1}$ min^{-2}
k_d	Differential parameter for PID model	µg $mmol^{-1}$
k_{ir}	Insulin clearance	min^{-1}
k_{iir}	Integral clearance rate, to simulate integral function	min^{-1}
k_{iar}	Insulin action increase rate, to delay insulin action	min^{-1}
$G(t)$	Glucose concentration	mmol l^{-1}
$I(t)$	Insulin concentration	µg l^{-1}
$I_a(t)$	Insulin action	mmol l^{-1} min
$I_i(t)$	Insulin integral/delay	µg l^{-1} min

Table 8.1: Model State Variables and Parameter Descriptions

8.4.1 Insulin Secretion

The basal levels of glucose and insulin are not fixed points in the biological mechanism. Instead, they are determined by the effect they have on each other in their steady states. The β-cell Mass Model by Topp, et al. has been developed in this way [119]; the basal levels of each are not defined, but are determined by the combination of parameters used. The model shows what can happen in the system if a reduction of insulin sensitivity occurs over a period of days or months.

This is a central point for model design as it is vital in ensuring that the parameters have relevance to the underlying biology. A classic PID controller could be related to a biological system by considering the set point as the basal glucose level and the error signal as the basal level minus the current level. Although having a set point for basal levels of glucose would produce similar results, it would not be a mechanistic representation of the underlying biology. In reality, this is not quite a valid analogy as a biological system does not have a defined set point, so the challenge is to design a model with similar terms to those present in a PID Controller, but without a set point.

The terms in the PID controller relate to the biological process as follows:

Proportional: $k_p\, G(t)$

This term simply creates the basal level under static conditions.

The proportional secretion rate is produced by taking the level present in the glucose compartment, shown in Figure 8.2.

Integral: $k_i\, I_i(t)$

This is non-trivial as the area under the glucose curve will increase over time, causing the system to become unstable. Hence the integral function must decay over time.

It is created by taking the concentration in the glucose compartment as the rate of change of a virtual compartment $I_i(t)$, as shown in equation 8.1.

Derivative: $k_d \frac{dG(t)}{dt}$

This is a rate of change, so the absolute value of the glucose does not matter.

This is simply taken as the rate of change of glucose, and is incorporated in equation 8.2.

8.4.2 Delayed and Sustained Insulin Action

As is evident from IVGTT experiments, a large initial amount of insulin action has little effect on the initial decrease of glucose. This can be explained in a number of ways, for example it may take the insulin time to bind to the receptor site [154].

Alternatively, consider a euglycaemic clamp experiment, where glucose is clamped by measuring the basal glucose level then infusing insulin at a constant rate and glucose at a variable, measured rate until the measured glucose level in the patient once more reaches a steady-state at the basal level, or in the case of a hyperglycaemic clamp, the set point. These experiments show a long delay

before insulin has affected the glucose level. It is therefore necessary to take into account the delay in insulin action and the fact that the insulin level must be sustained for a period of time before having an effect. Using a previously well-validated delay in [111] and [125], the insulin action compartment $I_a(t)$ for this model will be the same as the interstitial compartment in the Minimal Model and is incorporated in equation 8.3

8.4.3 Net Difference in Glucose

The glucose compartment has a number of inputs and a number of outputs. The relative rates of supply and disposal of glucose in this compartment determine the basal level. This is modelled in a clear manner in the β-cell Mass Model [119]. It has an appearance rate that is made up of all unknown appearance rates and all the disposal rates that can be calculated. The appearance rate cannot be established without tracer experiments [154], however as appearance rate is related to the amount of glucose present, obtaining an absolute value is unimportant.

Insulin has an effect on both the production rate of glucose and its disposal rate. However it is impossible to distinguish and quantify the effect on each when only peripheral glucose and insulin concentrations are measured as the end result, in terms of peripheral glucose concentration, is the same.

8.5 Model Analysis

8.5.1 Structural Identifiability

The problem with using a simplistic model, such as a 2-compartment model, is that it does not capture all the dynamics of the system - such as the variable insulin dynamics created by rapid changes in glucose [155] - and hence is not an accurate representation of the true physical process. On the other hand, a systems biology model would require a larger number of parameters which may allow different combinations of values to produce the same system output. In certain cases a variety of different parameter combinations could be used to fit the same data, making it impossible to tell which was actually correct. This would also make it impossible to validate the model especially with regards to determining a drugs mechanism of action and therefore render it practically useless. The solution is to create a model which is a balance between these two approaches, by using not only parameters that can be uniquely identified, but also incorporating a mechanistic structure that adequately describes the physical process and dynamics that are observed. This creates a need for a test on the postulated model to ensure that all parameters can be uniquely identified.

Such a test exists in the form of structural identifiability analysis, see Chapter 2. A system is said to be structurally globally identifiable if, with infinite, noise-free observations, there is only one possible set of parameters that can produce the output. Although real data will be neither infinite nor noise-free, structural

identifiability in this form is a theoretical step on the way to approaching numerical identifiability or parameter estimation with greater confidence.

8.5.2 Structural Identifiability Analysis of the Postulated Model

Glucose and insulin measurements can be taken for this model. The insulin integral compartment is just a representation of an integral function. The model can be treated as an uncontrolled non-linear system. All the model parameters, (equations: 8.5 - 8.9 below) including initial conditions, were considered unknown. The system equations are given by:

$$\frac{dI_i(t)}{dt} = G(t) - k_{iir}I_i \tag{8.5}$$

$$\frac{dI(t)}{dt} = k_p G(t) + k_i I_i(t) + k_d \frac{dG(t)}{dt} - k_{ir} I \tag{8.6}$$

$$\frac{dI_a(t)}{dt} = I(t) - k_{iar} I_a \tag{8.7}$$

$$\frac{dG(t)}{dt} = g_p - \big(g_r + k_{si} I_a(t)\big) G(t) \tag{8.8}$$

$$G(0) = g_0, = I(0) = i_o, I_i(0) = i_{i_0}, I_a(0) = i_{a_0} \tag{8.9}$$

There are various techniques for performing structural identifiability analysis [19]. The Lie-symmetry approach by Yates et al. [15], also described in Chapter 2, has been applied to the model introduced here as other techniques such as the Taylor series approach could not yield a solution due to the computational complexity of solving the parameters from the Taylor coefficients. The analysis is presented in Appendix 4 and was performed using Mathematica 7 [3]. Mathematica was selected for the analysis as it is excellent for complex symbolic

manipulation and performing the analysis by hand would be highly time-consuming and error-prone, even for the relatively low state-space dimension of this model.

System Observability is a prerequisite for the Lie-symmetry technique, so the Observability Rank Criterion (see Chapter 2) was applied to the model (see Appendix 4) with individual observations of *G(t)* and *I(t)*, which showed it to be observable.

Application of this approach concluded that the model is at least locally identifiable (as global identifiability cannot be established with the Lie-symmetry approach) when two specific parameters were known a priori: g_p which represents glucose production, and k_p, the proportional insulin secretion parameter.

This leads to issues with the following parameters:

g_p - This represents the amount of glucose entering the system, which is typically unknown. It can be estimated, for example from a tracer experiment, as the clearance is fractional so an exact value is not necessary. The value used here is taken from [119].

k_p - The proportional insulin secretion parameter is more difficult to estimate. However assuming that the integral component is negligible at steady state a rough estimate for k_p can be obtained using the known insulin clearance in equation 8.10, which has been derived from the steady state.

$$k_p \approx \frac{i_r I_{basal}}{G_{basal}} \quad 8.10$$

8.5.3 Steady States

As mentioned in the previous section, unlike some previous models this system does not have steady states dependent on parameters such as glucose and insulin basal levels. The system should tend to steady states based on the system parameters and the feedback components present.

At steady state, nothing is changing hence the derivative term, $k_d \frac{dG(t)}{dt}$, is zero. With a classic PID controller, there is an error signal entering the controller; however this is not the case with this system as there is no “set point" to derive an error signal from. The integral control is therefore required to introduce decay. This makes the calculations slightly complex as the steady state for this parameter is non-zero.

From the system equations (equations 8.1 to 8.4) the steady states can be calculated algebraically, for example from equation 8.1 we have:

$$I_{iss} = \frac{G_{ss}}{k_{iir}} \quad 8.11$$

Adding in the proportional control, the steady state for insulin becomes:

$$I_{ss} = \frac{k_i I_{iss} + I_p G_{ss}}{k_{ir}} \quad 8.12$$

From equation 8.3 the steady state for insulin action is given by:

$$I_{ass} = \frac{I_{ss}}{k_{iar}} \tag{8.13}$$

and the resulting steady state for glucose is given by:

$$G_{ss} = \frac{g_p}{g_r + k_{si} I_{ass}} \tag{8.14}$$

8.5.4 Parameter Estimation & Simulations

Parameter estimation was performed on IVGTT data from the data set (AliceIVGTT) as well as clamp data from (RuthClamp), both in Chapter 4, and human data from Bergman et al. in Chapter 6. The model was fitted using a PKPD tool developed in acslX [31] by James Yates and colleagues [15], which performs simulation and parameter fitting using a standardised modelling language and data input format. Outputs from this tool are shown in Table 8.2, Figure 8.3, Figure 8.4 and Figure 8.5. The Quasi-Newton approach was selected for its optimisation algorithm and Gear's stiff for its ODE solver Chapter 2.

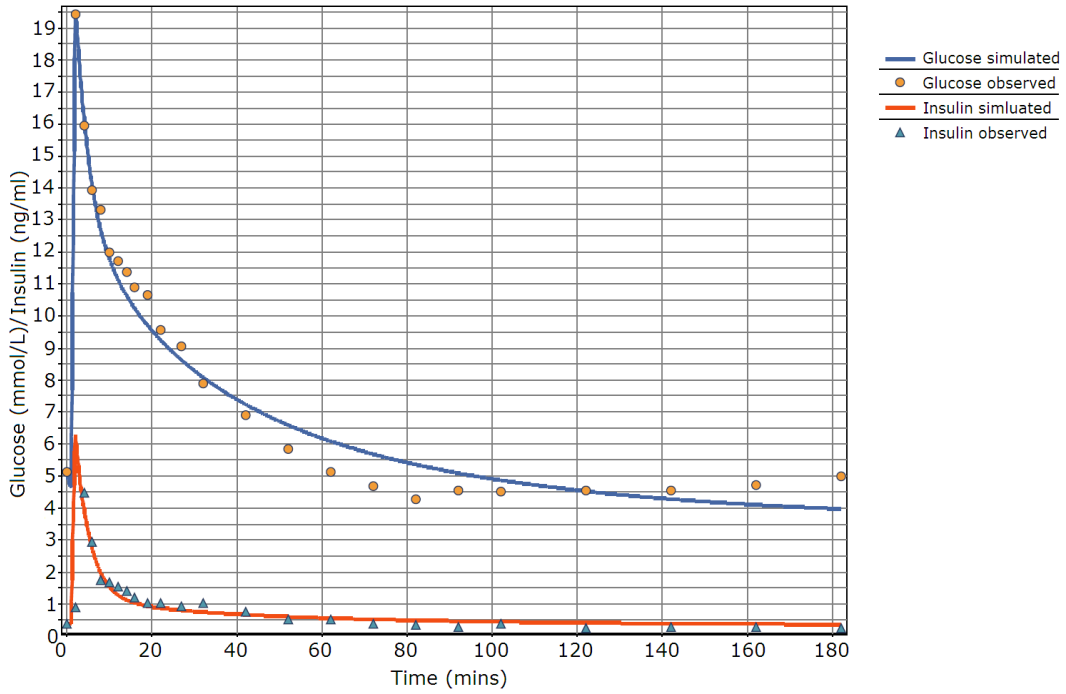

Figure 8.3: PID model insulin and glucose parameter fit on human IVGTT

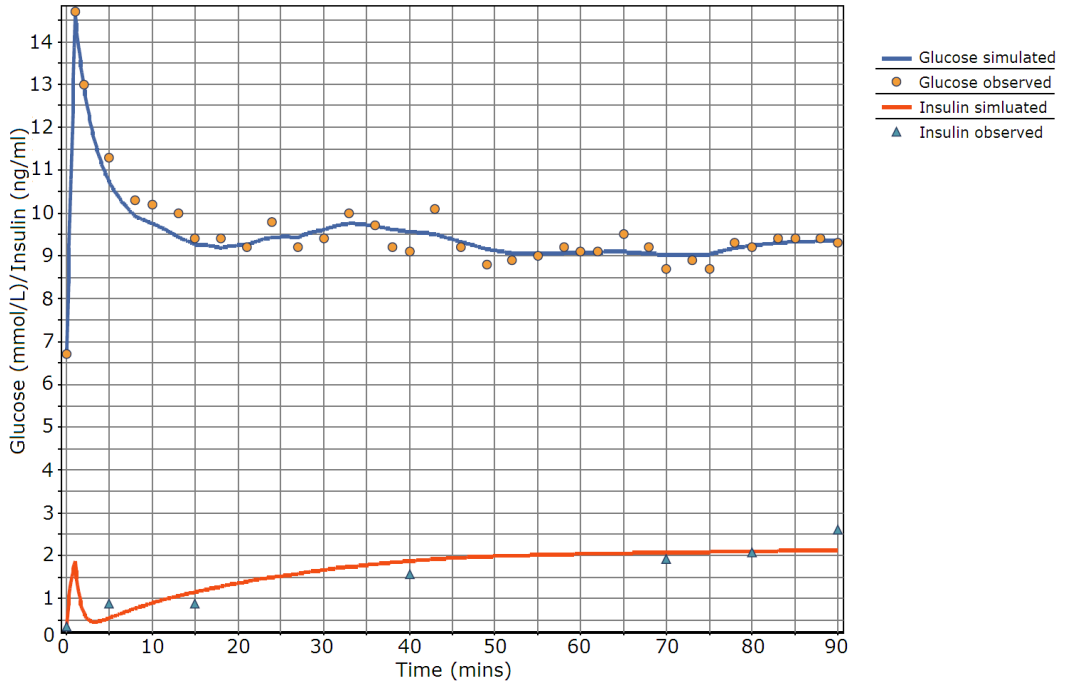

Figure 8.4: PID model insulin and glucose parameter fit on rat hyperglycaemic clamp

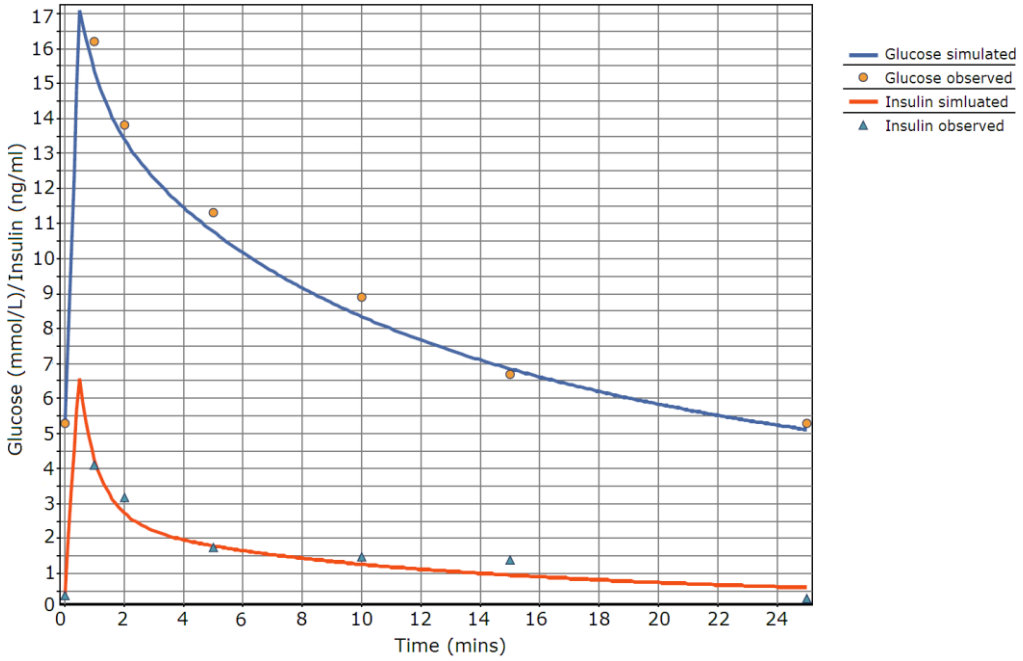

Figure 8.5: PID model insulin and glucose parameter fit on rat IVGTT

Parameter	Human IVGTT	Han Wistar IVGTT	Han Wistar Hyperglycaemic Clamp	Units
g_r	0.00159	0.0438	0.0413	min^{-1}
g_p [119]	0.033	0.033	0.033	$mmol\ l^{-1}\ min^{-1}$
k_{si}	0.00231	0.00105	0.00107	$ml\ ng^{-1}$
k_p *(Equation* 8.10*)*	0.0275	0.009274	0.00896	$\mu g\ mmol^{-1}\ min^{-1}$
k_i	0.00000158	0.000872	0.000256	$\mu g\ mmol^{-1}\ min^{-2}$
k_d	0.268	0.450	0.455	$\mu g\ mmol^{-1}$
k_{ir}	0.169	0.351	0.118	min^{-1}
k_{iir}	1.38E-19	1.38E-19	1.38E-19	min^{-1}
k_{iar}	0.114	0.0296	0.258	min^{-1}
G_0	5.11	5.8	6.7	$mmol\ l^{-1}$
I_0	0.379	0.879	0.348	$\mu g\ l^{-1}$
I_{a0}	0	0	0	$mmol\ l^{-1}\ min$
I_{i0}	0	0	0	$\mu g\ l^{-1}\ min$

Table 8.2: PID model parameter fit results

The parameter k_d is not well determined with respect to the hyperglycaemic clamp experiment, which could be due to the lack of data at the start of the clamp. According to the acslX tool, which automatically calculates confidence values for parameter estimates as described in Chapter 2 and [21], all other parameter estimates, shown in Table 8.2 are within 20% with 95% confidence.

8.5.5 Discussion

This model can produce a useful tool as it splits insulin secretion down to four parameters from the PID controller (k_p, k_i, k_d and k_{ir}). However the structural identifiability analysis shows that there are two unidentifiable parameters which had to be fixed from previously known data or steady-state conditions, meaning there is scope for improvement in the model if these could be removed.

As mentioned in Chapter 7, insulin clearance is affected by fed and fasted conditions and this is not taken into account in this model. Therefore, it would be useful to incorporate C-peptide kinetics into the model.

OGTTs were not addressed here; as this model attempts to be universal, it should be open to many different experimental scenarios so it would also be useful to test it against OGTT data. As other refinements to the model were identified at this stage, it was decided that these should be made before the model was validated with OGTT data.

8.6 Refinements

No model designed is a perfect representation of the original system, and therefore modelling is an iterative process. The model described above was not globally structurally identifiable; this was solved by fixing one parameter to steady state and another to known physiological values. However, under the definition of structural identifiability, these parameters or a combination of parameters could have an infinite number of possible values and would

therefore be meaningless. This is therefore a good point to consider whether these parameters are necessary for the model to be meaningful physiologically.

Consider first g_r, the parameter representing glucose effectiveness, which is the amount of glucose removed from the system independent of insulin in a resting state. Looking back at Chapter 3, we think about where this can actually occur. GLUT1 and GLUT2 will do this uptake, however uptake will be low and possibly also linear, therefore it can be seen that this would not appear in the model as g_p is the net glucose input to the system from the body. GLUT2 is a possible place for this uptake to occur; it appears in the pancreas and transports in small amounts of glucose for glucose sensing. However it is also expressed in large amounts to the liver and is the main input of glucose to the liver. This would be the obvious place where glucose effectiveness exists. However the glucose uptake in the liver is processed by an insulin-dependent pathway: glycogenesis. It may therefore be possible to say that there is no actual glucose effectiveness at rest. Structural identifiability tells us that we cannot work out the difference between glucose effectiveness and other parameters; therefore it can be considered a redundant parameter.

In a normal PID controller there is a set-point: the value to which a system seeks to return. It is therefore important that the controller always contains a term pushing it in the right direction. However in this model, no set-point exists but a constant level of insulin from the controller/pancreas must be maintained. Glucose is maintained above zero, therefore the integral term of the PID

controller maintains a secretion of insulin. This comes out in the reparameterisation of the k_p parameter $k_p \approx \frac{i_r I_{basal}}{G_{basal}}$ as it ends up as a fraction of the integral parameter. Again, the structural identifiability shows that the parameters will have an infinite set of possible values if k_p or k_i is left in; k_i shows useful second-phase responses to the glucose stimulus therefore k_p can be removed from the model. This makes the model simpler and more minimal and, as shown below, more robust.

This reduces the model equations as follows:

$$\frac{dI_i(t)}{dt} = G(t) - k_{iir} I_i \qquad 8.15$$

$$\frac{dI_a(t)}{dt} = I(t) - k_{iar} I_a$$

$$\frac{dI(t)}{dt} = k_i I_i(t) + k_d \frac{dG(t)}{dt} - k_{ir} I$$

$$\frac{dG(t)}{dt} = g_p - k_{si} I_a(t) G(t) + Fu(\mathrm{t})$$

The parameters are explained in Table 8.3 below.

Parameter	Description	Units
g_p	Glucose production rate	mmol l^{-1} min^{-1}
k_{si}	Insulin sensitivity, insulin-dependent glucose removal	ml ng^{-1}
k_i	Integral parameter for PID model	µg $mmol^{-1}$ min^{-2}
k_d	Differential parameter for PID model	µg $mmol^{-1}$

Parameter	Description	Units
k_{ir}	Insulin clearance	min^{-1}
k_{iir}	Integral clearance rate, to simulate integral function	min^{-1}
k_{iar}	Insulin action increase rate, to delay insulin action	min^{-1}
F	Input Gain (Bioavailability and Volume of Distribution)	ml^{-1}

Table 8.3: Refined model parameter descriptions

8.7 Simulation and Parameter Fitting

As this model is meant to help biologists analyse the data they produce and predict future experimental outcomes, it is necessary for the model to be in a form where they can access and understand it easily. Therefore, a software tool was developed to do this. This will be discussed in greater depth in Chapter 10. This tool was used to model the following data sets: (AliceIVGTT), (GeorgiaIVGTT), (RuthClamp), (AmieIVGTT) and (StevenOGTT) (see Chapter 4). The algorithms and methods used are detailed in Chapter 10.

8.8 Model Results

Figure 8.6 to Figure 8.8 and Table 8.4 to Table 8.8 are the parameter fits for (AliceIVGTT), (GeorgiaIVGTT) and (AmieIVGTT).

8.8.1 IVGTT Results

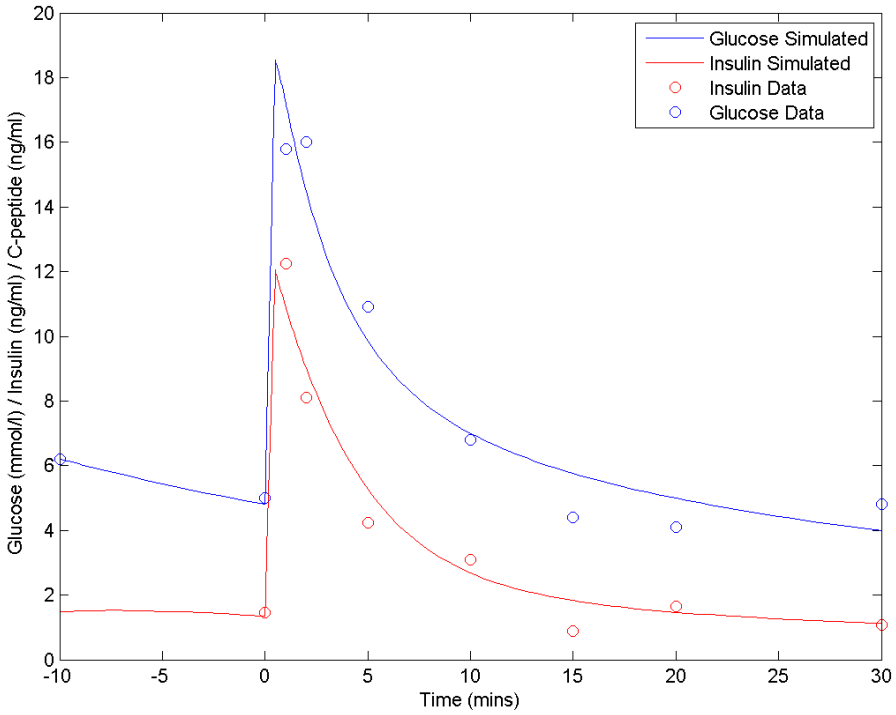

Figure 8.6: IVGTT parameter fit of a single subject

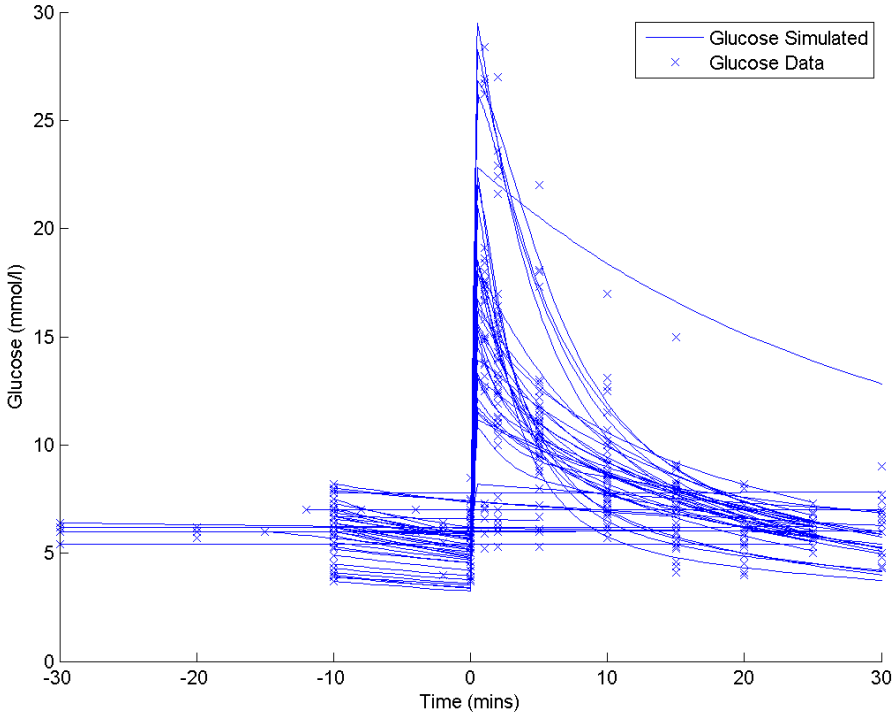

Figure 8.7: IVGTT parameter fit of glucose for all subjects

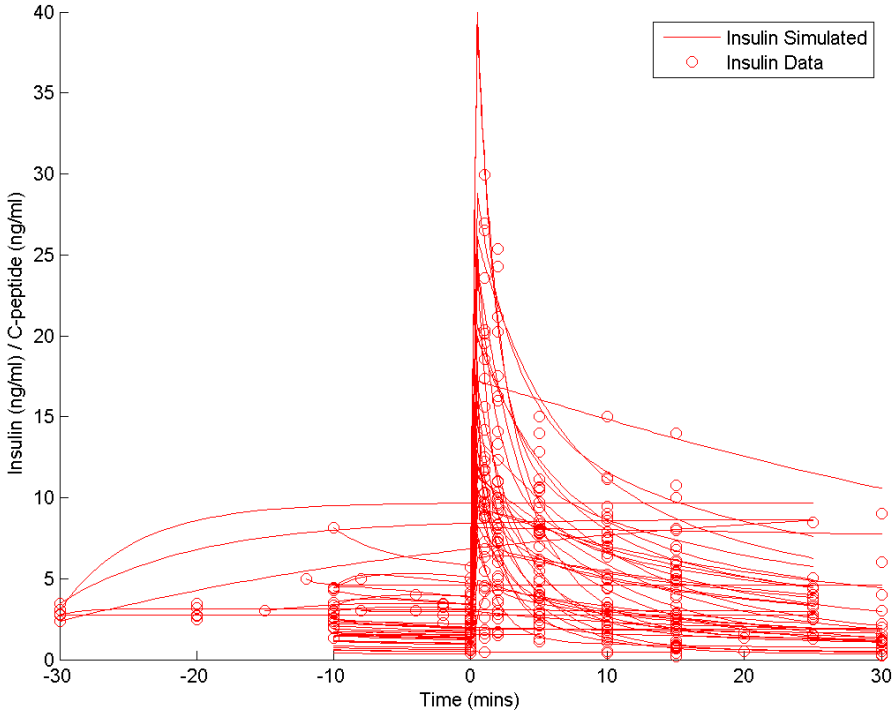

Figure 8.8: IVGTT parameter fit of insulin for all subjects

Data-base ID	Subject Ref	k_d (µg mmol^{-1})	k_{si} (ml ng^{-1})	k_i (µg mmol^{-1} min^{-2})	k_{iir} (min^{-1})	k_{ir} (min^{-1})	k_{iar} (min^{-1})	g_p (mmol l^{-1} min^{-1})	F (ml^{-1})	Residual
62	9	0.829 ± 0.0676	0.0416 ± 0.0808	1.07 ± 0.0289	12.1 ± 0.000685	0.334 ± 0.00543	2.39 ± 0.0911	0.000197 ± 5.68	0.0283 ± 0.0533	0.065
63	18	0.802 ± 0.0715	0.00962 ± 0.141	0.237 ± 1.05	4.29 ± 1.06	0.463 ± 0.0692	0.311 ± 0.132	0.000127 ± 3.91	0.0262 ± 0.0417	0.0283
64	23	1.46 ± 0.132	0.0339 ± 0.138	1.75 ± 0.18	7.21 ± 0.00749	0.75 ± 0.16	3.15 ± 0.0783	0.0002 ± 0.000186	0.0174 ± 0.0777	0.0744
65	26	1.28 ± 0.1	0.049 ± 0.639	1.28 ± 0.232	9.31 ± 0.224	0.557 ± 0.00158	3.44 ± 0.588	0.0002 ± 4.06	0.0264 ± 0.0818	0.0422
66	35	1.56 ± 0.0665	0.0358 ± 0.668	0.886 ± 1.66	14.5 ± 1.66	0.294 ± 0.0403	3.38 ± 0.643	0.000215 ± 5.69	0.0323 ± 0.0474	0.0546
67	42	0.492 ± 0.06	0.0721 ± 0.489	0.519 ± 0.638	23.8 ± 0.628	0.256 ± 0.0408	2.06 ± 0.467	0.000201 ± 5.32	0.0353 ± 0.045	0.0674
68	49	1.31 ± 0.0397	0.0231 ± 0.000332	0.582 ± 2.75	8.04 ± 2.74	0.357 ± 0.00019	1.76 ± 0.00882	0.000228 ± 3.51	0.0283 ± 0.032	0.0702
69	57	0.611 ± 0.0451	0.0291 ± 0.352	0.448 ± 0.527	18 ± 0.534	0.258 ± 0.0369	1.1 ± 0.333	0.000103 ± 3.34	0.0342 ± 0.0355	0.0501
70	45	0.608 ± 0.157	0.00934 ± 1.77	0.13 ± 1.78	3.6 ± 1.81	0.142 ± 0.0974	1.04 ± 1.73	0.000244 ± 3.71	0.0221 ± 0.13	0.063
71	46	0.509 ± 0.023	0.00317 ± 0.163	8.73 ± 3.4	89.6 ± 3.09	0.295 ± 0.424	0.238 ± 0.249	0.0802 ± 0.267	0.0209 ± 0.0313	0.0435

Data-base ID	Subject Ref	k_d (µg mmol^{-1})	k_{si} (ml ng^{-1})	k_i (µg mmol^{-1} min^{-2})	k_{iir} (min^{-1})	k_{ir} (min^{-1})	k_{iar} (min^{-1})	g_p (mmol l^{-1} min^{-1})	F (ml^{-1})	Residual
72	50	0.518 ± 0.0738	0.00642 ± 0.276	2.15 ± 4.81	64.2 ± 4.82	0.163 ± 0.0676	0.482 ± 0.268	0.000202 ± 4.37	0.0206 ± 0.0542	0.0489
73	53	0.506 ± 0.0561	0.00546 ± 0.235	0.77 ± 0.0422	26 ± 0.0492	0.181 ± 0.049	0.403 ± 0.232	0.000599 ± 2.28	0.0218 ± 0.0406	0.0256
74	54	1.66 ± 0.151	0.0144 ± 0.616	3.78 ± 4.97	48.4 ± 4.97	0.651 ± 0.0953	0.922 ± 0.574	0.000185 ± 5.71	0.00481 ± 0.108	0.0738
75	55	7.76 ± 0.00413	0.00345 ± 0.217	0.0471 ± 0.117	0.411 ± 0.171	0.698 ± 0.0371	0.26 ± 0.455	0.16 ± 0.3	0.00205 ± 0.041	0.0687
76	14	1.8 ± 1.71E+20	0.0227 ± 0.242	1.11 ± 0.995	10.6 ± 0.0222	0.413 ± 0.959	8.2 ± 0.108	0.000193 ± 7.75E-8	0.024 ± 6.39E+20	0.0338
77	30	1.84 ± 0.0117	7.46E-18 ± 18900000	0.52 ± 0.0138	23.6 ± 0.0125	0.0935 ± 0.0224	245E+16 ± 0.279	0.000277 ± 0.0788	0.024 ± 1790000	0.03
78	31	1.8 ± 23E+10	0.0155 ± 0.0298	1.34 ± 8.43	8.95 ± 0.33	0.636 ± 8.07	11.7 ± 1.29	0.000201 ± 0.0941	0.024 ± 859E+10	0.0143
79	43	1.8 ± 142E+10	0.051 ± 0.8	0.778 ± 0.134	15.2 ± 0.0897	0.813 ± 0.000265	3.66 ± 0.461	0.000197 ± 0.00161	0.024 ± 528E+10	0.0866

Table 8.4: IVGTT Four hour fasted

Data-base ID	Subject Ref	k_d ($\mu g\ mmol^{-1}$)	k_{si} ($ml\ ng^{-1}$)	k_i ($\mu g\ mmol^{-1}\ min^{-2}$)	k_{iir} (min^{-1})	k_{ir} (min^{-1})	k_{iar} (min^{-1})	g_p ($mmol\ l^{-1}\ min^{-1}$)	F (ml^{-1})	Residual
12	2.6	0.51 ± 0.0788	0.0338 ± 1.8	1.94 ± 0.467	6.31 ± 0.00672	0.595 ± 0.449	5.41 ± 1.79	0.0002 ± 0.0312	0.0187 ± 0.0308	0.0211
13	2.8	1.63 ± 0.0428	0.029 ± 0.0396	1.58 ± 0.0848	7.7 ± 0.0235	0.289 ± 0.0927	6.03 ± 0.0382	0.000202 ± 2.66	0.023 ± 0.0312	0.0161
14	3.13	0.0000000378 ± 0.163	0.0546 ± 0.00952	2190000000 ± 0.0157	412 ± 0.0333	15400000 ± 0.0211	5.96 ± 0.00469	0.000209 ± 0.112	0.0196 ± 0.013	0.024

Table 8.5: IVGTT eight hour fasted

Data-base ID	Subject Ref	k_d (µg mmol^{-1})	k_{si} (ml ng^{-1})	k_i (µg mmol^{-1} min^{-2})	k_{iir} (min^{-1})	k_{ir} (min^{-1})	k_{iar} (min^{-1})	g_p (mmol l^{-1} min^{-1})	F (ml^{-1})	Residual
1	1.1	1.89 ± 0.0803	0.026 ± 9.17	1.95 ± 1.65	6.13 ± 1.64	0.326 ± 0.205	7.01 ± 9.09	0.0002 ± 8.68	0.0241 ± 0.111	0.028
2	2.7	2.46 ± 0.000708	0.0208 ± 0.0269	2.54 ± 0.00735	5.35 ± 0.017	0.479 ± 0.00382	7.99 ± 0.0159	0.000201 ± 4.04	0.022 ± 0.0222	0.0119
3	2.1	1.61 ± 0.0737	0.021 ± 1.11	1.28 ± 5.66	9.22 ± 5.7	0.208 ± 0.111	5.09 ± 1.09	0.000206 ± 4.28	0.0205 ± 0.0367	0.0161
4	1.2	3.94 ± 0.0404	0.0155 ± 0.0442	3.69 ± 0.000805	6.01 ± 0.00673	1.05 ± 0.00104	3.3 ± 0.0125	0.000209 ± 0.0000514	0.0195 ± 0.0272	0.00886
5	1.5	4.06 ± 0.155	0.0228 ± 1.49	3.37 ± 3.22	4.16 ± 3.2	0.879 ± 0.102	5.44 ± 1.47	0.000193 ± 5.61	0.0291 ± 0.0158	0.0191
6	2.9	3.15 ± 0.0757	0.025 ± 0.0879	2.58 ± 0.0993	3.7 ± 0.0296	0.877 ± 0.11	5.17 ± 0.0769	0.000212 ± 3.9	0.0241 ± 0.0331	0.0109
7	2.11	3.95 ± 0.0733	0.0267 ± 1.19	2.28 ± 0.835	5.19 ± 0.834	0.622 ± 0.0789	6.06 ± 1.17	0.000201 ± 3.55	0.0287 ± 0.0339	0.0255
22	3	0.562 ± 0.0989	0.037 ± 1.67	1.17 ± 5.25	9.52 ± 5.46	0.235 ± 0.227	4.72 ± 1.66	0.000201 ± 6.1	0.025 ± 0.0322	0.00133
26	8	1.18 ± 0.0687	0.0236 ± 3.18	0.679 ± 4.25	22.9 ± 4.17	0.071 ± 0.3	7.68 ± 3.17	0.000203 ± 3.74	0.029 ± 0.0505	0.0238

Data-base ID	Subject Ref	k_d (µg mmol^{-1})	k_{si} (ml ng^{-1})	k_i (µg mmol^{-1} min^{-2})	k_{iir} (min^{-1})	k_{ir} (min^{-1})	k_{iar} (min^{-1})	g_p (mmol l^{-1} min^{-1})	F (ml^{-1})	Residual
28	9	0.583 ± 0.0174	0.0262 ± 0.00786	0.61 ± 0.0451	22 ± 0.13	0.0517 ± 0.0538	8.9 ± 0.0184	0.000213 ± 2.69	0.0226 ± 0.0103	0.00262
30	11	1.73 ± 0.0451	0.0202 ± 4.17	0.0609 ± 55.1	229 ± 55.1	0.0158 ± 0.0547	8.86 ± 4.16	0.000202 ± 5.14	0.0218 ± 0.0439	0.00884

Table 8.6: IVGTT fed

Data-base ID	Subject Ref	k_d (µg mmol^{-1})	k_{si} (ml ng^{-1})	k_i (µg mmol^{-1} min^{-2})	k_{iir} (min^{-1})	k_{ir} (min^{-1})	k_{iar} (min^{-1})	g_p (mmol l^{-1} min^{-1})	F (ml^{-1})	Residual
15	SS1	1.8 ± 1.09E+10	0.00886 ± 0.446	1.57 ± 0.395	7.65 ± 0.00374	0.411 ± 0.395	20.6 ± 0.287	0.000201 ± 0.000365	0.024 ± 4.08E+10	0.0182
16	SS2	1.8 ± 16.2	9.44E-10 ± 23200	1.58 ± 5.03	7.65 ± 0.0964	0.406 ± 5.03	193000000 ± 23600	0.000234 ± 0.265	0.024 ± 1240	0.014

Table 8.7: IVGTT saline infused, saline bolus

Data-base ID	Subject Ref	k_d (μg mmol^{-1})	k_{si} (ml ng^{-1})	k_i (μg mmol^{-1} min^{-2})	k_{iir} (min^{-1})	k_{ir} (min^{-1})	k_{iar} (min^{-1})	g_p (mmol l^{-1} min^{-1})	F (ml^{-1})	Residual
8	1.3	92.1 ± 0.0159	0.017 ± 0.359	16.5 ± 0.25	3.08 ± 0.249	9.17 ± 0.00137	3.72 ± 0.328	0.00022 ± 3.17	0.0399 ± 0.00385	0.0292
9	1.4	1.25 ± 1.8	0.0248 ± 99.4	2.68 ± 0.489	6.16 ± 2.54	0.729 ± 1.41	4.16 ± 98.4	0.000335 ± 2.07	0.017 ± 1.18	0.0297
10	2.12	0.945 ± 0.127	0.0476 ± 0.115	2.56 ± 0.000339	5.03 ± 0.0676	1.45 ± 0.0376	3.84 ± 0.0508	0.000204 ± 3.28	0.0178 ± 0.0446	0.0563
11	3.14	0.235 ± 0.0883	0.0489 ± 0.083	1.85 ± 0.476	9.92 ± 0.00682	0.638 ± 0.477	3.94 ± 0.0378	0.000214 ± 3.16	0.0262 ± 0.0287	0.0295

Table 8.8: IVGTT overnight fasted

8.8.2 Discussion of IVGTT

The main differences are between the eight hour fasted and the other groups, especially the four hour fasted and fed. There are statistically significant differences ($p<0.05$) between:

- the eight hour fasted and the four hour fasted in k_i, k_{iir} and k_{ir}
- and the eight hour and fed animals in k_{si}, k_i and k_{ir}.

These points are extremely interesting and show that there is a change in the insulin system due to changes in the fasting states. Changes in the insulin sensitivity (k_{si}) could be down to changes in lipid levels. High levels of lipids have been known to cause decreases in insulin sensitivity because they have an inhibitory effect on glucose uptake (see section 3.5). For changes of insulin sensitivity over time, see Chapter 8. Lipid levels were not measured in this experiment. Changes in insulin parameters could be due to blood flow changes (Chapter 7).

Parameters that have got a good fit are k_d, k_i, k_{iir} and k_{ir}. This means that the combination of this model and this test can produce an accurate measure for the first and second phases of insulin secretion. k_{si} and k_{iar} have low confidences suggesting that measuring insulin sensitivity in this combination is not reliable. This is expected as glucose clearance may be saturated. F and g_p also show low confidence. This may be due to an ambiguity in the system about where the glucose is entering the system.

Subjects 15 and 16 have many parameters with very low confidences. This is expected as the system has not been challenged with an IVGTT. From the data, subjects 76 and 77 appear to have responded incorrectly to the glucose stimulus. This may be due to the glucose not entering the system correctly so the subjects appear similar to subjects 15 and 16 and, therefore, have low parameter confidences.

8.8.3 Hyperglycaemic Clamp Results

Table 8.9 to Table 8.11 and Figure 8.9 to Figure 8.11 are parameter fits using (RuthClamp) in Chapter 4.

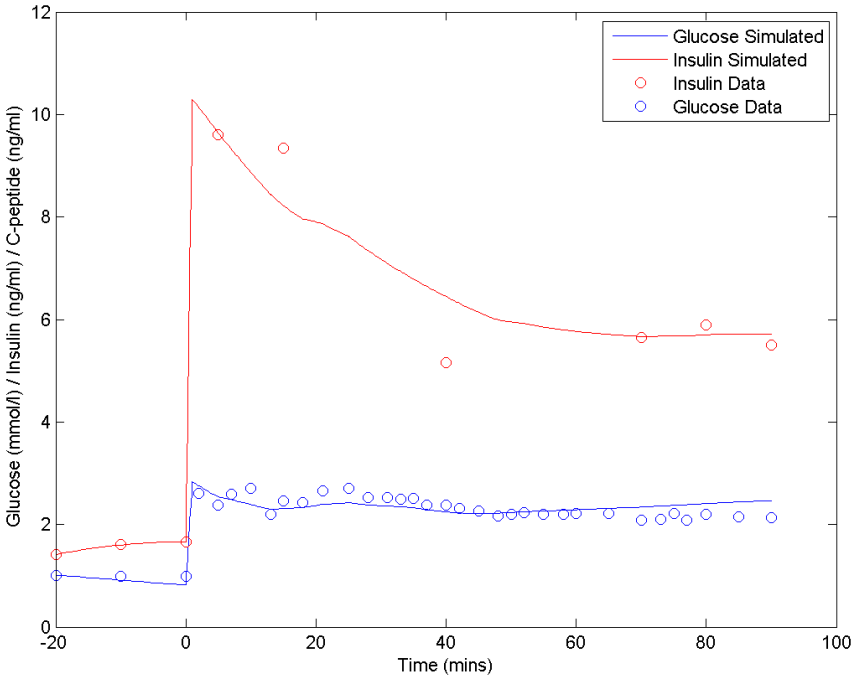

Figure 8.9: Hyperglycaemic clamp parameter fit of a single subject

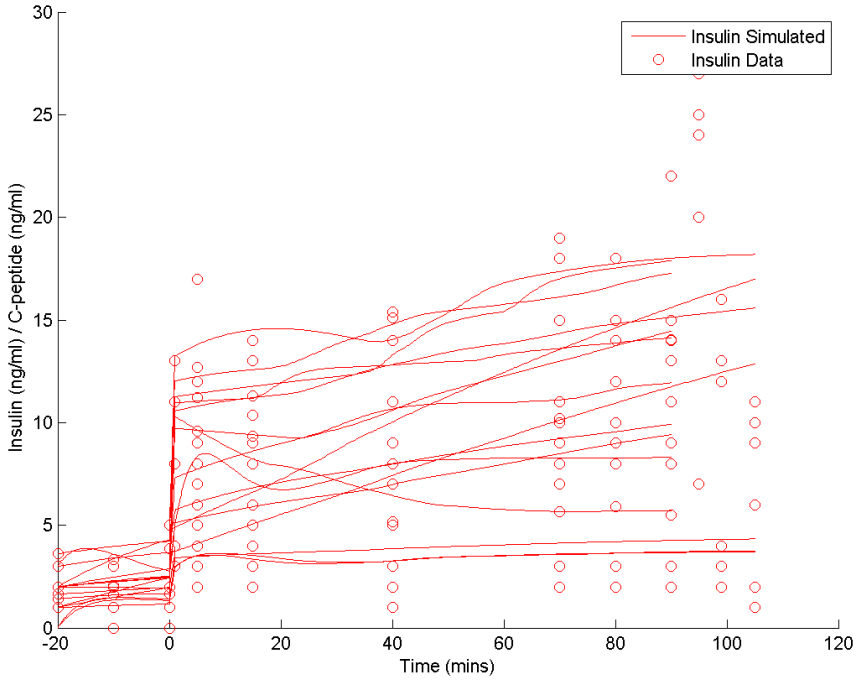

Figure 8.10: Hyperglycaemic clamp parameter fit of glucose for all subjects

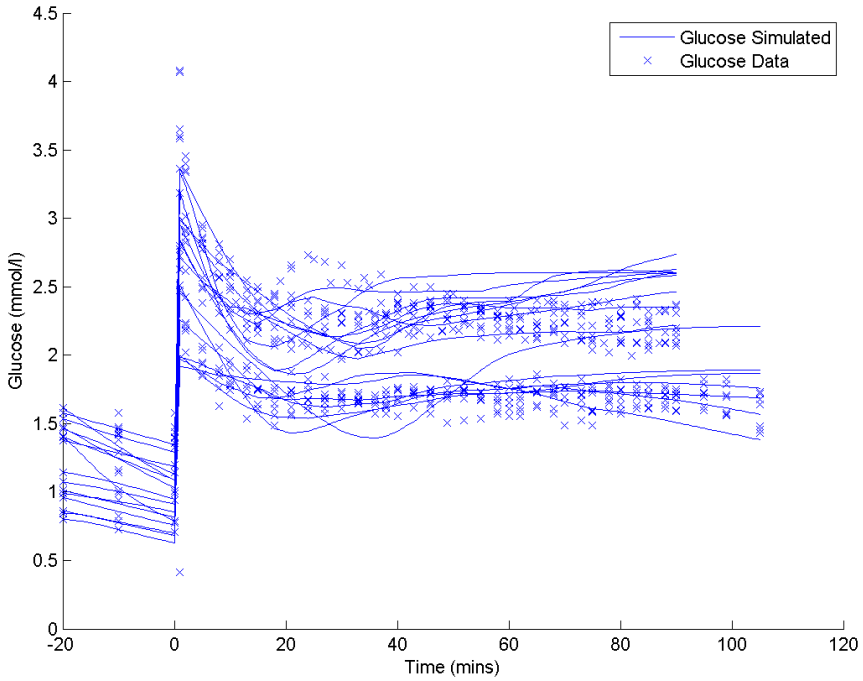

Figure 8.11: Hyperglycaemic clamp parameter fit of insulin for all subjects

Data-base ID	Subject Ref	k_d (µg mmol^{-1})	k_{si} (ml ng^{-1})	k_i (µg mmol^{-1} min^{-2})	k_{iir} (min^{-1})	k_{ir} (min^{-1})	k_{iar} (min^{-1})	g_p (mmol l^{-1} min^{-1})	F (ml^{-1})	Residual
48	3	0.618 ± 0.349	0.0257 ± 0.212	2.42 ± 0.0257	4.77 ± 0.00176	0.159 ± 0.0471	7.36 ± 0.115	0.000198 ± 0.000051	0.0043 ± 0.0729	0.0771
49	1	4.26 ± 0.101	0.0326 ± 3	0.461 ± 2.59	45.3 ± 2.59	1.04E-07 ± 17.5	7.29 ± 3.01	0.000209 ± 1.17	0.00538 ± 0.0178	0.0271
50	2	4.09 ± 0.0489	0.0381 ± 0.0983	1.21 ± 0.00899	7.56 ± 0.00608	0.077 ± 0.0202	4.37 ± 0.0446	0.000224 ± 0.00225	0.00724 ± 0.0491	0.0232
52	4	0.406 ± 0.471	0.0381 ± 0.0531	4.42 ± 0.0517	4.45 ± 0.00315	0.311 ± 0.0409	4.51 ± 0.0244	0.000223 ± 0.908	0.00675 ± 0.0266	0.0459
53	5	1.41 ± 0.326	0.0307 ± 0.0919	4.41 ± 0.00288	4.21 ± 4.56E-05	0.217 ± 0.000297	5.16 ± 0.0442	0.000213 ± 1.78	0.00672 ± 0.0427	0.101
54	6	1.76 ± 0.00332	0.029 ± 0.0391	0.945 ± 0.162	38.8 ± 0.12	0.0045 ± 0.0609	5.78 ± 0.0312	0.000371 ± 1.28	0.00489 ± 0.0188	0.0209
55	7	1.22 ± 0.273	0.0253 ± 0.000268	2.76 ± 6.95E-05	4.44 ± 0.0016	0.143 ± 3.72E-05	7.48 ± 5.39E-05	0.0002 ± 0.000353	0.00518 ± 0.024	0.137

Table 8.9: Hyperglycaemic clamp four hour fasted

Data-base ID	Subject Ref	k_d (μg mmol^{-1})	k_{si} (ml ng^{-1})	k_i (μg mmol^{-1} min^{-2})	k_{iir} (min^{-1})	k_{ir} (min^{-1})	k_{iar} (min^{-1})	g_p (mmol l^{-1} min^{-1})	F (ml^{-1})	Residual
42	14	1.26 ± 0.118	0.0337 ± 2.18	2.77 ± 1.74	4.41 ± 1.91	0.327 ± 0.688	5.43 ± 2.18	0.000198 ± 1.3	0.0028 ± 0.102	0.376
43	15	1.48 ± 0.102	0.0459 ± 0.995	2.49 ± 0.0612	4.84 ± 0.00202	0.245 ± 0.0861	4.06 ± 0.983	0.0002 ± 3.79	0.00426 ± 0.0678	0.146
44	16	1.55 ± 0.0633	0.0401 ± 2.78	1.53 ± 0.656	8.33 ± 0.628	0.0883 ± 0.336	4.53 ± 2.77	0.000138 ± 0.251	0.0032 ± 0.083	0.369
45	17	1.34 ± 0.182	0.0291 ± 0.138	3.36 ± 0.0487	3.56 ± 0.00174	0.124 ± 0.084	6.37 ± 0.0722	0.000201 ± 0.000051	0.00479 ± 0.0599	0.19
47	18	27.9 ± 0.108	0.017 ± 3.39	1.7 ± 8.11	35.8 ± 8.11	0.0318 ± 0.136	21.3 ± 3.39	0.00269 ± 0.078	0.000996 ± 0.0597	0.111

Table 8.10: Hyperglycaemic clamp eight hour fasted

Data-base ID	Subject Ref	k_d (µg mmol^{-1})	k_{si} (ml ng^{-1})	k_i (µg mmol^{-1} min^{-2})	k_{iir} (min^{-1})	k_{ir} (min^{-1})	k_{iar} (min^{-1})	g_p (mmol l^{-1} min^{-1})	F (ml^{-1})	Residual
36	9	2.84 ± 0.182	0.024 ± 0.000594	3.42 ± 0.00018	4.19 ± 0.00201	0.123 ± 0.000133	7.73 ± 0.000144	0.000206 ± 0.00119	0.0049 ± 0.0183	0.112
37	10	1.28 ± 0.513	0.0000914 ± 65	1.17 ± 13.2	12.1 ± 13.2	0.00126 ± 0.513	2190 ± 61	0.00536 ± 0.104	0.0000501 ± 0.564	0.155
39	12	1.91 ± 0.0841	0.035 ± 1.06	1.05 ± 3.41	19.8 ± 3.42	0.000816 ± 0.393	7.39 ± 1.06	0.000235 ± 0.618	0.00288 ± 0.0525	0.103
40	13	50.3 ± 0.0672	0.00139 ± 13.4	1.16 ± 8.78	15.4 ± 8.87	0.0648 ± 0.0532	135 ± 13.5	0.000243 ± 1.87	0.000737 ± 0.0592	0.108

Table 8.11: Hyperglycaemic clamp fed

8.8.4 Discussion of hyperglycaemic clamp

There is a statistically significant difference ($p<0.05$) for the results of the fed and eight hour fasted animals against the four hour fasted subjects for *F* (input gain of glucose – bioavailability/volume of distribution). This shows that the input gain of glucose has changed between different fasting states. In the eight hour fasted animals it has a greater input gain (0.0057 ml^{-1}), see Table 8.10. In the four hour fasted animals a smaller input gain was recorded (0.00411 ml^{-1}), see Table 8.9. This could be explained by there being missing glucose compartments in the model, in the case of the eight hour fasted animals all the glucose in extra compartments has been utilised whereas in the four hour case this has not happened.

There is a statistically significant difference ($p<0.05$) for the results of the fed against the other animals for k_{iar} (insulin action clearance rate). This shows that the insulin action clearance rate has changed between different fasting states. In the fed animals, the insulin action rate is highest which means that insulin acts for a shorter time.

The parameter fitting of the hyperglycaemic clamps worked well as the fits were close to the observed data. In some cases the fits did not match as closely as they could. This may have been because animal systems were under a lot of stress, therefore some animals might have acted erratically. Towards the end of the experiment, at 90 minutes, there is a large peak for most animals. This was due to an injection of Streptozotocin. This was done to release all the insulin from the

β-cells in order to measure how much insulin was left in the cells. This data point was left in as, in most cases, it was indistinguishable from the other data.

The residuals were low for most subjects and the confidences in the parameters were also high, except for k_{si}. This could be due to insulin dependent glucose clearance being saturated. The confidence in k_i for fed animals was low but also, in general, the parameters were more erratic than other animal states, for example database ID 40 had a large k_d. Looking at the graph, it can be seen that insulin secretion was increasing dramatically throughout the experiment while glucose infusion was relatively constant.

This study was also used with the C-peptide model, below, and the results are given in Chapter 7.

8.8.5 OGTT Results

In an OGTT experiment, the glucose is given orally and therefore takes a period of time to enter the system post absorption. It was therefore necessary to add this time delay into the model. Two attempts were made at modelling this delay. It is standard [13] to use a string of compartments to model the gut. One and two compartments were trialled on the data, however when parameter fitting was performed, the second compartment's parameters were fitted so that they had no impact on the resulting model output, i.e. the flow rate between compartments was set very low. As shown below, a one-compartment model for the gut is enough to adequately fit the data with the given data set. The data used is from (StevenOGTT); day 8 was used because it was at the end of the

experiment and would show the greatest difference between the animals used. The insulin secretion rates were taken from IVGTT data as the time points taken in these experiments were not taken at short enough intervals to be able to capture those parameters.

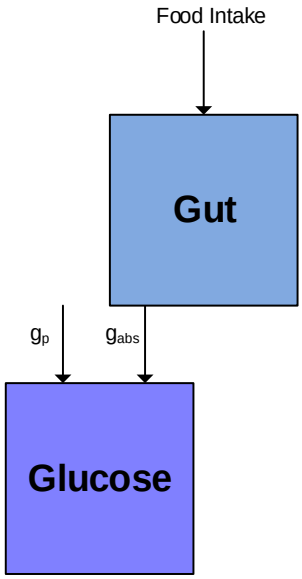

Figure 8.12: Gut Glucose Model for Short Term Model

The model is shown in Figure 8.12 and the system equations are given by:

$$\frac{dG(t)}{dt} = g_p - k_{si} I_a(t) G(t) + g_{abs} Gut(t) \qquad 8.16$$

$$\frac{dGUT(t)}{dt} = - g_{abs} Gut(t) + Fu(t)$$

Parameter	Description	Units
g_{abs}	Glucose absorption from gut	min^{-1}
F	Volume of distribution / bioavailability of glucose (Input gain of glucose)	ml^{-1}
$u(t)$	Input of glucose to the gut	$mmol\ min^{-1}$

Table 8.12: Gut Parameters for Short Term

8.8.6 Fitting OGTT

Figure 8.13 to Figure 8.15 and Table 8.13 to Table 8.16 are the results from parameter fitting (StevenOGTT).

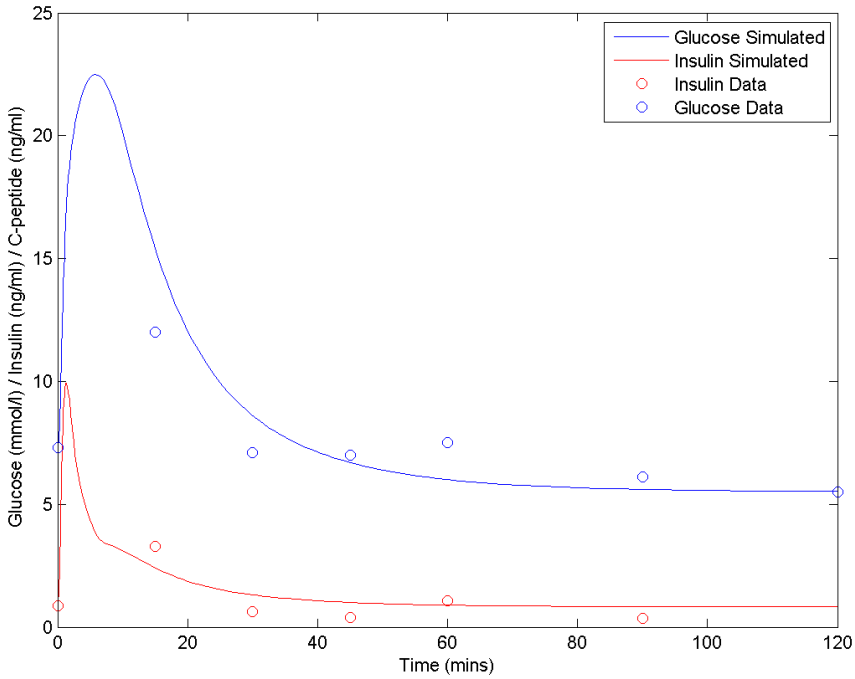

Figure 8.13: OGTT parameter fit for a single subject

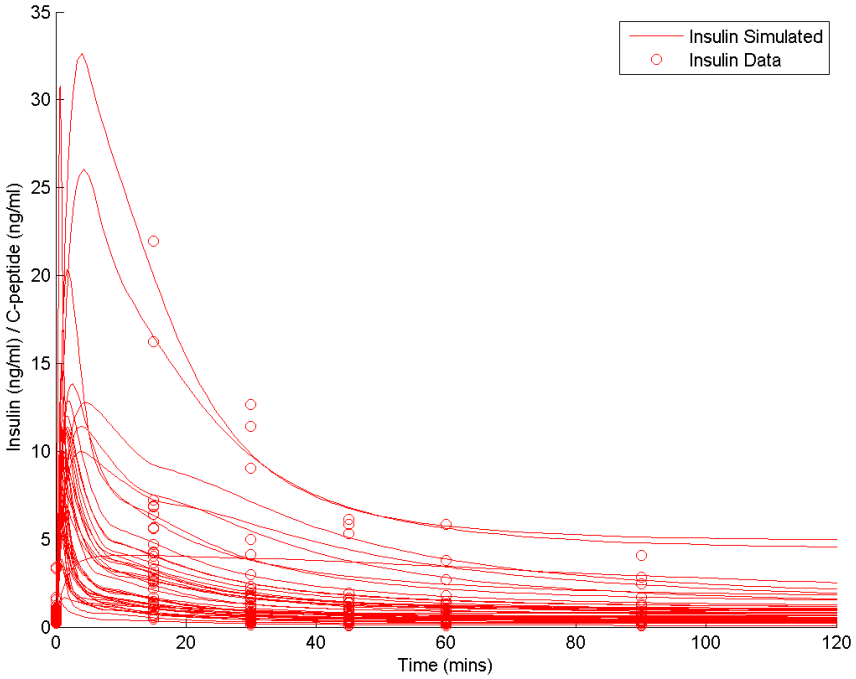

Figure 8.14: OGTT parameter fit of glucose for all subjects

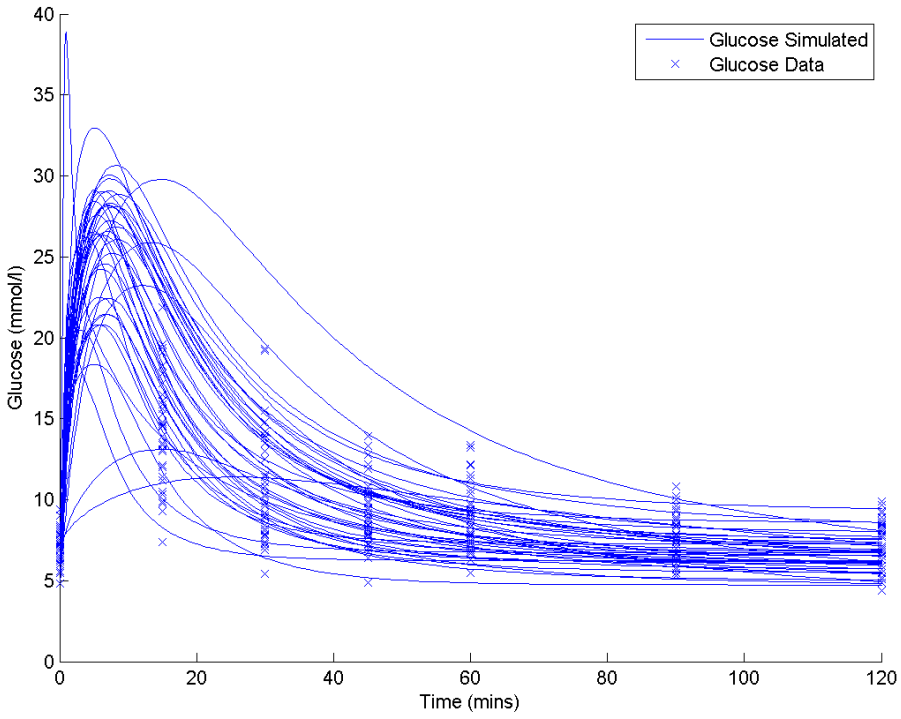

Figure 8.15: OGTT parameter fit of insulin for all subjects

Subject ref	k_{si} (ml ng^{-1})	k_{ir} (min^{-1})	k_{iar} (min^{-1})	g_p (mmol l^{-1} min^{-1})	k_{abs} (min^{-1})	Residual
4	0.148 ± 1.22	3.82 ± 0.0393	1.51 ± 1.18	0.138 ± 0.132	0.222 ± 0.154	0.0875
7	0.0828 ± 0.0968	1.92 ± 0.0698	1.69 ± 0.0921	0.0887 ± 0.222	0.143 ± 0.183	0.155
9	0.222 ± 1.34	2.08 ± 0.0621	2.01 ± 0.605	0.412 ± 0.69	0.419 ± 1.05	0.203
13	0.027 ± 1.74	1.79 ± 0.0223	1.22 ± 1.62	0.0608 ± 0.205	211 ± 30.7	0.0293
20	0.0914 ± 0.855	1.71 ± 0.0755	1.73 ± 0.532	0.26 ± 0.36	0.611 ± 0.979	0.263
22	0.0265 ± 0.686	0.534 ± 0.123	4.72 ± 0.668	0.0373 ± 0.395	4040 ± 2.02	0.57
28	0.0212 ± 0.044	2.45 ± 0.193	0.562 ± 0.00604	0.115 ± 0.543	0.427 ± 0.0979	0.187
30	0.14 ± 0.299	14.1 ± 0.0241	1.72 ± 0.301	0.112 ± 0.298	0.297 ± 0.345	0.509
34	0.103 ± 0.49	2.12 ± 0.0341	1.61 ± 0.477	0.183 ± 0.108	0.218 ± 0.125	0.0741
39	0.0657 ± 0.188	2.64 ± 0.046	1.22 ± 0.0575	0.131 ± 0.0976	0.379 ± 0.183	0.115

Table 8.13: OGTT Research Methods Diet 1 Glucose Tolerance Test

Subject ref	k_{si} (ml ng^{-1})	k_{ir} (min^{-1})	k_{iar} (min^{-1})	g_p (mmol l^{-1} min^{-1})	k_{abs} (min^{-1})	Residual
2	0.072 ± 0.406	1.1 ± 0.0699	2.2 ± 0.434	0.151 ± 0.26	0.255 ± 0.225	0.215
8	0.0679 ± 0.00262	1.76 ± 0.0277	2.71 ± 0.0339	0.113 ± 0.0755	0.298 ± 0.0994	0.376
10	0.122 ± 1.08	2.83 ± 0.0321	1.08 ± 0.979	0.351 ± 0.193	0.251 ± 0.209	0.0547
17	0.408 ± 0.0593	3.57 ± 0.000121	3.95 ± 0.145	0.12 ± 0.126	0.231 ± 0.155	0.0592
16	0.0695 ± 2.85	1.56 ± 0.0448	1.32 ± 2.76	0.212 ± 0.146	0.238 ± 0.173	0.11
21	0.102 ± 0.207	1.73 ± 0.0953	1.71 ± 0.176	0.529 ± 0.1	0.341 ± 0.132	0.319
25	0.145 ± 2.67	3.74 ± 0.0481	0.77 ± 2.44	0.186 ± 0.215	0.224 ± 0.0692	0.119
35	0.00701 ± 0.192	4.24 ± 0.0567	0.212 ± 0.177	0.0153 ± 0.394	1070 ± 0.274	0.156
32	0.145 ± 8.44	2.9 ± 0.0476	2.27 ± 8.45	0.136 ± 0.199	0.255 ± 0.541	0.0892
37	0.078 ± 0.826	3.34 ± 0.128	3.11 ± 0.597	0.0853 ± 0.417	0.258 ± 0.294	0.545

Table 8.14: OGTT Research Methods Diet 1 Meal Tolerance Test

Subject ref	k_{si} (ml ng^{-1})	k_{ir} (min^{-1})	k_{iar} (min^{-1})	g_p (mmol l^{-1} min^{-1})	k_{abs} (min^{-1})	Residual
1	0.0471 ± 0.00379	1.01 ± 0.000032	3.6 ± 0.00159	0.101 ± 0.0651	0.255 ± 0.039	0.0767
6	0.0719 ± 0.0317	1.65 ± 0.0239	3.32 ± 0.0713	0.187 ± 0.102	0.189 ± 0.161	0.0376
11	0.0246 ± 0.155	0.637 ± 0.0338	3.3 ± 0.0779	0.108 ± 0.0972	0.507 ± 0.338	0.0587
14	0.0441 ± 0.294	0.992 ± 0.0524	3.03 ± 0.184	0.113 ± 0.133	0.232 ± 0.136	0.19
18	0.061 ± 1.64	1.42 ± 0.0642	2.68 ± 1.64	0.167 ± 0.211	0.232 ± 0.188	0.203
24	0.03 ± 0.629	0.7 ± 0.167	5.8 ± 0.356	0.0335 ± 0.889	0.1 ± 0.58	0.462
26	0.0341 ± 2.13	0.357 ± 0.107	4.24 ± 2.12	0.0661 ± 1.18	0.0247 ± 0.134	0.388
31	0.042 ± 0.592	0.913 ± 0.0881	4.16 ± 0.386	0.0598 ± 0.753	0.271 ± 0.242	0.199
33	0.0391 ± 1.14	2.66 ± 0.0517	1.44 ± 1.11	0.119 ± 0.215	0.286 ± 0.184	0.154
38	0.0251 ± 0.0342	0.278 ± 0.0272	7.13 ± 0.0803	0.0939 ± 0.121	0.206 ± 0.121	0.0467

Table 8.15: OGTT High Fat Diet Glucose Tolerance Test

Subject ref	k_{si} (ml ng^{-1})	k_{ir} (min^{-1})	k_{iar} (min^{-1})	g_p (mmol l^{-1} min^{-1})	k_{abs} (min^{-1})	Residual
3	0.0612 ± 0.206	1.04 ± 0.151	4.69 ± 0.0886	0.0864 ± 0.163	0.497 ± 0.988	0.203
5	0.051 ± 0.0901	1.49 ± 0.00591	3.37 ± 0.118	0.117 ± 0.0558	0.206 ± 0.245	0.172
12	0.0491 ± 4.49	1.23 ± 0.0374	3.54 ± 4.43	0.0463 ± 0.294	0.389 ± 0.322	0.061
15	0.0538 ± 0.0912	1.07 ± 0.0715	2.84 ± 0.092	0.168 ± 0.111	0.278 ± 0.209	0.219
19	0.0373 ± 0.367	0.619 ± 0.0423	4.56 ± 0.306	0.0636 ± 0.243	0.24 ± 0.328	0.081
23	0.116 ± 0.164	2.46 ± 0.0526	1.28 ± 0.196	0.412 ± 0.255	0.0416 ± 0.197	0.123
27	0.0658 ± 0.0678	1.53 ± 0.0279	2.59 ± 0.0773	0.15 ± 0.13	0.445 ± 0.127	0.0505
29	0.0307 ± 0.68	0.409 ± 0.0589	4.95 ± 0.551	0.14 ± 0.208	0.00234 ± 0.475	0.3
36	0.0624 ± 0.124	1.24 ± 0.0523	4.45 ± 0.0177	0.109 ± 0.205	0.734 ± 0.146	0.11
40	0.0269 ± 0.637	0.207 ± 0.0422	8.45 ± 0.532	0.0848 ± 0.192	0.382 ± 0.464	0.0932

Table 8.16: OGTT High Fat Diet Meal Tolerance Test

8.8.7 Discussion of OGTT

The main differences are between the high fat diet and the non-high fat diet. There is a significant difference ($p<0.05$) on the parameter insulin sensitivity (k_{si}). This shows that a high fat diet has a measurable effect on insulin sensitivity. This is exactly what would be expected (see Chapter 3).

Insulin clearance (k_{ir}) and insulin action clearance (k_{iar}) are significant differently ($p<0.05$) lower in the high fat diet (except for RM1GTT with k_{ir}; this could be because subject 30 was an outlier).

Glucose production (g_p) is significantly different ($p<0.05$) between RM1GTT and the high fat diet (HDGTT and HFDMTT).

Glucose absorption (k_{abs}) is not statistically significantly different between groups showing that diet does not seem to affect glucose absorption rate.

Very few data points were taken in this test so, from the model stand point, there is uncertainty in how fast the glucose could enter the system. This could explain why there is variable confidence in the k_{abs} parameter. The k_{si} parameter also shows signs of uncertainty for similar reasons. The rest of the parameters show a reasonable level of confidence.

From the graphs, Figure 8.13 to Figure 8.15, it can be seen that there is a large peak of insulin within the first 15 minutes. This has been simulated to be the case as the parameters have been taken from the IVGTT. Due to limitations in the

experiment, it was not possible to take readings so close to the dose being given. This would be interesting for future study.

8.9 C-peptide

As seen in previous chapters, Chapter 5 and Chapter 7, there has been a well-defined model developed for C-peptide kinetics [57]. It is a simple step to combine this C-peptide model into the model presented above. To do this, we state that the insulin secretion seen previously is the real insulin secretion before the insulin is cleared by the liver; so the GSIS terms from the model above are the terms for C-peptide secretion. This assumes that the output seen in the periphery is a fraction of that seen in the portal vein. In this model the term *S(t)* is the secretion of insulin and C-peptide in molar quantities because, as stated previously, insulin and C-peptide are secreted in equal molar quantities. The system model is shown in Figure 8.16 and *S(t)* is given by:

$$S(t) = k_i I_i(t) + k_d \frac{dG(t)}{dt} \qquad 8.17$$

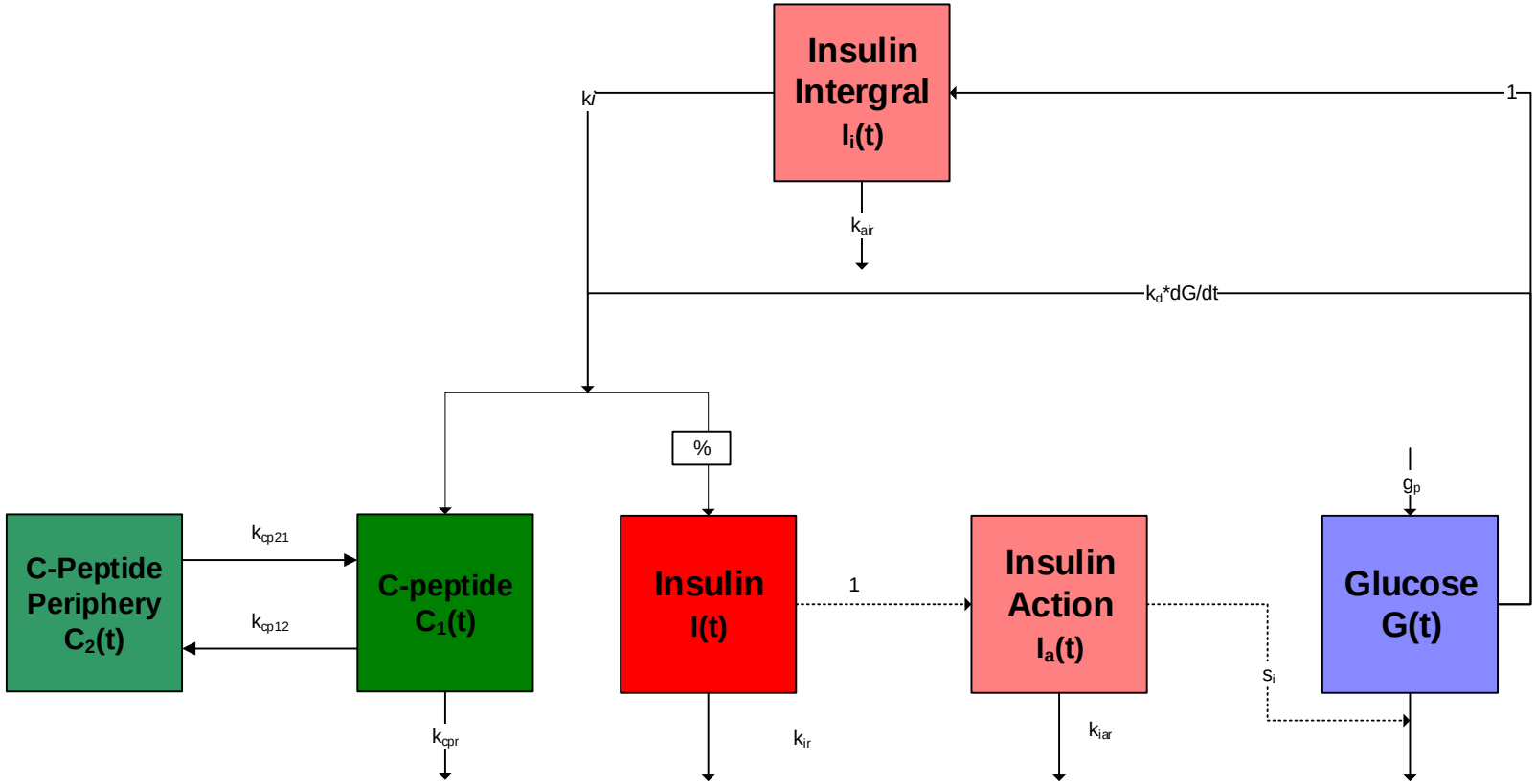

Figure 8.16: Full C-peptide Short Term Model

In Chapter 7, hepatic blood flow changes were used to model changes in insulin clearance. In this situation, it was decided not to include this model because, if another factor alters insulin appearance in the periphery and insulin clearance, this will produce misleading results in the model. Therefore, it is more relevant to show the fraction of insulin appearance in the periphery and clearance. Parameter estimation was performed in the same way with the C-peptide part of the model on data sets (AliceIVGTT), and (RuthClamp). The results can be seen in Figure 8.17 to Figure 8.20. The parameters are in Table 8.17 and the system equations are given by:

$$\frac{dI_i(t)}{dt} = G(t) - k_{iir}I_i \qquad 8.18$$

$$\frac{dI_a(t)}{dt} = I(t) - k_{iar}I_a$$

$$\frac{dI(t)}{dt} = S(t) - k_{ir}I$$

$$\frac{dG(t)}{dt} = g_p - k_{si}I_a(t)G(t)$$

$$\frac{dC_1(t)}{dt} = \frac{1}{frac}S(t) + k_{cp21}C_2(t) - k_{cp12}C_1(t) - k_{cpr}C_1(t)$$

$$\frac{dC_2(t)}{dt} = -k_{cp21}C_2(t) + k_{cp12}C_1(t)$$

Parameter	Description	Units
$frac$	Fraction of C-peptide observed compared to insulin	min
k_{cp21}	Flow of C-peptide from compartment 2 to compartment 1	min^{-1}
k_{cp12}	Flow of C-peptide from compartment 1 to compartment 2	min^{-1}
k_{cpr}	Clearance rate of C-peptide	min^{-1}

Table 8.17: C-Peptide Parameters for Short Term Model

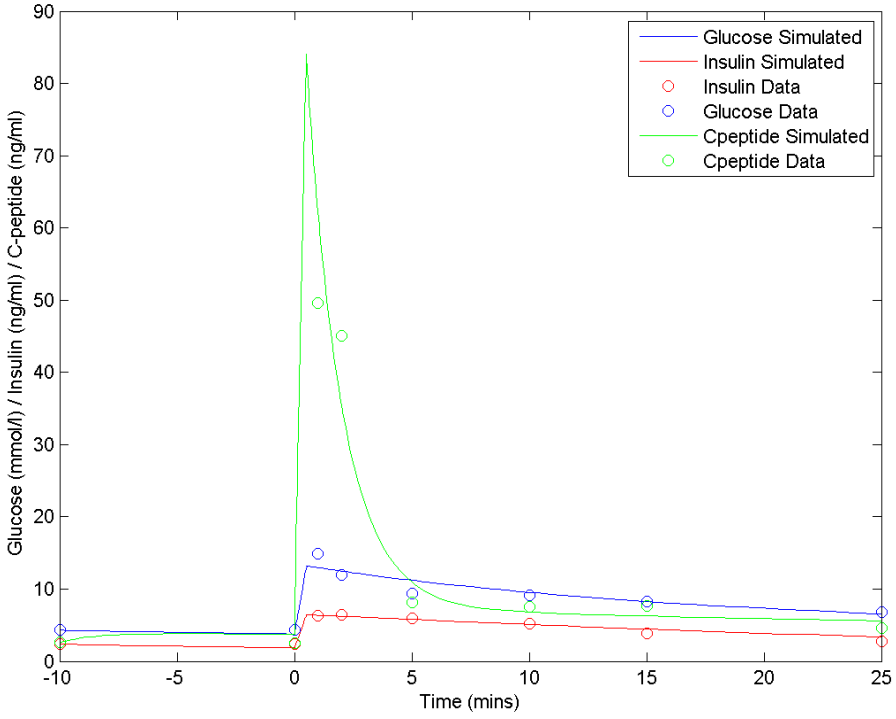

Figure 8.17 IVGTT parameter fit of a single subject

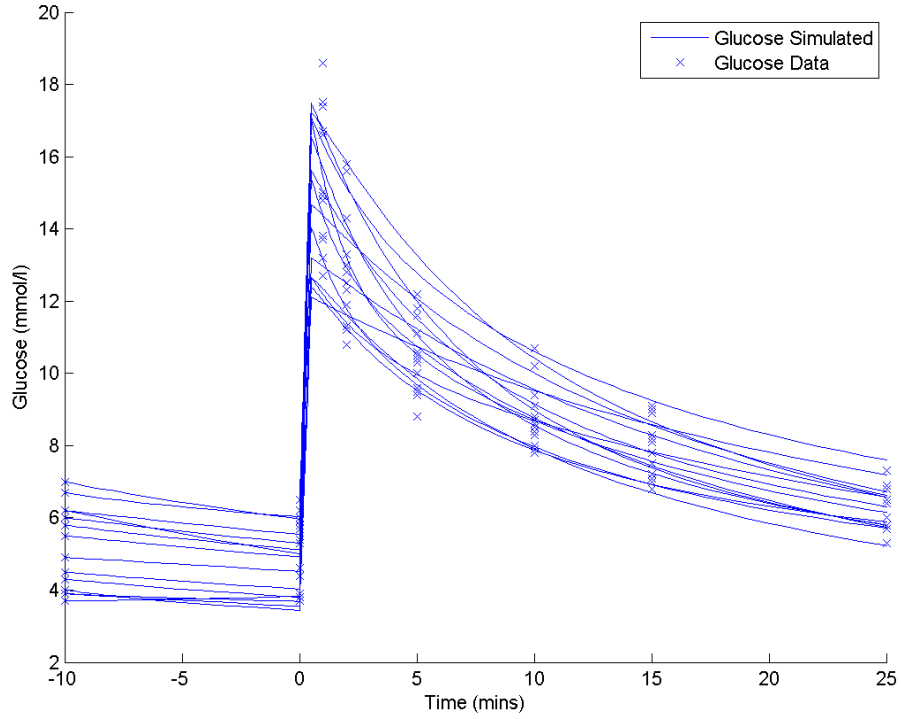

Figure 8.18 IVGTT parameter of glucose for all subjects

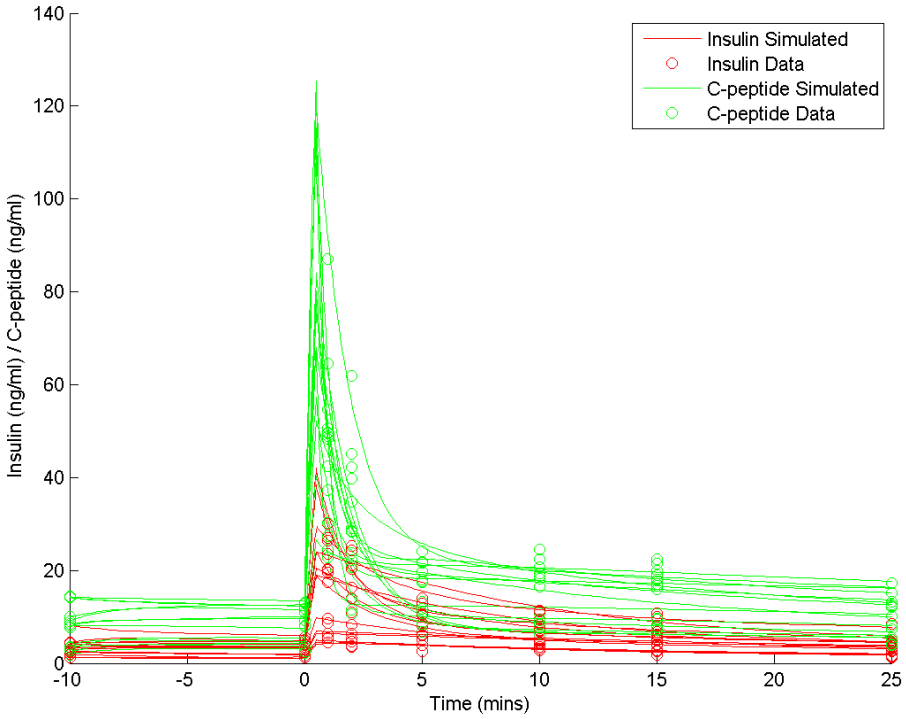

Figure 8.19 IVGTT parameter fit of all subjects with insulin and C-peptide

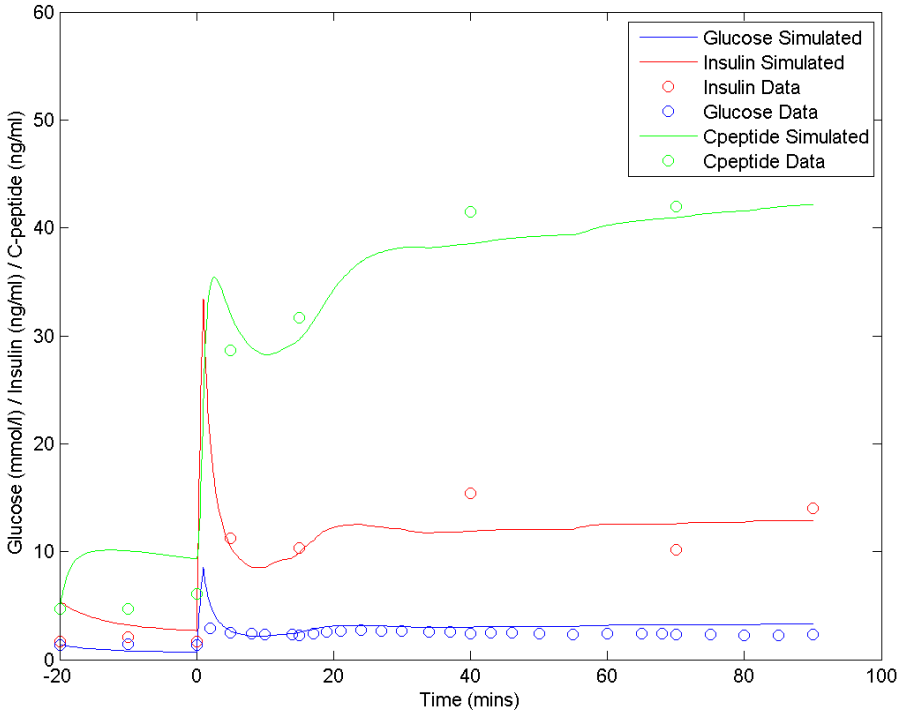

Figure 8.20 Clamp individual fit of a single subject

All the data for hyperglycaemic clamp fitting are given in Appendix 4.

8.9.1 Conclusions

It can be seen there are good fits with all the above experiments (IVGTT, hyperglycaemic clamp and OGTT) both with and without C-peptide present. Being able to predict exactly where to take measurements to get the best confidence with the parameters allows scientists to optimise the readings taken and therefore to get the most out of the experiments performed. Taking fewer readings on animals also reduces the animals' stress, which is good from the point of view of both animal welfare and reliability of data. The way to work out the optimal point to take readings is through sensitivity analysis.

8.10 Sensitivity analysis

The concept of sensitivity analysis was introduced in Chapter 2. This model is designed primarily for use with acute/short-term experiments. These experiments are usually quite intense, however due to limitations such as blood sample volumes, the logistics of working with many animals and other constraints mentioned in Chapter 4. large numbers of time points are not always available. Therefore it is important to know when are the most informative times to sample.

Sensitivity analysis was performed on this model using automatic differentiation. In this context, automatic differentiation involves differentiating the model with respect to the parameters at the same time as simulating the model. This has several advantages over differentiation: it is less tedious and error-prone than manual differentiation and allows alterations to the model to be reflected in the differentiation immediately.

The automatic differentiation method used here is performed by a piece of MATLAB code written by [24] which uses substitution of functions and operators to perform successive differentiations using the chain rule. As this method is analytical it therefore provides an exact solution, not an approximation. As it is done with parameter substitution, it is fast. This creates a set of differential equations, defined in equation 2.27 from section 2.7, which can be simulated at the same time as the model differential equations. There is little or no noticeable difference in performance when simulating these ODEs alongside the model

ODEs. The MATLAB code used to generate this matrix has been included in Appendix 6.

This produces results that show the effect that each parameter has on each state. These can be shown as either absolute effects on the state by the parameter or as relative effects of changing the parameter on the state. As the parameters in this model have a large range of magnitudes, showing relative parameter effects is more relevant. These can then be summed for each state to view a combined sensitivity of state against time. This is useful for seeing which time points are most beneficial for sampling.

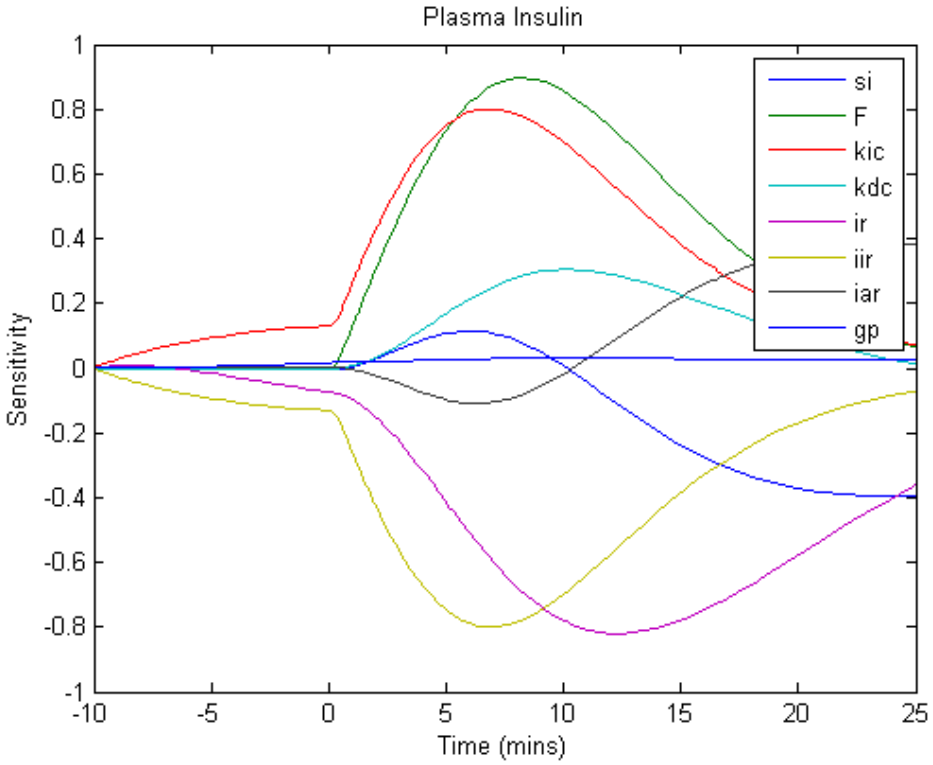

Figure 8.21 Relative sensitivity analysis of insulin on an IVGTT

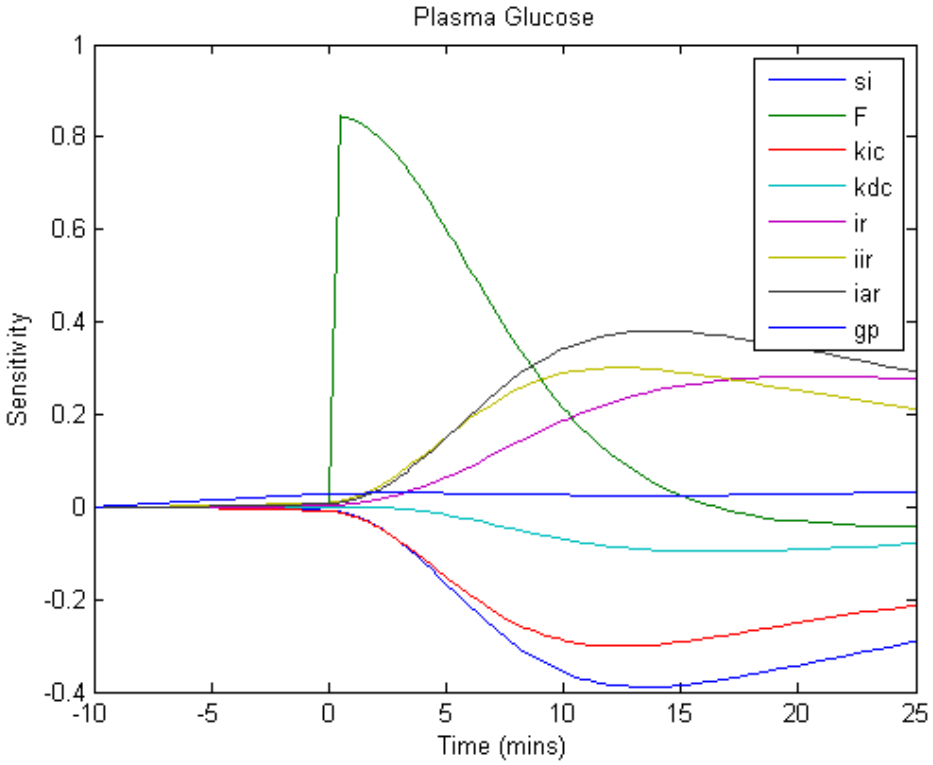

Figure 8.22 Relative sensitivity analysis of glucose on an IVGTT

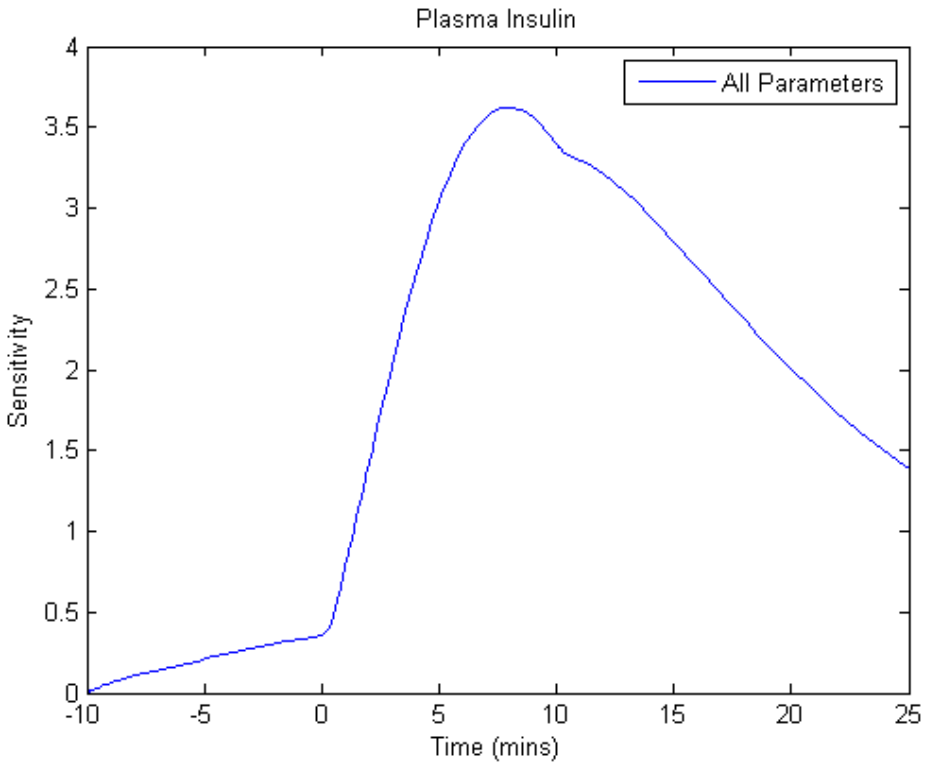

Figure 8.23 Sum of relative sensitivities of all parameters on insulin on an IVGTT

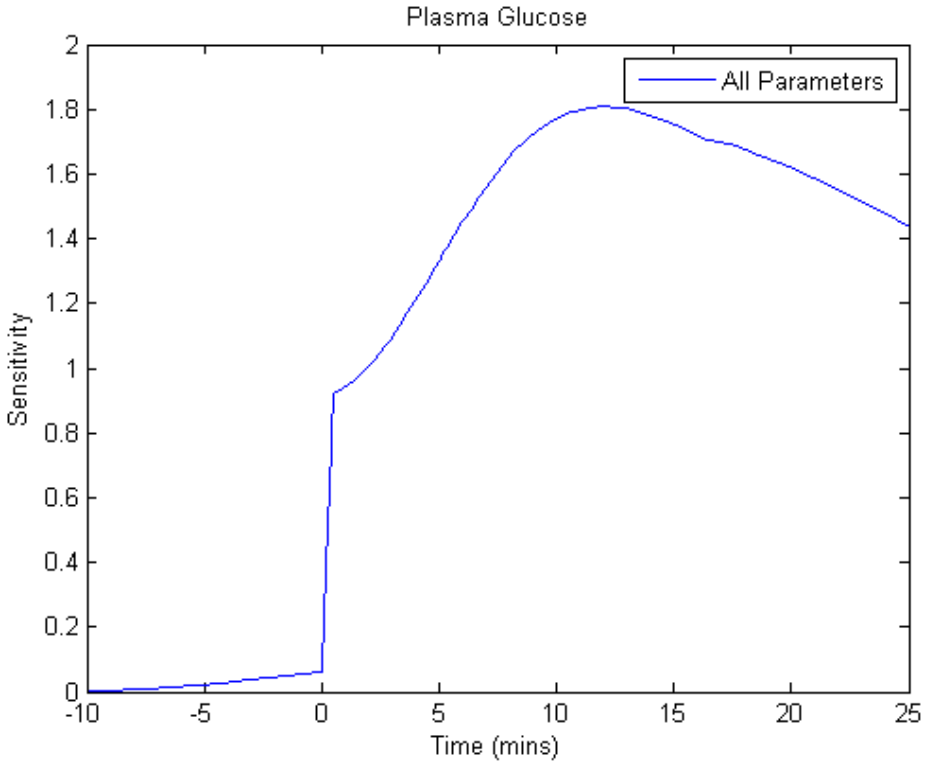

Figure 8.24: Sum of relative sensitivities of all parameters on glucose on an IVGTT

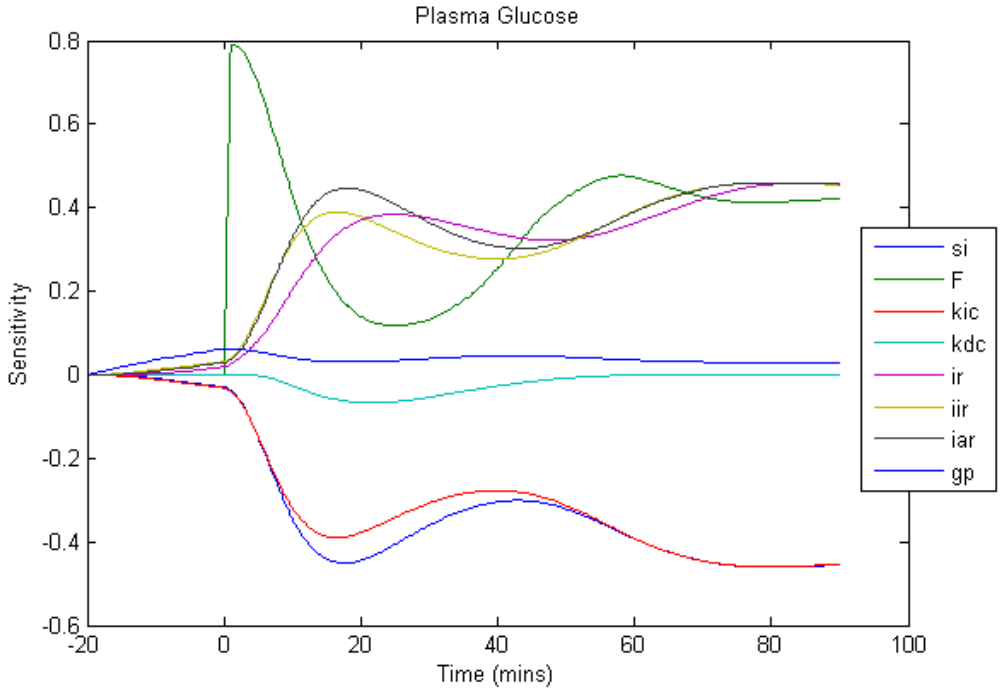

Figure 8.25 Relative sensitivity analysis of glucose on a hyperglycaemic clamp

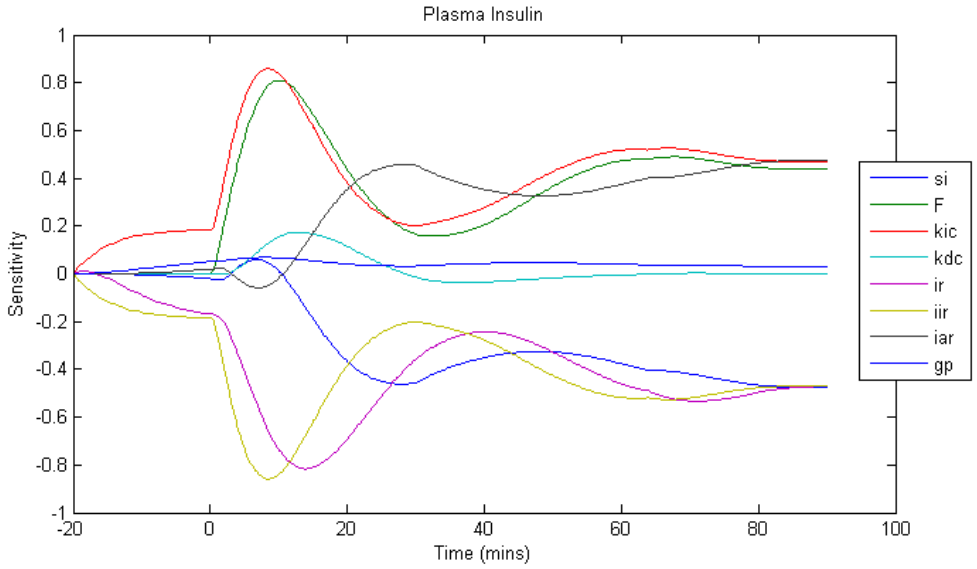

Figure 8.26: Relative sensitivity analysis of insulin on a hyperglycaemic clamp

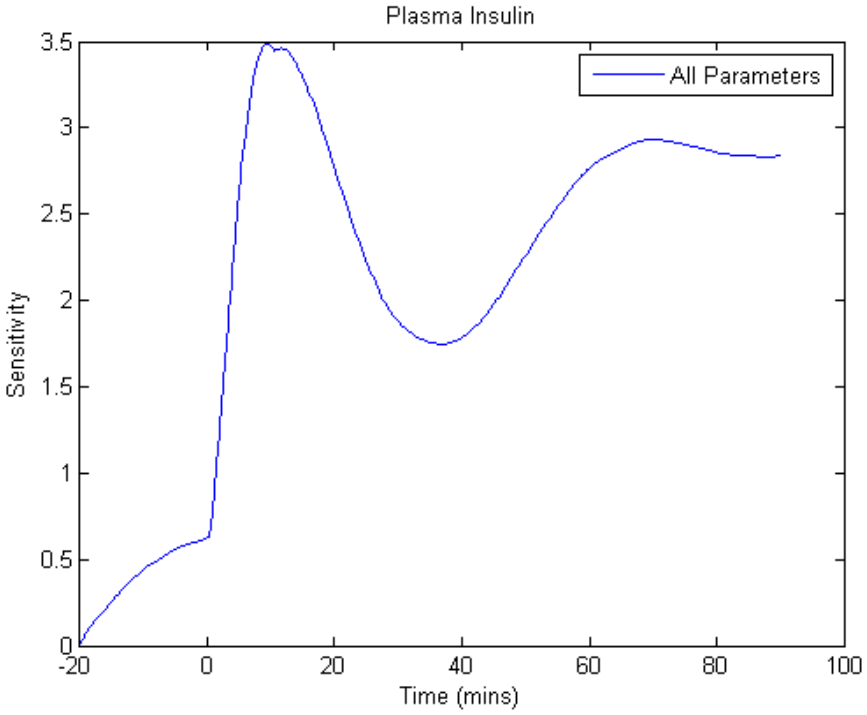

Figure 8.27 Sum of relative sensitivities of all parameters of insulin on a hyperglycaemic clamp

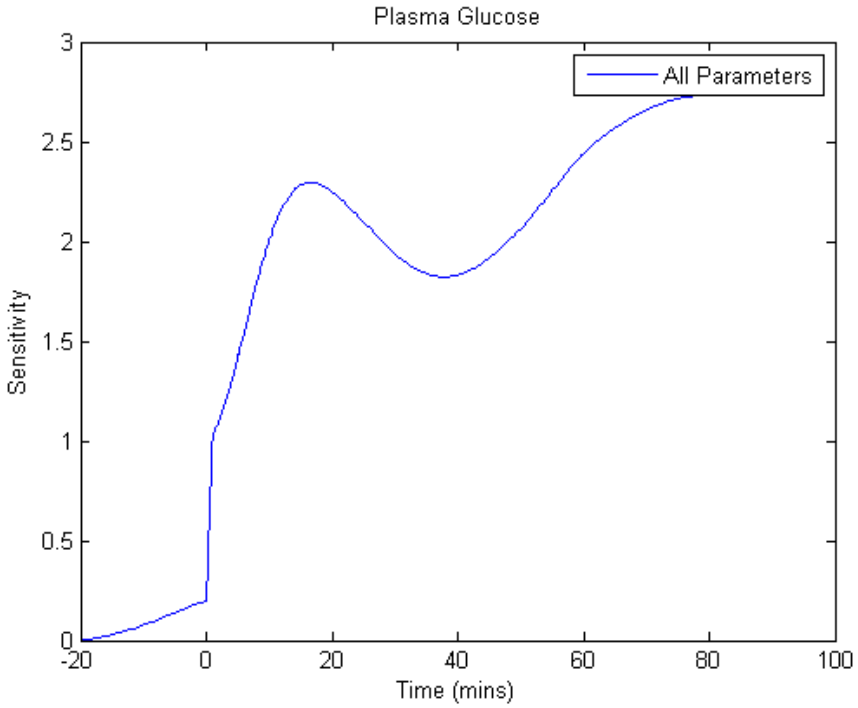

Figure 8.28 Sum of relative sensitivities of all parameters of glucose on a hyperglycaemic clamp

Overall from the sensitivity analysis (Figure 8.21 to Figure 8.28) it is evident that, for most parameters, it is best to measure in the early stages of the experiment, i.e. within the first 20 minutes. It also shows, however, that there is merit in measuring the system when it has reached a steady state, especially for the hyperglycaemic clamp. In all experiments, g_p is the least influential parameter and F is the most influential parameter.

It is valuable to note that the relative sensitivities of all parameters except for g_p have similar magnitudes and, therefore, from these experiments the parameter confidence should be high.

8.11 Conclusions

The aim of this chapter was to design a mathematical model for the glucose homeostatic system that was mechanistic, had key parameters that could identify disease, could predict future experiments and help with experimental design. The model should also be universal, i.e. not confined to a specific test such as an IVGTT; not have an explicit parameter for steady state values; it should be stable and minimal in form.

The model presented is mechanistic as it contains parameters, such as k_d which represents docked insulin granules in the cell. A reduction in such a parameter could represent a failure in the β-cells to produce insulin. Other disease states can be seen mechanistically in other parameters such as k_{si}, changes in insulin sensitivity; k_i, changes in gradual insulin secretion; and g_p, changes in normal constant glucose production. When the model is run on fasted and unfasted animals, key parameters change which match the biological system. These factors will be discussed further in Chapter 9.

That this model can predict other experiments was shown above by using parameters from the IVGTT which gave a reasonable fit to the OGTT. This model is, therefore, not restricted to a single test.

The model does not have any parameters for steady state but reaches a steady state naturally.

The model went through a process of model minimisation to refine the key parameters.

The model can help with experimental design through sensitivity analysis, allowing key time points to be picked for measurements.

Chapter 9: Long Term Modelling

This chapter is concerned with the simulation of disease progression over the longer term (i.e. days and months). The model used is based on the β-cell Mass Model [119]. It incorporates the short-term model previously discussed in Chapter 8 to show how it is possible to have a complete model that can represent both short-term and long-term aspects of the glucose-insulin system. The model output is compared to (not fitted to using an optimisation algorithm) Zucker and ZDF data collected at AstraZeneca, Alderley Park, Cheshire.

9.1 β-cell Mass Model

This model is based on a model created in 2000 by Topp et al.[119]. These authors set up a three compartment model, with the compartments representing insulin, glucose and β-cell mass (see Figure 9.1).

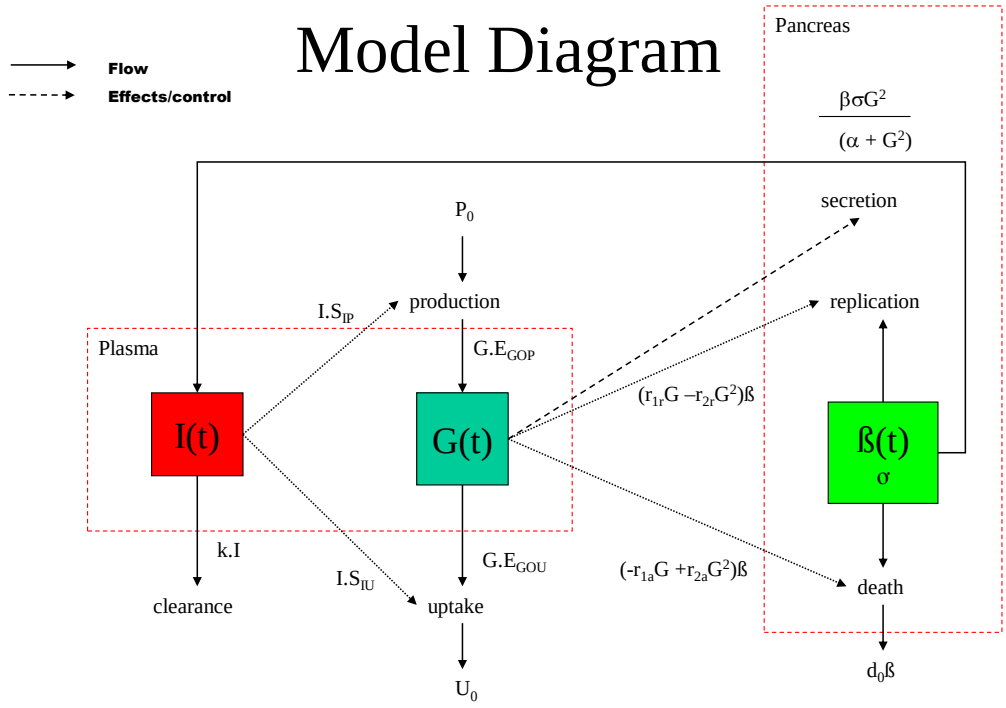

Figure 9.1: β-cell mass model diagram

The model and analysis concentrated primarily on long-term, rather than short-term, aspects of the system, i.e. changes which occur over days rather than minutes or hours. Therefore the glucose and insulin concentrations in this model could be considered as the basal levels of glucose and insulin. The differential equation describing rate of change of glucose in the model includes terms

representing the rate of appearance of glucose minus glucose effectiveness and insulin sensitivity, and is given by:

$$\frac{dG(t)}{dt} = R_o - \big(E_{go} + S_I I(t)\big)G(t) \qquad 9.1$$

where *G(t)* is glucose concentration, R_0 is the net rate of production at zero glucose, $E_{go}$is the total glucose effectiveness at zero insulin and S_I is the total insulin sensitivity.

The differential equation describing rate of change of insulin has terms representing insulin secretion, based on glucose and β-cell mass in a Hill function, and a clearance function, and is given by:

$$\frac{dI(t)}{dt} = \frac{\beta\sigma G(t)^2}{(\alpha + G(t)^2)} - kI(t) \qquad 9.2$$

The differential equation describing rate of change of β-cell mass comprises terms representing the natural death rate of β-cells, a rate of growth of β-cells based on the level of glucose, and a decrease in β-cells which is also based on glucose, and is given by:

$$\frac{d\beta(t)}{dt} = (-d_0 + r_1 G(t) - r_2 G(t)^2)\beta(t) \qquad 9.3$$

The combination of the parameters d_0, r_1 and r_2 create a system which can adapt to changing levels of glucose. For example, if the glucose level is below

100mg/dl, the β-cell mass will decrease which will in turn lower insulin and return glucose to an acceptable level (i.e. 100mg/dl); if the glucose level lies between 100 and 250mg/dl, β-cell mass will increase, meaning insulin will increase and glucose levels will decrease towards 100mg/dl. With glucose below 250mg/dl the system adapts, based on glucose levels; with glucose levels over 250mg/dl, glucose toxicity comes into play and reduces β-cell mass, which leads to decreased insulin levels and results in ever-increasing glucose levels in a runaway situation, see Figure 9.2.

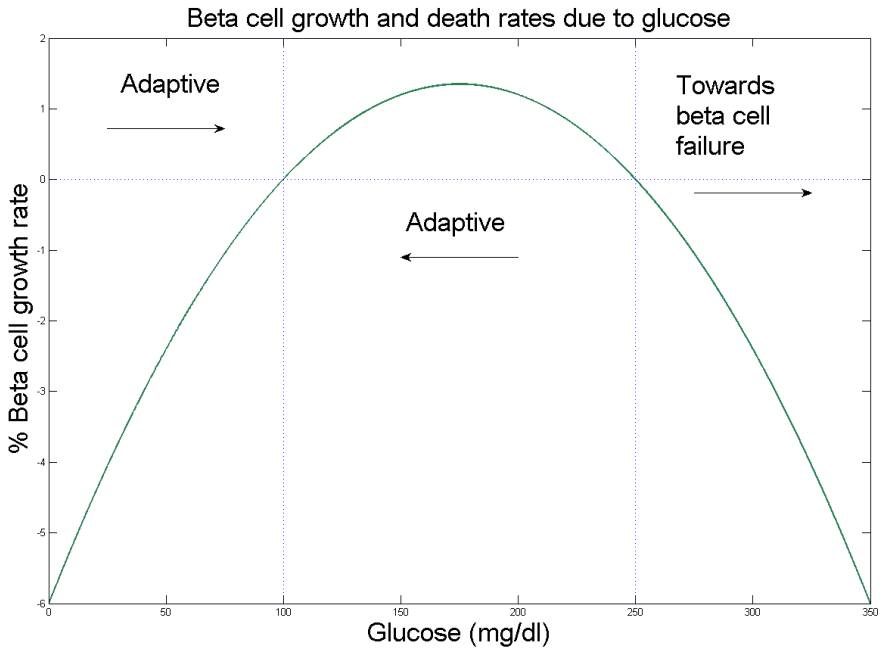

Figure 9.2: β*-cell growth and death rates due to glucose*

9.2 Data

ZDF and Zucker data were taken from (JoChronic) and glucose and insulin profiles were taken on several days over a 40 day study. As the model was in

concentration units of mg dl^{-1} for glucose and μU ml^{-1} for insulin, all data have been converted to these units from the mM and ng ml^{-1} that were originally used.

9.3 Modifications

9.3.1 Incorporating Short-Term Model

The short-term model presented in Chapter 8 was incorporated into this long-term model, with a few modifications. The first is insulin secretion: as it is related to β-cell mass, integral and derivative terms have been incorporated in the long-term model for β-cell mass. The second is insulin action, which was removed as time points in the long-term model are hours apart (as opposed to minutes in the short-term model) so the fast dynamics of the insulin action are not present in the data in Chapter 8 (see equation 9.4). The third modification involved removing glucose effectiveness, as discussed earlier in Chapter 8.

Finally, as the animals used here were in a diseased state and hyperinsulinaemic, i.e. insulin was saturating glucose disposal compared to a normal, insulin-sensitive rat, Michaelis-Menten type kinetics were incorporated and applied to insulin sensitivity. K_M was set to 100mg/dl of insulin, following the same assumptions as the β-cell Mass Model that that is the stable equilibrium point, therefore V_{max} is assumed to be twice the steady-state sensitivity of insulin. These adjustments mean that the parameters in the short-term model are not exactly equivalent to those in the long-term model. The modified system equations are therefore given by:

$$\frac{dI(t)}{dt} = k_d \frac{dG(t)}{dt} + k_i I_i(t) - k_{ir} I \qquad 9.4$$

$$\frac{dG(t)}{dt} = R_o - \frac{S_I I(t) G(t) V_{max}}{G(t) + K_m} + g_{abs} G_{gut}(t) - R_c(t)$$

9.3.2 Meal Feeding

As with the short-term modelling of OGTT in Chapter 8, this model required the addition of a single compartment to represent a delay in the intake of food into the system. Unlike an OGTT, however, glucose was taken in differently; instead of being given a single dose at a specific time, animals were eating over a four hour period. The assumption was made that, as rats had been fasted for an extended period of time, the rate of feeding would be high at the start of the feeding period and would slow down over the course of the four hour period. A trapezoidal function was therefore used for the rate of feeding. This trapezoidal function was normalised to have an area of one, with a single parameter for the steepness of the slope - see Figure 9.3. This trapezoidal function could then be multiplied by the actual amount of glucose ingested to give an input to the gut compartment. This is given by:

$$\frac{dG_{gut}(t)}{dt} \qquad 9.5$$

$$= \begin{cases} -g_{abs} G_{gut}(t) + g_{feed}(\mathrm{g_m t} + \mathrm{g_c}) & t_{start} < t < t_{finish} \\ -g_{abs} G_{gut}(t) & everwhere\ else \end{cases}$$

where

$$g_c = \frac{1}{t_{finish} - t_{start}}(1 + g_{slope})$$

$$g_m = \frac{\frac{1}{t_{finish} - t_{start}}(1 + g_{slope}) - g_c}{t_{finish} - t_{start}}$$

This, together with the gut compartment and an appropriate value for g_{abs} (gut absorption), produces glucose concentrations that lie within approximately 10% of the mean of the data. Figure 9.3 shows a typical meal feed produced by trapezoidal function.

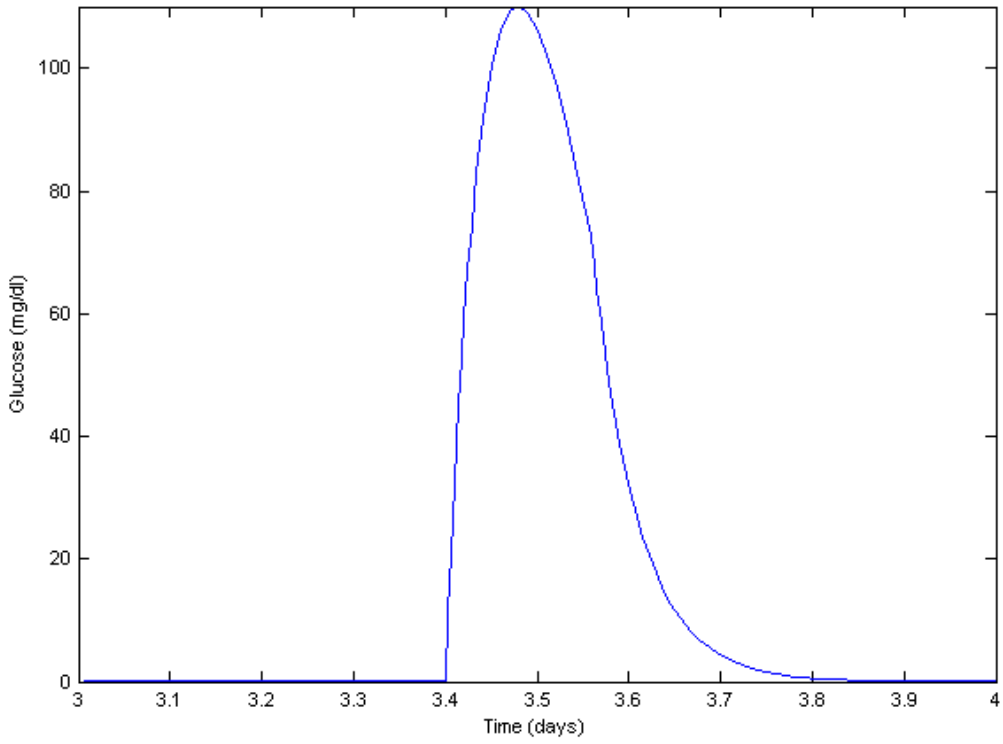

Figure 9.3: Gut glucose concentration as produced by the trapezoidal function

9.3.3 Renal Clearance

As explained above, when a subject's glucose level is above 250mg/dl, the β-cell Mass Model shows a runaway reduction in β-cell mass. Some of the animals from

which data for this model were obtained are hyperinsulinaemic and hyperglycaemic (i.e. with glucose levels above 250mg/dl), and do not see a rapid decay in β-cell mass as would be predicted by the β-cell Mass Model, but instead see only a small reduction in β-cell mass. 250mg/dl is either coincidentally (or by design but unmentioned by the creators of the model) close to renal clearance of glucose [156], which is not included in the β-cell Mass Model. In previous models, such as the AIDA Model and Cobelli's Model, detailed in Chapter 5, renal clearance has been incorporated; it was therefore also incorporated in the long-term model here and represented by a piecewise function for renal clearance with parameter values taken from the AIDA model, as follows:

$$R_c(t) = \begin{cases} -\mathrm{r_c}(\mathrm{G(t)} - \mathrm{r_t}) & G(t) > r_t \\ 0 & everwhere\ else \end{cases} \qquad 9.6$$

9.3.4 Disease Progression

9.3.4.1 Insulin Sensitivity

It was hypothesised that a way of introducing disease progression into the model would be to represent insulin sensitivity by a decaying exponential function [119].This hypothesis was adopted for the long-term model presented here. It was also noted in the experimental data that the ratio between insulin and glucose (i.e. insulin sensitivity) changed over time, reinforcing the need for this adaptation. Thus the system equation for insulin sensitivity is given by:

$$\frac{dS_I(t)}{dt} = -c_s.S_I(t) \qquad 9.7$$

9.3.4.2 First-Phase Insulin Secretion

It is apparent from the Zucker and ZDF data collected at AstraZeneca that basal insulin secretion varies between groups of animals and over time. It is also apparent that the first-phase insulin secretion changes and, in the case of the meal-fed animals, it decreases in comparison to the basal level of insulin secretion. Therefore the model was modified so that the level of first-phase insulin secretion changes over time. This was done in a similar way to the modification made for insulin sensitivity, i.e. using a decaying exponential function. This was not intended to reflect a specific reason behind change in first-phase insulin secretion, only to quantify the rate of change. Thus the system equation for first-phase insulin secretion is given by:

$$\frac{dk_d(t)}{dt} = -c_d.k_d(t) \qquad 9.8$$

9.4 Software Tool

A simple software tool was created to perform the simulation of this model, see Figure 9.4, the code for which is given in Appendix 5. It was set-up so that the experimental data could be visualised and the model simulated. It was written in MATLAB using the in-built GUI editor (see Appendix 5). As this model is stiff (see Chapter 2), the ODE solver `ode23tb` was used, which is an implicit Runge-Kutta

algorithm. This solver simulates a response representing a 40 day period within a few seconds. The software allows parameters to be changed and re-simulated easily. It does not have any parameter fitting capabilities and is purely used for simulation given realistic parameter values and initial conditions. See Table 9.1 below.

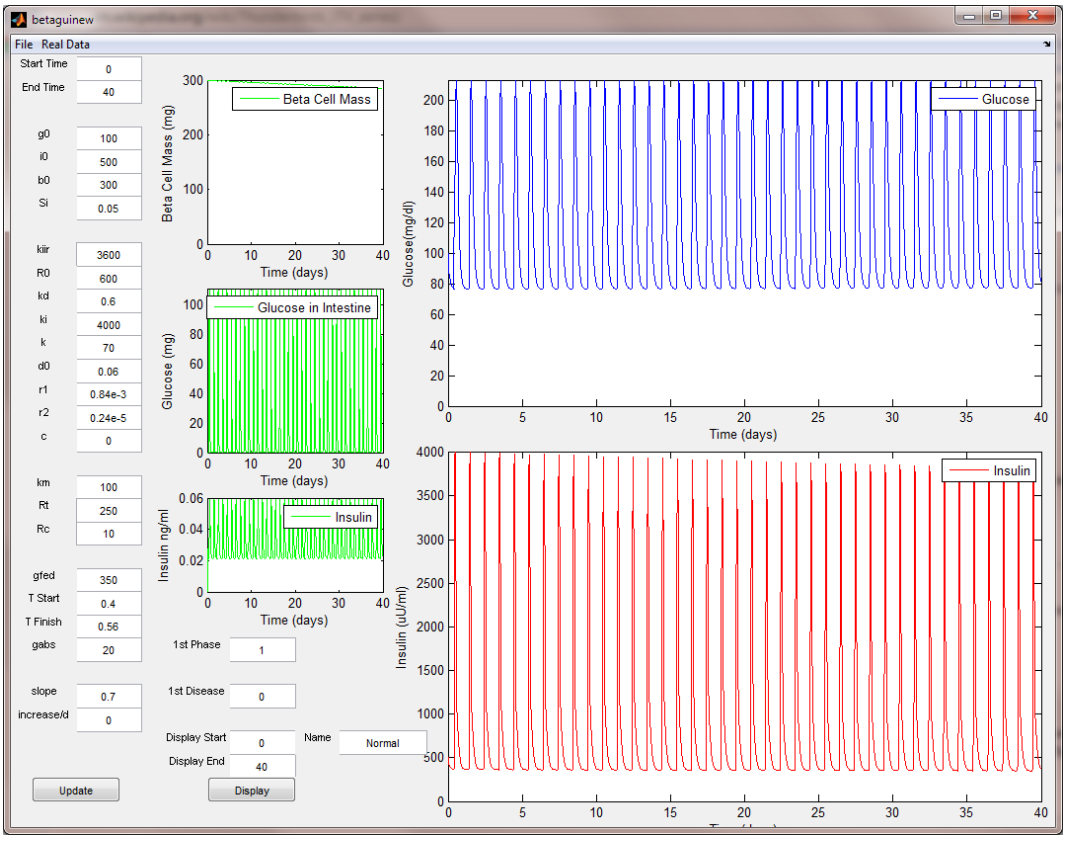

Figure 9.4: Long term modelling simulation tool

Parameter	Description	Value	Units	Source
	Initial Conditions			
g_0	Starting level of glucose	100	mg dl^{-1}	[119] Data
i_0	Starting level of insulin	500	µU ml^{-1}	Data
b_0	Starting level of β-cell mass	300	mg	[119]
g_{gut}	Starting level of gut glucose	0	mg dl^{-1}	Assuming empty gut
	Insulin Kinetics			
k_d (k_{d0})	First-phase insulin secretion -differential (starting value)	0.7	µU ml^{-1} $mgdl^{-1}$	Chapter 8
k_i	Second-phase insulin secretion -integral	4000	µU ml^{-1} $mgdl^{-1}$ day^{-2}	Chapter 8
k_{iir}	Second-phase insulin secretion time constant	3600	day^{-1}	Chapter 8
k	Insulin clearance	432	d^{-1}	[119]
c_d	First-phase insulin secretion decay		day^{-1}	See above

Parameter	Description	Value	Units	Source
	Glucose Kinetics			
R_0	Net rate of glucose production		mg dl^{-1} d^{-1}	[119]
k_m	k_m of insulin sensitivity		mg dl^{-1}	See above
S_I (S_{I0})	Insulin sensitivity (starting value)	0	ml μU^{-1} d^{-1}	[119]
c_{SI}	Insulin sensitivity decay	0	day^{-1}	[119]
	β-*cell Kinetics*			
d_0	Natural β-cell death		d^{-1}	[119]
r_1	Rate constant of β-cell growth		mg^{-1} dl d^{-1}	[119]
r_2	Rate constant of β-cell death		mg^{-2} dl^2 d^{-1}	[119]

Parameter	Description	Value	Units	Source
	Glucose gut kinetics			
g_{abs}	Glucose absorption from the gut	24	day^{-1}	See above [118]
g_{slope}	Slope of trapezoidal function		fraction (unit-less)	See above
t_{start}	Feeding start time		day	Data
t_{end}	Feeding end time		day	Data
g_{fed}	Glucose ingested		mg	Data

Table 9.1: Parameters in long-term model

9.5 Comparison with Experimental Data

The model was compared with real experimental data to see if it produced realistic results. As this model could be considered to be over-parameterised for the system modelled, parameter optimisation via an optimisation algorithm is unlikely to be successful so was not used. Therefore, changes in parameters are educated estimates of changes to biological mechanisms in order to demonstrate that this model can produce responses that compare well with real data.

9.5.1 Zucker Chow Fed Rat Experimental Protocol

In this situation, a Zucker rat is meal fed with a chow diet; 7.42% Fat vs 42% for High Fat diet which is low fat but provides the same calorific intake as the high fat diet given to animals later in this chapter. In this situation the Zucker rat is hyperinsulinaemic, but maintains reasonable glycaemic control, i.e. insulin is above the normal level - such as that of a Han Wistar rat - glucose returns to the basal level of 80-100mg dl^{-1}

9.5.1.1 Necessary Changes in Parameters

As these animals were hyperinsulinaemic, it is reasonable to lower insulin sensitivity and alter k_d, k_i, k_{iir} and k. The parameter values used are given in Table 9.2.

Parameter	Value
k_d	0.7 µU ml $^{-1}$mgdl^{-1}
k_i	4000 µU ml $^{-1}$mgdl^{-1} day^{-2}
k_{iir}	3600 day^{-1}
k	70 d^{-1}

Table 9.2: Parameters altered based on Zucker chow fed data

Note that the values have not changed from Table 9.1 as those values were set in this model. The results from this can be seen in Figure 9.5 to Figure 9.7.

9.5.1.2 Long-term Graphs

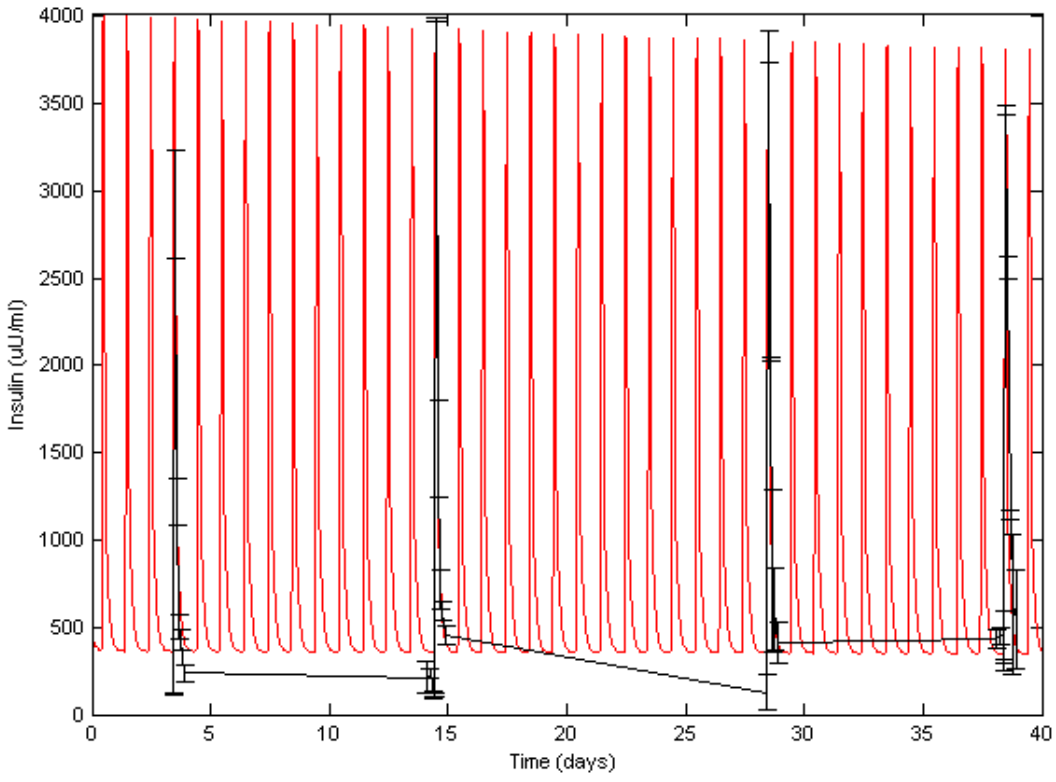

Figure 9.5: Zucker chow fed data - whole study simulations with insulin mean values and standard errors in black and simulated insulin in red

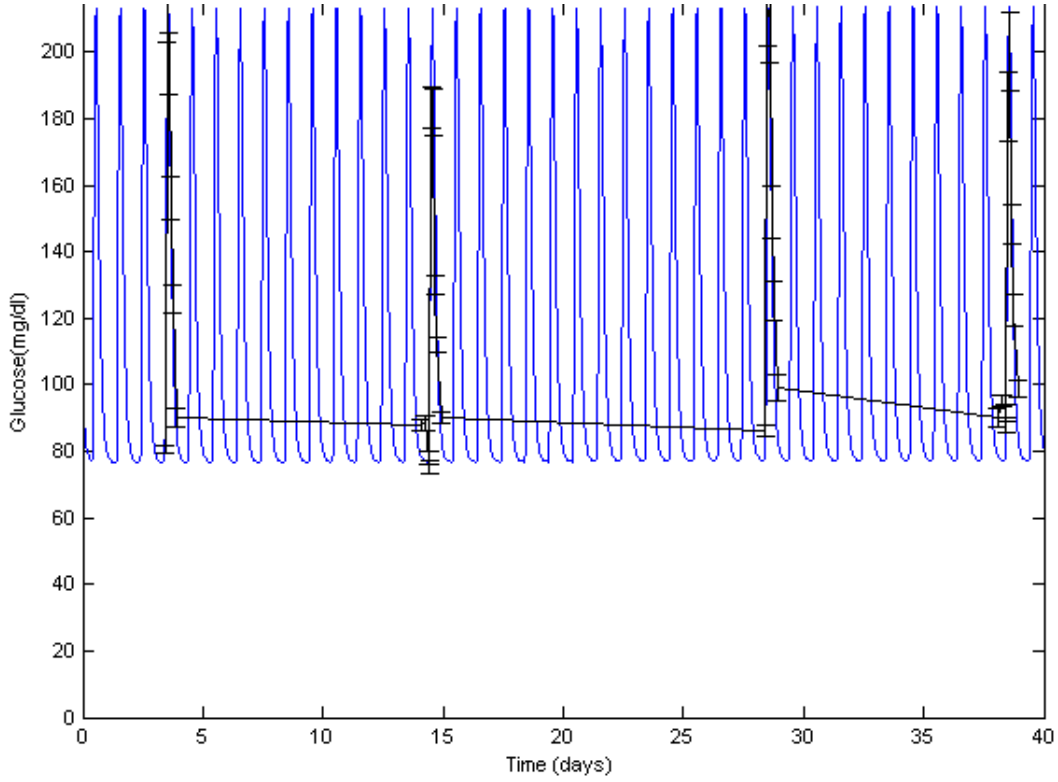

Figure 9.6: Zucker chow fed data - whole study simulations with glucose mean values and standard errors in black and simulated glucose in blue

9.5.1.3 Day Graphs

Day 3

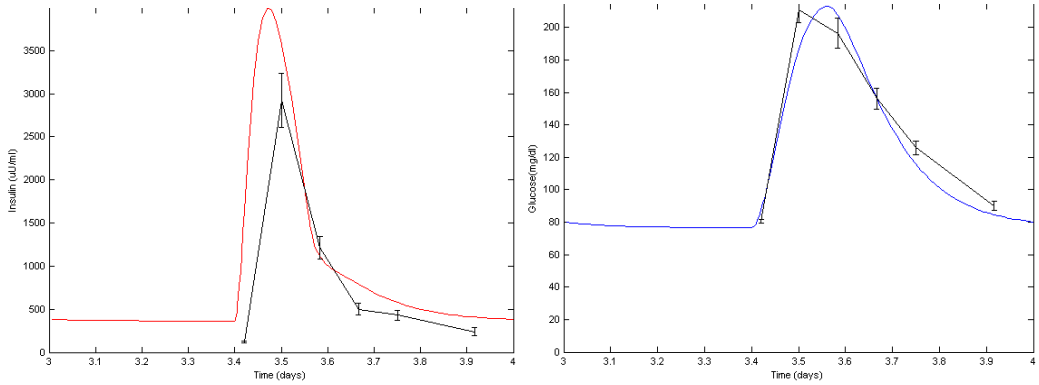

Day 14

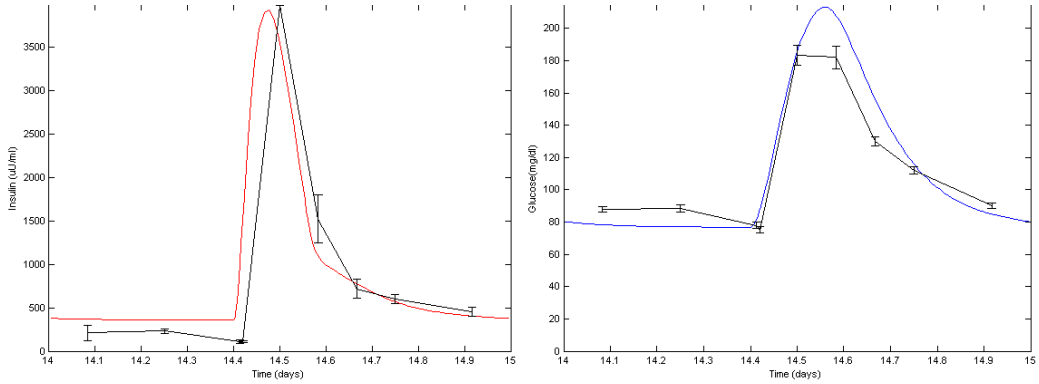

Day 28

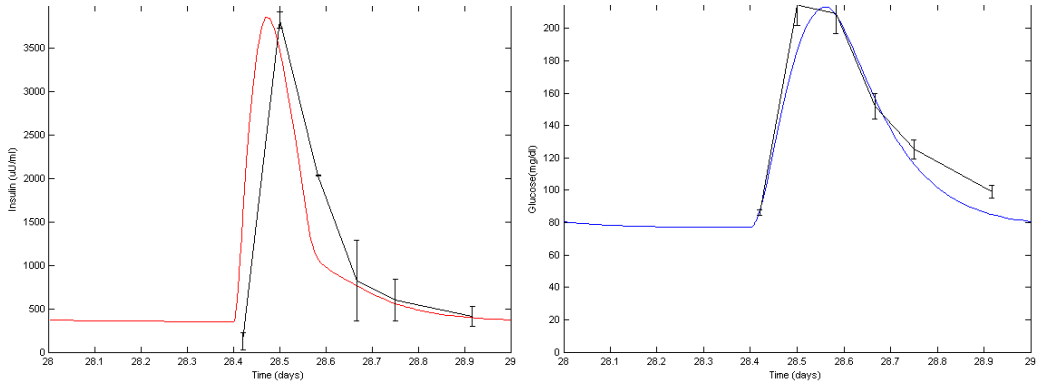

Day 38

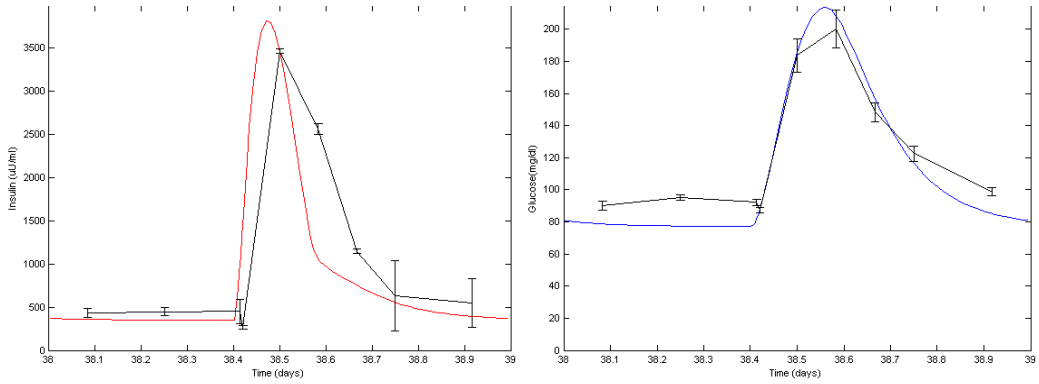

Figure 9.7: Zucker chow fed data - day simulations with real data in black, simulated insulin in red and simulated glucose in blue

The above graphs, Figure 9.5 to Figure 9.7, show that this model can produce realistic results for the Zucker chow fed, meaning that it represents animals in a non-diseased state.

9.5.2 Zucker High Fat Fed Rat Experimental Protocol

The only difference from the previous experimental set-up here is that the diet was changed to the 42% fat content diet. The model was set up identically; the profiles were initially similar, but changed throughout the study.

9.5.2.1 Necessary Changes in Parameters

It was anticipated that insulin sensitivity would decrease over time, however this did not take into account the fact that first-phase insulin secretion was also decreasing and therefore c_d was decreased accordingly. The parameter values used are given in Table 9.3. The results from this can be seen in Figure 9.8 to Figure 9.10.

Parameter	Value
S_I	0.02 day^{-1}
c_d	0.06 day^{-1}

Table 9.3: Parameters altered based on Zucker high fat fed data

9.5.2.2 Long-term Graphs

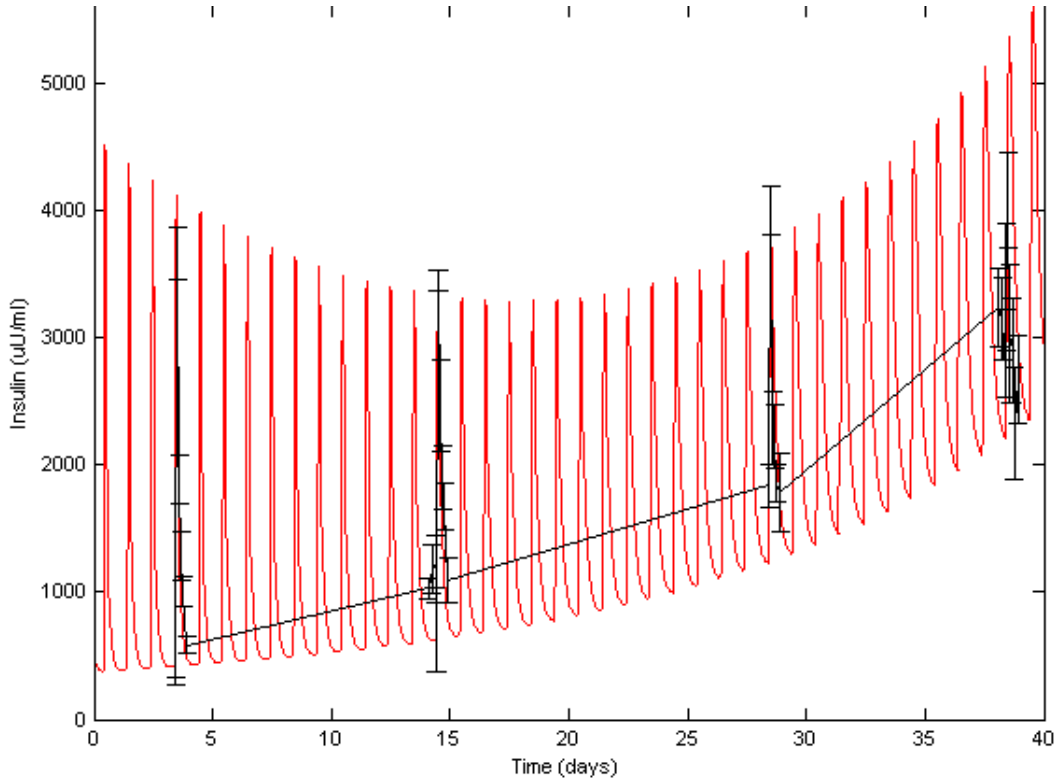

Figure 9.8: Zucker high fat fed data - whole study simulations with insulin mean values and standard errors in black and simulated insulin in red

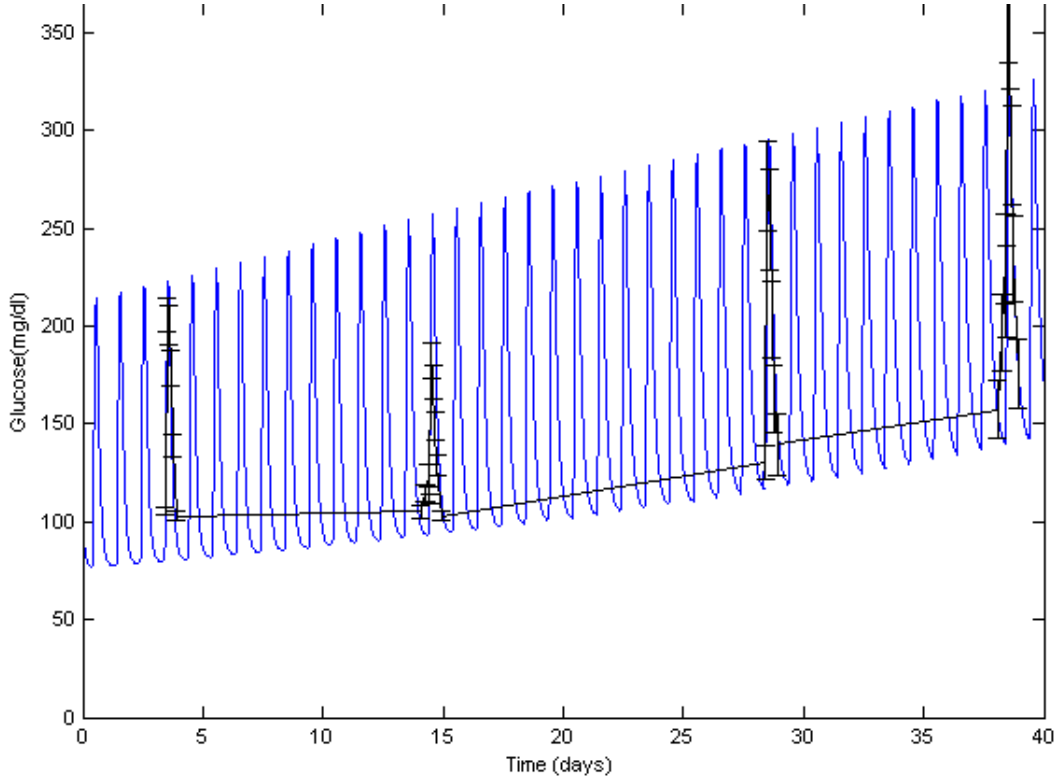

Figure 9.9: Zucker high fat fed data - whole study simulations with glucose mean values and standard errors in black and simulated glucose in blue

9.5.2.3 Day Graphs

Day 3

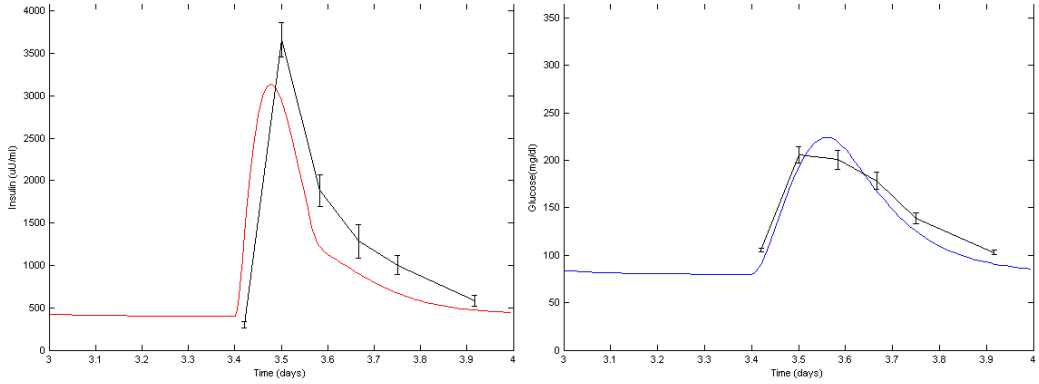

Day 14

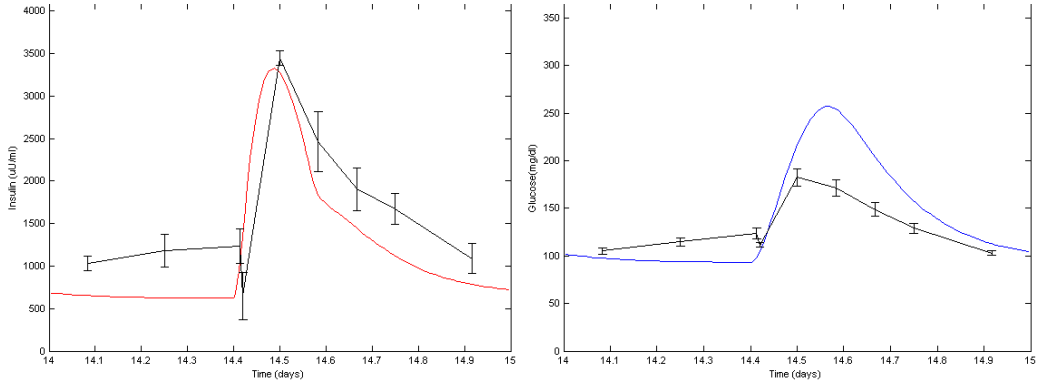

Day 28

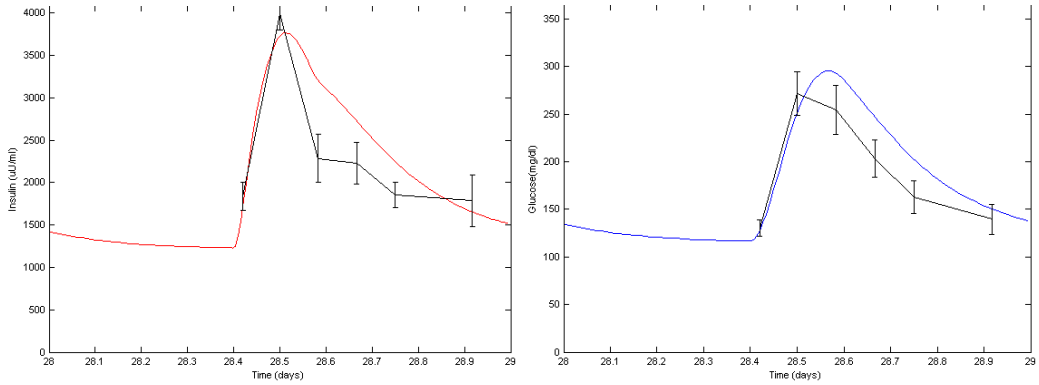

Day 38

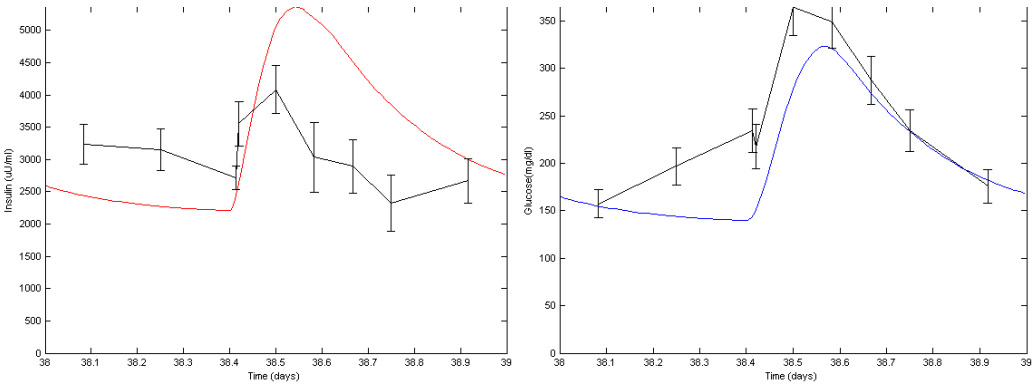

Figure 9.10: Zucker high fat fed data - day simulations with real data in black, simulated insulin in red and simulated glucose in blue

Figure 9.8 to Figure 9.10 show that, by altering a few parameters, we can simulate a Zucker rat going into a diseased state which means that we can experiment with changing certain physiological parameters of a rat to see the resulting effect.

9.5.3 ZDF Chow Fed Rat Experimental Protocol

In this situation, it was noted that the chow diet seemed to improve the condition of the ZDF animals.

9.5.3.1 Necessary Changes in Parameters

In this study, both glucose and insulin sensitivity remained constant throughout. Insulin, however, decreased but, as the animals were hyperinsulinaemic, insulin disposal was saturated so falling levels of insulin had no effect on glucose levels. The only aspect which did change throughout the experiment, therefore, was first-phase insulin secretion, which decreased. The only change required to the

original base set of parameters was first-phase insulin secretion decay, c_d, which was set at 0.04 day^{-1}. The results can be seen in Figure 9.11 to Figure 9.13.

9.5.3.2 Long-term Graphs

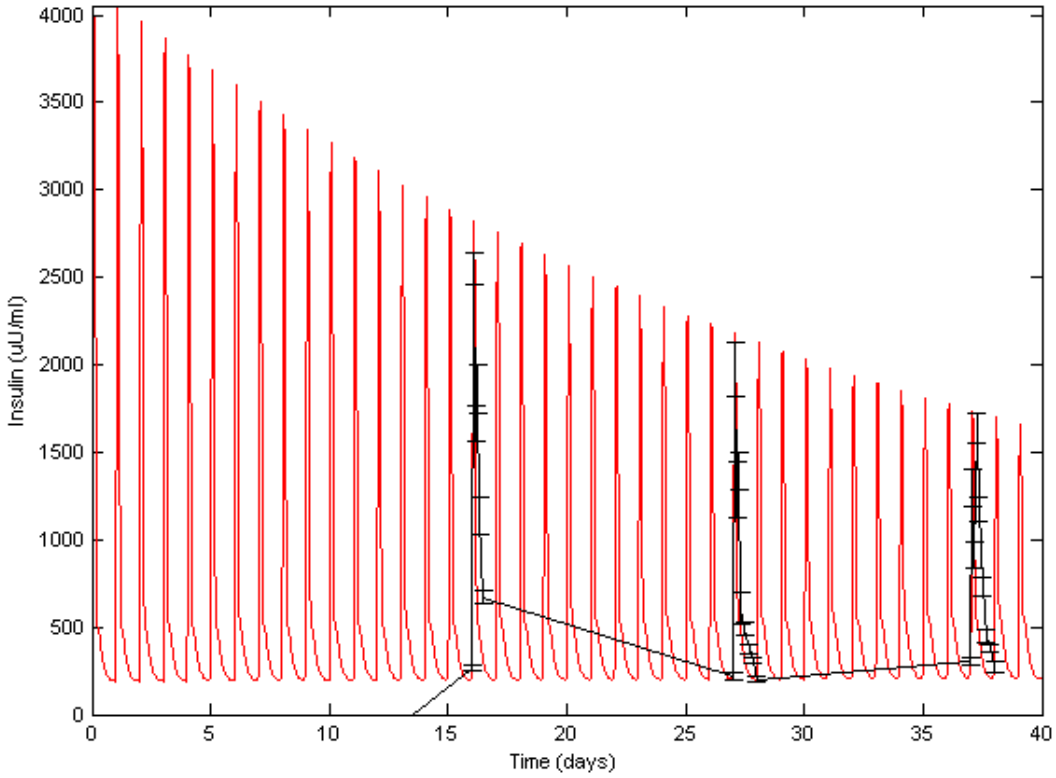

Figure 9.11: ZDF data - whole study simulations with insulin mean values and standard errors in black and simulated insulin in red

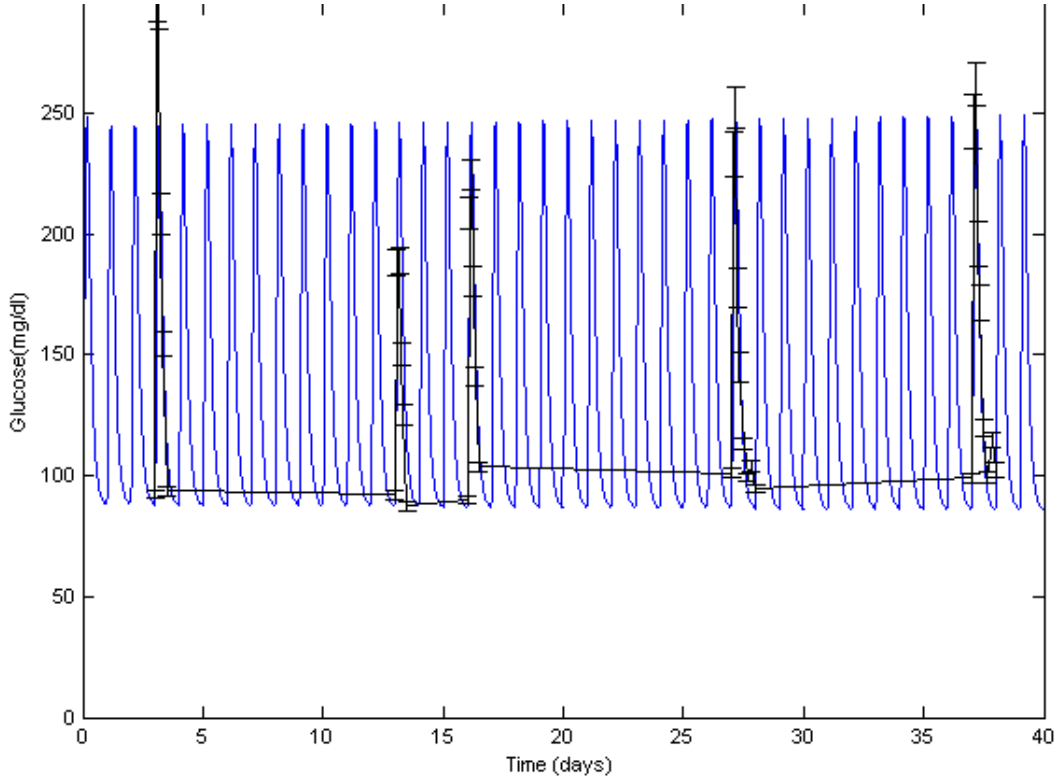

Figure 9.12: ZDF data - whole study simulations with glucose mean values and standard errors in black and simulated glucose in blue

9.5.3.3 Day Graphs

Day 16

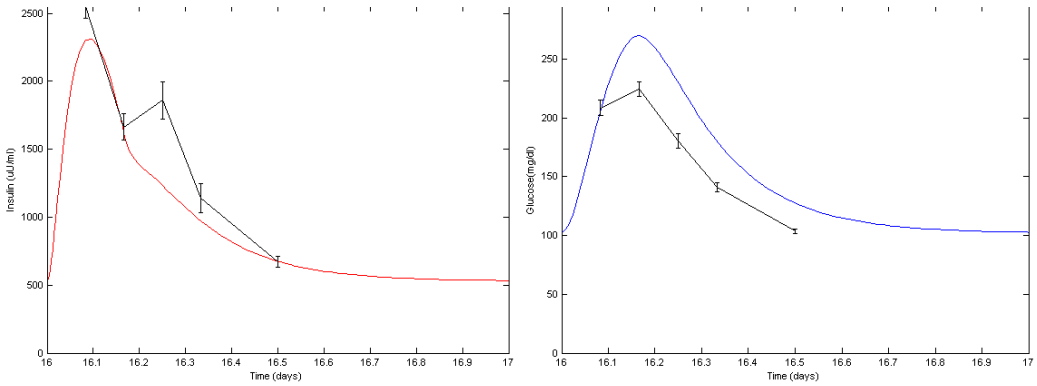

Day 27

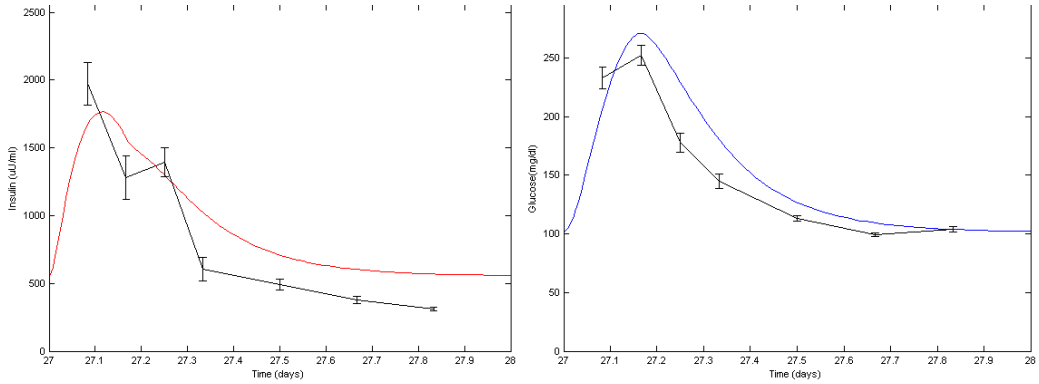

Day 38

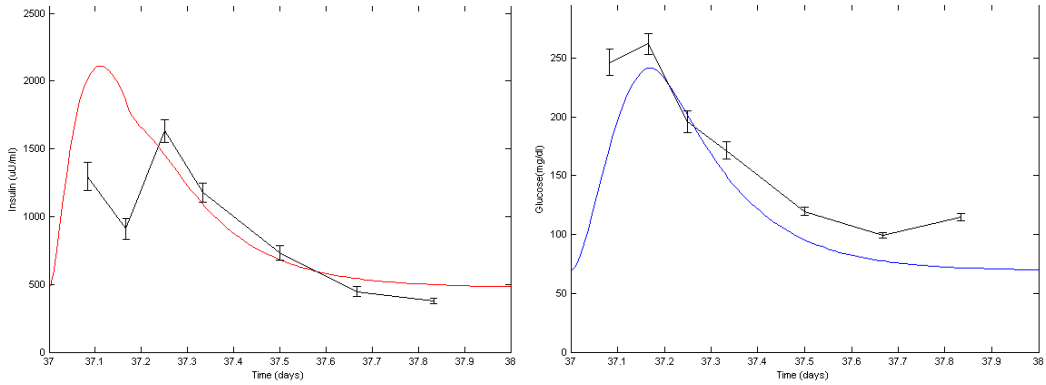

Figure 9.13: ZDF data - day simulations with real data in black, simulated insulin in red and simulated glucose in blue

Figure 9.11 to Figure 9.13 show that this model can produce reasonable predictions of the diseased state. These animals, however, are in a highly diseased state and so are metabolically stressed which means that the insulin secretion is exacerbated and this is not captured by this model. The insulin levels are very high and well above the saturation of insulin sensitivity so this two-phase insulin secretion has little or no effect on the glucose profile.

9.5.4 Conclusions and Discussion

Here, the short-term and long-term models have been combined to produce a fully-coupled, continuous model of the glucose-insulin system. It has been shown that glucose and insulin models can be combined to simulate a reasonable representation of the long-term dynamics and disease progression of subjects.

As this model is over-parameterised and there are only data from two compartments, it is difficult to draw any firm biological conclusions because the same graphs could be produced from different sets of parameters. However, parameters which have been altered to produce the results mechanistically make sense in the biological context. This makes the model a potentially useful predictive or experimental tool rather than an analytical tool.

The model does not explain biologically certain aspects of the system, in particular insulin sensitivity decreasing in the Zucker high fat fed animal. It does not provide a mechanistic reason for this decrease, therefore further modelling work should be carried out to link in possible causes such as lipid metabolism; the effects of lipids on the glucose-insulin system were mentioned in Chapter 3 and could be incorporated into this model. The other aspect which is not covered is why first-phase insulin secretion decreases whereas second-phase insulin secretion seems to remain in-line with basal levels. Again, the model does not provide an explanation for the reason behind this.

Chapter 10: Software Tool for Modelling Glucose, Insulin and C-peptide Dynamics

10.1 Aim and Purpose

A software tool to allow the use of modelling in their day-to-day operations is an important deliverable for AstraZeneca. It is important to AstraZeneca that non-mathematical scientists are able to perform modelling and simulation to allow them to use the concept of modelling in the same way that they use statistics. They can use it as a tool to analyse and predict system outcomes, to give more information about the data they have collected, to produce more meaningful conclusions and to gain a better understanding of the underlying biology of a system.

There are various requirements to ensure that the software tool is useful to non-mathematical scientists at AstraZeneca. The software tool must be robust so that it does not produce erroneous results. It must be simple to use and present results in an appropriate form for non-mathematical scientists to interpret. It must be well-integrated into the existing AstraZeneca set-up so that using the software will not create additional work and it will be seen as an easily accessible, accepted and worthwhile tool.

10.2 Specification

The functions the software tool will perform will be as follows:

- Simulations of the glucose, insulin and C-peptide system given a set of parameters.
    - Be able to select the most appropriate model.
- It will be able to fit data to a model to produce parameters.
    - The fitted parameters will be given confidence values.
    - Given groups of data, it will be able to calculate statistical significance between the groups.
- It will be able to produce graphs of the results for individual and grouped data.

It will take data from these sources:

- Toolkits used by the department, e.g. the CVGI toolkit.
- A plain spreadsheet.

It will be able to run on a standard build of AstraZeneca computer which is of Windows Vista 32-bit with various specifications.

It will be user-friendly so that a non-mathematician will be able to use it and understand the results.

10.3 Software Construction

10.3.1 Overview

MATLAB [4] was used to construct the software tool as it provides functions and features, such as ODE solvers and optimisation algorithms, which are essential for modelling and simulation in this context. It also provides a method of outputting data graphically for the end user to make results easier to interpret. However, MATLAB lacks more advanced programming features, such as object-orientation, needed for developing a complete modelling tool. In addition, if every person that wishes to use the tool had to have a full licence for MATLAB with toolkits, this would be very cost-prohibitive. The way round this is to use the MATLAB compiler to create a stand-alone application which can be accessed from other programming languages. This gives the advantage that the functionality of MATLAB can be used alongside the programming features of a language such as Java, and also means that the application can be freely distributed without the need for a full MATLAB licence for each individual user. MATLAB can be compiled to work with a range of programming languages; in this case Java was used as it provided all the desired features, such as object-orientation, and was the language with which the author was most familiar.

10.3.2 Structure

The overall structure of the software tool is shown in Figure 10.1, below.

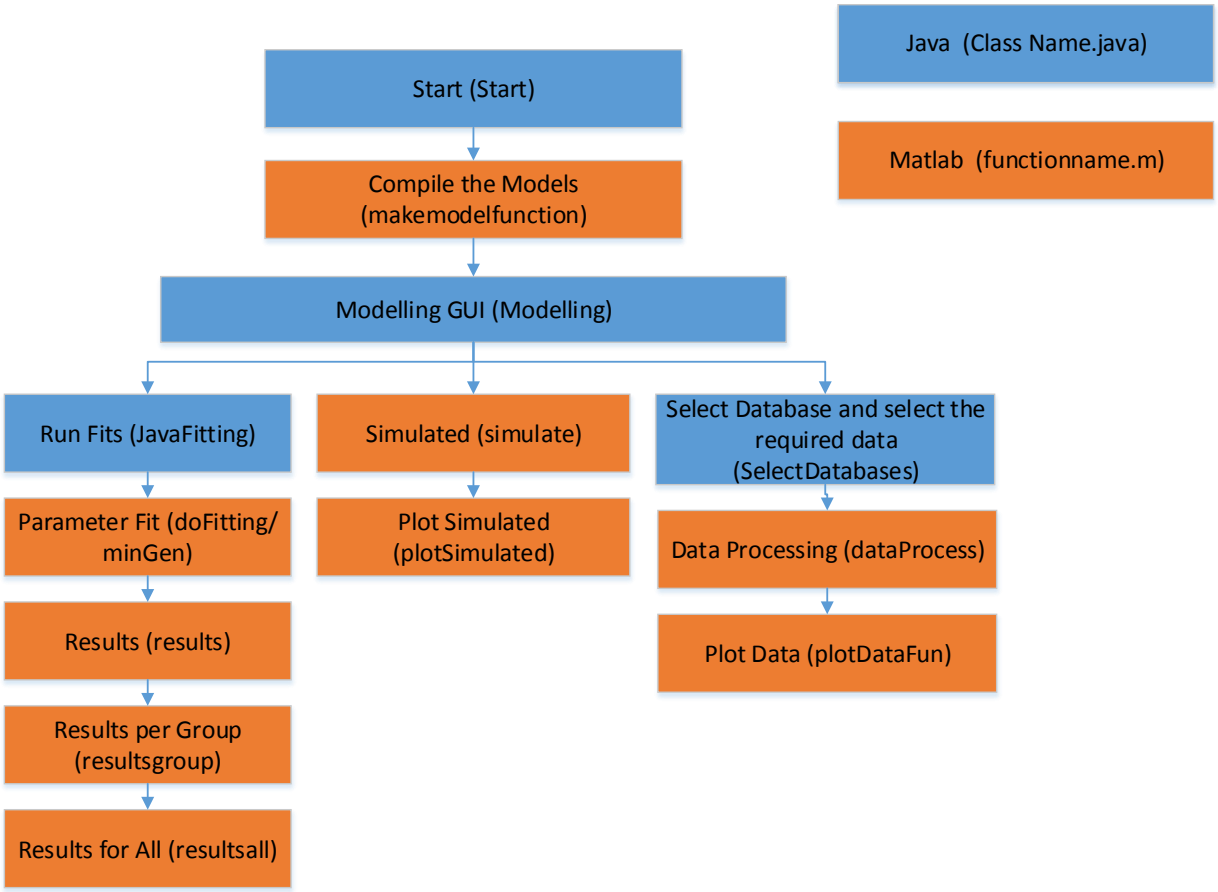

Figure 10.1: General overview of code structure

10.3.2.1 MATLAB Components

The MATLAB components primarily perform the arithmetic and data display functions. One component performs graphical display for parameters and immediate simulations of the model and model simulation. Another performs fitting and formats results.

These components are separate to allow fitting and results formatting to be executed on a remote system if required in the future (e.g. if fitting is too numerically intensive for the user's machine). This would be possible as Java can be used to control both MATLAB components and the RMI (Remote Method Invocation) interface could divide workload between separate machines as required. Note that this aspect has not currently been implemented, but the structure of the MATLAB components would allow for this in the future.

10.3.2.2 Java Components

The Java project is split into five packages. `interfaces` contains any Java interfaces required, including the database connection interface which is extended for each standard framework (e.g. the IVGTT toolkit). `structures` contains any nodes used in the database section of the Java components, such as objects containing groups, profile and subjects. `fitting` contains the link between the two MATLAB components. `gui` contains graphical interfaces for the user to select certain parts of the databases. Finally, `start` sets up the environment to run MATLAB in Java.

10.4 Software Function

10.4.1 Model Input

Models are input to the software tool in a standard format developed in XML. This format requires a list of states, parameters with initial estimates and differential equations which define the model. The data in this format are interpreted by MATLAB to create functions called by an integration algorithm when the model is simulated. An example of the XML format are given in Figure 10.2.

```
<model>
  <name>ID Model</name>
  <states>

    <state>
      <name>glucose plasma</name>
      <symbol>G</symbol>
      <equation>
        dGdt =gp -IA*G*si
      </equation>
      <observable />
      <initial>
        G0
      </initial>

      <input>IV</input>
      <inputequation>
        F
      </inputequation>

    </state>
    <state>
      <name>Insulin Integral</name>
      <symbol>II</symbol>
      <equation>
        dIIdt = G-II*kiir
      </equation>
      <initial>
        G0/kiir
      </initial>

    </state>
    <state>
      <name>Insulin</name>
      <symbol>I</symbol>
      <equation>
        dIdt = kd*max((dGdt),0) + II*ki - kir*I
      </equation>
      <observable/>
      <initial>
        I0
      </initial>

    </state>
    <state>
      <name>Insulin Action</name>
      <symbol>IA</symbol>
      <equation>
        dIAdt = I-IA*kiar
      </equation>
      <initial>
        I0/kiar
      </initial>
    </state>
  </states>

  <parameters>
    <parameter>
      <name>kd</name>
      <value>1.7968 </value>
            <description>1st Phase Insulin
Secretion</description>
    </parameter>
    <parameter>
      <name>si</name>
      <value>0.026</value>
<description>Insulin Sensivity</description>
    </parameter>
    <parameter>
      <name>ki</name>
      <value>1</value>
<description>2nd Phase Insulin Secretion</description>
    </parameter>
    <parameter>
      <name>kiir</name>
      <value>12</value>
<description>2nd Phase Insulin Secretion Delay (time
constant)</description>
    </parameter>
    <parameter>
      <name>kir</name>
      <value>0.7</value>
<description>Insulin Clearance</description>
    </parameter>
    <parameter>
      <name>kiar</name>
      <value>7.00</value>
<description>Insulin Action Delay (Time
Constant)</description>
    </parameter>
    <parameter>
      <name>gp</name>
      <value>0.0002</value>
<description>Glucose Production</description>
    </parameter>
    <parameter>
      <name>F</name>
      <value> 0.024 </value>
<description>Bioaviabiliy of Glucose</description>
    </parameter>
  </parameters>

</model>
```

Figure 10.2: Example model XML code

10.4.2 Data Input

The vast majority of data at AstraZeneca are stored in spreadsheets, with each different user having their own spreadsheet design and layout. There have been attempts to standardise the spreadsheet formats. One example is the CVGI toolkit which is used for storing data from OGTT experiments, however this does not include IVGTT or hyperglycaemic clamp data. It stores data in a Microsoft Access database which is easily accessible and data are easy to extract via an Excel spreadsheet front-end. There is also an IVGTT toolkit which also stores data in a database (Oracle, rather than Microsoft Access), again with an Excel front end which produces an easily readable spreadsheet. This toolkit is used with IVGTT data, but can also be extended for hyperglycaemic clamp data.

OGTT, IVGTT and hyperglycaemic clamp data can all be used within the model presented in Chapter 8. It is therefore useful, to save data re-entry, to be able to extract data from the CVGI and IVGTT toolkits directly. This saves time and prevents copying errors entering the data, as well as simplifying use of the software tool from the user's point of view. The software tool therefore imports data from these sources and uses Java to transform them to fit in a common framework. Different methods are required to import data from different sources: for example, the CVGI toolkit imports data via a Microsoft Access ODBC (Open Database Connectivity) driver then uses an ODBC-JDBC (Java Database Connectivity) bridge which allows the data to be transferred into Java.

Data from all the different sources are placed into a standard framework of Java objects. This ensures that MATLAB can deal with data from all sources easily and consistently. It also allows for easy data manipulation, including selecting data by the group of animals and selecting which groups of animals should be compared.

10.4.2.1 Additional Data Processing

For most experiments, the data input are sufficient for modelling directly. However hyperglycaemic clamp data are unique in that there are two sets of data that are recorded for glucose: blood glucose concentration and plasma glucose concentration. As explained in Chapter 4, haemacel is used to stabilise the volume of distribution in the subject. This can affect blood glucose measurements, but plasma glucose measurements remain unaffected. Plasma glucose measurements are taken less frequently than blood glucose measurements, however at each time point a plasma glucose measurement is taken there is also a blood glucose measurement taken. This allows the ratio between plasma and blood glucose levels to be calculated at these time points.

The software tool takes the mean of these ratios over the course of the experiment. The mean ratio is then used to correct blood glucose measurements – which are taken more frequently and therefore provide more data points – and it is these corrected blood glucose measurements which are used for fitting.

10.4.3 Interface

The interface was made as simple as possible to make parameter fitting straightforward for the user. The tool has two screens: a main screen, shown in Figure 10.3, and a data selection screen, shown in Figure 10.4.

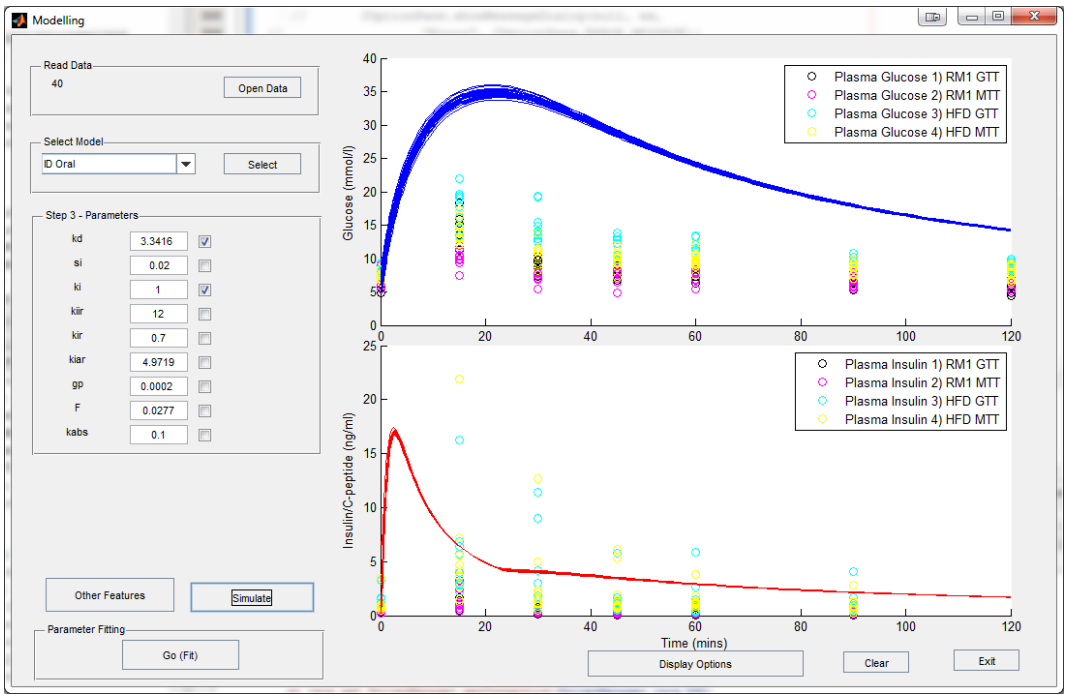

Figure 10.3: Software tool – main display screen shot

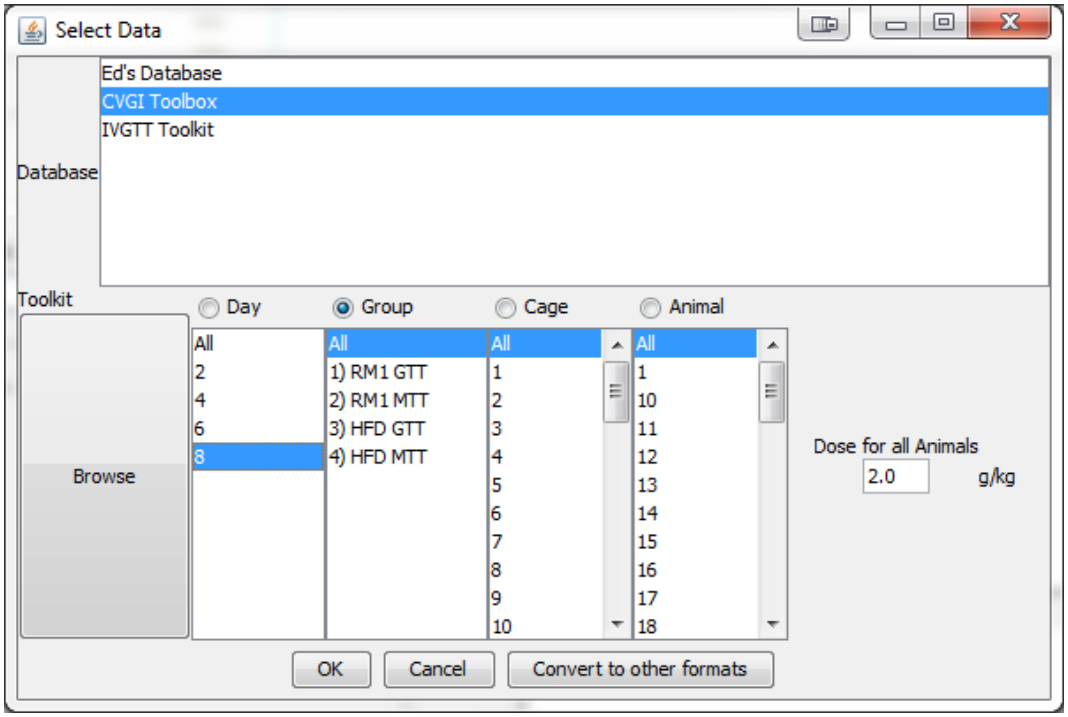

Figure 10.4: Software tool – select database screen shot

10.4.4 Parameter Estimation

The software tool performs parameter estimation by the Quasi-Newton algorithm [36]. It goes through each subject in turn performing the parameter fit, simulating the model using ode15s algorithm [30] and fitting using GLS (Generalised Least Squares, described in Chapter 2). For each subject it produces graphs of fits of insulin and glucose data (and C-peptide where applicable) and creates an Excel spreadsheet containing fitted parameter values. It also calculates parameter confidence values using equations 2.23 and 10.2 via the Hessian matrix, *H*, derived from the unconstrained fit function in MATLAB (`fminunc`) as described further in Chapter 2, given by:

$$C(\hat{p}) = \frac{2}{N - n_p} E(\hat{p}) H(\hat{p})^{-1} \qquad 10.1$$

where $\hat{p}$ is the set of parameter estimates, *N* is the number of time points, *n* is the number of parameters fitted, *E* is the output from the residual function and *H* is the Hessian matrix. In addition:

$$\delta_i = \pm t_{N-n_p}^{1-\left(\frac{\alpha}{2}\right)} \sqrt{C(ii)} \qquad 10.2$$

for $i = 1, \ldots, n_p$ where $t_{N-n_p}^{1-\left(\frac{\alpha}{2}\right)}$ is a two-tailed Student's t distribution for confidence level α and $N\text{-}n_p$ degrees of freedom.

10.4.5 Statistical Analysis

As well as providing parameter estimates for a given model and data set, the software tool also performs a two-tailed Student's t-test on every combination of sets of parameter values. This is provided to the user in an Excel spreadsheet so they can see if there are any statistically significant differences between groups that are reflected in the parameter estimates.

10.5 Software Use

The hope is that this software tool will be used by AstraZeneca in their day-to-day analysis.

10.6 Conclusions

This software tool will allow non-mathematical based scientists to access complex modelling without the need for vast amounts of expertise in modelling.

It will help to improve their decisions about experiments they perform as well as enabling them to obtain more detailed information from previously gathered data.

Chapter 11: Conclusions and Discussion

11.1 Discussion

The main model in the field of glucose-insulin dynamics has previously been the Minimal Model developed by Bergman et al. [111] It can only be used in an IVGTT. It is structurally identifiable for insulin and glucose being observable as well as just glucose on its own (under certain assumptions). It does not reach a steady state value after the experiment has finished. The parameters in the model may not have any physiological relevance, such as *h*, the threshold value for insulin release. It was thus necessary to develop or find a new model that would cater for more tests.

There are other models in the field that bring useful insights into the glucose and insulin system. However no one model does everything that is required for this thesis, therefore it was necessary to develop a new model.

In developing a new model it was, therefore, necessary to investigate the glucose and insulin system with as much data as possible. C-peptide was also collected at AstraZeneca. This was useful for working out the level of insulin secretion as it was suspected that insulin clearance may not be constant. The fraction of insulin observed in the ad-lib fed animals was statistically significantly higher than the 8 and 16 hour fasted animals. This meant that it was important to include C-peptide in a mathematical model of the glucose and insulin system.

It was observed that the insulin response to a glucose stimulus was similar to that of a proportional-integral-derivative controller that is found in engineering systems. The system equations were changed slightly to fit in better with a

biological system as , for example, in this biological system there is no error signal. Other elements of the model were taken from the minimal model and others. The model then was further reduced by removing the proportional control in the model. This model was structurally identifiable. This model was successfully applied to IVGTTs and hyperglycaemic clamps. With the addition of a compartment for all absorption it was also successfully applied to OGTTs.

It was also useful to be able to model the progression of long term changes of subjects into diabetes. Using a combination of Topp et al [119] and the short term model it was possible to simulate (not to parameter fit) the varying different factors that could result in diabetes. Therefore it was possible to use this as a tool for testing hypotheses to see whether certain parameter changes over time would lead to the disease progression as expected. For example, it was able to demonstrate what would happen with a gradual decrease in insulin sensitivity.

A software tool was made that allowed AstraZeneca staff to parameter fit their data to IVGTTs, hyperglycaemic clamps and OGTTs. It could also be used on other experiments not yet thought of. The models that could be fitted were the integral derivative model, with and without C-peptide and with or without glucose absorption.

11.2 Conclusion

The aim of this thesis was to develop an integrated mathematical model of glycaemic control that predicts both short-term and long-term glucose

regulation. This thesis has covered these two requirements in Chapter 8 and Chapter 9.

An additional aim to this thesis was to make it understandable to any person with an interest. This has hopefully has been accomplished by a thesis that does not require wide knowledge of either biology or mathematics to understand and a software tool that can be used by anyone.

The objectives of this thesis were mostly met as follows:

Objectives	**Where/how they were met**
“To review and evaluate the different mathematical models of glycaemic control.”	This was met in Chapter 5.
"To modify/develop existing mathematical models and determine how existing glucose and insulin data from animal (rat and mouse) studies fit.”	This was done throughout the thesis but specifically in Chapter 6, Chapter 8 and Chapter 9.
"To apply the new model to the evaluation of glucose stimulated insulin secretion using new data.”	This was done in Chapter 8.
"To develop an integrated desktop utility for modelling and analysing glycaemic control and insulin secretion in animal	This was done in Chapter 10.

Objectives	**Where/how they were met**
models of diabetes.”	
"To develop methods for determining pancreatic degeneration and function from measurable, but indirect, parameters such as glucose, C-peptide and insulin levels.”	This was done in Chapter 7 and Chapter 9.
"To include in the model physiological control parameters that address counter-regulatory systems, such as lipid levels and β-cell mass.”	This was done in Chapter 9. Lipid levels were not specifically dealt with but they can be seen as a factor that affects insulin sensitivity. It should be an area of future work however, due to lack of time and data, it was not done on this occasion. β-cell mass was covered but not measured due to the difficulty in obtaining the data.
"To apply the model to the design of future studies evaluating pancreatic changes and effects on glycaemic control.”	This was mainly done by designing experiments to measure C-peptide secretion which in turn helps future understanding of insulin secretion. The software tool allows for future experiments that have not yet been designed to be used with the model.

11.3 Future Work

Insulin sensitivity has a major role in type-2 diabetes. It is therefore important that changes to it are properly understood. Lipids are the main contributing factor to changes in insulin sensitivity (see Chapter 9). Therefore for long term modelling it will be important to look into them in greater depth to understand their relationship with diabetes disease progression.

The primary aim of this thesis was to design a mathematical model for glucose and insulin secretion. The parameter fitting was based on individual subjects. It would provide more mathematically robust results if population modelling using this model was performed. This work was planned to be done by AstraZeneca (as of 2013 some of this work has been done [157]).

References

[1] R. Macey and G. Oster, "Berkley Madonna," vol. 8.3, ed, 2007.

[2] Maplesoft, "Maple," 12 ed, 2010.

[3] Wolfram, "Mathematica," vol. 7, ed, 2009.

[4] Mathworks, "MATLAB," ed, 2007.

[5] Pharsight, "WinNonLin," vol. 5.2.1, ed. http://www.pharsight.com/, 2008.

[6] E. Watson, "AstraZeneca/University of Warwick Studentship Agreement," ed, 2006.

[7] Who. (2006, Web Page). *Definition and diagnosis of diabetes mellitus and intermediate hyperglycemia : report of a WHO/IDF consultation*. Available: http://www.who.int/diabetes/publications/Definition and diagnosis of diabetes_new.pdf

[8] M. Gould, "Diabetes costs NHS £1m an hour, charity says," in *Guardian*, ed, 2008.

[9] M. Chappell and N. D. Evans, "Physiological & Compartmental Modelling Master Level Module Lecture Notes," ed. University of Warwick, 2007.

[10] E. R. Carson and C. Cobelli, *Modelling methodology for physiology and medicine*. San Diego, Calif.: Academic Press 2000.

[11] H. T. Banks, M. Davidian, J. R. Samuels, and K. L. Sutton, "An Inverse Problem Statistical Methodology Summary," ed, 2009, pp. 249-302.

[12] C.C.Bissell, *Control Engineering*, 2nd ed. London: CRC Press, 1994.

[13] D. Kaplan and L. Glass, *Understanding nonlinear dynamics*: New York : Springer-Verlag, c1995., 1995.

[14] K. Godfrey, *Compartmental models and their application*. London: Academic Press, 1983.

[15] J. W. T. Yates, N. D. Evans, and M. J. Chappell, "Structural identifiability analysis via symmetries of differential equations," *Automatica,* vol. 45, pp. 2585-2591, 2009.

[16] M. J. Chapman, K. R. Godfrey, M. J. Chappell, and N. D. Evans, "Structural identifiability for a class of non-linear compartmental systems using linear/non-linear splitting and symbolic computation," *Mathematical biosciences,* vol. 183, pp. 1-14, 2003.

[17] N. D. Evans, M. J. Chapman, M. J. Chappell, and K. R. Godfrey, "Identifiability of uncontrolled nonlinear rational systems," *Automatica,* vol. 38, pp. 1799-1805, 2002.

[18] M. J. Chappell and R. N. Gunn, "A procedure for generating locally identifiable reparameterisations of unidentifiable non-linear systems by the similarity transformation approach," vol. 148, ed, 1998, pp. 21-41.

[19] M. J. Chappell, K. R. Godfrey, and S. Vajda, "Global identifiability of the parameters of nonlinear systems with specified inputs: a comparison of methods," vol. 102, ed, 1990, pp. 41-73.

[20] "BioMathMed," in *Parameter Estimation in Physiological Models*, Lipari, 2009.

[21] S. Marsili-Libelli, S. Guerrizio, and N. Checchi, "Confidence regions of estimated parameters for ecological systems," *Ecological Modelling,* vol. 165, pp. 127-146, 2003.
[22] N. D. Evans and M. J. Chappell, "Extensions to a procedure for generating locally identifiable reparameterisations of unidentifiable systems," vol. 168, ed, 2000, pp. 137-159.
[23] H. T. Banks, S. Dediu, and S. L. Ernstberger, "Sensitivity functions and their uses in inverse problems," *Journal of Inverse and Ill-posed Problems,* vol. 15, pp. 683-708, 2007.
[24] M. Fink, "myAD," ed. http://gosh.gmxhome.de/, 2006.
[25] S. Vajda, K. R. Godfrey, and H. Rabitz, "Similarity transformation approach to identifiability analysis of nonlinear compartmental models," *Mathematical biosciences,* vol. 93, pp. 217-248, 1989.
[26] J. W. Yates, "Structural identifiability of physiologically based pharmacokinetic models," *Journal of Pharmacokinetics and Pharmacodynamics,* vol. 33, pp. 421-439, 2006.
[27] K. A. Keating and J. F. Quinn, "Estimating Species Richness: The Michaelis-Menten Model Revisited," *Oikos,* vol. 81, p. 411, 1998.
[28] E. Watson, S. Poucher, M. J. Chappell, and J. Teague, "Short term and long term disease mathematical modelling of diabetes in Zucker and ZDF rats," *Diabetologia,* vol. 52, pp. S240-S240, 2009.
[29] S. Vajda, "Similarity transformation approach to identifiability analysis of nonlinear compartmental models," *Mathematical biosciences,* vol. 93, p. 217, 1989.
[30] L. F. Shampine and M. W. Reichelt, "The MATLAB ODE Suite," *SIAM Journal on Scientific Computing,* vol. 18, pp. 1-22, 1997.
[31] T. G. The Aegis, "acslX," vol. 2.4.2.1, ed, 2008.
[32] S. O. Fatunla, *Numerical Methods for Initial Value Problems in Ordinary Differential Equations (Computer Science and Scientific Computing)* vol. First Edition: Academic Pr, 1988.
[33] (Web Page). *Regression*. Available: http://download.oracle.com/docs/cd/E11882_01/datamine.112/e12216/regress.htm
[34] J. C. Lagarias, J. A. Reeds, M. H. Wright, and P. E. Wright, "Convergence Properties of the Nelder--Mead Simplex Method in Low Dimensions," *SIAM Journal on Optimization,* vol. 9, p. 112, 1998.
[35] D. F. Shanno, "Conditioning of Quasi-Newton Methods for Function Minimization," *Mathematics of Computation,* vol. 24, p. 647, 1970.
[36] Mathworks, "Optimisation Toolbox," vol. %6, ed, 2007.
[37] M. Fink, J. J. Batzel, and H. Tran, "A Respiratory System Model: Parameter Estimation and Sensitivity Analysis," *Cardiovascular Engineering,* vol. 8, pp. 120- 134, 2007.
[38] R. T. Haftka and H. M. Adelman, "Recent developments in structural sensitivity analysis," *Structural and Multidisciplinary Optimization,* vol. 1, pp. 137-151, 1989.

[39] M. Bliss, *Discovery of Insulin*. Chicago: Chicago University Press, 1983.
[40] R. N. Bergman, "Orchestration of glucose homeostasis: from a small acorn to the California oak," *Diabetes,* vol. 56, pp. 1489-1501, 2007.
[41] T. Barnett and S. Kumar, *Obesity and diabetes*. Chichester: Wiley, 2004.
[42] P. Rorsman and E. Renstrom, "Insulin granule dynamics in pancreatic beta cells," *Diabetologia,* vol. 46, pp. 1029-1045, 2003.
[43] M. J. Brady and A. R. Saltiel, "Insulin and Glucagon," in *eLS*, ed Chichester: John Wiley & Sons, Ltd, 2001.
[44] E. Ferrannini, J. D. Smith, C. Cobelli, G. Toffolo, A. Pilo, and R. A. Defronzo, "Effect of insulin on the distribution and disposition of glucose in man," *J Clin Invest,* vol. 76, pp. 357-364, 1985.
[45] M. Daniel Lane, "Energy Balance, Obesity and Type-2 Diabetes," in *eLS*, ed Chichester: John Wiley & Sons, Ltd, 2001.
[46] L. Poretsky, *Principles of Diabetes Mellitus*. New York: Springer, 2002.
[47] S. M. Haffner, "Type 2 diabetes: Unravelling its causes and consequences: A compendium of classical papers," ed: Cambridge: Medical Publications, 2002.
[48] J. G. Salway, *Metabolism at a Glance* vol. 2. Oxford: Wiley-Blackwell, 1999.
[49] (Web Page). *BBC - GCSE Bitesize: Compounds in living organisms*. Available: http://www.bbc.co.uk/schools/gcsebitesize/science/add_ocr/biosphere/biocompoundsrev1.shtml
[50] M. W. King, "Glycogen, Starch and Sucrose Synthesis," in *eLS*, ed Chichester: John Wiley & Sons, Ltd, 2001.
[51] E. T. Harper and R. A. Harris, "Glycolytic Pathway," in *eLS*, ed Chichester: John Wiley & Sons, Ltd, 2001.
[52] G. D. Lopaschuk and J. R. B. Dyck, "Glycolysis Regulation," in *eLS*, ed: John Wiley & Sons, Ltd, 2001.
[53] J. C. Wallace and G. J. Barritt, "Gluconeogenesis," in *eLS*, ed Chichester: John Wiley & Sons, Ltd, 2001.
[54] G. Williams and J. C. Pickup, *Handbook of Diabetes*, 4th ed. Oxford: Wiley-Blackwell, 2004.
[55] O. Cabrera, D. M. Berman, N. S. Kenyon, C. Ricordi, P. O. Berggren, and A. Caicedo, "The unique cytoarchitecture of human pancreatic islets has implications for islet cell function," *Proceedings of the National Academy of Sciences of the United States of America,* vol. 103, pp. 2334-2339, 2006.
[56] L. Marzban, G. Trigo-Gonzalez, X. Zhu, C. J. Rhodes, P. A. Halban, D. F. Steiner*, et al.*, "Role of -Cell Prohormone Convertase (PC)1/3 in Processing of Pro-Islet Amyloid Polypeptide," *Diabetes,* vol. 53, pp. 141-148, 2003.
[57] E. Van Cauter, F. Mestrez, J. Sturis, and K. S. Polonsky, "Estimation of insulin secretion rates from C-peptide levels. Comparison of individual

and standard kinetic parameters for C-peptide clearance," *Diabetes,* vol. 41, pp. 368-377, 1992.

[58] G. Toffolo, F. De Grandi, and C. Cobelli, "Estimation of beta-cell sensitivity from intravenous glucose tolerance test C-peptide data. Knowledge of the kinetics avoids errors in modeling the secretion," *Diabetes,* vol. 44, pp. 845-854, 1995.

[59] R. M. Watanabe and R. N. Bergman, "Accurate measurement of endogenous insulin secretion does not require separate assessment of C-peptide kinetics," *Diabetes,* vol. 49, pp. 373-382, 2000.

[60] G. Toffolo, E. Breda, M. K. Cavaghan, D. A. Ehrmann, K. S. Polonsky, and C. Cobelli, "Quantitative indexes of beta-cell function during graded up&down glucose infusion from C-peptide minimal models," *American journal of physiology.Endocrinology and metabolism,* vol. 280, pp. E2-10, 2001.

[61] E. Breda, M. K. Cavaghan, G. Toffolo, K. S. Polonsky, and C. Cobelli, "Oral glucose tolerance test minimal model indexes of beta-cell function and insulin sensitivity," *Diabetes,* vol. 50, pp. 150-158, 2001.

[62] D. Langin, "Diabetes, insulin secretion, and the pancreatic beta-cell mitochondrion," *The New England journal of medicine,* vol. 345, pp. 1772-1774, 2001.

[63] D. J. Drucker and M. A. Nauck, "The incretin system: glucagon-like peptide-1 receptor agonists and dipeptidyl peptidase-4 inhibitors in type 2 diabetes," *The Lancet,* vol. 368, pp. 1696-1705, 2006.

[64] J. C. Hutton, "The insulin secretory granule," *Diabetologia,* vol. 32, pp. 271-281, 1989.

[65] T. K. Bratanova-Tochkova, H. Cheng, S. Daniel, S. Gunawardana, Y. J. Liu, J. Mulvaney-Musa*, et al.*, "Triggering and augmentation mechanisms, granule pools, and biphasic insulin secretion," *Diabetes,* vol. 51 Suppl 1, pp. S83-S90, 2002.

[66] S. G. Straub and G. W. Sharp, "Glucose-stimulated signaling pathways in biphasic insulin secretion," *Diabetes/metabolism research and reviews,* vol. 18, pp. 451-463, 2002.

[67] S. O. R. Sudhesh Kumar, *Insulin Resistance: Insulin Action and Its Disturbances in Disease*: John Wiley and Sons, 2005.

[68] (Web Page). *SLC2A4 - solute carrier family 2 (facilitated glucose transporter), member 4*. Available: http://www.genenames.org/data/hgnc_data.php?hgnc_id=11009

[69] S. Kumar and S. O'Rahilly, *Insulin resistance insulin action and its disturbances in disease*: Chichester, West Sussex, England ; J. Wiley, c2005., 2005.

[70] I. Raz, J. S. Skyler, and E. Shafrir, *Diabetes: From Research to Diagnosis and Treatment*. London: Taylor & Francis, 2002.

[71] M. Muratoglu, J. Kuyumjian, and N. Kalant, "First-pass hepatic uptake and utilization of glucose in the rat," *The Biochemical journal,* vol. 233, pp. 245-248, 1986.

[72] L. Yano, H. Yano, and K. Taketa, "Portal blood flow during and after high-intensity physical exercise in rats: response of plasma endothelin-1 and catecholamine," *Hepatology Research,* vol. 11, pp. 1-11, 1998.
[73] J. Burggraff, "Liver blood flow in clinical pharmacology assessment with echo-Doppler," Dissertation/Thesis, University of Leiden, Neatherlands, 1998.
[74] D. Lebrec and C. Girod, "Comparison of the circulation between fed and fasted normal and portal hypertensive rats," *Journal of pharmacological methods,* vol. 15, pp. 359-365, 1986.
[75] C. B. Jensen, "Insulin Secretion and Cellular Glucose Metabolism after Prolonged Low-Grade Intralipid Infusion in Young Men," *Journal of Clinical Endocrinology & Metabolism,* vol. 88, pp. 2775 - 2783, 2003.
[76] (Web Page). *WHO | Diabetes*. Available: http://www.who.int/dietphysicalactivity/publications/facts/diabetes/en/
[77] (Web Page). *Unite for Diabetes | World Diabetes Day*. Available: http://www.worlddiabetesday.org/the-campaign/unite-for-diabetes
[78] U. K. Diabetes. (2008, Web Page). *Diabetic Complications*.
[79] F. R. Kaufman, L. C. Gibson, M. Halvorson, S. Carpenter, L. K. Fisher, and P. Pitukcheewanont, "A Pilot Study of the Continuous Glucose Monitoring System: Clinical decisions and glycemic control after its use in pediatric type 1 diabetic subjects," *Diabetes care,* vol. 24, pp. 2030-2034, 2001.
[80] C. Cobelli, "Subcutaneous model predictive closed-loop control of type 1 diabetes: from in silico to human studies," in *EASD/JDRF Symposium: Artificial pancreas technologies - progress towards a mechanical closed-loop system to restore euglycaemia*, Vienna, 2009.
[81] F. Juvenile Diabetes Research, "FDA Approves Computer Simulator to Model Diabetes, Test Artificial Pancreas Algorithms," in *The JDRF Emerging Technologies E-Newsletter* vol. Emerging Technologies In Diabetes Research, ed, 2008, pp. 1-1-4.
[82] H. E. Turner and J. A. H. Wass, *Oxford Handbook of Endocrinology and Diabetes (Oxford Handbooks Series)*: Oxford University Press, USA, 2009.
[83] M. B. Zemel, "Insulin resistance vs. hyperinsulinemia in hypertension: insulin regulation of Ca2+ transport and Ca(2+)-regulation of insulin sensitivity," *The Journal of nutrition,* vol. 125, pp. 1738S-1743S, 1995.
[84] (Web Page). *Animals in Scientific Procedures | Home Office*. Available: http://scienceandresearch.homeoffice.gov.uk/animal-research/?version=1
[85] (Web Page). *Understanding Animal Research*. Available: http://understandinganimalresearch.org.uk/
[86] AstraZeneca, "Protocol Documentation used internally at AstraZenca," ed, 2006.
[87] (Web Page). *AstraZeneca Corporate Responsibility - Animal Research*. Available: http://www.astrazeneca.com/responsibility/research-ethics/49574471/animal-research/
[88] AstraZeneca, "AstraZeneca Internal Animal Ethics Guidlines," ed, 2010.

[89] C. River. (2014). *Han Wistar Rat* Available: http://www.criver.com/products-services/basic-research/find-a-model/wistar-han-igs-rat

[90] B. L. Kasiske, M. P. O'Donnell, and W. F. Keane, "The Zucker rat model of obesity, insulin resistance, hyperlipidemia, and renal injury," *Hypertension,* vol. 19, pp. I110-I115, 1992.

[91] M. S. Phillips, Q. Liu, H. A. Hammond, V. Dugan, P. J. Hey, C. J. Caskey*, et al.*, "Leptin receptor missense mutation in the fatty Zucker rat," *Nature genetics,* vol. 13, pp. 18-19, 1996.

[92] B. Ferrari, M. Arnold, R. D. Carr, W. Langhans, G. Pacini, T. B. Bodvarsdottir*, et al.*, "Subdiaphragmatic vagal deafferentation affects body weight gain and glucose metabolism in obese male Zucker (fa/fa) rats," vol. 289, ed, 2005, pp. R1027-R1034.

[93] C. T. Montague, I. S. Farooqi, J. P. Whitehead, M. A. Soos, H. Rau, N. J. Wareham*, et al.*, "Congenital leptin deficiency is associated with severe early-onset obesity in humans," *Nature,* vol. 387, pp. 903-908, 1997.

[94] M. Ozata, I. C. Ozdemir, and J. Licinio, "Human leptin deficiency caused by a missense mutation: multiple endocrine defects, decreased sympathetic tone, and immune system dysfunction indicate new targets for leptin action, greater central than peripheral resistance to the effects of leptin, and spontaneous correction of leptin-mediated defects," *The Journal of clinical endocrinology and metabolism,* vol. 84, pp. 3686-3695, 1999.

[95] D. T. Finegood, M. D. McArthur, D. Kojwang, M. J. Thomas, B. G. Topp, T. Leonard*, et al.*, "Beta-cell mass dynamics in Zucker diabetic fatty rats. Rosiglitazone prevents the rise in net cell death," *Diabetes,* vol. 50, pp. 1021-1029, 2001.

[96] (Web Page). *JAX Mice Database - 000664 C57BL/6J*. Available: http://jaxmice.jax.org/strain/000664.html

[97] P. J. Bingley, P. Colman, G. S. Eisenbarth, R. A. Jackson, D. K. McCulloch, W. J. Riley*, et al.*, "Standardization of IVGTT to predict IDDM," *Diabetes care,* vol. 15, pp. 1313-1316, 1992.

[98] J. O. Clausen, K. Borch-Johnsen, H. Ibsen, R. N. Bergman, P. Hougaard, K. Winther*, et al.*, "Insulin sensitivity index, acute insulin response, and glucose effectiveness in a population-based sample of 380 young healthy Caucasians. Analysis of the impact of gender, body fat, physical fitness, and life-style factors," *The Journal of clinical investigation,* vol. 98, pp. 1195-1209, 1996.

[99] S. Wang, R. MacDonald, and S. Loxham, "private communications about experiments at AstraZeneca," ed, 2010.

[100] R. N. Bergman, M. Ader, K. Huecking, and G. Van Citters, "Accurate Assessment of -Cell Function: The Hyperbolic Correction," *Diabetes,* vol. 51, pp. 212S-220, 2002.

[101] F. Belfiore, S. Iannello, and G. Volpicelli, "Insulin Sensitivity Indices Calculated from Basal and OGTT-Induced Insulin, Glucose, and FFA Levels," *Molecular genetics and metabolism,* vol. 63, pp. 134-141, 1998.

[102] S. Wang, "OGTT Procedure," vol. OGTT procedure discussion over practicalities, ed, 2010.
[103] G. I. Uwaifo, S. J. Parikh, M. Keil, J. Elberg, J. Chin, and J. A. Yanovski, "Comparison of insulin sensitivity, clearance, and secretion estimates using euglycemic and hyperglycemic clamps in children," *The Journal of clinical endocrinology and metabolism,* vol. 87, pp. 2899-2905, 2002.
[104] D. Elahi, "In praise of the hyperglycemic clamp. A method for assessment of beta-cell sensitivity and insulin resistance," *Diabetes care,* vol. 19, pp. 278-286, 1996.
[105] R. Macdonald, A. Gyte, and S. Loxham, "Clamp and IVGTT Procedure," vol. Clamp and IVGTT procedure discussion over practicalities, ed, 2010.
[106] "Roche Accu-Chek," vol. 2010, ed.
[107] (Web Page). *Millipore - ELISA, Enzyme-linked immunosorbent assay and ELISA assays*. Available: http://www.millipore.com/immunodetection/id3/elisa
[108] (Web Page). *Mercodia - C-peptide ELISA*. Available: http://www.mercodia.se/index.php?page=productview2&prodId=13
[109] S. Schwartz, E. Taylor, J. Ward, and R. Ng. (2008, Accuracy of Four Blood Glucose Monitoring Systems. *(Journal, Electronic)*. Available: http://www.abbottdiabetescare.co.uk/_resources/media/documents/hcps/clinical_papers/accuracycomparison_fslite.pdf
[110] V. W. Bolie, "Coefficients of normal blood glucose regulation," *Journal of applied physiology,* vol. 16, pp. 783-788, 1961.
[111] R. N. Bergman, Y. Z. Ider, C. R. Bowden, and C. Cobelli, "Quantitative estimation of insulin sensitivity," *The American Journal of Physiology,* vol. 236, pp. E667-E677, 1979.
[112] R. N. Bergman, C. R. Bowden, and C. Cobelli, "The minimal model approach to quantification of factors controlling glucose disposal in man," in *Carbohydrate Metabolism: Quantitative Physiology and Mathematical Modelling*. vol. 1, R. N. Bergman and C. Cobelli, Eds., ed Chichester: John Wiley & Sons Ltd, 1981, pp. 269-287.
[113] A. De Gaetano and O. Arino, "Mathematical modelling of the intravenous glucose tolerance test," *Journal of mathematical biology,* vol. 40, pp. 136-168, 2000.
[114] D. R. Matthews, J. P. Hosker, A. S. Rudenski, B. A. Naylor, D. F. Treacher, and R. C. Turner, "Homeostasis model assessment: insulin resistance and beta-cell function from fasting plasma glucose and insulin concentrations in man," *Diabetologia,* vol. 28, pp. 412-419, 1985.
[115] J. C. Levy, D. R. Matthews, and M. P. Hermans, "Correct homeostasis model assessment (HOMA) evaluation uses the computer program," *Diabetes care,* vol. 21, pp. 2191-2192, 1998.
[116] T. M. Wallace, J. C. Levy, and D. R. Matthews, "Use and abuse of HOMA modeling," *Diabetes care,* vol. 27, pp. 1487-1495, 2004.
[117] "AIDA v4.3a freeware diabetes software simulator program of glucose-insulin action," ed.

[118] E. D. Lehmann and T. Deutsch, "AIDA2: a Mk. II automated insulin dosage advisor," *Journal of Biomedical Engineering,* vol. 15, pp. 201-211, 1993.
[119] B. Topp, K. Promislow, G. deVries, R. M. Miura, and D. T. Finegood, "A model of beta-cell mass, insulin, and glucose kinetics: pathways to diabetes," *Journal of theoretical biology,* vol. 206, pp. 605-619, 2000.
[120] U. Picchini, S. Ditlevsen, and A. De Gaetano, "Modeling the euglycemic hyperinsulinemic clamp by stochastic differential equations," *Journal of mathematical biology,* vol. 53, pp. 771-796, 2006.
[121] U. Picchini, A. De Gaetano, S. Panunzi, S. Ditlevsen, and G. Mingrone, "A mathematical model of the euglycemic hyperinsulinemic clamp," *Theoretical Biology and Medical Modelling,* vol. 2, p. 44, 2005.
[122] C. Dalla Man, R. A. Rizza, and C. Cobelli, "Mixed meal simulation model of glucose-insulin system," *Conference proceedings : ...Annual International Conference of the IEEE Engineering in Medicine and Biology Society.IEEE Engineering in Medicine and Biology Society.Conference,* vol. 1, pp. 307-310, 2006.
[123] A. Mari, O. Schmitz, A. Gastaldelli, T. Oestergaard, B. Nyholm, and E. Ferrannini, "Meal and oral glucose tests for assessment of beta -cell function: modeling analysis in normal subjects," *AJP - Endocrinology and Metabolism,* vol. 283, pp. E1159-1166, 2002.
[124] C. Dalla Man, D. M. Raimondo, R. A. Rizza, and C. Cobelli, "GIM, simulation software of meal glucose-insulin model," *Journal of diabetes science and technology,* vol. 1, pp. 323-330, 2007.
[125] H. E. Silber, P. M. Jauslin, N. Frey, R. Gieschke, U. S. H. Simonsson, and M. O. Karlsson, "An Integrated Model for Glucose and Insulin Regulation in Healthy Volunteers and Type 2 Diabetic Patients Following Intravenous Glucose Provocations," *The Journal of Clinical Pharmacology,* vol. 47, pp. 1159-1171, 2007.
[126] P. M. Jauslin, H. E. Silber, N. Frey, R. Gieschke, U. S. H. Simonsson, K. Jorga*, et al.*, "An integrated glucose-insulin model to describe oral glucose tolerance test data in type 2 diabetics," *The Journal of Clinical Pharmacology,* vol. 47, pp. 1244-55, 2007.
[127] H. E. Silber, N. Frey, and M. O. Karlsson, "An integrated glucose-insulin model to describe oral glucose tolerance test data in healthy volunteers," ed: Uppsala University, Division of Pharmacokinetics and Drug Therapy; Uppsala University, Division of Pharmacokinetics and Drug Therapy.
[128] H. E. Silber, J. Nyberg, A. C. Hooker, and M. O. Karlsson, "Optimization of the intravenous glucose tolerance test in T2DM patients using optimal experimental design," ed: Uppsala University, Division of Pharmacokinetics and Drug Therapy.
[129] H. Silber, "Integrated Modeling of Glucose and Insulin Regulation Following Provocation Experiments," Dissertation/Thesis, Acta Universitatis Upsaliensis, Uppsala, 2009.
[130] G. Pacini and R. N. Bergman, "MINMOD: a computer program to calculate insulin sensitivity and pancreatic responsivity from the frequently

sampled intravenous glucose tolerance test," *Computer Methods and Programs in Biomedicine,* vol. 23, pp. 113-122, 1986.

[131] R. C. Boston, D. Stefanovski, P. J. Moate, A. E. Sumner, R. M. Watanabe, and R. N. Bergman, "MINMOD Millennium: a computer program to calculate glucose effectiveness and insulin sensitivity from the frequently sampled intravenous glucose tolerance test," vol. 5, ed, 2003, pp. 1003-1015.

[132] G. Frangioudakis, A. C. Gyte, S. J. G. Loxham, and S. M. Poucher, "The intravenous glucose tolerance test in cannulated Wistar rats: A robust method for the in vivo assessment of glucose-stimulated insulin secretion," *Journal of pharmacological and toxicological methods,* vol. 57, pp. 106-113, 2008.

[133] K. Færch, C. Brøns, A. C. Alibegovic, and A. Vaag, "The disposition index: adjustment for peripheral vs. hepatic insulin sensitivity?," *The Journal of physiology,* vol. 588, pp. 759-764, 2010.

[134] S. Standring and H. D. Gray, *Gray's anatomy: the anatomical basis of clinical practice*. [Edinburgh]: Churchill Livingstone/Elsevier, 2008.

[135] A. N. Peiris, R. A. Mueller, M. F. Struve, G. A. Smith, and A. H. Kissebah, "Relationship of Androgenic Activity to Splanchnic Insulin Metabolism and Peripheral Glucose Utilization in Premenopausal Women," *The Journal of Clinical Endocrinology & Metabolism,* vol. 64, pp. 162-169, 1987.

[136] C. N. Jones, D. Pei, P. Staris, K. S. Polonsky, Y.-I. Chen, and G. M. Reaven, "Alterations in the glucose-stimulated insulin secretory dose-response curve and in insulin clearance in nondiabetic insulin-resistant individuals," *Journal of Clinical Endocrinology & Metabolism,* vol. 82, pp. 1834-1838, 1997.

[137] C. Cobelli and G. Pacini, "Insulin secretion and hepatic extraction in humans by minimal modeling of C-peptide and insulin kinetics," *Diabetes,* vol. 37, pp. 223-231, 1988.

[138] M. A. Hedaya, *Basic Pharmacokinetics (Pharmacy Education Series)*: TF-CRC, 2007.

[139] J. G. Hattersley, "Mathematical modelling of immune condition dynamics: a clinical perspective," Dissertation/Thesis, University of Warwick, Coventry, 2009.

[140] S. Dutta and R. C. Reed, "A Multiphasic Absorption Model Best Characterizes Gastrointestinal Absorption of Divalproex Sodium Extended-Release Tablets," *The Journal of Clinical Pharmacology,* vol. 46, pp. 952-957, 2006.

[141] T. J. Cornwell, "A simple maximum entropy deconvolution algorithm," *Astron.Astrophys.,* vol. 143 %6, pp. 77-83, 1985.

[142] J. Skilling, "Maximum Entropy Image Restoration: General Algorithm," *Mon.Not.R.astr.Soc.,* vol. 211 %6, pp. 111-124, 1984.

[143] M. K. Charter, "Maximum Entropy and Its Application to the Calculation of Drug Absorption Rates," *J.Pharmacokinet.Biopharm.,* vol. 15 %6, pp. 645-655, 1987.

[144] F. Madden, K. Godfrey, M. Chappell, R. Hovorka, and R. Bates, "A comparison of six deconvolution techniques," *Journal of pharmacokinetics and pharmacodynamics,* vol. 24, pp. 283-299, 1996.
[145] "Non-parametric Prediction of Free-Light Chain Generation in Multiple Myeloma Patients," in *17th World Congress The International Federation of Automatic Control*, Seoul, Korea.
[146] I. G. M. C. V. Stovin and J. Hattersley, "The use of deconvolution techniques to identify the fundamental mixing characteristics of urban drainage struc- tures," in *In Proceedings of the 8th International Conference on Urban Drainage Modelling*, Tokyo, Japan.
[147] M. J. Box, "A Comparison of Several Current Optimization Methods, and the use of Transformations in Constrained Problems," *The Computer Journal,* vol. 9, pp. 67-77, 1966.
[148] N. Gould and P. Toint, "Nonlinear scaling for bound-constrained optimization," ed, 2004.
[149] H. S. Brown, M. Halliwell, M. Qamar, A. E. Read, J. M. Evans, and P. N. Wells, "Measurement of normal portal venous blood flow by Doppler ultrasound," *Gut,* vol. 30, pp. 503-509, 1989.
[150] S. Chillistone and J. Hardman, "Factors affecting drug absorption and distribution," *Neonatal/pharmacology,* vol. 9, pp. 167-171, 2008.
[151] A. Kotronen, S. Vehkavaara, A. Seppälä-Lindroos, R. Bergholm, and H. Yki-Järvinen, *Effect of liver fat on insulin clearance* vol. 293, 2007.
[152] W. S. Bowman and M. J. Rand, *Textbook of pharmacology / W. C. Bowman, M. J. Rand*. Boston, Mass.: Blackwell Scientific, 1980.
[153] Y. Kwon, *Handbook of Essential Pharmacokinetics, Pharmacodynamics and Drug Metabolism for Industrial Scientists* vol. 1st: Springer, 2001.
[154] M. J. Muller, U. Paschen, and H. J. Seitz, "Glucose production measured by tracer and balance data in conscious miniature pig," *AJP - Endocrinology and Metabolism,* vol. 244, pp. E236-E244, 1983.
[155] J. J. Lima, N. Matsushima, N. Kissoon, J. Wang, J. E. Sylvester, and W. J. Jusko, "Modeling the metabolic effects of terbutaline in [beta]2-adrenergic receptor diplotypes[ast]," *Clinical pharmacology and therapeutics,* vol. 76, pp. 27-37, 2004.
[156] H. C. Grady and E. M. Bullivant, "Renal blood flow varies during normal activity in conscious unrestrained rats," *The American Journal of Physiology,* vol. 262, pp. R926-32, 1992.
[157] J. W. Yates and E. M. Watson, "Estimating insulin sensitivity from glucose levels only: Use of a non-linear mixed effects approach and maximum a posteriori (MAP) estimation," *Computer methods and programs in biomedicine,* vol. 109, pp. 134-143, 2013.

Appendices

Appendix 1: Data Collection

Contents of the CD:

A database with the data collected for this thesis as well as the original data from:

AliceIVGTT

AmieIVGTT

GeorgiaIVGTT

JoChronic

RuthClamp

RuthCPeptide

StevenOGTT

Appendix 2: Minimal Model

Contents:

SI Taylor Series Approach

Edmund Watson (E.M.Watson@warwick.ac.uk)

Setting up the Model

Minimal Model for Glucose and Insulin

```
x'[t_] :=- p2*x[t] + p3*(i[t]-ib)
g'[t_]:=x[t]*g[t]+p1*(gb-g[t])
i'[t_]:=-n*i[t]+Gamma*(g[t]-h)*m[t]
m'[t_]:=1
x[0] = 0;
g[0]=Go;
i[0]=Io;
m[0]=0;
yg[t_] :=  g[t];
yi[t_] := i[t];
subst = {p1 → p1b , p2 → p2b, p3 → p3b,h →hb, n → nb ,
Gamma → Gammab,Io → Iob,Go → Gob};
```

Creating the Coefficients

k is the number of coefficients wanted to be created.
As there are 2 observable states, there are 2 sets of produced coefficients, ya and yb.

```
k=4;
ya = {yg[0],D[yg[t],t]};
For[j = 2,j<k,ya= Join[ya,{D[ya[[j]],t]} ] ; j++]
yi[0];
yb = {yi[0],D[yi[t],t]};
For[l = 2,l<k,yb= Join[yb,{D[yb[[l]],t]} ] ; l++]
TableForm[Simplify[ya]]
TableForm[Simplify[yb]]
coeffs ={ ya,yb} /. t→0;
coeffsPBar = coeffs /. subst;
eqns = coeffs - coeffsPBar;
```

```
{ {Go},
{gb p1+g[t] (-p1+x[t])},
{gb p1 (-p1+x[t])+g[t] (p1^2-ib p3+p3 i[t]-(2 p1+p2)
x[t]+x[t]^2)},
{Gamma p3 g[t]^2 m[t]+gb p1 (p1^2-2 ib p3+2 p3 i[t]-2 (p1+p2)
x[t]+x[t]^2)-g[t] (p1^3-3 ib p1 p3-ib p2 p3+Gamma h p3 m[t]+p3
i[t] (n+3 p1+p2-3 x[t])-3 p1^2 x[t]-3 p1 p2 x[t]-p2^2 x[t]+3
ib p3 x[t]+3 p1 x[t]^2+3 p2 x[t]^2-x[t]^3)}}
{ {Io},
{-n i[t]+Gamma (-h+g[t]) m[t]},
{n^2 i[t]+Gamma (-h+h n m[t]+gb p1 m[t])+Gamma g[t] (1-m[t]
(n+p1-x[t]))},
{-n^3 i[t]-Gamma (-h n-2 gb p1+m[t] (h n^2+gb p1 (n+p1)-gb p1
x[t]))+Gamma g[t] (-n-2 p1+2 x[t]+m[t] (n^2+n p1+p1^2-ib p3+p3
i[t]-(n+2 p1+p2) x[t]+x[t]^2))}}
```

Solving the parameters

```
soln = Simplify
       [Solve[eqns==0,{p1b,p2b,p3b,hb,nb,Gammab,Iob, Gob}]]
{{hb→h,p2b→p2,Gammab→Gamma,
        Iob→Io,nb→n,p3b→p3,Gob→Go,p1b→p1}}
```

Taylor Series

Minimal Model

Setting up the Model

>

$$eqn := \{diff(x1(t),t) = x2(t)*x1(t) + p1*(x1b - x1(t)), diff(x4(t),t) = 1, diff(x2(t),t) = -p2*x2(t) + p3*(x3(t) - x3b), x1(0) = x1o, x2(0) = 0, x3(0) = x3o, diff(x3(t),t) = -n*x3(t) + \Gamma*(x1(t) - h)*x4(t)\};$$

$$eqn := \left\{ \frac{d}{dt} x1(t) = x2(t)\, x1(t) + p1\,(x1b - x1(t)), \frac{d}{dt} x4(t) = 1, \frac{d}{dt} x2(t) = -p2\, x2(t) + p3\,(x3(t) - x3b), x1(0) = x1o, x2(0) = 0, x3(0) = x3o, \frac{d}{dt} x3(t) = -n\, x3(t) + \Gamma\,(x1(t) - h)\, x4(t) \right\}$$

$$[1]$$

> $y1(t) := x1(t) : \quad y3(t) := x3(t) :$

> **Creating the Coefficients**

```
k := 5 :
ya := Vector([eval(y1(0), eqn), eval(diff(y1(t), t), eqn)]) :
yb := Vector([ eval(limit(ya[1], t = 0), eqn), eval(limit(ya[2], t = 0), eqn)]) :
printlevel := 0 :
for i from 2 by 1 to k do
ya := Vector([ya , eval(diff(ya[i], t), eqn)]);
yb := Vector([yb, eval(limit(ya[(i + 1)], t = 0), eqn)]);
end do;


yc := Vector([eval(y3(0), eqn), eval(diff(y3(t), t), eqn)]) :
yd := Vector([ eval(limit(yc[1], t = 0), eqn), eval(limit(yc[2], t = 0), eqn)]) :
for j from 2 by 1 to k do
yc := Vector([yc , eval(diff(yc[j], t), eqn)]);
yd := Vector([yd, eval(limit(yc[(j + 1)], t = 0), eqn)]);
end do;
 coeffents := Vector([yb, yd]);
```

$$coeffents := \begin{bmatrix} 1 .. 12\ Vector_{column} \\ Data\ Type: anything \\ Storage: rectangular \\ Order: Fortran\_order \end{bmatrix}$$

> Finding the Result

> coeffentsb := subs({p1 = p1b, p2 = p2b, p3 = p3b, h = hb, Gamma = Gammab, x1o = x1ob, x3o = x3ob, n = nb}, coeffents);

results := coeffents-coeffentsb;

$$coeffentsb := \begin{bmatrix} 1 .. 12\ Vector_{column} \\ Data\ Type: anything \\ Storage: rectangular \\ Order: Fortran\_order \end{bmatrix}$$

$$results := \begin{bmatrix} 1 .. 12\ Vector_{column} \\ Data\ Type: anything \\ Storage: rectangular \\ Order: Fortran\_order \end{bmatrix}$$

> $solve(convert(results, list), \{p1b, p2b, p3b, hb, nb, Gammab, x1ob, x3ob\});$

$$\{hb = h, p3b = p3, p1b = p1, x3ob = x3o, Gammab = Gammab, nb = n, p2b = p2, x1ob = x1o\}$$

>

Identifiability Analysis

Edmund Watson + James Chapman

```
x[t_]:={x1[t],x2[t],x3[t],x4[t]}

x1'[t_]:= f[x[t],p][[1]]
x2'[t_]:= f[x[t],p][[2]]
x3'[t_]:= f[x[t],p][[3]]
x4'[t_]:= f[x[t],p][[4]]

x1[0]= 0;
x2[0]= G0;
x3[0]= J0;
x4[0]= 0;
xbar[t_]:={Xbar[t],Gbar[t],Jbar[t],Kbar[t]}
Xbar'[t_]:= f[xbar[t],pbar][[1]]
Gbar'[t_]:= f[xbar[t],pbar][[2]]
Jbar'[t_]:= f[xbar[t],pbar][[3]]
Kbar'[t_]:= f[xbar[t],pbar][[4]]


Xbar[0]= 0;
Gbar[0]= Gbar0;
Jbar[0]=Jbar0;
Kbar[0]= 0;

p :={p2,p3,p1,n,h,γ,ib,gb,G0,J0}
pbar :={p2bar,p3bar,p1bar,nbar,hbar,γbar,ib,gb,Gbar0,Jbar0}
```

System f (x(t, p), p)

```
f[x_,p_]:={-p[[1]] x[[1]]+ p[[2]](x[[3]] - p[[7]]),-x[[1]] x[[2]]
+ p[[3]](p[[8]] -x[[2]]),-p[[4]] x[[3]]+ p[[6]](x[[2]]-
p[[5]])x[[4]],1}

h[x_]:={0,1,0,1}  x
 u1[x_] := h[x][[2]];
u1bar[x_] :=h[x][[2]];


u2[x_] := h[x][[4]];
u2bar[x_] :=h[x][[4]];


mu3 = Map[D[u1[x[t]],#]&,x[t]].f[x[t],p];
mu3bar = Map[D[u1bar[x[t]],#]&,x[t]].f[x[t],pbar];
u3[x_]:=mu3 /. {x1[t]→
x[[1]],x2[t]→x[[2]],x3[t]→x[[3]],x4[t]→x[[4]]}
u3bar[x_]:=mu3bar /. {x1[t]→
x[[1]],x2[t]→x[[2]],x3[t]→x[[3]],x4[t]->x[[4]]}

mu4 = Map[D[u3[x[t]],#]&,x[t]].f[x[t],p];
mu4bar = Map[D[u3bar[x[t]],#]&,x[t]].f[x[t],pbar];
```

```
u4[x_]:=mu4 /. {x1[t]→
x[[1]],x2[t]→x[[2]],x3[t]→x[[3]],x4[t]→x[[4]]}
u4bar[x_]:=mu4bar /. {x1[t]→
x[[1]],x2[t]→x[[2]],x3[t]→x[[3]],x4[t]->x[[4]]}

H[x_] := {u1[x],u2[x],u3[x],u4[x]}
Hbar[x_] := {u1bar[x],u2bar[x],u3bar[x],u4bar[x]}

Jacob :=  Transpose[Map[D[H[x[t]],#]&,x[t]]]
MatrixForm[Jacob]
MatrixForm[Jacob /. t→0]

 (_{
  {0, 1, 0, 0},
  {0, 0, 0, 1},
  {-x2[t], -p1-x1[t], 0, 0},
  {-p1 (gb-x2[t])+p2 x2[t]-(-p1-x1[t]) x2[t]+x1[t] x2[t], (-p1-
x1[t])^2+p2 x1[t]-p3 (-ib+x3[t]), -p3 x2[t], 0}
 }_)
 (_{
  {0, 1, 0, 0},
  {0, 0, 0, 1},
  {-G0, -p1, 0, 0},
  {G0 p1-(-G0+gb) p1+G0 p2, p1^2-(-ib+J0) p3, -G0 p3, 0}
 }_)
MatrixRank[Jacob/. t→0]
4
ϕ[x_] := {λ1,λ2,λ3,λ4}

eqns = Simplify[H[ϕ[x[t]]]-Hbar[x[t]]]
Simplify[ Solve[eqns==0, {λ1,λ2,λ3,λ4}]];

{λ2-x2[t],λ4-x4[t],gb (p1-p1bar)-(p1+λ1) λ2+(p1bar+x1[t]) x2[t],-
(p1+λ1) (gb p1-(p1+λ1) λ2)+λ2 (ib p3+p2 λ1-p3 λ3)+(p1bar+x1[t])
(gb p1bar-(p1bar+x1[t]) x2[t])-x2[t] (p2bar x1[t]+p3bar (ib-
x3[t]))}
ϕ[x_] := {λ1,λ2,λ3,λ4}/. Solve[eqns==0, {λ1,λ2,λ3,λ4}][[1]] /.
{x1[t]→ x[[1]],x2[t]→x[[2]],x3[t]→x[[3]],x4[t]->x[[4]]}
eqnzero = (x[t]  /. {t→0}) -( ϕ[xbar[t]] /. {t→0})
resultszero = Simplify[Solve[eqnzero==0 , p]]
{-((gb p1-Gbar0 p1-gb p1bar+Gbar0 p1bar)/Gbar0),G0-Gbar0,J0-
1/(Gbar0 p3) (-((gb p1bar (gb p1-Gbar0 p1-gb p1bar+Gbar0
p1bar))/Gbar0)+gb p1 p2-Gbar0 p1 p2-gb p1bar p2+Gbar0 p1bar
p2+Gbar0 ib p3-Gbar0 ib p3bar+Gbar0 Jbar0 p3bar),0}


{{G0→Gbar0,J0→(ib p3-ib p3bar+Jbar0
p3bar)/p3,gb→Gbar0},{G0→Gbar0,J0→(ib p3-ib p3bar+Jbar0
p3bar)/p3,p1→p1bar}}
 equation[n_] :=Simplify[f[ϕ[x[t]],p][[n]] -
Total[Map[D[ϕ[x[t]][[n]],#]&,x[t]]]f[x[t],pbar][[n]]]

 equation[1]

 -((gb (p1-p1bar) (gb p1bar+ib p3bar+x1[t] (p2bar-x2[t])-p1bar
x2[t]-p3bar x3[t]))/x2[t]^2)
```

```
 equan =Simplify[f[ϕ[x[t]],p] -
Transpose[Map[D[ϕ[x[t]],#]&,x[t]]].f[x[t],pbar]];

 equan[[3]]

 1/(p3 x2[t]^3) (2 gb^3 p1bar^2 (-p1+p1bar)+gb^2 (p1-p1bar) p1bar (n+3
p1bar+p2+3 x1[t]) x2[t]-gb (p1-p1bar) x2[t]^2 (n p1bar+p1bar^2+n
p2+p1bar p2-ib p3bar+(n+2 p1bar+p2-p2bar) x1[t]+x1[t]^2+p3bar
x3[t])+(p3 γ-p3bar γbar) x2[t]^4 x4[t]+x2[t]^3 (n p1 p2-n p1bar p2-
ib n p3+ib n p3bar+ib p2 p3bar-ib p2bar p3bar+(n-p2bar) (-
p2+p2bar) x1[t]+(-n+nbar-p2+p2bar) p3bar x3[t]-h p3 γ x4[t]+hbar
p3bar γbar x4[t]))

Simplify[equation[3]-equan[[3]]]

1/(p3 x2[t]^3) ((-p2+p2bar) γbar x2[t]^4 x4[t]+2 gb^2 (p1-p1bar) p1bar
(gb p1bar+nbar x3[t]+hbar γbar x4[t])+x2[t]^3 (-ib p2 p3bar+ib
p2bar p3bar+p2bar (-p2+p2bar) x1[t]+(p2-p2bar) (nbar+p3bar) x3[t]-
gb p1 γbar x4[t]+gb p1bar γbar x4[t]+hbar p2 γbar x4[t]-hbar p2bar
γbar x4[t])+gb (p1-p1bar) x2[t]^2 (p1bar^2+p1bar p2-ib
p3bar+x1[t]^2+(nbar+p3bar) x3[t]+hbar γbar x4[t]+p1bar γbar
x4[t]+p2 γbar x4[t]+x1[t] (2 p1bar+p2-p2bar+γbar x4[t]))-gb (p1-
p1bar) x2[t] (3 gb p1bar^2+gb p1bar p2+nbar (p1bar+p2) x3[t]+2 gb
p1bar γbar x4[t]+hbar p1bar γbar x4[t]+hbar p2 γbar x4[t]+x1[t] (3
gb p1bar+nbar x3[t]+hbar γbar x4[t])))

 equationt[1]

 -((gb (p1-p1bar) (gb p1bar+ib p3bar+x1[t] (p2bar-x2[t])-p1bar
x2[t]-p3bar x3[t]))/x2[t]^2)

 equation3a = Simplify[equation[3] /. p1bar □p1]

 1/p3 (-ib n p3+ib n p3bar+n (-p2+p2bar) x1[t]+(-n p3bar+nbar (p2-
p2bar+p3bar)) x3[t]-h p3 γ x4[t]+hbar p2 γbar x4[t]-hbar p2bar
γbar x4[t]+hbar p3bar γbar x4[t]+p3 γ x2[t] x4[t]-p2 γbar x2[t]
x4[t]+p2bar γbar x2[t] x4[t]-p3bar γbar x2[t] x4[t])

cf3a1 = Simplify[Coefficient[equation3a, {x1[t]}]/.{x2[t]→
0,x3[t]→0 , x4[t]→0}];
cf3a2 = Simplify[Coefficient[equation3a, {x2[t] x4[t]}]/.{x1[t]→
0,x3[t]→0 }];
cf3a3= Simplify[Coefficient[equation3a, { x3[t]}]/.{x2[t]→
0,x1[t]→0 , x4[t]→0}];
cf3a4= Simplify[Coefficient[equation3a, {x4[t] }]/.{x2[t]→
0,x1[t]→ 0,x3[t]→0 }];
cf3a5= Simplify[equation3a/.{x2[t]→ 0,x1[t]→ 0,x3[t]→0
,x4[t]→0}];
Simplify[equation3a -(x1[t]*cf3a1+x2[t] x4[t]
*cf3a2+x3[t]*cf3a3+x4[t]*cf3a4 + cf3a5)]

 {0}
 cf2 = Simplify[Coefficient[equation[1],
{x1[t]/x2[t]^2}]/.{x3[t]→0 , x4[t]→0}];
cf3 = Simplify[Coefficient[equation[1],
{x3[t]/x2[t]^2}]/.{x1[t]→0 , x4[t]→0}];
```

```
cf1= Simplify[Coefficient[equation[1], {x1[t]/x2[t]}]/.{x3[t]→0 ,
x4[t]→0}];
cf4= Simplify[Coefficient[equation[1],
{1/x2[t]}]/.{x1[t]→0,x3[t]→0 , x4[t]→0}];
cf5= Simplify[Coefficient[equation[1],
{1/x2[t]^2}]/.{x1[t]→0,x3[t]→0 , x4[t]→0}];
Simplify[equation[1] - (
cf2*x1[t]/x2[t]^2+cf3*x3[t]/x2[t]^2+cf1*x1[t]/x2[t]+
cf4/x2[t]+cf5/x2[t]^2 )]
```

```
{0}
solutions = {cf1,cf2,cf3,cf4,cf5,cf3a1,cf3a2,cf3a3,cf3a4,cf3a5}
{{gb (p1-p1bar)},{gb (-p1+p1bar) p2bar},{gb (p1-p1bar) p3bar},{gb
(p1-p1bar) p1bar},{-gb (p1-p1bar) (gb p1bar+ib p3bar)},{(n (-
p2+p2bar))/p3},{(p3 γ-(p2-p2bar+p3bar) γbar)/p3},{(-n p3bar+nbar
(p2-p2bar+p3bar))/p3},{(-h p3 γ+hbar (p2-p2bar+p3bar)
γbar)/p3},(ib n (-p3+p3bar))/p3}
results = Simplify[Solve[solutions==0 , p]]
Solve::svars: Equations may not give solutions for all "solve"
variables. More…
{{gb→0,n→0,γ→0,p2→p2bar-
p3bar,p3→p3bar},{p1→p1bar,n→0,γ→0,p2→p2bar-
p3bar,p3→p3bar},{gb→0,n→0,γ→0,p2→p2bar-
p3bar},{p1→p1bar,n→0,γ→0,p2→p2bar-
p3bar},{gb→0,n→nbar,h→hbar,γ→γbar,p2→p2bar,p3→p3bar},{p1→p1bar,n
→nbar,h→hbar,γ→γbar,p2→p2bar,p3→p3bar},{ib→0,gb→0,n→nbar,h→hbar,
γ→(p3bar γbar)/p3,p2→p2bar},{n→nbar,ib→0,gb→0,h→hbar,γ→(p3bar
γbar)/p3,p2→p2bar},{p1→p1bar,ib→0,n→nbar,h→hbar,γ→(p3bar
γbar)/p3,p2→p2bar}}
```

```
MatrixForm[results]
```

```
(_{
 {{gb→0,n→0,γ→0,p2→p2bar-p3bar,p3→p3bar}},
 {{p1→p1bar,n→0,γ→0,p2→p2bar-p3bar,p3→p3bar}},
 {{gb→0,n→0,γ→0,p2→p2bar-p3bar}},
 {{p1→p1bar,n→0,γ→0,p2→p2bar-p3bar}},
 {{gb→0,n→nbar,h→hbar,γ→γbar,p2→p2bar,p3→p3bar}},
 {{p1→p1bar,n→nbar,h→hbar,γ→γbar,p2→p2bar,p3→p3bar}},
 {{ib→0,gb→0,n→nbar,h→hbar,γ→(p3bar γbar)/p3,p2→p2bar}},
 {{n→nbar,ib→0,gb→0,h→hbar,γ→(p3bar γbar)/p3,p2→p2bar}},
 {{p1→p1bar,ib→0,n→nbar,h→hbar,γ→(p3bar γbar)/p3,p2→p2bar}}
}_)
test1 = gf2*x1[t]/x2[t]^2+gf3*x3[t]/x2[t]^2+gf1*x1[t]/x2[t]+
gf4/x2[t]+gf5/x2[t]^2
test2 = Simplify[D[test1,t]];
test3 = Simplify[D[test2,t]];
test4 = Simplify[D[test3,t]];
test5 = Simplify[D[test4,t]];

syseqn = {test1,test2,test3,test4,test5};
```

```
gf5/x2[t]^2+(gf2 x1[t])/x2[t]^2+gf4/x2[t]+(gf1 x1[t])/x2[t]+(gf3
x3[t])/x2[t]^2
Solve[syseqn == 0,{gf1,gf2,gf3,gf4,gf5}]
```

```
 {{gf1→0,gf2→0,gf3→0,gf4→0,gf5→0}}
 test31 =x1*gf31+x2 x4 *gf32+x3*gf33+x4*gf34 + gf35 /.{ x1 →
x1[t],x2→x2[t],x3→x3[t],x4→x4[t]}
test32 = Simplify[D[test31,t]];
test33 = Simplify[D[test32,t]];
test34 = Simplify[D[test33,t]];
test35 = Simplify[D[test34,t]];
syseqn3a = {test31,test32,test33,test34,test35};

gf35+gf31 x1[t]+gf33 x3[t]+gf34 x4[t]+gf32 x2[t] x4[t]

Solve[syseqn3a == 0,{gf31,gf32,gf33,gf34,gf35}]
{{gf35→0,gf34→0,gf31→0,gf32→0,gf33→0}}
```

Appendix 3: C-peptide

Contents of the CD:

MATLAB code

Results

Appendix 4: Short Term Modelling

Contents:

Observability Rank Criterion

Minimal Model

Model Definition

```
 x[t] := {x1[t],x2[t],x3[t]}
p :={x10,x20,x30,Ro,Ego,Si,kp,ki,kd,n,intn}
f[x_,p_]:={p[[4]]- (p[[5]] +(p[[6]] *x[[2]]))*x[[1]],
p[[7]]*x[[1]]  -p[[10]]*x[[2]] + x[[3]]*p[[8]]+ p[[9]]*x[[1]]',
x[[1]]- p[[11]]*x[[3]]}

h[x_] := {1,0,0,0}
```

Observability Rank Criterion

Lie derivation

```
 c =Map[D[h[x[t]] .x[t],#]&,x[t]]
{{0,0,0,0}.{x1[t],x2[t],x3[t]}+{1,0,0,0}.{1,0,0},{0,0,0,0}.{x1[t],
x2[t],x3[t]}+{1,0,0,0}.{0,1,0},{0,0,0,0}.{x1[t],x2[t],x3[t]}+{1,0,
0,0}.{0,0,1}}
 ca = c.f[x[t],p]
 c.{Ro-x1[t] (Ego+Si x2[t]),kp x1[t]-n x2[t]+ki x3[t]+kd
x1[t]',x1[t]-intn x3[t]}
 ob1 =  Map[D[ca[[1]],#]&,x[t]];
 MatrixForm[ob1]
 (_{
  {-x2[t]},
  {-p1-x1[t]},
  {0},
  {0}
 }_)
 ob1a = ob1.f[x[t]]
{(-p1-x1[t]) (p1 (gb-x2[t])-x1[t] x2[t])-x2[t] (-p2 x1[t]+p3 (-
ib+x3[t]))}
 ob2  =   Map[D[ob1a[[1]],#]&,x[t]];
 MatrixForm[ob2]
 (_{
  {-p1 (gb-x2[t])+p2 x2[t]-(-p1-x1[t]) x2[t]+x1[t] x2[t]},
  {(-p1-x1[t])^2+p2 x1[t]-p3 (-ib+x3[t])},
  {-p3 x2[t]},
  {0}
 }_)
 ob2a = ob2.f[x[t]]
{(p1 (gb-x2[t])-x1[t] x2[t]) ((-p1-x1[t])^2+p2 x1[t]-p3 (-
ib+x3[t]))+(-p1 (gb-x2[t])+p2 x2[t]-(-p1-x1[t]) x2[t]+x1[t] x2[t])
(-p2 x1[t]+p3 (-ib+x3[t]))-p3 x2[t] (-n x3[t]+γ (-h+x2[t]) x4[t])}
 ob3  =   Map[D[ob2a[[1]],#]&,x[t]];
 MatrixForm[ob3]
 (_{
  {(p2-2 (-p1-x1[t])) (p1 (gb-x2[t])-x1[t] x2[t])-p2 (-p1 (gb-
x2[t])+p2 x2[t]-(-p1-x1[t]) x2[t]+x1[t] x2[t])-x2[t] ((-p1-
x1[t])^2+p2 x1[t]-p3 (-ib+x3[t]))+2 x2[t] (-p2 x1[t]+p3 (-
ib+x3[t]))},
  {(-p1-x1[t]) ((-p1-x1[t])^2+p2 x1[t]-p3 (-ib+x3[t]))+(2 p1+p2+2
x1[t]) (-p2 x1[t]+p3 (-ib+x3[t]))-p3 γ x2[t] x4[t]-p3 (-n x3[t]+γ
```

```
(-h+x2[t]) x4[t])},
  {n p3 x2[t]-p3 (p1 (gb-x2[t])-x1[t] x2[t])+p3 (-p1 (gb-x2[t])+p2
x2[t]-(-p1-x1[t]) x2[t]+x1[t] x2[t])},
  {-p3 γ x2[t] (-h+x2[t])}
 }_)
H := {c,ob1,ob2,ob3}
MatrixForm[H]
 (_{
  {0, 1, 0, 0},
  {-x2[t], -p1-x1[t], 0, 0},
  {-p1 (gb-x2[t])+p2 x2[t]-(-p1-x1[t]) x2[t]+x1[t] x2[t], (-p1-
x1[t])^2+p2 x1[t]-p3 (-ib+x3[t]), -p3 x2[t], 0},
  {(p2-2 (-p1-x1[t])) (p1 (gb-x2[t])-x1[t] x2[t])-p2 (-p1 (gb-
x2[t])+p2 x2[t]-(-p1-x1[t]) x2[t]+x1[t] x2[t])-x2[t] ((-p1-
x1[t])^2+p2 x1[t]-p3 (-ib+x3[t]))+2 x2[t] (-p2 x1[t]+p3 (-
ib+x3[t])), (-p1-x1[t]) ((-p1-x1[t])^2+p2 x1[t]-p3 (-ib+x3[t]))+(2
p1+p2+2 x1[t]) (-p2 x1[t]+p3 (-ib+x3[t]))-p3 γ x2[t] x4[t]-p3 (-n
x3[t]+γ (-h+x2[t]) x4[t]), n p3 x2[t]-p3 (p1 (gb-x2[t])-x1[t]
x2[t])+p3 (-p1 (gb-x2[t])+p2 x2[t]-(-p1-x1[t]) x2[t]+x1[t] x2[t]),
-p3 γ x2[t] (-h+x2[t])}
 }_)
MatrixForm[H0 = H /. {x1[t] → 0,x2[t]→g0,x3[t]→i0,x4[t]→0}]
 (_{
  {0, 1, 0, 0},
  {-g0, -p1, 0, 0},
  {g0 p1-(-g0+gb) p1+g0 p2, p1^2-(i0-ib) p3, -g0 p3, 0},
  {(-g0+gb) p1 (2 p1+p2)-p2 (g0 p1-(-g0+gb) p1+g0 p2)+2 g0 (i0-ib)
p3-g0 (p1^2-(i0-ib) p3), i0 n p3+(i0-ib) (2 p1+p2) p3-p1 (p1^2-(i0-
ib) p3), g0 n p3-(-g0+gb) p1 p3+(g0 p1-(-g0+gb) p1+g0 p2) p3, -g0
(g0-h) p3 γ}
 }_)
 Dimensions[H0]
 {4,4}
MatrixRank[H0]
 4
```

Lie Symmetries PID

```
SetDirectory["C:/Documents and Settings/Edmund Watson/My
Documents/Subversion/Documents/PhD/Mathematica/Symmetry/IntroToSym
metry"];
Needs["SymmetryAnalysis`IntroToSymmetry`"];
 inputequation1="D[x1[t],t]-p[4]+ (p5[t] +(p6[t] *x4[t]))*x1[t]";
inputequation2="D[x2[t],t] -p[7]*x1[t]  +p10[t]*x2[t] -
x3[t]*p8[t]- p9[t]*D[x1[t],t]";
inputequation3="D[x3[t],t]-x1[t]+ p11[t]*x3[t]";
inputequation4="D[x4[t],t]-x2[t]+p12[t]*x4[t]";
inputequation5="D[p4[t],t]";
inputequation6="D[p5[t],t]";
inputequation7="D[p6[t],t]";
inputequation8="D[p7[t],t]";
inputequation9="D[p8[t],t]";
inputequation10="D[p9[t],t]";
inputequation11="D[p10[t],t]";
inputequation12="D[p11[t],t]";
inputequation13="D[p12[t],t]";
 rulesarray={"D[x1[t],t]->-(-p4[t]+ (p5[t] +(p6[t]
*x4[t]))*x1[t])",
   "D[x2[t],t] ->-(-p7[t]*x1[t]  +p10[t]*x2[t] - x3[t]*p8[t]-
p9[t]*x1[t])",
   "D[x3[t],t]->-(-x1[t]+ p11[t]*x3[t])",
   "D[x4[t],t]->x2[t]-p12[t]*x4[t]","D[p4[t],t]->0",
   "D[p5[t],t]->0","D[p6[t],t]->0","D[p7[t],t]->0","D[p8[t],t]-
>0","D[p9[t],t]->0","D[p10[t],t]->0","D[p11[t],t]-
>0","D[p12[t],t]->0"};
 independentvariables={"t"};
dependentvariables={"x1","x2","x3","x4","p4","p5","p6","p7"
,"p8","p9","p10","p11","p12"};
 frozennames={""};
p=1;
r=0;
xseon=1;
internalrules=1;

FindDeterminingEquations[independentvariables,dependentvariables,f
rozennames,p,r,xseon,inputequation1,rulesarray,internalrules];
zdeterminingequations1=zdeterminingequations;
FindDeterminingEquations[independentvariables,dependentvariables,f
rozennames,p,r,xseon,inputequation2,rulesarray,internalrules];
zdeterminingequations2=zdeterminingequations;
FindDeterminingEquations[independentvariables,dependentvariables,f
rozennames,p,r,xseon,inputequation3,rulesarray,internalrules];
zdeterminingequations3=zdeterminingequations;
FindDeterminingEquations[independentvariables,dependentvariables,f
rozennames,p,r,xseon,inputequation4,rulesarray,internalrules];
zdeterminingequations4=zdeterminingequations;
FindDeterminingEquations[independentvariables,dependentvariables,f
rozennames,p,r,xseon,inputequation5,rulesarray,internalrules];
zdeterminingequations5=zdeterminingequations;
FindDeterminingEquations[independentvariables,dependentvariables,f
rozennames,p,r,xseon,inputequation6,rulesarray,internalrules];
```

```
zdeterminingequations6=zdeterminingequations;
FindDeterminingEquations[independentvariables,dependentvariables,f
rozennames,p,r,xseon,inputequation7,rulesarray,internalrules];
zdeterminingequations7=zdeterminingequations;
FindDeterminingEquations[independentvariables,dependentvariables,f
rozennames,p,r,xseon,inputequation8,rulesarray,internalrules];
zdeterminingequations8=zdeterminingequations;
FindDeterminingEquations[independentvariables,dependentvariables,f
rozennames,p,r,xseon,inputequation9,rulesarray,internalrules];
zdeterminingequations9=zdeterminingequations;
FindDeterminingEquations[independentvariables,dependentvariables,f
rozennames,p,r,xseon,inputequation10,rulesarray,internalrules];
zdeterminingequations10=zdeterminingequations;
FindDeterminingEquations[independentvariables,dependentvariables,f
rozennames,p,r,xseon,inputequation11,rulesarray,internalrules];
zdeterminingequations11=zdeterminingequations;
FindDeterminingEquations[independentvariables,dependentvariables,f
rozennames,p,r,xseon,inputequation12,rulesarray,internalrules];
zdeterminingequations12=zdeterminingequations;
FindDeterminingEquations[independentvariables,dependentvariables,f
rozennames,p,r,xseon,inputequation13,rulesarray,internalrules];
zdeterminingequations13=zdeterminingequations;
zdeterminingequations=Join[zdeterminingequations1,zdeterminingequa
tions2,zdeterminingequations3,zdeterminingequations4,zdeterminingequations5,zdeterminingequations6,zdeterminingequations7,zdeterminingequations8,zdeterminingequations9,zdeterminingequations10,zdeterminingequations11,zdeterminingequations12,zdeterminingequations13]
;

SolveDeterminingEquations[independentvariables,dependentvariables,
r,xseon,zdeterminingequations,1]
TableForm[xsefunctions]
TableForm[etafunctions]
 {
 {xse1[z1_, z2_, z3_, z4_, z5_, z6_, z7_, z8_, z9_, z10_, z11_,
z12_, z13_, z14_]=a10 + a12*z10 + a13*z11 + a14*z12 + a15*z13 +
a16*z14 + a111*z6 + a112*z7 + a113*z8 + a114*z9}
}
 {
 {eta1[z1_, z2_, z3_, z4_, z5_, z6_, z7_, z8_, z9_, z10_, z11_,
z12_, z13_, z14_]=0},
 {eta2[z1_, z2_, z3_, z4_, z5_, z6_, z7_, z8_, z9_, z10_, z11_,
z12_, z13_, z14_]=0},
 {eta3[z1_, z2_, z3_, z4_, z5_, z6_, z7_, z8_, z9_, z10_, z11_,
z12_, z13_, z14_]=0},
 {eta4[z1_, z2_, z3_, z4_, z5_, z6_, z7_, z8_, z9_, z10_, z11_,
z12_, z13_, z14_]=0},
 {eta5[z1_, z2_, z3_, z4_, z5_, z6_, z7_, z8_, z9_, z10_, z11_,
z12_, z13_, z14_]=b50 + b52*z10 + b53*z11 + b54*z12 + b55*z13 +
b56*z14 + b511*z6 + b512*z7 + b513*z8 + b514*z9},
 {eta6[z1_, z2_, z3_, z4_, z5_, z6_, z7_, z8_, z9_, z10_, z11_,
z12_, z13_, z14_]=0},
 {eta7[z1_, z2_, z3_, z4_, z5_, z6_, z7_, z8_, z9_, z10_, z11_,
z12_, z13_, z14_]=0},
 {eta8[z1_, z2_, z3_, z4_, z5_, z6_, z7_, z8_, z9_, z10_, z11_,
z12_, z13_, z14_]=b80 + b82*z10 + b83*z11 + b84*z12 + b85*z13 +
b86*z14 + b811*z6 + b812*z7 + b813*z8 + b814*z9},
```

```
 {eta9[z1_, z2_, z3_, z4_, z5_, z6_, z7_, z8_, z9_, z10_, z11_,
z12_, z13_, z14_]=0},
 {eta10[z1_, z2_, z3_, z4_, z5_, z6_, z7_, z8_, z9_, z10_, z11_,
z12_, z13_, z14_]=0},
 {eta11[z1_, z2_, z3_, z4_, z5_, z6_, z7_, z8_, z9_, z10_, z11_,
z12_, z13_, z14_]=0},
 {eta12[z1_, z2_, z3_, z4_, z5_, z6_, z7_, z8_, z9_, z10_, z11_,
z12_, z13_, z14_]=0},
 {eta13[z1_, z2_, z3_, z4_, z5_, z6_, z7_, z8_, z9_, z10_, z11_,
z12_, z13_, z14_]=0}
}
```

Minimised ID – Similarity 4 state

```
g'[t_]:=-ia[t]*g[t]*si+gp
j'[t_]:=-n*j[t]+ii[t]*ki+kd*g'[t]
ii'[t_]:=g[t]-ii[t]*kiir
ia'[t_] := j[t] - kair*ia[t]
x1[0] = x1o;
x2[0] = 0;
x3[0] = x3o;
y1 = j[t];
y = g[t];
p ={si,gp,n,ki,kd,kiir,kair};
 G=Append[{},Map[D[y /. t->0,#]&,p]];
calrow:=Module[{},y = D[y,t]; r = Map[D[y /. t->0,#]&,p]; G =
Append[G,r]]
For[i=1,i<7,i++,calrow]

H=Append[{},Map[D[y1 /. t->0,#]&,p]];
calrow:=Module[{},y = D[y,t]; r = Map[D[y /. t->0,#]&,p]; G =
Append[G,r]]
For[i=1,i<7,i++,calrow]


 $Aborted
 MatrixForm[G]
Dimensions[G]
G = Append[G,H]
Dimensions[G]

 {7,7}
 MatrixRank[G]
 6
 gr = RowReduce[G]
gs = Simplify[gr]


{{1,0,0,0,0,0,0},{0,1,0,0,0,0,0},{0,0,1,0,0,0,0},{0,0,0,1,0,0,0},{
0,0,0,0,1,0,0},{0,0,0,0,0,1,0},{0,0,0,0,0,0,1},{0,0,0,0,0,0,0}}

{{1,0,0,0,0,0,0},{0,1,0,0,0,0,0},{0,0,1,0,0,0,0},{0,0,0,1,0,0,0},{
0,0,0,0,1,0,0},{0,0,0,0,0,1,0},{0,0,0,0,0,0,1},{0,0,0,0,0,0,0}}
 MatrixForm[ns = NullSpace[G]]
 {}
 z = {z1[t],z2[t],z3[t],z4[t],z5[t],z6[t]};
 DSolve[{z1'[t]==ns[[1]][[1]], z1[0]==θ1},{z1[t]},t]
 {{z1[t]→θ1}}
 z1 = θ1;z2 = θ2;z3 = θ3;z4 = θ4;z5 = θ5;z6 = θ6;z7 = θ7 + t; z8 =
θ8;z9 = θ9;z10 = θ10;

psi1[t_,z_]:={z[[1]],z[[2]],z[[3]],z[[4]],z[[5]],z[[6]],z[[7]]+t,z
[[8]],z[[9]],z[[10]]}
psi2[t_,z_]:={z[[1]],z[[2]],z[[3]],z[[4]],z[[5]],z[[6]]+t,z[[7]],z
[[8]],z[[9]],z[[10]]}
psi3[t_,z_]:={z[[1]],z[[2]],z[[3]],z[[4]],z[[5]]+t,z[[6]],z[[7]],z
[[8]],z[[9]],z[[10]]}
```

```
psi4[t_,z_]:={z[[1]],z[[2]],z[[3]],z[[4]]+t,z[[5]],z[[6]],z[[7]],z
[[8]],z[[9]],z[[10]]}
psi5[t_,z_]:={z[[1]]+t,z[[2]],z[[3]],z[[4]],z[[5]],z[[6]],z[[7]],z
[[8]],z[[9]],z[[10]]}
psi6[t_,z_]:={z[[1]],z[[2]]+t,z[[3]],z[[4]],z[[5]],z[[6]],z[[7]],z
[[8]],z[[9]],z[[10]]}
psi7[t_,z_]:={z[[1]],z[[2]],z[[3]]+t,z[[4]],z[[5]],z[[6]],z[[7]],z
[[8]],z[[9]],z[[10]]}
psi8[t_,z_]:={z[[1]],z[[2]],z[[3]],z[[4]],z[[5]],z[[6]],z[[7]],z[[
8]]+t,z[[9]],z[[10]]}
psi9[t_,z_]:={z[[1]],z[[2]],z[[3]],z[[4]],z[[5]],z[[6]],z[[7]],z[[
8]],z[[9]]+t,z[[10]]}
psi10[t_,z_]:={z[[1]],z[[2]],z[[3]],z[[4]],z[[5]],z[[6]],z[[7]],z[
[8]],z[[9]],z[[10]]+t}

 Ψ =
psi1[σ1,psi2[σ2,psi3[σ3,psi4[σ4,psi5[σ5,psi6[σ6,psi7[σ7,psi8[σ8,ps
i9[σ9,psi10[σ10,{θ1,θ2,θ3,θ4,θ5,θ6,θ7,θ8,θ9,θ10}]]]]]]]]]]
{θ1+σ5,θ2+σ6,θ3+σ7,θ4+σ4,θ5+σ3,θ6+σ2,θ7+σ1,θ8+σ8,θ9+σ9,θ10+σ10}
 Ψinv = Simplify[Solve[p==Ψ,{σ1,σ2,σ3,σ4,σ5,σ6,σ7,σ8,σ9,σ10}]]
 {{σ5→p1-θ1,σ6→p2-θ2,σ7→p3-θ3,σ4→h-θ4,σ3→n-θ5,σ2→Gamma-θ6,σ1→Io-
θ7,σ8→Go-θ8,σ9→gb-θ9,σ10→ib-θ10}}
 Ψ inv= Ψinv  /. {θ1 → 0,θ2→ 0,θ3→ 0,θ4→ 0,θ5→ 0,θ6→ 0,θ7→ 0,θ8→
0,θ9→ 0,θ10→ 0}
{{σ5→p1,σ6→p2,σ7→p3,σ4→h,σ3→n,σ2→Gamma,σ1→Io,σ8→Go,σ9→gb,σ10→ib}
}
```

Minimised ID – Similarity 6 state

```
g'[t_]:=-ia[t]*g[t]*si+gp
j'[t_]:=-n*j[t]+fac*(ii[t]*ki+kd*g'[t])
ii'[t_]:=g[t]-ii[t]*kiir
ia'[t_] := j[t] - kair*ia[t]
cp1'[t_]:= -cr*cp1[t] -k12*cp1[t]+k21*cp2[t] + ii[t]*ki+kd*g'[t]
cp2'[t_] := +k12*cp1[t]-k21*cp2[t]
g[0] = go;
j[0] = io;
ii[0] = iio;
ia[0] =iao;
cp1[0] = cp1o;
cp2[0] =cp2o;
y = j[t];
y1 = g[t];
y2 = cp1[t];
p ={si,gp,n,ki,kd,kiir,kair,fac,cr,k12,k21};
 G=Append[{},Map[D[y /. t->0,#]&,p]];
calrow:=Module[{},y = D[y,t]; r = Map[D[y /. t->0,#]&,p]; G =
Append[G,r]]
For[i=1,i<12,i++,calrow]


MatrixForm[G]

 MatrixRank[G]
 7
 gr = RowReduce[G]
gs = Simplify[gr]


{{1,0,0,0,0,0,0},{0,1,0,0,0,0,0},{0,0,1,0,0,0,0},{0,0,0,1,0,0,0},{
0,0,0,0,1,0,0},{0,0,0,0,0,1,0},{0,0,0,0,0,0,1},{0,0,0,0,0,0,0}}

{{1,0,0,0,0,0,0},{0,1,0,0,0,0,0},{0,0,1,0,0,0,0},{0,0,0,1,0,0,0},{
0,0,0,0,1,0,0},{0,0,0,0,0,1,0},{0,0,0,0,0,0,1},{0,0,0,0,0,0,0}}
 MatrixForm[ns = NullSpace[G]]
 {}
 z = {z1[t],z2[t],z3[t],z4[t],z5[t],z6[t]};
 DSolve[{z1'[t]==ns[[1]][[1]], z1[0]==θ1},{z1[t]},t]
 {{z1[t]→θ1}}
 z1 = θ1;z2 = θ2;z3 = θ3;z4 = θ4;z5 = θ5;z6 = θ6;z7 = θ7 + t; z8 =
θ8;z9 = θ9;z10 = θ10;

psi1[t_,z_]:={z[[1]],z[[2]],z[[3]],z[[4]],z[[5]],z[[6]],z[[7]]+t,z
[[8]],z[[9]],z[[10]]}
psi2[t_,z_]:={z[[1]],z[[2]],z[[3]],z[[4]],z[[5]],z[[6]]+t,z[[7]],z
[[8]],z[[9]],z[[10]]}
psi3[t_,z_]:={z[[1]],z[[2]],z[[3]],z[[4]],z[[5]]+t,z[[6]],z[[7]],z
[[8]],z[[9]],z[[10]]}
psi4[t_,z_]:={z[[1]],z[[2]],z[[3]],z[[4]]+t,z[[5]],z[[6]],z[[7]],z
[[8]],z[[9]],z[[10]]}
psi5[t_,z_]:={z[[1]]+t,z[[2]],z[[3]],z[[4]],z[[5]],z[[6]],z[[7]],z
[[8]],z[[9]],z[[10]]}
psi6[t_,z_]:={z[[1]],z[[2]]+t,z[[3]],z[[4]],z[[5]],z[[6]],z[[7]],z
[[8]],z[[9]],z[[10]]}
```

```
psi7[t_,z_]:={z[[1]],z[[2]],z[[3]]+t,z[[4]],z[[5]],z[[6]],z[[7]],z
[[8]],z[[9]],z[[10]]}
psi8[t_,z_]:={z[[1]],z[[2]],z[[3]],z[[4]],z[[5]],z[[6]],z[[7]],z[[
8]]+t,z[[9]],z[[10]]}
psi9[t_,z_]:={z[[1]],z[[2]],z[[3]],z[[4]],z[[5]],z[[6]],z[[7]],z[[
8]],z[[9]]+t,z[[10]]}
psi10[t_,z_]:={z[[1]],z[[2]],z[[3]],z[[4]],z[[5]],z[[6]],z[[7]],z[
[8]],z[[9]],z[[10]]+t}

 Ψ =
psi1[σ1,psi2[σ2,psi3[σ3,psi4[σ4,psi5[σ5,psi6[σ6,psi7[σ7,psi8[σ8,ps
i9[σ9,psi10[σ10,{θ1,θ2,θ3,θ4,θ5,θ6,θ7,θ8,θ9,θ10}]]]]]]]]]]
{θ1+σ5,θ2+σ6,θ3+σ7,θ4+σ4,θ5+σ3,θ6+σ2,θ7+σ1,θ8+σ8,θ9+σ9,θ10+σ10}
 Ψinv = Simplify[Solve[p==Ψ,{σ1,σ2,σ3,σ4,σ5,σ6,σ7,σ8,σ9,σ10}]]
 {{σ5→p1-θ1,σ6→p2-θ2,σ7→p3-θ3,σ4→h-θ4,σ3→n-θ5,σ2→Gamma-θ6,σ1→Io-
θ7,σ8→Go-θ8,σ9→gb-θ9,σ10→ib-θ10}}
 Ψ inv= Ψinv  /. {θ1 → 0,θ2→ 0,θ3→ 0,θ4→ 0,θ5→ 0,θ6→ 0,θ7→ 0,θ8→
0,θ9→ 0,θ10→ 0}
{{σ5→p1,σ6→p2,σ7→p3,σ4→h,σ3→n,σ2→Gamma,σ1→Io,σ8→Go,σ9→gb,σ10→ib}
}
```

Appendix 5: Long Term Modelling

The CD contains the GUI for long term modelling.

Appendix 6: Software Tool for Modelling Glucose, Insulin and C-peptide Dynamics

Software tool is on the CD.